Evapotranspiration Measurement and Modeling for a Green Roof System

By

Gerald Zaremba

A Thesis Submitted to

Department of Civil and Environmental Engineering

College of Engineering

in partial fulfillment of the requirements

for the degree of

MASTER OF SCIENCE

In

Civil Engineering

April 2015

Villanova University

Villanova, PA

Statement by Author

This dissertation has been submitted in partial fulfillment of requirements for an advanced degree at the Villanova University and is deposited in the University Library to be made available to borrowers under rules of the Library.

Brief quotations from this dissertation are allowable without special permission, provided that accurate acknowledgment of source is made. Requests for permission for extended quotation from or reproduction of this manuscript in whole or in part may be granted by the head of the major department or the Associate Dean for Graduate Studies and Research of the College of Engineering when in his or her judgment the proposed use of the material is in the interests of scholarship. In all other instances, however, permission must be obtained from the author.

Acknowledgments

First of off, I would like to thank my advisors Dr. Wadzuk, Dr. Traver, and Dr. Welker for their help and guidance through the course of my master's degree at Villanova University. Additionally, I would like to thank Professor David Brandes at Lafayette College for inspiring me to continue my education in water resources.

I would also like to thank everyone at the VUSP, grad students past and present for their help with projects as well as for all of the stimulating intellectual discussion on everything from green infrastructure and climate change down too softball strategies and song choices at karaoke.

In addition to the VUSP there are several people within the department who without, all operations at the VUSP would cease to a halt. Linda DeAngelis, for her help with all things paperwork, ordering, and figuring out how to pay for things, Sonali Joshi for helping with all things communications and outreach related, and George Pappas, for everything he does which could not be possibly summarized in this section.

I would also like to thank the PA DEP Growing Greener Grants for providing funding for this research as well as the VUSP partners for providing funding for our day to day operations as an organization.

Lastly I would like to thank my parents and sister for their continued support throughout the course of my graduate studies. Without their love and support none of this would have been possible.

Abstract

As populations continue to move into America's cities and the urban landscape continues to sprawl out, stormwater management will continue to be a pressing matter. In the near future, designers and engineers will have to mitigate the effects of stormwater with unique and dynamic stormwater control measures (SCMs). While green roofs are still an emerging technology in the United States, they hold promise as a way to mitigate most of the runoff from smaller storms (typically 2.5cm or less) directly at the source. Unfortunately, for many municipalities and regulatory agencies, green stormwater infrastructure is not credited for evapotranspiration (ET) even though it can account for around 75% of a green roofs water budget during April through November.

To tackle this problem, research at Villanova University has been tracking and studying the performance of a weighing lysimeter for 6 years (2009-2014) as well as an entire green roof for 2 full years (2013-2014). Results from the weighing lysimeter showed ET accounting for 68% of the total precipitation for 2009, 88% for 2010, 74% for 2011, 77% for 2012, 75% for 2013, and 80% for 2014 between the months of April and November. For the entire green roof system, ET accounted for 62% and 56% of the precipitation for 2013 and 2014, respectively. It was found that this difference in performance was due to the different drainage scenarios of the two systems. Where the weighing lysimeter was fully enclosed with no drain, the media was able to become fully saturated allowing for the retention of nearly 40mm of water while the green roof could only reach field capacity, retaining about 20mm. This difference in total retention allowed more water to be available for ET between storms for the lysimeter, optimizing its performance.

A model based off of the Hargreaves equation for reference ET was created to predict performance of the system. Utilizing a reduction factor based on soil moisture as well as a simple day to day water budget accounting system, results for the model were close to observed field conditions. Data from the weighing lysimeter was used for the development and calibration of the model and the average error across all 6 years was 74mm with the model underpredicting ET in all years but 2009. When applied to the entire green roof, the model overpredicted overflow by 37mm in 2013 and underpredicted for 2014 by 36mm.

As engineers progress in analyzing and designing stormwater infrastructure for the urban environment, the idealized design storm methodology should be put aside in favor of continuous simulation. The idea that SCMs are static systems is not appropriate when considering the effects climatic variables, as well as antecedent moisture conditions, have on a system's performance. With the results presented in this research, it is believed that this model can serve as an acceptable method for predicting the antecedent moisture condition within a green roof system for continuous simulation.

TABLE OF CONTENTS

List of Figures

List of Tables

Nomenclature

ET_o	Reference Evapotranspiration [mm/day]
ET_a	Actual Evapotranspiration [mm/day]
ET_{Lys}	Evapotranspiration from Lysimeter [mm/day]
W	Weight of Lysimeter
Q_r	Overflow [mm]
P	Precipitation [mm]
T	Temperature [^oC]
T_r	Terrestrial Radiation [mm/day]
R_a	Terrestrial Radiation [MJ m^{-2} day^{-1}]
d_r	Inverse Relative Distance Earth to Sun
φ	Site Latitude [radians]
G_{sc}	Solar Constant [0.0820 MJ m^{-2} min^{-1}]
ω_s	Sunset Hour Angle [radians]
δ	Solar Decimation [radians]

CHAPTER 1. INTRODUCTION

1.1 Research Objectives

The overall objective of the current research was twofold. The first was to build upon previous green roof work performed with the use of a weighing lysimeter at Villanova's green roof, and to compare it to the performance of the entire green roof site. Secondly, to develop a model to predict how the green roof has performed in order to better understand the effects evapotranspiration (ET) had on system performance and serve as a design tool for future green roofs. To go about this, several smaller objectives were set:

- Analyze how the weighing lysimeter has performed over the course of 6 years of measured data.
- Analyze the performance of the entire green roof using overflow data for 2013 and 2014.
- Compare the two systems and analyze the differences between performances based on the differences between the two designs.
- Develop a predictive model for estimating annual performance of each green roof system based on measured climatic variables as well as design parameters.
- Compare the results from the model to the field measurements to assess its validity.

1.2 Stormwater Background

As the world has become more and more developed, populations have always centered around areas of trade and commerce. In today's society, cities have become particularly attractive for younger people who want to live closer to their jobs as well as be near all of the conveniences of modern life. This process of populations moving from rural areas and the spread of cities

outward is known as urbanization. As of 2013, nearly two thirds of the US population lived in cities with this number still increasing (Cohen 2015).

The hydrologic cycle is comprised of all processes that affect water in the natural environment. This includes but is not limited to precipitation, evaporation and transpiration, infiltration into pervious surfaces, groundwater flow, surface runoff from impervious surfaces, as well as flow through rivers and streams, and surface storage. When one of these processes is altered, in order to maintain a mass balance, another process or combination of processes must also change (Hess, 2014). With urbanization comes the need for infrastructure and development, and with this comes the conversion of pervious surfaces to impervious surfaces. As we transform the native environment from meadows and forests to roadways and rooftops, the natural response to the hydrologic cycle is severely altered. Precipitation that used to be primarily soaked up into the ground or held up in surface storage, is now unable to infiltrate and is rapidly conveyed over smoother impervious surfaces, as seen in Figure 1.1. This allows stormwater to make its way to main channels, such as rivers and streams, quicker and in greater volumes. This can lead to severe erosion in some places, as well as cause flash flooding in low lying areas.

When planners and engineers first started developing infrastructure, the idea at the time was to convey the water as quickly as possible off site and downstream to ensure the safety of users (Berndtsson 2010). This was often done with large pipes, gutters and culverts and often times utilized existing sanitary sewer systems for this purpose. The problem with this is storm events; the existing sanitary sewer systems could not handle the additional surge of water and often times became backed up causing floods of raw sewage in some places, or combined sewer overflows (CSOs) where raw sewage is discharged directly into a receiving body of water in others. Today in Philadelphia, CSOs are still discharged at over 160 points into the Schuylkill

and Delaware Rivers (PWD 2011). Combined sewer overflows are both harmful to the native species of plants and animals and citizens who use the water for recreational purposes and municipal use.

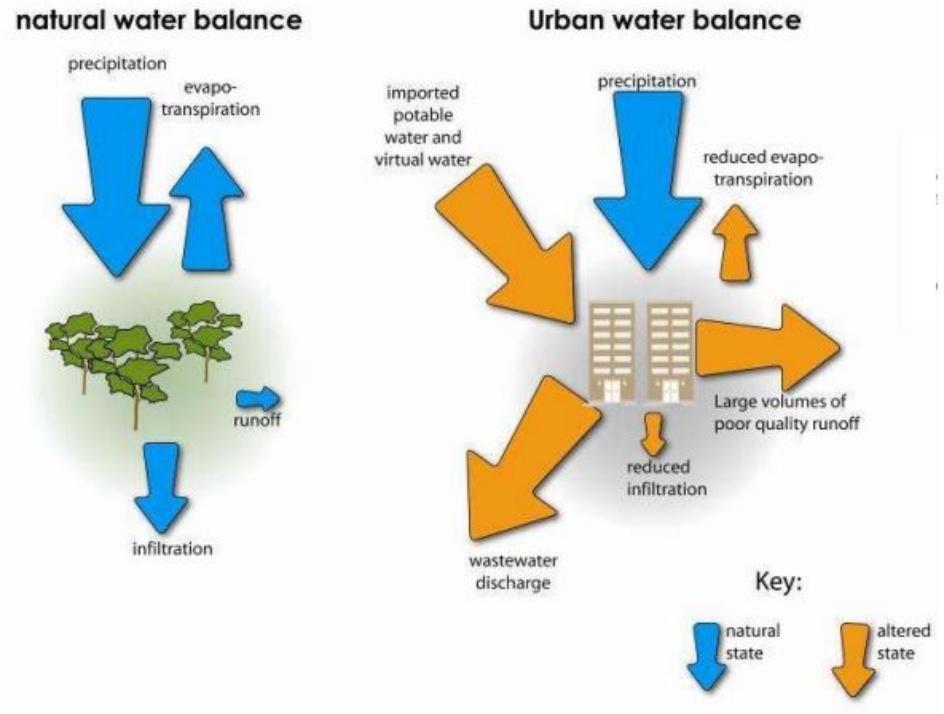

Figure 1.1 Impacts of Urbanization on the Hydrologic Cycle (Hoban and Wong 2006)

To combat these problems, engineers turned to reducing peak flow rates by creating large detention basins with controlled outflows. This methodology has often times been called “grey infrastructure” (Spatari et al. 2011) as it utilizes large concrete structures to control stormwater. These detention basins were often times designed to capture larger rain events, which was what was believed to be causing most of the problems with stormwater. However, as we civil engineers progressed as a profession, we came to realize that most of the storms we experienced, particularly in the Philadelphia area, were typically less than 1 inch of precipitation yet these

smaller events still caused a significant amount of CSOs (Mayor's Office Of long-Term Planning and Sustainability, 2008). It was only in the late 90s and early 2000s when the idea of capturing and treating the smaller events on site with "green infrastructure" such as stormwater control measures (SCMs) or best management practices (BMPs) has become a common practice.

Structural SCMs are stormwater control devices that are physically constructed such as rain gardens, pervious asphalt/concrete sites, or green roofs, as opposed to non-structural SCMs which are practices that mitigate the effects of urbanization such as street sweeping to help remove pollutants, or using previously developed areas rather than green areas for new development. One of the key ideas behind SCMs is to employ them on a smaller site scale meaning, rather than have one large detention basin for a community, have each parcel mitigate its own stormwater within the confines of its property. This helps spread the cost of stormwater infrastructure as well as help reduce the size of stormwater control measures; additionally it distributes the environmental burden and benefit of stormwater treatment.

1.3 Green Roofs and Crediting Evapotranspiration

In November 2000 a 3.4 acre piece of land sold within Manhattan for $345 million. This equates to approximately $2,300 per square foot (Haughwout et al. 2008). With prices of real estate this high, property owners and developers may be hesitant or unwilling to build ground level SCMs, such as rain gardens; this may make the use of green roofs particularly attractive for sites such as these. Green roofs provide an excellent opportunity for controlling stormwater within an urban environment. Rooftops comprise a large portion of the impervious surfaces within an urban environment and are a relatively unused and overlooked space (Fassman-Beck et al. 2013).

Intensive green roofs typically consist of a thin growing media overtop a storage and drainage layer. The media is typically planted with smaller drought resistant plants such as sedums and a few herbaceous species. The main idea behind this is to mimic a natural undeveloped surface on a rooftop where peak stormwater flows can be mitigated as well as total volume reduced. While green roofs can be one of the costliest SCMs on a per square foot basis; when paired with their other benefits such as insulation, roof protection, and aesthetic benefits, their cost can be more bearable for property owners.

One of the main problems with crediting green roofs appropriately is the lack of sufficient long-term studies attesting to their performance (Fassman-Beck et al. 2013). Although green roofs have been around for centuries, particularly in Europe, their popularity and reception in the United States has been slow to take off. Because of this dearth many cities and municipalities rely on legacy methods for evaluating green roofs, such as with the use of the National Resource Conservation Service (NRCS) curve number methodology (NRCS 1986). Designed as a simplified method to calculate stormwater runoff from small urbanized watersheds, this method is not appropriate for evaluating green roofs which do not have the same hydrology as the areas used to develop the method.

The issue with providing a set number on a green roofs performance lies in how it functions. Unlike other SCMs that rely on infiltration as the primary means for mitigating stormwater, a green roof relies primarily on its ability to retain water within its media and then evapotranspiration (ET) of this water over time. This means that a green roof's performance is highly dependent on key climactic variables such as rainfall depth and intensity, solar radiation, and temperature (Carpenter and Kaluvakolanu 2011; Voyde et al. 2010; Fassman-Beck et al. 2013). Fassman-Beck et al. (2015), compiled green roof runoff data from sites around the world

and determined curve numbers for green roofs of varying depth and composition, and categorized them into climate regions. While the study was comprehensive of various types of roofs, the authors still were not proponents of the use of the curve number and offered their findings as a basis for crediting green roofs with data backed research.

Most municipalities and regulating authorities however do not allow for crediting of ET within SCMs (Wadzuk 2013). The concern is that because ET is a highly energy dependent process, it is variable throughout the year, and therefore difficult to account for on a design storm basis. However, many regulating authorities are receptive to the idea of allowing credit for ET if the science is there and it can be done in a simple way. With this, researchers around the globe have been working diligently on trying to understand the complex processes within green roofs to develop an easy to use standard for green roofs. The current research at Villanova is primarily focused on understanding ET and how it plays a role in performance of green roofs.

CHAPTER 2. LITERATURE REVIEW

This chapter will explore three distinct areas pertaining to the present research. First, a brief overview of green roofs and how their system components interact and affect performance will be provided. Next, an outline of current green roof crediting standards, as well as current proposed modeling techniques will be explored. Lastly, an examination of evapotranspiration (ET) estimation techniques will be discussed, as well as their applicability to green roofs.

2.1 Green Roof Overview

2.1.1 Green Roof Background

Green roofs are alternative roof covers that have been growing in popularity recently, especially in urban areas. Green roofs can be designed to help mitigate stormwater runoff, provide an additional layer of insulation for a roof, as well as increase the aesthetic component of the building. When using a green roof as a stormwater control measure (SCM) they can be one of the costliest stormwater management systems, however when paired with their other benefits the cost can be less overwhelming for a building owner (EPA 2008).

Green roofs have been around in some form or another for centuries. Historically, Northern Europeans have used this technology primarily as an insulating measure to help protect them from the cold weather (Magill 2007). The modern green roofs which we are familiar with today were developed around the 1960s in Germany. While their popularity around Europe spread rapidly during the 1980s, their appearance in the United States was not significant until the 2000s. Because of this delay, the cost for green roofs in Germany are significantly less than in the United States due to the market size and experience in the field (Philippi 2006). There are fewer companies producing green roof materials in the United States, as well as fewer

professionals experienced with the installation of green roofs, therefore prices tend to be significantly higher in the United States than in Germany. The average price per square foot of installed green roof was $18.50 in Germany as compared to $47.30 in the United States (Figure 2.1) (Philippi 2006).

Figure 2.1 Green Roof Costs USA vs. Germany (Philippi 2006)

Green roofs are typically categorized as either extensive, semi-intensive, or intensive and are distinguished by their depth of growing media as well as typical plant varieties (Green Roof Technologies, no date). Extensive green roofs, such as the green roof at Villanova University, are typically classified by their thinner media depths (typically less than 150mm) and their use of mostly sedums as well as a few grasses and herbaceous species. Extensive green roofs are typically chosen for their lower costs, the need of only minimal maintenance, and the need for fewer structural modifications to support their lighter weight (typically 30psf). Extensive green

roofs also do not typically have permanent irrigation systems and should only require temporary watering during initial plant establishment and during periods of extreme drought (Miller 2003).

Intensive green roofs are typically thicker and have a depth of media greater than 200mm. Intensive green roofs can typically support more native species and even small trees or shrubberies (FLL 2002) and can often times be used as an outdoor public space. These systems typically have a permanent irrigation system and require regular maintenance.

Semi-intensive green roofs are a hybrid design of both systems. They typically include between 100mm and 200mm of growing media, however these systems typically have a permanent irrigation system installed. Because of the increased thickness of the media and the irrigation system, plant species that are typically not tolerant to droughts can be used. Although similar to extensive green roofs, semi-intensive green roofs shift more towards the grasses and herbaceous species of plants and these systems can even be used as an ornamental garden adding to the aesthetic component of the roof. (Green Roof Technologies no date; Green Roof Guide no date)

2.1.2 Components of Green Roofs

Green roof systems include many components that must work together to provide the user with an effective and efficient design while ensuring the structural integrity and preventing water damage. When a green roof is installed, typically the existing roof is resealed to ensure the building will not be susceptible to water damage (e.g., leaking, extended ponding). A protective barrier is installed to prevent the materials used from puncturing the newly sealed roof. Above that, a drainage layer consisting of an expanded plastic board or a porous media, such as gravel, is installed to help convey any water drained by gravity to the roof drain. The drainage layer is topped by a filter fabric, to ensure no fine particles can clog and restrict drainage, and finally a

growing media layer with various types of vegetation. To ensure any surrounding structure is not damaged by the green roof, as well as to ensure any surface runoff can be quickly conveyed to the roof drain, a rock barrier is typically installed around the perimeter of the roof.

The key components that affect the performance of the system during a storm are the growing media, the type of drainage layer, and the rock perimeter. For ET, the media choice as well as vegetation type can have a significant effect on long-term performance. (Fassman-Beck et al., 2013)

2.1.2.1 Media Choice and Thickness

FLL guidelines provide suggestions for various media types to be used in green roofs. These systems can range from improved soil mixtures (such as soil found on site) for intensive green roofs, to mineral aggregate mixtures and vegetation matting for extensive green roofs (FLL 2002). Typical grain sizes range from 0.07mm up to 18mm with the range of particle size distributions shown in Figure 2.2. Clay and silts should not exceed 15% by mass and organic content should range from 6% to 8% for multiple course green roof projects.

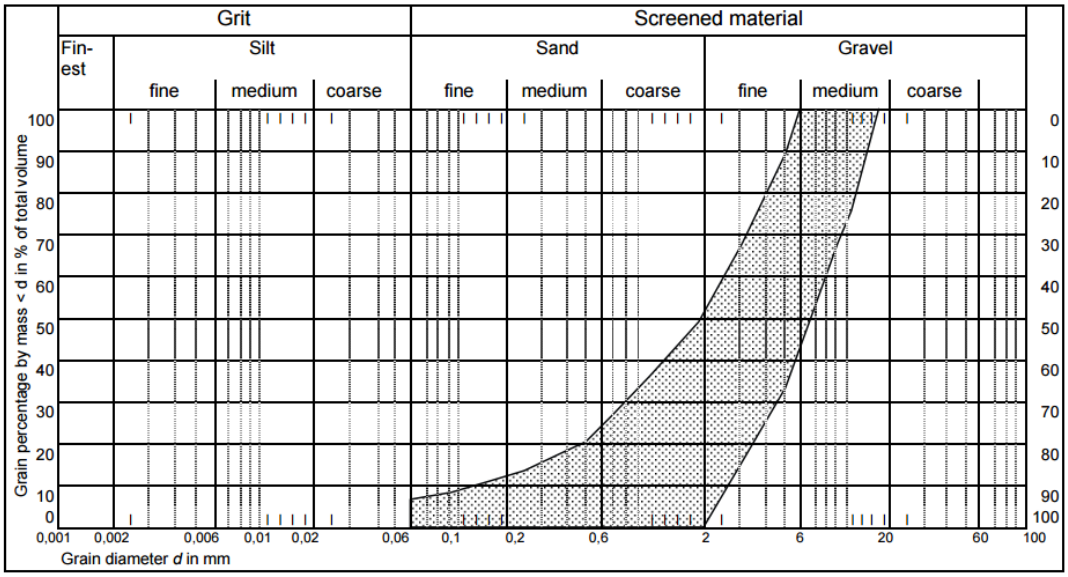

Figure 2.2 Grain Size Distribution for Single Course Extensive Green Roofs (FLL 2002)

Ranges for extensive green roof growing media thickness typically are from 50-150mm (2 to 6in). As media thickness increases, total stormwater retention increases (Fassman and Simcock 2012; VanWoert et al. 2005a; VanWoert et al. 2005b). VanWoert et al. (2005b) found that although water holding capacity increases as media thickness increases, once that has been exhausted, all other precipitation will become direct runoff regardless of media thickness. However, peak flows are delayed due to the increased travel time through the media (Fassman-Beck et al. 2013).

Fassman-Beck et al. (2013) found that this apparent difference in performance only applies on an event to event basis. When comparing different media depths ranging from 50-150mm across four different green roofs, cumulative performance across the four roofs was not significant. This is attributed to the predominance of rainfall events with less total precipitation than the storage capacity of the system.

In a study performed by Graceson et al. (2013), 12 different media compositions were compared in terms of water holding capacity and total annual retention. The different media compositions were sorted into either a sedum supporting media and tested at a depth of 75mm, or a meadow species supporting media planted at 150mm. Grain size distributions for each sample varied and were comprised of either crushed brick, crushed tile, or fly ash. Over an analysis period from December 2009 to June 2010 the authors found that for all of the samples, except the sedum samples comprised of crush tiles, there was not a significant difference in cumulative retention amongst the samples though their water holding capacity ranged from 20 to 30%. This is believed to be caused by the amount of rainfall events with precipitation less than the holding capacity of the system.

Media thickness can also play other important roles for green roofs particularly in more extreme environments. Boivin et al. (2001) found that deeper media can help prevent damaging frost for some herbaceous species minimizing the need for replanting in the spring. In addition, thicker media layers and the additional water retention associated with them can help to minimize stress on plants and can help promote healthier plant growth (Monterusso et al. 2005; VanWoert et al. 2005b).

2.1.2.2 Drainage Layer

Most green roofs in the United States, regardless of type, include a drainage layer. The two primary types of drainage layers are media composed systems and expanded plastic “egg carton” drainage boards. The expanded plastic boards are becoming increasingly popular especially in retrofits because of their light weight and high void-space. While media based drainage layers are typically heavier in nature and may have reduced void-space, their lower hydraulic conductivity compared to plastic drainage boards helps in increasing the time of travel to an

outflow structure and thus also further delays the peak of the hydrograph (Fassman-Beck et al., 2013). Regardless of drainage layer type, it is imperative that a filter fabric is used to separate the growing media from the drainage layer. This filter fabric allows water to pass easily into the drainage layer, but prevents the fines and organics from clogging the void-space of the drainage layer.

2.1.2.3 Vegetation

It has been shown that one of the main limitations for plant health and survivability on green roofs is water availability (VanWoert et al. 2005a; Wolf and Lundholm 2008). The lack of consistent watering regime often times limits the choice of plants, which typically leads to the selection of more drought resistant and usually non-native species (Nagase and Dunnett 2010).

It is important to have a number of diverse species on a green roof system. By varying the types of plants used, a green roof can be more resilient to the varying conditions of the seasons. Typically on green roof systems with 50mm (2in) of media, plant species are limited by root size and type. For these thinner media profiles, species are typically limited to sedums and herbs because of their shallow root structures, as well as their ability to tolerate stressed water conditions. As media thickness increases, plant species can become more diverse. As the profile thickness increases to 10cm (4in), perennial plants can start to survive. When the media profile exceeds 15cm (6in), in addition to the change in media type, these profiles can support grasses as well as shrubs and small trees. (FLL 2002)

2.1.2.4 Rock Perimeter

The primary role of the rock perimeter of a green roof is to allow surface runoff to be conveyed quickly to the roof drain and to protect the surrounding building from damage due to plant

growth. While these rock perimeters are essential, they reduce the amount of greened surface. In a review performed by Fassman-Beck et al. (2013), the authors found that although one of their test locations (the Tamaki mini-roofs) had the highest water retention capacity as well as the thickest depths, their peak flows were statistically higher than the other studied roofs. It is hypothesized that this could be a result of the greater of proportion of rock perimeter to greened surface compared to the other two roof setups.

2.2 Green Roof Design Standards and Crediting

2.2.1 Green Roof Design Standards

While there is currently not a widely accepted United States specific design guide for green roofs, many designers and engineers refer to the Forschungsgesellschaft Landschaftsentwicklung Landschaftsbau e.V. (FLL) Richlinien für die Planung, Ausführung and Plege von Dachbegrünung, which is the German “Guidelines for the Planning, Execution and Upkeep of Green-Roof Sites”. The FLL Guidelines provide design specifications for every aspect of green roof design from specific system components specifications, to plant selection and maintenance requirements. The FLL Guidelines also provide standards for calculating and monitoring green roof performance. The FLL guidelines are based off of years of data and millions of square feet of greened roofs. (Green Roof Technologies no date)

In 2014 the American Society for Testing and Materials (ASTM) released ASTM E2777-14, which is the “Standard Guide for Vegetative (Green) Roof Systems”. This standard is the start of an American design guide for green roofs. Much like in the beginning of the geo-textile era where many of their test standards were based off of standards for testing fabrics and clothing (Welker 2014), the green roof guidelines refer to many standards from the soils testing area for

media design and selection, as well as the geosynthetic specifications for filter fabrics and drainage boards (ASTM E2777-14). In the last few years however, there have been six new ASTM standards directly related to green roof design. These methods include a testing method for determining saturated water permeability of drainage media for green roofs (ASTM E2396), standardized methods of calculating live and dead loads from green roofs (ASTM E2397), test methods to determine water capture and media retention of composite drainage layers (ASTM E2398), test methods for determining maximum media density for dead load analysis (ASTM E2399), a guide for selecting, installing, and maintaining plants in a green roof system (ASTM E2400), and lastly a specification for the use of expanded shale, clay, and slate as the mineral component of green roof media (ASTM E2788).

2.2.2 Current State Regulations

While many states and local municipalities have different design regulations for green roofs used as SCMs, most seem to incorporate traditional runoff methods, such as the NRCS Curve Number method or the rational method. A look into a few of the regional design guides highlights the wide array of standards. For Philadelphia, the total area of the green roof may be considered disconnected impervious cover to encourage the use of this technology. Since green roofs do discharge runoff, designers must use the curve number method with a curve number of 86 to calculate discharge for stormwater regulations. Designers may use other curve numbers if appropriate citations are included in their proposal. While the city does not provide specific requirements or design standards, other than that media thickness must not be less than 76mm (3in), they do provide general guidelines on materials as well as media selection and refer the designer to the FLL guidelines (PWD 2011).

New York City requires that green roofs media must be at least 10cm (4in) thick. The city provides material and media guidelines for the design of green roofs as well as maintenance and plant species recommendations. For stormwater runoff calculations, they apply a runoff coefficient of 0.7 using the rational method. Storage is taken as the void space within the media and drainage layer and is limited by the weir elevation of the outflow structure (NYC DEP 2012).

Washington D.C. allows for the total volume of the void space within the system to be used in part to manage a portion of the 2yr and 15yr storm events (DDOE 2012). Maryland's BMP manual requires the use of the curve number method for calculating stormwater runoff. The curve number used is based off of media thickness and ranges from 94 for a 50mm (2in) thick media to a 77 for a 200mm (8in) thick media roof. They also require the use of an additional treatment to compensate for the loss of groundwater recharge from a green roof (MDE 2000).

2.3 Evapotranspiration

Evapotranspiration is one of the major components of the hydrologic cycle; without evapotranspiration (ET), there could be no precipitation. Evapotranspiration is a process that is often times overlooked when discussing stormwater regulations. This section will explore some of the key concepts of ET.

2.3.1 Evapotranspiration Concepts

Evaporation is the process in which water is converted to water vapor and lost to the atmosphere (Allen et al. 1998). The primary climactic factors affecting evaporation from standing water is solar radiation, surface area and wind. While solar radiation provides most of the energy required for evaporation, wind speed can have a significant impact on the rate of evaporation. A study by

Chow (1964) found that a 5mph wind could increase evapotranspiration by 20% and a 15mph wind could increase evapotranspiration by 50% over a similar timespan relative to still air. Surrounding land use (fetch) can also have a significant effect on ET by increasing moisture content of air and decreasing the vapor pressure gradient (Allen et al. 1998)

Transpiration is the process by which water is lost through plant stomata. Different species of plants use different amounts of water depending primarily on stomatal resistance, climactic conditions, and soil water availability. Plant density, crop roughness, reflectivity, and plant root characteristics can cause different levels of transpiration under similar climactic characteristics (Allen et al. 1998).

Evapotranspiration is the combined effort of evaporation from surface water storage or wetted surface as well as water loss through plant transpiration, although it is nearly impossible to differentiate between the two (Allen et al. 1998). Evapotranspiration typically accounts for roughly 70% of the total precipitation, but can range from 40% of the total precipitation for the northwest and northeast to upwards of 100% in the southwest during times of drought (Hanson 1991). Annual ET rates are typically estimated by conservation of mass. Inflows and outflows from a watershed, as well as consumptive uses within a watershed, are all summed and subtracted from total precipitation. Any difference in these values is attributed to ET. For Villanova's green roof system, ET is calculated in a similar way with precipitation representing total inflows and an outflow measuring device that records any overflow; the difference between these values is taken as ET for the system. For Villanova's weighing lysimeter, which will be discussed further in chapter 3, ET is taken as the negative change in weight since there is no underdrain; this is typically performed on a daily time scale.

2.3.2 Seasonal Trends and Variability

Evapotranspiration rates tend to coincide with the seasonal trends of solar radiation. Higher rates of ET occur during the summer and lower rates in the winter. For green roofs, this seasonal variability can have a significant impact on the water retention performance throughout the year. Several research projects have shown that lower ET rates in the winter months, paired with the seasonally different rainfall patterns can significantly reduce water retention on a storm to storm basis and in some studies down to 0% when test plots were saturated at the time of rainfall due to the lack of storage space from lower ET rates (Graceson et al. 2013; Schroll et al. 2011; Stovin 2010; VanWoert et al. 2005a).

2.3.3 Instrumentation for Measuring Evapotranspiration

There are three main types of instrumentation and equipment used for measuring potential evapotranspiration (PET): atmometers such as the ET Gage®, evaporation pans and tanks, and evapotranspirometers or lysimeters. Each provides a reference ET for a specific application. There are measurement limits and errors associated with each method.

Atmometers are smaller instruments that measure ET by measuring the loss of water from a porous surface such as a ceramic or paper disk (WMO 2008). Water is wicked up from a reservoir within the device to the wetted surface; ET is measured by calculating the loss of water within the reservoir. Different coverings can be used to simulate different types of crops for agricultural uses (WMO 2008). The surface of the disk must remain clean of any dirt or debris as clogged pores can cause significant errors in measurements.

Evaporation pans and tanks are used to measure potential evaporation from free surface water bodies and are used regularly in the agricultural world for determining crop watering regimes.

The three main types of pans and tanks are the United States class A pan, the Russian GGI-3000 pan, and the Russian $20m^2$ tank. Each of these is simply a large circular pan filled with water. Evapotranspiration is measured by taking the difference in water surface within the tank or pan as well as accounting for any precipitation that may increase the level within the pan. The United States class A pan sits above the surface typically on a wooden support 3-5cm above the ground surface, whereas the Russian pan, with its conical bottom, is buried within the ground with the rim 7.5cm above the ground surface. The Russian tank, which is 2m deep, is also buried with the rim 7.5cm above the ground surface.

Many pans and tanks can be instrumented with data loggers and pressure transducers or ultrasonic sensors for a more accurate or continuous record of ET. Errors or differences in measurements across systems can in large part be attributed to the different exposures or treatments of the pan. For example, the Russian pans and tanks are painted and buried within the ground to help minimize the effect of radiation on the side of the pans unlike the US pans which are fully exposed and left in bare metal. Additionally, evaporation from the pans can be very sensitive to coverings. For example, protecting pans from birds and debris using a 25mm hexagonal wire mesh resulted in a roughly 10% drop in ET from pans over the course of a 2 year study (WMO 2008).

Evapotranspirometers or lysimeters are scale representations of a soil cross section with typical vegetation included. The two main types of lysimeters are percolation type or weighing type. Percolation type lysimeters contain all of the media and have a singular outflow opening where any water drained by gravity is measured to close the water balance. This type of lysimeter is typically used for long-term studies rather than short term because of its inherent inability to track current moisture conditions within the soil. Conversely, weighing lysimeters are self-

contained mesocosms in which the entire profile is weighed at any time interval. Changes in weight are attributed to a change in soil moisture condition of the profile. Some weighing lysimeters can be combined systems and are equipped with a percolate collection system in which each component can be independently measured. The weighing lysimeter used on Villanova's green roof is a weighing lysimeter without drainage outlet or percolate collection system. Evapotranspiration rates from the lysimeter are calculated on a daily basis. Wadzuk et al. (2013) determined that ET can be calculated from a water balance as shown in equation 2.1.

$$ET_{lys} = W_0 - W_{24} + P - Q_r \qquad \textbf{(Equation 2.1)}$$

Where W_0 is the weight of the lysimeter at midnight beginning of day, W_{24} is the weight of the lysimeter at midnight end of day, P is weight of precipitation, and Q_r is overflow. Overflow is estimated by taking the summation of weight at the beginning of the day and the weight of precipitation, and subtracting the weight max of the year (weight of the lysimeter when it is completely full of water); if this value is positive it is taken as overflow, if it is negative it is set to zero (no overflow).

2.3.4 Calculating ET

When applying models for predicting ET, meteorological data is typically not recorded at that particular site so it must be assumed that meteorological data from a nearby station will be representative of the actual field conditions. Unfortunately the parameters needed for many physically based evapotranspiration models can have significant variation over space and time. (Beven 1979)

The Penman equation (Penman 1948) and the later revised Penman-Monteith (Monteith 1965) equation is highly dependent on the values used for predicting aerodynamics and canopy resistance more so than on climactic variables (Beven 1979). Because of this, green roof site layout and relation to nearby structures may be very hard to accurately represent when attempting to use these more complex means to estimate reference ET.

Because of the higher need for data and information for the Penman-Monteith equation, paired with the sensitivity described above, many hydrologic models use simplified empirical methods for calculating potential and actual ET (Zhao et al. 2013). The Hargreaves model is an empirical model used to predict potential evapotranspiration and is considered relatively accurate for obtaining estimates for longer time periods (several days) in the agricultural community. While other physical based models require many inputs, the Hargreaves model simply needs daily temperature, which is easily procured, as well as terrestrial radiation, which is calculated from latitude and time of year. (Hargreaves and Samani 1985; Hargreaves and Allen 2003)

2.3.5 Green Roof Modeling

Traditionally, many models for green roof performance have been focused on modeling the flow of water through the media and obtaining runoff volumes on a storm-by-storm basis. Unfortunately, the characteristics of the growing media that make it excellent for water retention, also make it extremely difficult to model. Because of the large grain sizes, there can exist macropores in the media that are useful for storing water, but can severely impact the media's hydraulic conductivity (Liu and Fassman-Beck, 2014). Liu and Fassman-Beck (2014) found the best way to model this was with the use of a dual porosity model in Hydrus. In a continuous simulation model proposed by She and Pang (2009), green roof infiltration was modeled using Green and Ampt. However, due to the lack of a physically-based ET model, the authors used an

exponential decay function based on soil moisture conditions. The model showed about a 10% difference from the observed conditions and the authors conceded the need for a more accurate prediction of ET to better predict the starting moisture condition of the media. Even though evapotranspiration has minimal effect on a catchment's immediate response to rainfall, soil moisture loss between rain events from ET can significantly affect the antecedent moisture condition of a media (Beven 1979) dictating how a catchment may respond in the next event.

Another area of research interest for some has been to attempt to standardize curve numbers for different green roof designs. Fassman-Beck et al. (2015) have analyzed roofs from different climate regions as well as varying green roof designs. While the authors do not endorse the use of the curve number method for green roof planning, their purpose was to have an established set of curve number values that were based off of actual tested and monitored roofs, rather than estimating a curve number from design guides.

CHAPTER 3. METHODOLOGY

This chapter will explore the construction and instrumentation of the green roof at Villanova University. An overview of how measurements are interpreted into performance for both the green roof and a weighing lysimeter will be discussed. Lastly, a background of how the system was modeled will be provided before the results of these comparisons and model are discussed in chapter 4.

3.1 General Green Roof Background

This section will discuss the design of Villanova's green roof test site, as well as the basic meteorological instrumentation and data logging equipment.

3.1.1 Green Roof Design

Villanova University is located approximately 11 miles northwest of Philadelphia, Pennsylvania in Radnor Township. Villanova's green roof site was constructed atop the Center for Engineering Education and Research (CEER) building in the summer of 2006. It is situated on a smaller portion of the roof, approximately 54 m^2 (580ft^2), overtop one of the universities many coffee shops, "Holy Grounds", and serves as an aesthetic piece for faculty and students as they make their way up the main staircase to the third floor. Figure 3.1 shows the roof prior to construction and Figure 3.2 shows the roof just after it was completed in 2006.

Figure 3.1: Site of Green Roof Prior to Installation June 1, 2006 (VUSP)

Figure 3.2: Green Roof Site Just After Completion (VUSP)

The roof is classified as an extensive green roof with a growing media thickness of around 10cm (4in). The roof is comprised of an area approximately 43m^2 (467ft^2) of Rooflite MC Extensive media which is manufactured by Skyland USA, LLC. The media is lightweight weighing in between 0.70 and 0.85g/cm^3 (44-53lb/ft^3) and has a very high water-holding capacity of approximately 35-65% of its total volume. Specs for Rooflite MC Media can be found in Appendix A. The media sits above a drainage layer consisting of Optigreen 25mm waffled plastic sheets, commonly referred to as “cups” or “egg cartons”. The high void space of the drainage layer allows for any stormwater that is unable to be retained to quickly make its way to the roof drain and the cups allow for the additional collection of approximately 5mm (0.2in) of stormwater (Breuning, personal correspondence 2014) Specifications for the drainage board can be found in Appendix A. The media is separated from the drainage board by a layer of nonwoven 200g/m^2 Optigreen filter fabric that serves to prevent media and fines from clogging the drainage board, while still allowing roots from vegetation to pass through and utilize the additional water being stored within the drainage layer (Figure 3.3).

Figure 3.3: Optigreen Filter Fabric Overlaying Expanded Plastic Drainage Board (VUSP)

The media was originally planted with a diverse list of 12 sedum species as well as five additional perennial species at approximately three plugs per square foot. An original planting plan can be found in (Appendix A). However, the roof was replanted following severe droughts in 2010 and since then, sedums have become the predominant species on the roof.

Surrounding the vegetated portion of the roof is a river rock perimeter ranging between 15 and 20cm (6-8in) wide and 10cm (4in) thick. This rock perimeter serves as a buffer to prevent any damage to nearby structures from plant intrusion, as well as to convey any surface runoff as quickly as possible to the drain to prevent surface ponding and inundation. This rock perimeter is approximately 5.5m^2 (59ft^2) and accounts for approximately 10% of the green roof system. Installation of the rock perimeter can be seen in Figure 3.4.

Figure 3.4: Installation of the Rock Perimeter Adjacent to Existing Wall. (VUSP)

Also contributing to the total area of the system is an area of aluminum flashing covering the parapet walls surrounding the green roof. This area, while common to most systems, consists of approximately 10% of the total system area (5m^2 or 56ft^2). The flashing perimeter drains directly to the protective rock perimeter and this additional runoff is handled by the singular 8cm (3in) drain in the southern corner of the roof responsible for removing any excess stormwater from the entire system.

3.1.2 Meteorological Instrumentation

The green roof site has served as a research site for the Villanova Urban Stormwater Partnership (VUSP) since it was first instrumented in 2008. Since evapotranspiration (ET), as well as green roof performance, is highly dependent on weather conditions, a full meteorological station has been installed on the roof for monitoring. All meteorological parameters are recorded in 5 minute

time increments by a Campbell Scientific CR1000 data logger located in the southern corner of the roof (Figure 3.5).

Figure 3.5: Location of Campbell Scientific Data Logger and Met-One Anemometer (VUSP)

Any rainfall on the system is measured using an 8 inch tipping bucket rain gauge situated in the center of the roof. The center of the roof was chosen because it was believed to provide the most accurate representation of rainfall on the system given the proximity of the nearby walls of the building (Figure 3.6).

Figure 3.6: Site of Rain Gauge, Temperature, Relative Humidity, and Solar Radiation Instrumentation. (VUSP)

Prior to March 2014, an American Sigma Model 2149 tipping rain gauge was used similar to most of the other SCM sites around campus. In March of 2014, a Met-One Model 375 heated tipping bucket rain gauge was installed to facilitate the measurement of the liquid equivalent of snowfall and sleet during the winter months. Both rain gauges had a similar resolution of 0.01 in per tip and similar accuracies of 1% for rainfall between 1 and 3in/hr. Because the location of the green roof does not permit for the recommended spacing from nearby structures (nearby

obstructions should be at least twice the distance away from the rain gauge as they are high) (Met-One Manual, 1994), an additional American Sigma 2149 rain gauge is situated on the rooftop of CEER approximately 45m (150ft) away from the primary rain gauge. This additional rain gauge serves as a check for precipitation data, as well as a reliable backup should the primary rain gauge fail to record properly.

Additional weather parameters measured include temperature and relative humidity, wind speed, and incoming solar radiation. Temperature and relative humidity are measured using a Vaisala HMP 60 probe inside of a RM Young 6 plate radiation shield to minimize any artificial data resulting from solar radiation. Incoming solar radiation is measured using a LI-COR LI200X silicon pyranometer and wind speed is measured using a Met-One model 014A anemometer. Locations for all meteorological instrumentation can be found in Figure 3.7.

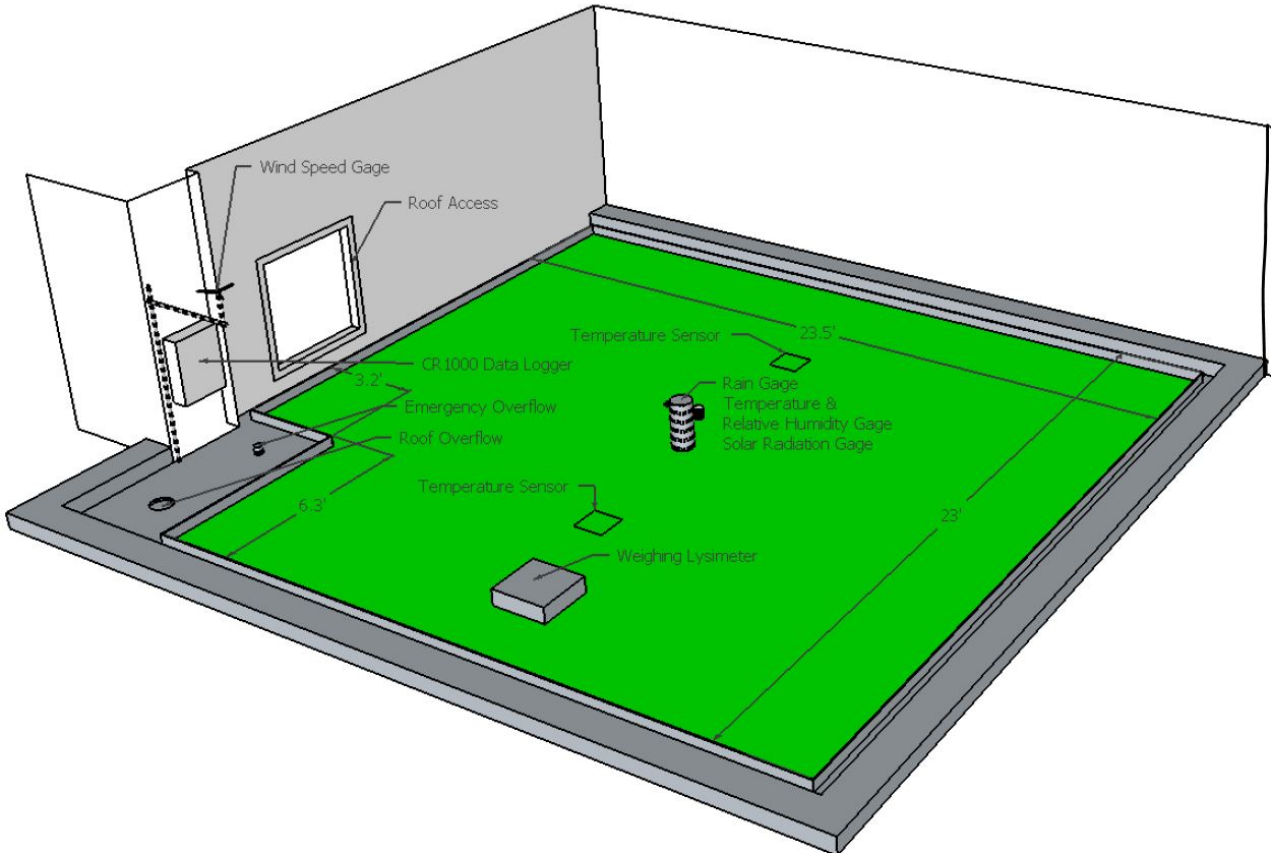

Figure 3.7: Schematic of Green Roof and Instrumentation (Feller, 2010)

3.2 Green Roof vs Lysimeter Performance

3.2.1 Performance Instrumentation

In order to measure the total retention and the ET performance of the green roof system, two key instrumentation setups are needed. For measuring total retention for the green roof, equipment hooked up to the gutter system measures total volume and flow rate that drains from the system. For measuring ET directly, a weighing lysimeter is used as a means to close the mass balance.

3.2.1.1 Weighing Lysimeter

On the roof (Figure 3.7) sits a 45.7cm × 45.7cm × 10cm (18in ×18in × 4in) weighing lysimeter. The lysimeter is filled with the same Rooflite MC extensive growing media described in Section

3.1.1 and is planted with various sedums representative of the entire green roof's plantings. The lysimeter sits atop three Sentran model PF3-B-100-020 compression load cells each with a capacity of 45kg (100lbs) (Appendix B). Weights of the lysimeter are taken every 5 minutes and are recorded by the CR1000 data logger. The weighing lysimeter, unlike the actual green roof, does not have the Optigreen drainage board used in the rest of the green roof and does not have an underdrain. Due to the lack of an underdrain, overflow will not be achieved until the 10cm cross section of media has reached full saturation and surface runoff is forced to spill over the side of the lysimeter.

Annual calibration of the load cells is performed to ensure that the instrumentation is still measuring within acceptable limits. To perform a calibration, three different weight amounts (typically 5, 10, and 15lb) are placed on the lysimeter for 30 minutes each. Load cell readings are compared prior to and after the procedure to ensure the readings return to their initial value as well compared to the amount of weight added to the lysimeter. Three different weights are used to establish whether any error is a linear relationship or not. Results from the 2013 calibration can be seen in Table 3.1. The lysimeter showed an accurate response to the weight added with the highest % error coming in at 2.1% and most being less than 1%. The lysimeter returned almost to its previous weight only losing 0.1lbs. over the course of the 3.5 hour calibration timeframe. This could be possibly attributed to some ET from the system since the average air temperature for that day was 24 degrees Celsius.

Table 3.1: Results from 2013 Calibration.

	Weight	Vs. pre	% error	Vs. post	% error
Pre Weight	73.5			0.1	
Added 7 lb.	80.3	6.9	2.1	7.0	0.6
Added 10 lb.	83.5	10.0	0.4	10.1	0.6
Added 17 lb.	90.5	17.0	0.3	17.1	0.4
Post Weight	73.4	-0.1			

3.2.1.2 Overflow Instrumentation

In 2011, instrumentation to measure overflow from the green roof was first installed ($Q_{r,roof}$). This setup originally included an Omega FP8501A flow meter as well as a 12in Thelmar weir with a Senix ToughSonic ultrasonic distance sensor for verification. It was found that the minimum flow rate for the paddle wheel sensor was 2.52×10^{-5} M^3/s (0.4gpm), which exceeded the typical low flow rates. Because of this, a modified 12 in High Sierra Model 2400 tipping bucket rain gauge (Appendix B) was installed to act as a metering gauge for measuring flows from 0 to $3.15X10^{-6}$ M^3/s (0.0gpm to 0.05gpm). Flows exceeding $3.15X10^{-6}$ M^3/s (0.05gpm) are measured using the existing Thelmar weir (Appendix B) and ultrasonic distance sensor setup. A view of the overflow instrumentation can be seen in Figure 3.8.

Figure 3.8: Metering Tipping Bucket (Left) and Thelmar weir (Right) Used for Overflow Measurements. (VUSP)

Calibration and maintenance of the overflow instrumentation includes verifying monthly that the tipping bucket mechanism is both level and free of any debris or obstruction that may hinder readings. Calibration and maintenance of the weir is performed by visually inspecting the system for any leaks or damage, and adding water behind the weir until it is crested. Once the weir has been crested, readings from the ultrasonic sensor are taken and compared to the established datum. An alternative method for verification is to compare flow rates of both the tipping bucket and the weir when flows are around the crossover point of $3.15X10^{-6}$ M^3/s (0.05gpm). As of the most recent calibration in 2014, the original datum of 9.09cm (3.58in) was still acceptable.

3.2.2 Comparison Methodology

One of the primary objectives of this research was to verify whether the weighing lysimeter's ET data was indicative of the actual performance of the green roof. To go about this, the data from each system was compared both on a long-term growing season (April through November) time scale, as well as on a smaller event based or daily based time scale.

3.2.2.1 Water Budget Calculations

Evapotranspiration rates from the lysimeter are calculated on a daily basis. Wadzuk et al. (2013) determined that ET can be calculated from a water balance as shown in Equation 3.1:

$$\boldsymbol{ET_{Lys} = W_0 - W_{24} + P - Q_{rlys}} \quad \textbf{(Equation 3.1)}$$

where W_0 is the weight of the lysimeter at midnight beginning of day, W_{24} is the weight of the lysimeter at midnight end of day, P is weight of precipitation (calculated from rain gauge data), and Q_{rlys} is overflow. Overflow is estimated by Equation 3.2:

$$\boldsymbol{Q_{rlys} = W_0 + P - W_{max,year}} \quad \textbf{(Equation 3.2)}$$

where $W_{max,year}$ is the maximum weight of the lysimeter (weight of the lysimeter when it is completely saturated). If the $Q_{r,lys}$ value is positive it is taken as overflow, if it is negative it is set to zero (no overflow). Changes in weights are then converted into equivalent depths of water in millimeters using the unit weight of water.

The storm events from the entire green roof are categorized by a dry time of at least 6 hours between rainfalls and precipitation totaling 1.25mm (0.05in) or more. Because of this it is possible to have multiple rain events in one day; however this has so far been an unlikely occurrence with only 14 such events being recorded over the course of the 2012 through 2014. Because of the long drainage time associated with green roofs, new rain events can start before

the roof has had a chance to completely finish draining from the previous event and therefore events need to be classified as to whether or not they had a chance to completely drain. For events in which overflow was not complete, analysis needs to be done to determine whether the events need to be combined into one event. For the purpose of the water budgets used in this thesis, data was analyzed on a monthly and yearly basis so the need to decipher when events started and ended and which events should be combined is not needed. However, for plotting storm event size vs overflow, storms where overflow was not complete before the next rainfall were not used for analysis.

Long-term comparisons of the two systems are made by closing the water balance for the growing season. For the lysimeter, daily time step values of precipitation, measured ET (ET_{lys}) as well as calculated overflow (Q_{rlys}) are summed over the course of the growing season. For the entire green roof's performance, cumulative precipitation is compared with the cumulative overflow ($Q_{r,roof}$) for the season and ET_{roof} is estimated as the difference between the two. Since infiltration on a green roof is impossible, the rainfall loading on the green roof is 1:1, and the storage volume of the green roof can be considered negligible for long-term comparisons, ET is the only other component of the typical water budget. Evapotranspiration for the lysimeter and the roof can be calculated as:

$$\boldsymbol{ET_{annual} = P_{annual} - Q_{r,annual}} \qquad \textbf{(Equation 3.3)}$$

Where P_{annual} is equal to cumulative precipitation over the study period and $Q_{r,annual}$ is the cumulative overflow for the same time period. For measurements for the entire green roof, volume is measured directly in gallons and then converted to an equivalent depth over the entire green roof including rock perimeter and flashing. System comparisons were performed on a

monthly and annual (growing season) basis due to the lack of a way to directly measure ET on a shorter time scale. Due to the different scales of the systems, systems were compared on a basis of equivalent depths. Any percentages for either overflow or ET are taken as the percent of total precipitation for the study period because there is some storage within the media

3.3 Green Roof System Modeling

This section will discuss the setup of the model used for predicting ET within green roofs. Because of the inherent sensitivity of and the large amounts of input parameters required for the Penman-Monteith and FAO56 discussed in Chapter 2, the Hargreaves method was chosen as the basis of the ET model for predicting reference ET. An analysis was performed over the 6 years of data available to determine the validity of using the simpler Hargreaves equation for reference evapotranspiration over the data intensive FAO56. Results for this analysis will be discussed in Section 4.3.

3.3.1 Hargreaves Equation

For estimating reference evapotranspiration (ET_0), the Hargreaves model as summarized by Hargreaves et al. (2003), is typically used for agriculture. It is used here because it only needs easily obtainable maximum and minimum daily temperature data and the calendar day as inputs. For this, ET_0 (in mm) can be calculated using Equation 3.4:

$$\boldsymbol{ET_0 = 0.0023 \times (T_{max} - T_{min})^{0.5} \times (T_{max} + 17.8) \times T_r} \qquad \textbf{(Equation 3.4)}$$

where T_{max} is the maximum daily temperature in ^{o}C, T_{min} is the minimum daily temperature in ^{o}C, and T_r is terrestrial radiation on any given Julian day (mm/D). (Hargreaves and Samani, 1985).

T_r (or R_a) can be calculated using the following equation from Allen et al. (1998, equation 21):

$$\boldsymbol{R_a = \frac{24(60)}{\pi} G_{sc} d_r [\omega_s \, sin(\varphi) \, sin(\delta) + cos(\varphi) \, cos(\delta) \, sin(\omega_s)]} \qquad \textbf{\textit{(Equation 3.5)}}$$

where Ra is terrestrial radiation in MJ m^{-2} day^{-1}, d_r is the inverse relative distance Earth-Sun, φ is the site latitude in radians, G_{sc} is a solar constant taken as 0.0820 MJ m^{-2} min^{-1}, ω_s is the sunset hour angle in radians, and δ is the solar decimation in radians.

d_r and δ can be calculated using the following relationships (Allen et al 1998, equations 23 &24):

$$\boldsymbol{dr = 1 + 0.033 cos\left(\frac{2\pi}{365} J\right)} \qquad \textbf{(Equation 3.6)}$$

$$\boldsymbol{\delta = 0.409 sin\left(\frac{2\pi}{365} J - 1.39\right)} \qquad \textbf{(Equation 3.7)}$$

where J is the number of the Julian day in the year (i.e. January 1st being number 1 and December 31st being either 365 or 366).

The sunset hour angle can be found using equation 3.8 (Allen et al 1998, equation 25):

$$\boldsymbol{\omega_s = arccos[-tan(\varphi) tan(\delta)]} \qquad \textbf{(Equation 3.8)}$$

For converting R_a from MJ m-2 day-1 to mm day-1 required for the Hargreaves equation, R_a is multiplied by the conversion factor of 0.408, which is the inverse of the latent heat of vaporization. (Allen et al. 1998)

3.3.2 Soil Moisture Extraction Functions

One of the key issues using predictive ET equations, such as the Hargreaves equation, is they are assumed to predict accurately when there is a sufficient amount of freely available water. Because of this, the model discussed within this thesis employs a reduction factor for the amount of reference ET (ET_o) multiplied by the limiting soil moisture extraction function (SMEF) to obtain the actual ET (ET_a):

$$\boldsymbol{ET_a = ET_0 \times (SMEF)} \qquad \textbf{(Equation 3.9)}$$

The soil moisture extraction functions discussed below and analyzed for this proposed model are all based off of a simple relationship of the available soil moisture relative to the maximum available soil moisture. This relationship of soil moisture (RAT) can be most simply represented by equation 3.10:

$$\boldsymbol{RAT = \left(\frac{SMT}{SMC}\right)} \qquad \textbf{(Equation 3.10)}$$

where SMT is actual soil moisture (represented here by available water) and SMC is the field capacity of the soil (taken here as the maximum storage capacity).

Five relationships summarized by Zhao et al. (2013) were applied to the green roof data with the Hargreaves Equation to determine the best fit. Each relationship provides a different reduction factor depending on the available soil moisture. The five equations analyzed are (equations 3.11-3.15):

$$\boldsymbol{ET_a = ET_o \times (RAT^2/(RAT^2 + (1 - RAT)^2))} \qquad \textbf{(Equation 3.11)}$$

$$\boldsymbol{ET_a = ET_o \times 2RAT^2 \left[\frac{1}{1+RAT^{RAT}}\right]} \qquad \textbf{(Equation 3.12)}$$

$$ET_a = ET_o \times 2RAT\left[\frac{1}{1+RAT^{RAT}}\right] \quad \textbf{(Equation 3.13)}$$

$$ET_a = ET_o \times RAT^2 \quad \textbf{(Equation 3.14)}$$

$$ET_a = ET_o \times RAT \quad \textbf{(Equation 3.15)}$$

Figure 3.9 shows the relationship of the ratio of soil moisture to the reduction factor of each equation. Some of the functions put a higher importance on lower available water scenarios and a lower importance on more saturated conditions, such as equation 3.13. Equations 3.11 and 3.13 allow for higher ET rates under more saturated conditions and equation 3.15 has a linear (1:1) relationship across all moisture conditions. Equation 3.12 is nearly linear however it further reduces actual ET when soil moisture conditions are approximately 75% or less of the maximum soil moisture. Equation 3.14 reduces actual evapotranspiration the most across all ranges of soil moisture. This could be representative of a clayey soil where it may be particularly difficult to pull the water out of the system. The relationship that works best for each model should be chosen based on the soil water characteristic curve as well as the leaf area index of the study area (Zhao et al, 2013). For the purpose of this study, Equation 3.13 was limited to peak at 1, meaning actual evapotranspiration can equal reference evapotranspiration even if the soil moisture is slightly below maximum however, actual evapotranspiration can never exceed reference evapotranspiration.

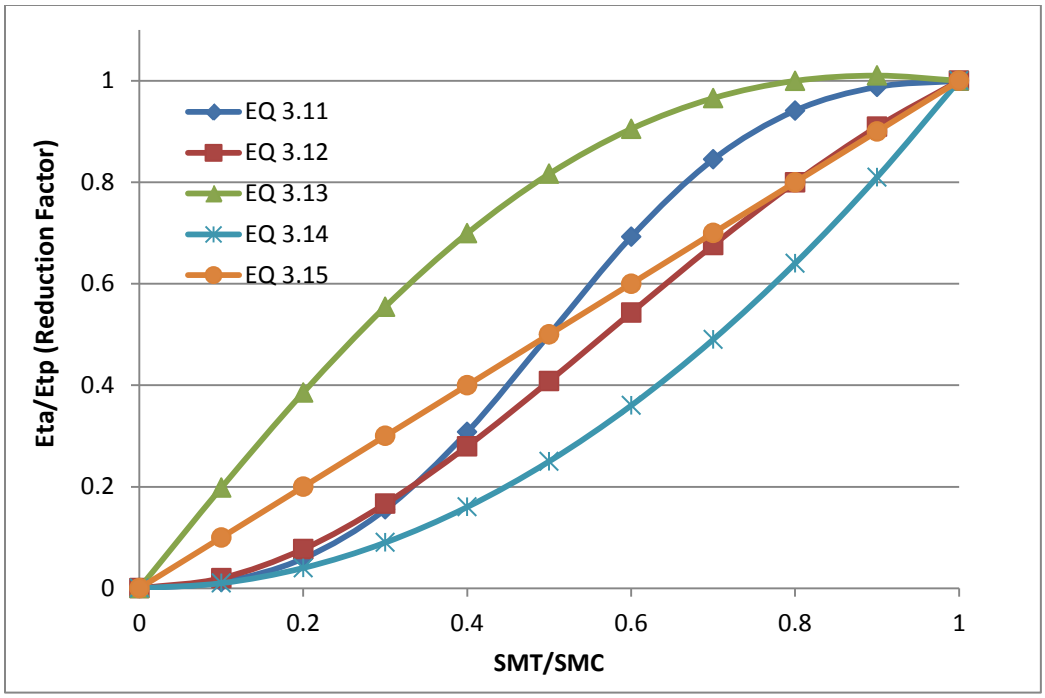

Figure 3.9: Plot of the Soil Moisture Extraction Functions above (Reproduced from Zhao et al. 2013)

3.3.3 Simple Accounting System

The proposed model uses a simple conservation of mass budget to account for inflows (precipitation) and outflows (overflow and ET). All inflows and outflows are added or calculated on a daily basis and influence the following day's available water for ET. Total storage of the green roof is estimated by taking the thickness of the green roof media and the drainage board and multiplying it by the field capacity of the media or by the void space of the drainage board. Because of the timescale used, the media is assumed to never be at complete saturation (either it has drained to field capacity or it has not reached field capacity) so anything above the field capacity is assumed to be overflow. In the case of the weighing lysimeter, since there is no underdrain and therefore no free drainage by gravity, total storage volume was taken as the volume of the media at complete saturation.

The proposed model starts on January 1st (day 1) assuming the roof has full storage potential (media completely dry). The time until the roof reaches full saturation is considered the warm up time for the model. Because the measured data available from Villanova's green roof is only considered from April through November (to eliminate snowfall events) the model completes the warm up time prior to the start of analysis (April 1st). Winter months are not considered in the model because prior to 2014, the weather station on the green roof did not include a heated rain gauge so liquid equivalents of water from snow was unknown.

Available storage is calculated on a daily time step. It is taken as the previous day's (n-1) storage volume minus day before (n-1) precipitation plus day before (n-1) ET or overflow. Overflow is taken as any event where rainfall exceeds available storage. Available water is assumed to be the maximum storage capacity less the available storage. Once available water is calculated, it (along with maximum available water) is used to calculate the soil moisture extraction function and obtain a reduction factor for ET. This reduction factor is then multiplied by the daily reference ET to obtain the daily total of evapotranspiration from the system.

The available storage of any day can be summarized by equation 3.16:

$$\boldsymbol{S_A = S_{n-1} - P + ET_{n-1} + Q_{rn-1}} \qquad \textbf{(Equation 3.16)}$$

where S_A is available storage, S_{n-1} is previous day's storage, P is precipitation, ET_{n-1} is ET from the previous day, and Q_{rn-1} is overflow from the previous day.

CHAPTER 4. RESULTS AND DISCUSSION

This chapter is divided into two distinct portions. The first portion will summarize the performance of the weighing lysimeter for 2009 through 2014, present the performance of the entire green roof system for 2013 and 2014, and provide an analysis of the differences between the two systems. The second portion of this chapter will discuss the results of the model proposed for predicting green roof evapotranspiration and overflow, as well as its potential applicability to other models and green roofs.

4.1 System Comparison

This section will discuss the overall performance of the green roof weighing lysimeter from 2009 through 2014 and compare it to the results obtained from monitoring and measuring the overflow from the entire green roof for 2012 through 2014. The annual performance will be compared to the annual rainfall patterns for the study period. Lastly, a comparison between the freely drained green roof and the lysimeter will be analyzed based on the key design differences between the two systems.

4.1.1 Weighing Lysimeter Performance

Since its installation in 2008, the weighing lysimeter has been monitoring parameters every 5 minutes to yield ET on a daily basis, as described in Section 3.2.2.1. The results from 2009 to 2011 were summarized by Wadzuk et al. (2013) and performance from 2012 through 2014 have since been analyzed; all 6 years are presented here (Table 4.1), which is notable as most green roof ET studies range from a few weeks to one or two years (Fassman-Beck et al. 2013). Total measured ET for the annual study period (April through November) ranged anywhere between 65% and 90% of the rainfall in that period with an average of 78% (±6%) of the rainfall. Further,

the historical observed annual ET volume of 600mm (Church et al. 1995) is 71% of the annual historical rainfall, which is less than the 8-month average observed ET from the green roof lysimeter. Any difference between the sum of annual overflow and ET and total annual rainfall is assumed to be the change in storage from April 1st to the end of the study period November 30th. This change in storage can also represent the change in moisture condition within the lysimeter. The amount of ET each year is remarkably consistent with the average annual ET around 750mm (±110mm) for the weighing lysimeter. The average 8-month ET is greater than the observed annual historical ET (600mm) by 25%. The observed lysimeter ET is greater than the historical ET most likely for several reasons, but primarily because of the design of the lysimeter that enhances water storage to make water available for ET that may not naturally occur over a watershed.

Table 4.1: Annual Performance of ET and Overflow from the weighing Lysimeter

	Hist.	**2009**	**2010**	**2011**	**2012**	**2013**	**2014**	**Avg.**	**Std. Dev.**
Rainfall (mm)	845[1]	1152	819	1345	894	901	848	984	197
Overflow (mm)		336	144	356	203	232	180	239	89
Evapotranspiration (mm)	600 [2]	784	718	990	690	680	675	751	110
Evapotranspiration (%)		68	88	74	77	75	80	78	6

* Analysis for 2014 was cut off at November 25th due to an early snowfall on the 26th.
[1] NOAA historical Weather Data for Philadelphia
[2] Church et al. (1995)

While the historical rainfall for the region is around 845mm (NOAA) and the average rainfall for the study period was 984mm, yearly comparisons may not necessarily provide a strong basis for comparison. When trying to discuss overall performance for green roof systems, given their dynamic nature, trying to normalize their performance into a “typical year” may not be

appropriate. For example, 2014 which had 848mm of rainfall was a drought year for the system because the summer months experienced less total rainfall as compared to 2012 which had a fairly consistent rainfall across the study period. In 2011, which had rainfall exceeding the historical average by over 300mm, there were droughts in June and July where the system was in a stressed phase.

Monthly ET and overflow volumes were also calculated and analyzed (Table 4.2). Again, any discrepancies in the monthly mass balance are attributed to a change in storage or moisture condition from the start to the end of the month. Because ET is a slow process, rainfall towards the end of one month can lead to increased storage within the system and therefore allow more water to be available for ET in the following months. For example, August 2013 had a total rainfall of 145mm (5.7in) yet only had 104mm (4.1in) of ET (Table 4.2). In the following month, September 2013, there was a cumulative rainfall of 52mm (2in) yet there was 74mm (2.9in) of measured ET. Therefore the average rate of ET of 3mm/d for the first 10 days of September had to be dictated by the moisture condition of the media which was related to the rainfall in August, particularly the 32mm (1.27in) rainfall on August 28th.

It is interesting to note that the majority of overflow resulted from months where precipitation was greater than 100mm or in typically cooler months (October and November). This observation confirms that ET is highly dependent on available water within the system, as well as the energy needed to vaporize water for evaporation. In months with rainfall exceeding 100mm, there was not sufficient storage within the lysimeter to retain all of the rainfall leading to overflow. Once the rainfall is lost to overflow, it is gone and cannot be evapotranspirated from the system at a later time even though there may be enough energy. Further, during these rainy months, rain events were more frequent so there may not have been not sufficient time between

events to fully recover storage capacity from saturated conditions (i.e., there was not enough time to dry out the media). During the cooler months (e.g. late September, October, and November) a similar trend can be seen. Although there was typically less rainfall in November, compared to May through September across the 6 years studied, there was significant overflow in 2012, 2013, and 2014. This is because although monthly rainfall was relatively less than warmer, higher rainfall months, there was less energy available for ET. Therefore, it took longer to regain storage space within the system between storms, which led to smaller rain events producing overflow.

As a way to highlight and analyze how the performance of the system is changing over the course of the entire study period, Figure 4.1 through Figure 4.6 were created to show daily as well as cumulative performance data for the weighing lysimeter for 2009 through 2014. Monthly plots were also created for comparing performance on a monthly time scale and can be found in Appendix C. On the plots, daily values of ET and overflow are represented by bar graphs in green and red, respectively, and daily rainfall totals are represented by blue dots with values on the left axis. Cumulative curves for rainfall are shaded in light blue and cumulative measured ET is represented by light green. In some instances where the cumulative ET exceeds cumulative rainfall (especially in the beginning of analysis period) this is attributed to the moisture condition before the analysis starts on April 1st.

Table 4.2: Lysimeter Monthly Rainfall, ET and Overflow for 2009 through 2014

	2009			2010			2011		
Month	Rain (mm)	ET (mm)	Overflow (mm)	Rain (mm)	ET (mm)	Overflow (mm)	Rain (mm)	ET (mm)	Overflow (mm)
April	116	112	13	71	98	0	135	140	31
May	147	101	43	113	132	8	94	113	0
June	120	110	8	103	107	0	45	53	0
July	143	114	0	164	131	30	81	73	0
August	268	124	144	41	46	0	421	188	192
September	131	91	39	108	29	12	263	187	88
October	171	79	88	163	120	94	209	157	45
November	55	53	1	56	55	0	97	79	0
	2012			**2013**			**2014***		
Month	Rain (mm)	ET (mm)	Overflow (mm)	Rain (mm)	ET (mm)	Overflow (mm)	Rain (mm)	ET (mm)	Overflow (mm)
April	89	58	0	76	107	0	214	93	123
May	144	125	38	91	105	0	136	109	37
June	47	82	0	261	92	130	72	126	0
July	117	111	0	102	113	8	111	102	0
August	169	130	38	145	104	53	100	94	0
September	119	95	27	52	74	0	95	55	0
October	165	56	77	84	56	8	90	53	0
November	48	35	23	89	28	31	87	44	20

* Analysis for November 2014 was cut off at November 25th due to an early snowfall on the 26th.

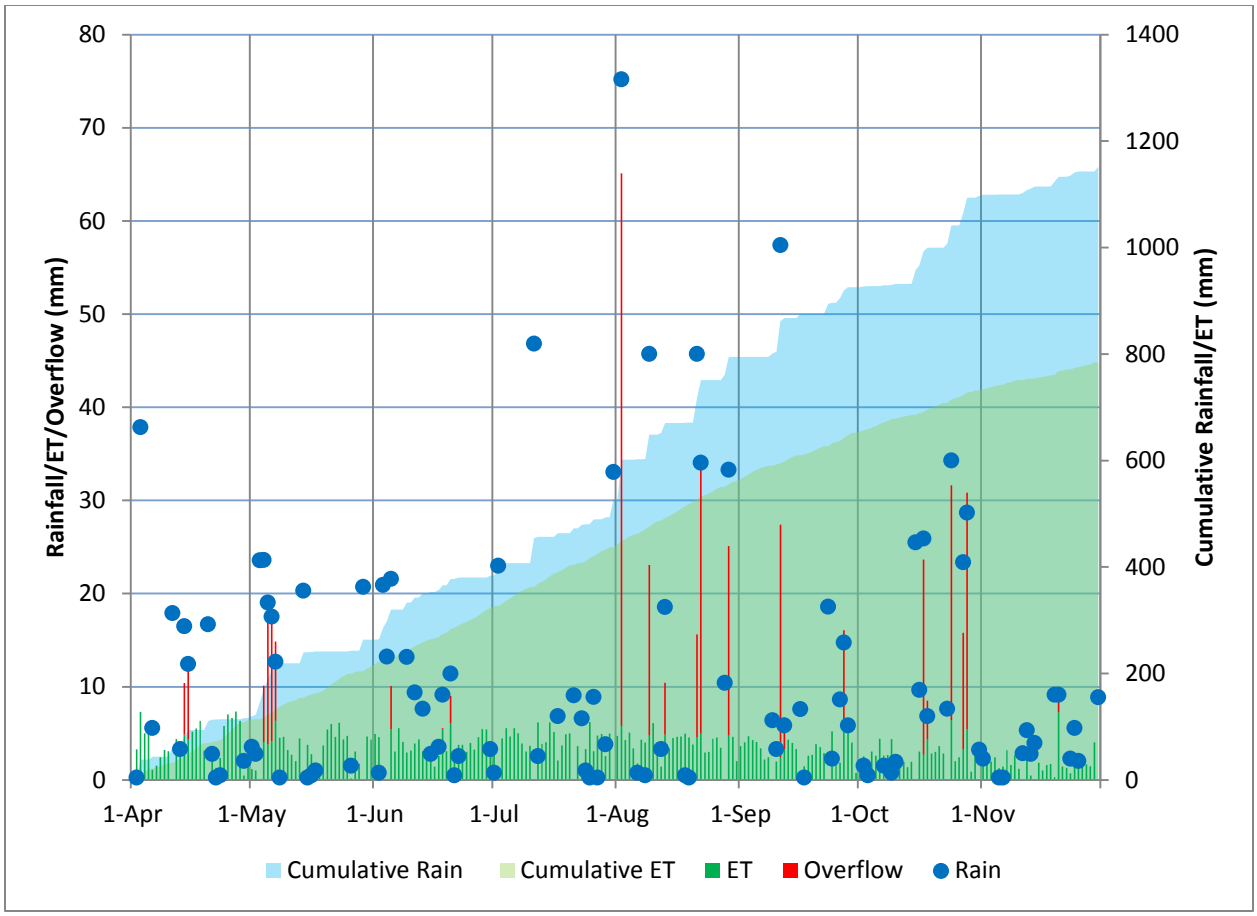

Figure 4.1: Cumulative Performance of Lysimeter for 2009. Daily values of ET and overflow are represented by bar graphs in green and red, respectively, and daily rainfall totals are represented by blue dots with values on the left axis. Cumulative curves for rainfall are shaded in light blue and cumulative measured ET is represented by light green.

In 2009, which was a wetter and cooler year, there was a cumulative rainfall of 1152mm (45.35in) and a total cumulative ET of 784mm (30.9in) (Figure 4.1). The rate of increase of ET remains fairly constant from May until September at around 4mm/d, after which the ET rate continues to increase, just at a slower rate of 2.5mm/d. It is also interesting to note how the difference between cumulative ET and cumulative rainfall increases whenever there was an event producing overflow (e.g. August 2nd 2009). These same phenomenas can be seen throughout all 6 years of available data.

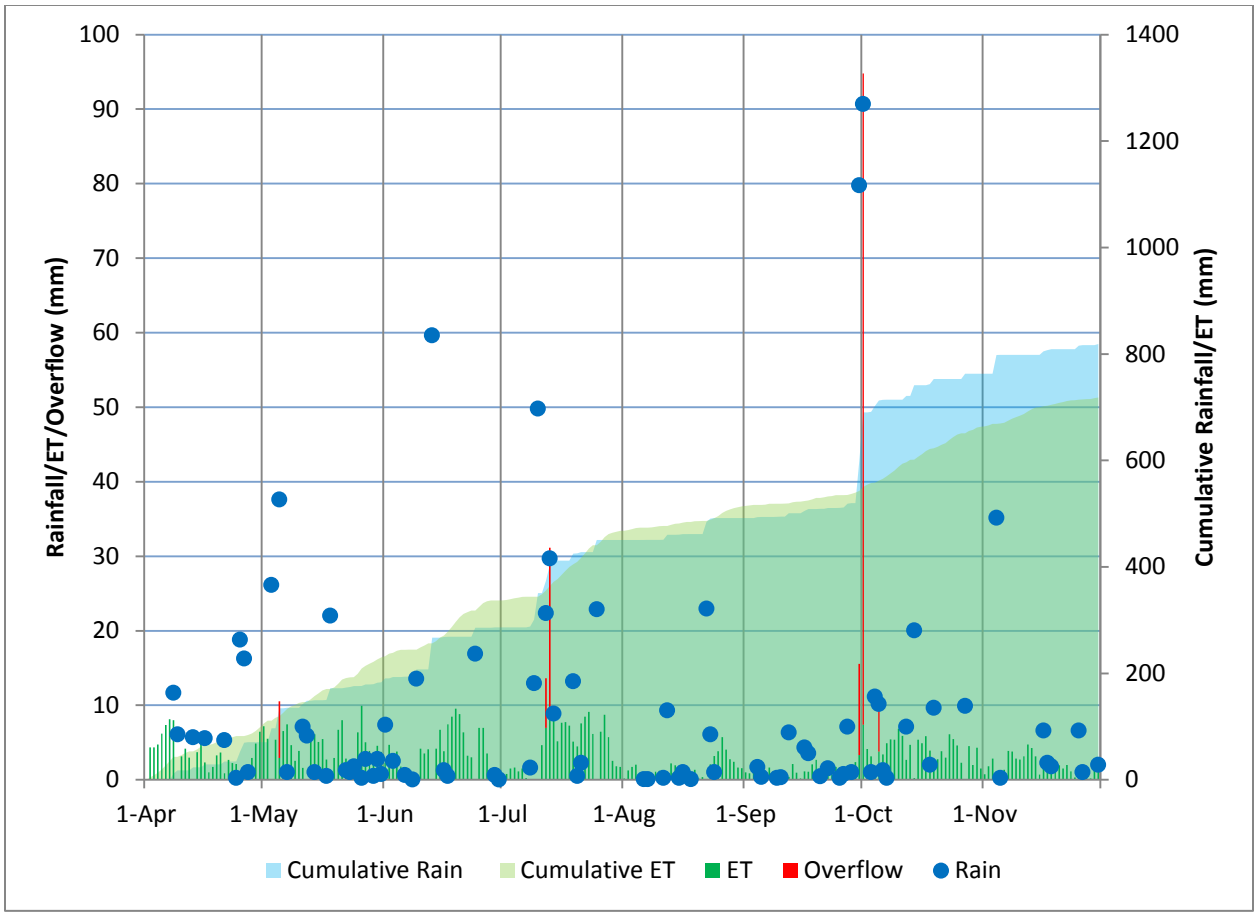

Figure 4.2: Cumulative Performance of Lysimeter for 2010. Daily values of ET and overflow are represented by bar graphs in green and red, respectively, and daily rainfall totals are represented by blue dots with values on the left axis. Cumulative curves for rainfall are shaded in light blue and cumulative measured ET is represented by light green.

2010 experienced droughts in August and September. This can be seen by the shallow slope of the cumulative ET in Figure 4.2. Starting in mid July the slope decreases to about 1mm/d as compared to the previous months which were closer to 4mm/d. On October 1st however, significant rainfall was able to replenish the soil moisture within the system; there was a huge spike in net rainfall as well as overflow. From this point on the slope of cumulative ET increased to 4mm/d and remained fairly constant until the cooler weather came in mid November where teas dropped down to 2mm/d.

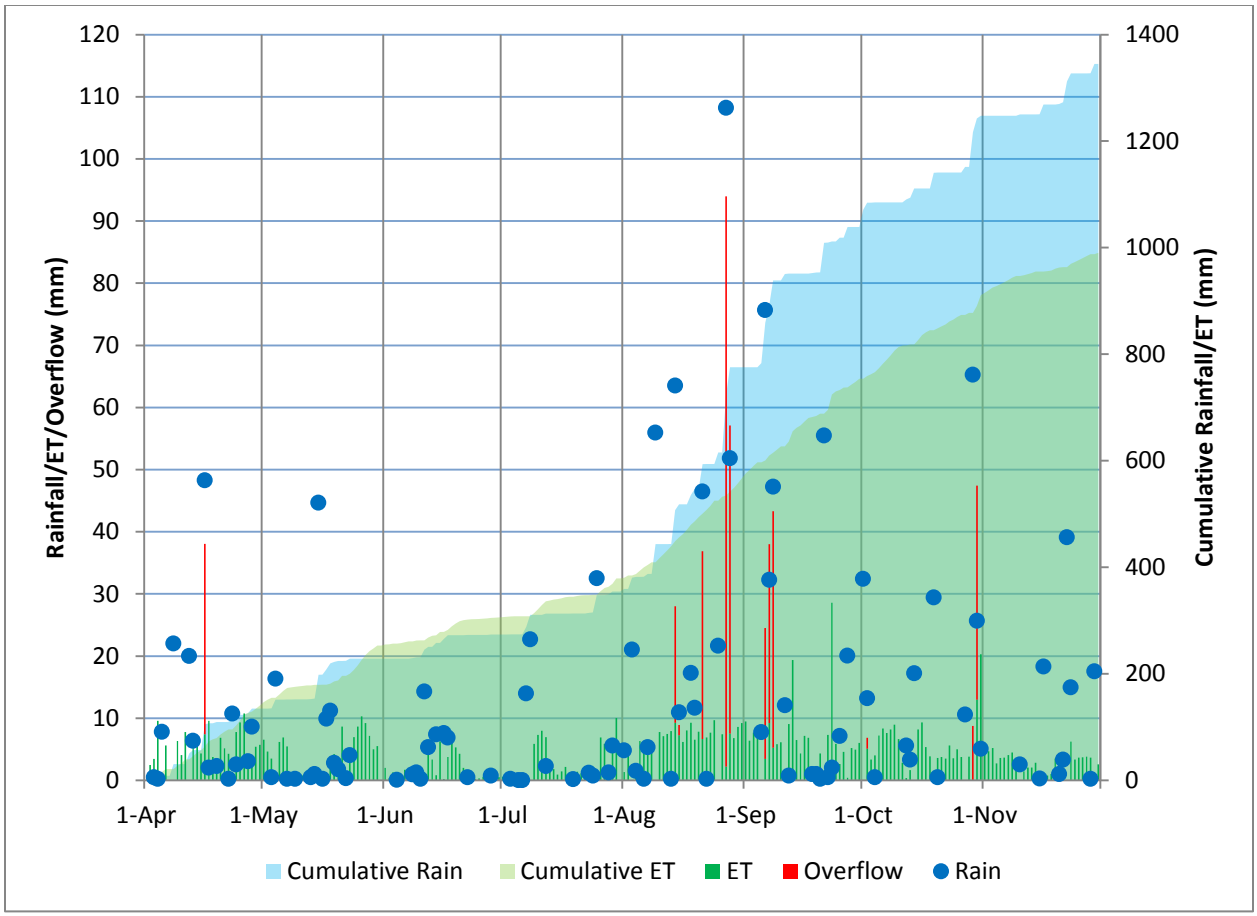

Figure 4.3: Cumulative Performance of Lysimeter for 2011. Daily values of ET and overflow are represented by bar graphs in green and red, respectively, and daily rainfall totals are represented by blue dots with values on the left axis. Cumulative curves for rainfall are shaded in light blue and cumulative measured ET is represented by light green.

2011 had a few large rain events in April and May that allowed the ET rate to remain fairly constant (Figure 4.3) until droughts in June and July caused the rate of ET to decrease and level off from 4mm/d to 2mm/d. In late July and early August, ET rates increased to average 6mm/d as several small storms helped to increase the available water. On August 27th, Hurricane Irene passed through the area and produced almost 190mm (7.5in) of rainfall. This can be seen by the spike in overflow and cumulative rainfall. Overall, 2011 had the highest average daily ET at 4mm/d as compared to 3mm/d for all other years.

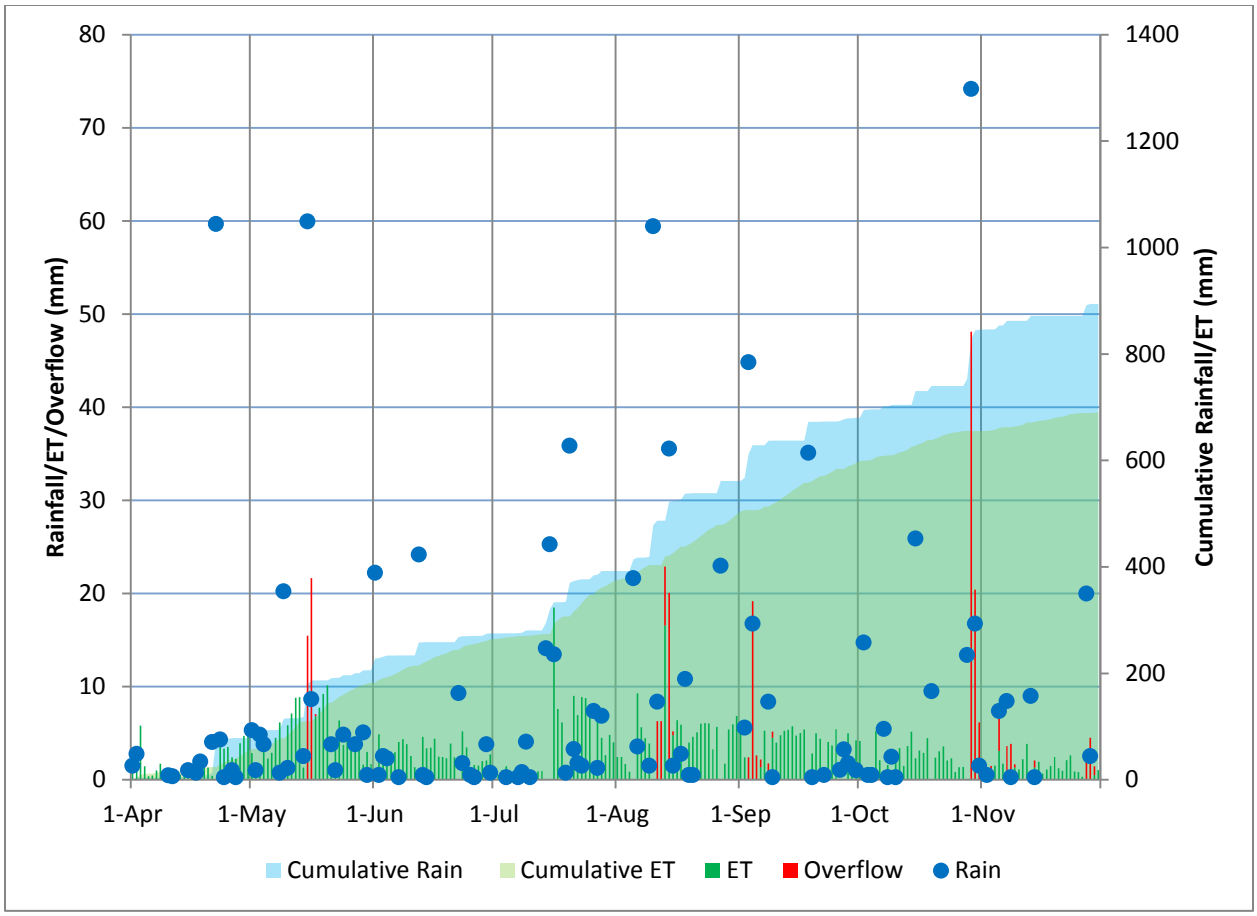

Figure 4.4: Cumulative Performance of Lysimeter for 2012. Daily values of ET and overflow are represented by bar graphs in green and red, respectively, and daily rainfall totals are represented by blue dots with values on the left axis. Cumulative curves for rainfall are shaded in light blue and cumulative measured ET is represented by light green.

2012 was the most average year with no single daily rainfall exceeding 75mm (2.95in). While April was dryer than previous years (2009 and 2011) its rainfall did exceed 2010; however, water from storms in late march 2010 allowed ET rates to be around 4mm/d in 2010 as opposed to 2mm/d in 2012. Daily ET rates remained fairly constant around 4mm/d, but spiked in May and August to 5mm/d, this coincides with the two larger events producing overflow (Figure 4.4). While there was no single daily rainfall greater than 75mm, Hurricane Sandy was 3-days long (67hr) with a total of 103mm (4.06in) of rainfall that produced over 75mm of overflow.

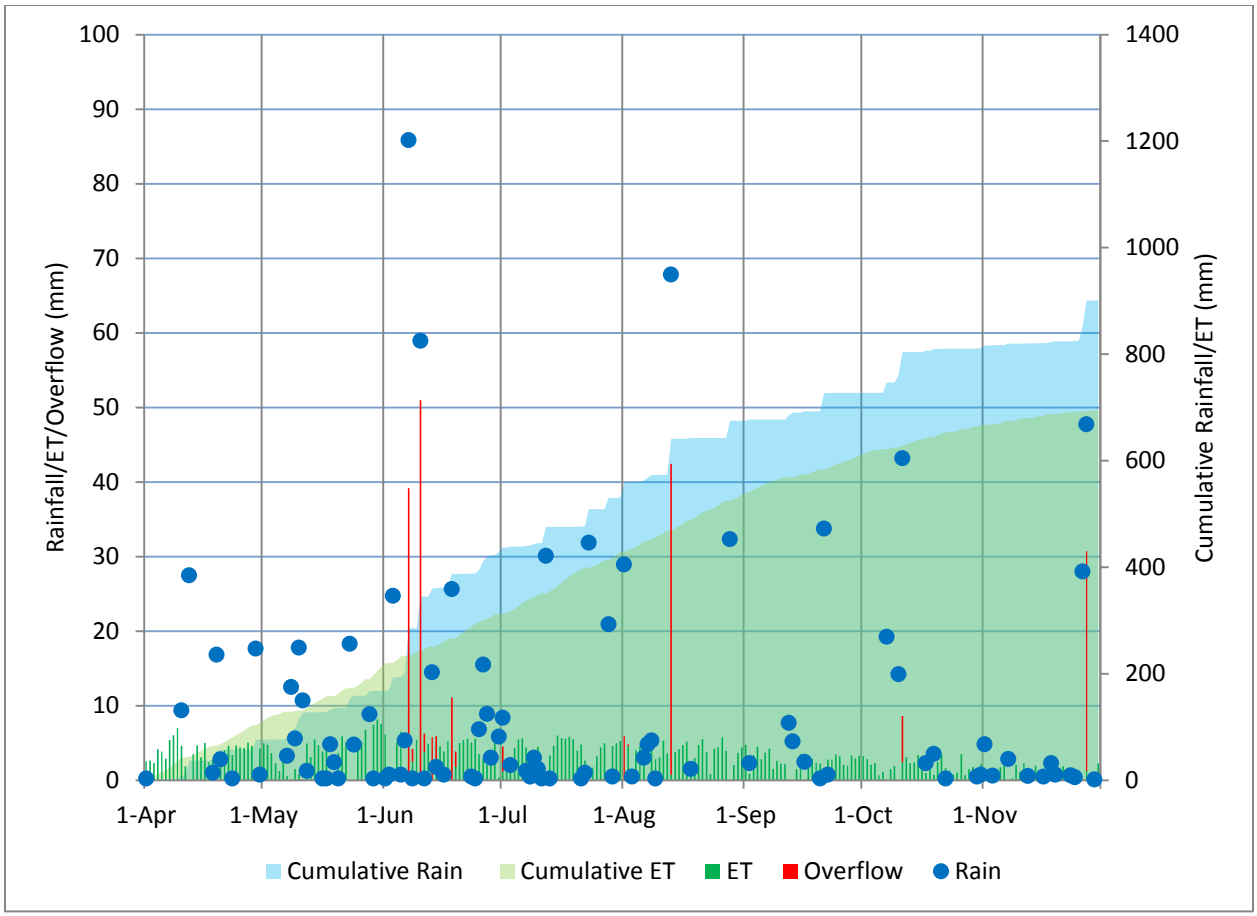

Figure 4.5: Cumulative Performance of Lysimeter for 2013. Daily values of ET and overflow are represented by bar graphs in green and red, respectively, and daily rainfall totals are represented by blue dots with values on the left axis. Cumulative curves for rainfall are shaded in light blue and cumulative measured ET is represented by light green.

2013 (Figure 4.5) had a drier spring (April and May) than typical with rainfall totaling about 160mm (6.3in) as compared to other years where rainfall for this time period generally exceeded 200mm (7.9in). Evapotranspiration rates remained constant at 4mm/d until September when due to a combination of less than typical rainfall as compared to other study years, and cooler temperatures, daily ET rates decreased to 3mm/d in September, then further down to 2mm/d and 1mm/d for October and November, respectively.

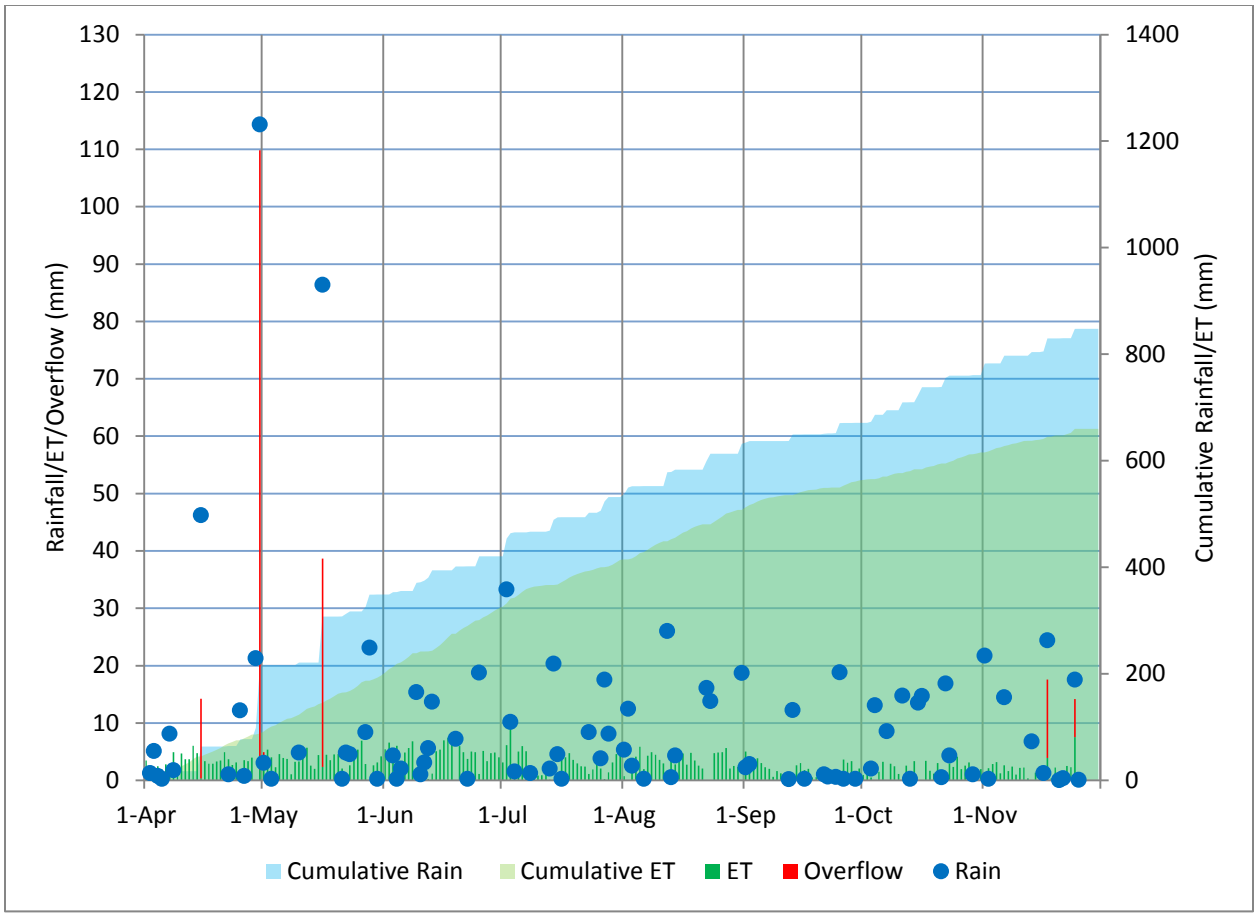

Figure 4.6: Cumulative Performance of Lysimeter for 2014. Daily values of ET and overflow are represented by bar graphs in green and red, respectively, and daily rainfall totals are represented by blue dots with values on the left axis. Cumulative curves for rainfall are shaded in light blue and cumulative measured ET is represented by light green.

2014 (Figure 4.6) was an unusual year in that large storms in April and May produced most of the cumulative overflow for the system. However, these large events allowed the lysimeter to become fully saturated, and paired with the fairly constant rainfall through July, attributed to the daily ET rate of 4mm/d to continue through August. While the analysis was cut off at November 25th due to an unseasonably early snowfall, ET rates remained constant at approximately 3mm/d until mid-November.

4.1.2 Entire Roof Performance

Overflow instrumentation was installed in late 2011 for monitoring the performance of the entire green roof. Data collection and analysis started on April 1st 2012 and is still ongoing. Due to complications during 2012 with the new instrumentation, some of the data is incomplete so an analysis of only 2013 and 2014 is provided. A summary of annual performance can be seen in Table 4.3. Estimated ET is taken as the remainder of precipitation and overflow since infiltration on the green roof is impossible and change in storage can be considered negligible over the long-term.

Table 4.3: Annual Performance of Entire Green Roof

	Historical	2013		2014*	
Rainfall (mm)	845 [1]	901		848	
Overflow (mm, % rainfall)		338	38%	380	44%
Estimated Evapotranspiration (mm, % rainfall)	600 [2]	563	62%	468	56%

* Analysis for 2014 was cut off at November 25th due to an early snowfall on the 26th.
[1] NOAA historical Weather Data for Philadelphia
[2] Church et al. (1995)

While taking the difference between overflow and precipitation works well on a long-term mass balance, on a shorter time scale the results may be misleading. Table 4.4 summarizes monthly performance for the entire green roof for 2013 and 2014. A challenge with using this system is the lysimeter calculates overflow on a more instantaneous basis by estimating what the additional weight of the lysimeter should have been and taking the difference as overflow at the end of the day. For the entire green roof, the overflow can take several days to complete as the roof drains by gravity. This means if it rains on April 30th, all overflow from the lysimeter is calculated at the end of that day, whereas on the entire green roof, overflow could have been

going on for several days into May which artificially added to May's total overflow event though the precipitation was from April.

Table 4.4: Green Roof Monthly Overflow Summary

Month	2013				2014*			
	Rain (mm)	Overflow (mm)	Percent of Total	Estimated ET (mm)	Rain (mm)	Overflow (mm)	Percent of Total	Estimated ET (mm)
April	76	2	3%	74	214	152	71%	62
May	91	17	19%	74	136	97	71%	39
June	261	109	42%	152	72	10	14%	62
July	102	33	32%	69	111	7	6%	104
August	145	75	52%	70	100	18	18%	82
September	52	6	11%	46	39	2	5%	37
October	84	39	46%	45	90	38	42%	52
November	89	56	63%	33	87	56	64%	31

* Analysis for November 2014 was cut off at November 25th due to an early snowfall on the 26th.

Figure 4.7 and Figure 4.8 plot cumulative overflow and cumulative rainfall for the green roof system. Daily overflow is represented by the red bar graph; rainfall is represented by the blue dots. Cumulative rainfall is represented by the light blue shaded region and cumulative overflow by the red shaded region. 2013 had around ten events that contributed a significant portion of overflow to the system (Figure 4.7). Since ET is back calculated by taking the difference between the cumulative rainfall and the cumulative overflow, daily average ET can then be assumed to be the difference between the two divided by the study period. In the case of 2013, it was found this difference was 563mm (22.2in) and the total time analyzed was 244 days. This means that the average rate of ET was approximately 2.3mm/d.

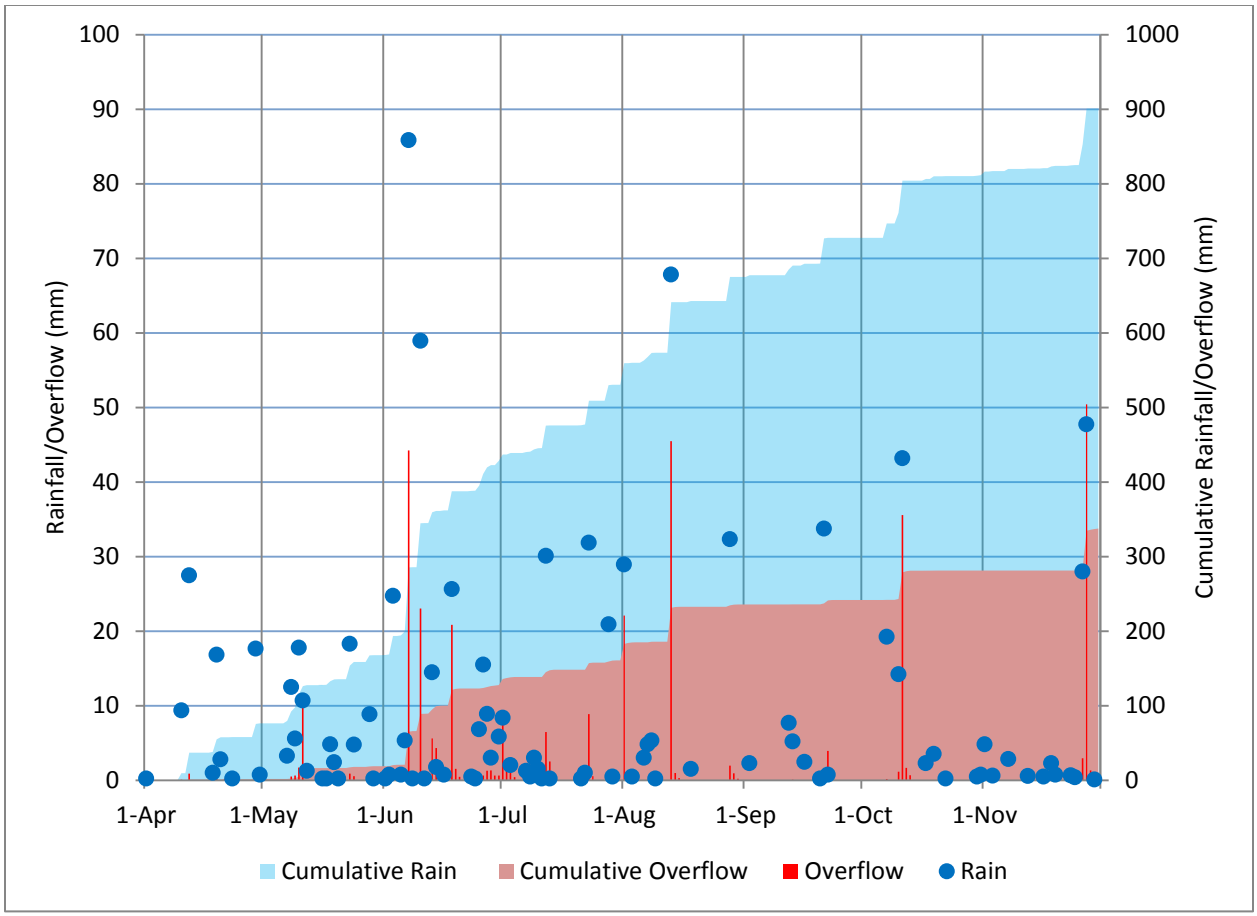

Figure 4.7: Plot of Cumulative Rain and Cumulative Overflow for Green Roof during 2013. Daily overflow is represented by the red bar graph; rainfall is represented by the blue dots. Cumulative rainfall is represented by the light blue shaded region and cumulative overflow by the red shaded region.

For 2014 (Figure 4.8) there were around six events that contributed a significant portion of overflow to the system, mostly early on in the year in April and May. As discussed before for 2013, the daily average ET calculated as this difference between rainfall and overflow was 468mm (18.4in) and the total time analyzed was 239 days. This yields an average rate of ET of approximately 2mm/d.

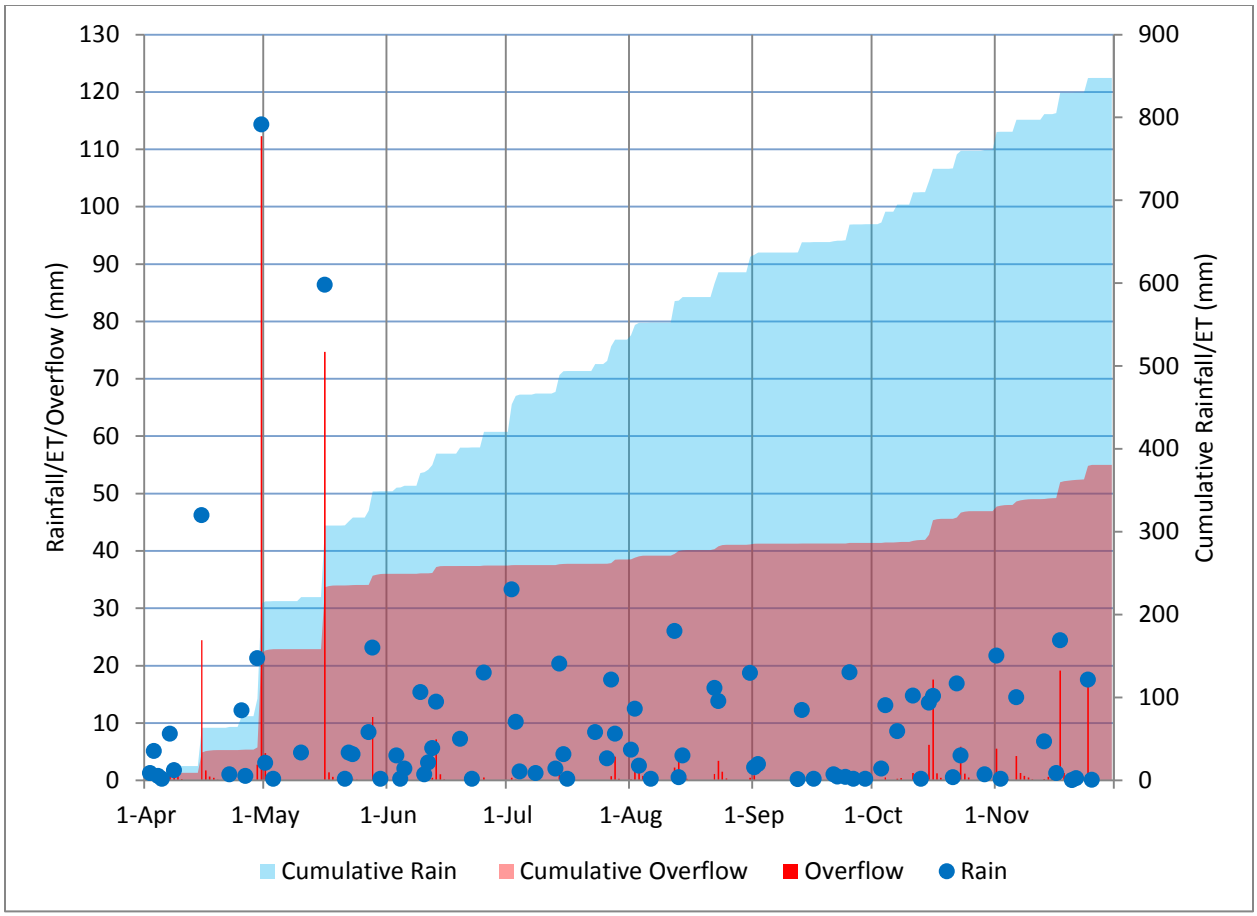

Figure 4.8: Plot of Cumulative Rain and Cumulative Overflow for Green Roof during 2014. Daily overflow is represented by the red bar graph; rainfall is represented by the blue dots. Cumulative rainfall is represented by the light blue shaded region and cumulative overflow by the red shaded region.

4.1.3 System Comparisons and Discussion

The 2009 sampling season was a wetter and colder year than typical for the Philadelphia area and explains why ET percentages were lower than the other years at 68% (Table 4.1). During 2010 there was a significant drought in August and September; however the rest of the year was fairly typical for the area so ET rates were on the upper bound of about 90%. The 2011 season had droughts in June and July; however Hurricane Irene produced almost 190mm of rain over a 2 day period that contributed to a large portion of the years overflow. Since most of the water was lost

from these larger events, it was unavailable for the lysimeter to use for ET so only about 74% of the annual volume was attributed to ET. The 2012 season was relatively average for the region with a fairly even rainfall distribution over the course of the study period and no extreme events. Since there were no extreme events, there was minimal overflow during the course of the season yielding an ET in the upper range at 83%. Although similar to 2010 and 2012 in total precipitation, 2013 experienced three times the average rainfall for June and July. *"June's rainfall total was the highest ever in Philadelphia, with a total of 10.56 inches. That surpassed the record of 10.06 inches set in 1938"* (Philly.com 2013). Because of this unusually wet June, there was a significant amount of overflow similar to Hurricane Irene in 2011, therefore 2013 had a comparable ET percentage of 75%. 2014 was primarily a drought year for the region. Although total precipitation was on par with the historical average for the region, nearly 25% of the rainfall can be attributed to two large storms events in late April and mid-May. These periods of higher than average rainfall inundate the system and do not allow adequate recovery time for storage space within the system therefore creating more total overflow and less ET. Throughout the rest of the 2014 season though, there was almost no overflow so annual ET was high at 80% of the total precipitation.

While the lysimeter was comparable to the green roof on an annual basis for 2013 (75% of the rainfall went to ET for the lysimeter and 62% of rainfall was retained on the entire green roof, a difference of 13%, (Table 4.1 and Table 4.3) despite their different designs) the relationship did not hold true for 2014. The 2014 yearly performance showed approximately 52% of total rainfall retained (48% lost to overflow) as opposed to 78% of total rainfall going to ET from the lysimeter (i.e. a difference of 26%, double that of 2013). There was similar ET from the lysimeter in 2013 and 2014 (i.e. 680mm and 675mm, respectively, Table 4.1). This leads to the

question of what elements of the design and which climate parameters drive the higher retention (i.e., 2013) to fully realize the potential of green roofs and ET as a stormwater volume reduction strategy. It is believed that the relatively poor retention/ET performance from the green roof in 2014 is due to the larger storms that occurred in 2014, particularly the approximately 135mm (5.25in) event on April 29th, as well as the approximately 90mm (3.5in) event on May 16th. Combined, these storms had 225mm of rainfall that produced over 190mm of green roof overflow (7.5in), or 84% of the rainfall was converted to overflow. This overflow accounted for nearly half of the total overflow for the entire year from the green roof. In the case of the lysimeter, the same storm events only produced 144mm (5.6in) of overflow combined with the lysimeter retaining approximately 49mm (1.9in) of the May event and 27mm (1in) of the April event. It is believed that from larger storms, such as these two events, the rock perimeter as well as the protective aluminum flashing around the roof can generate a significant amount of overflow leading to reduced observed performance. This phenomenon is similar to surface runoff from a basin, for smaller events, the rock perimeter and flashing does not play as significant a role because there is some depression storage within the system that is able to capture smaller storms. It is events like these that highlight the need for a standardized method to account for overflow generated by these portions of the green roof system. To highlight the significant impact extreme events can have on the green roof system, if April is eliminated from the 2014 analysis; the lysimeter measured 84% ET while the entire green roof estimated 74%. This approximately 10% difference in performance is more closely related to that seen in 2013.

On a monthly basis the lysimeter performance matched up fairly well to the entire roof's performance particularly during the warmer summer months in (June - September) (Table 4.2 and Table 4.4, Figure 4.9 and Figure 4.10). For 2013, the monthly trends appear to be consistent,

with June, July, August, October, and November producing the majority of the overflow (Figure 4.9). For 2014, although the entire green roof did generate some overflow for June through October as opposed to the lysimeter, which did not, the total monthly overflow volume for these months was always less than 20% of the total monthly rainfall. While the volume of the total overflow was different between the two systems, the response of each system was similar in that if overflow from one system changed from one month to another, the same trend can be seen in the other system. This difference between the lysimeter and roof is expected given the different carrying capacities of the roof discussed in chapter 3 and seen in Figure 4.11 and Figure 4.12.

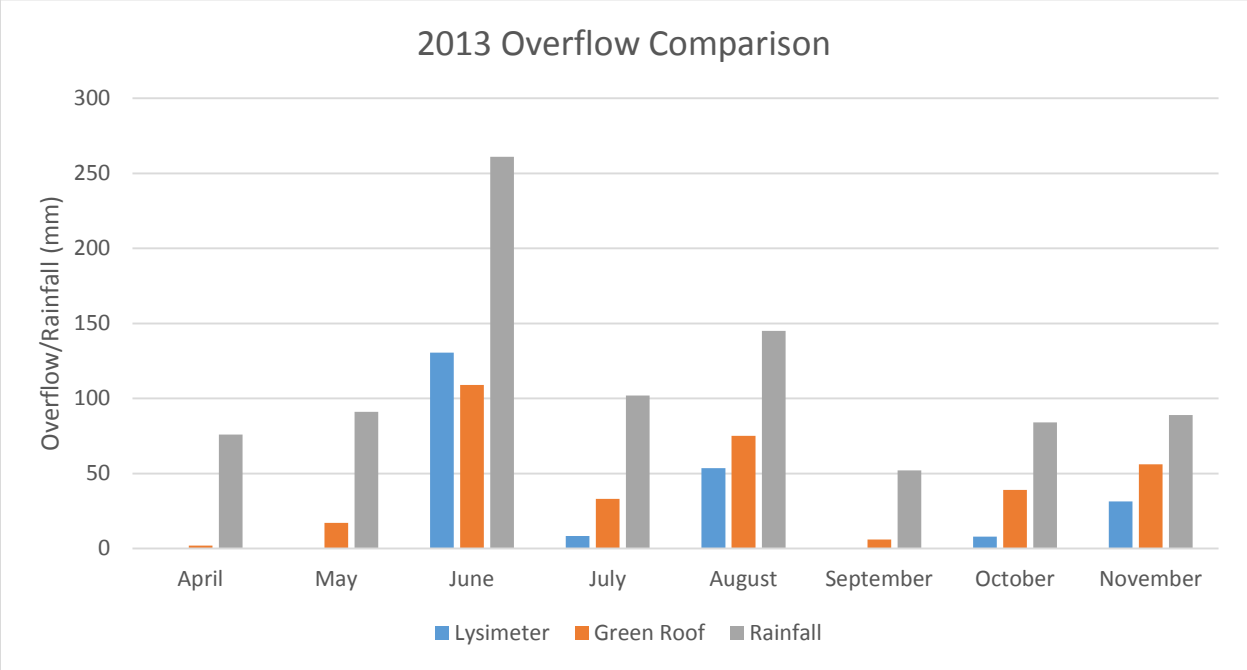

Figure 4.9: Overflow Volumes for Lysimeter and Green Roof for 2013

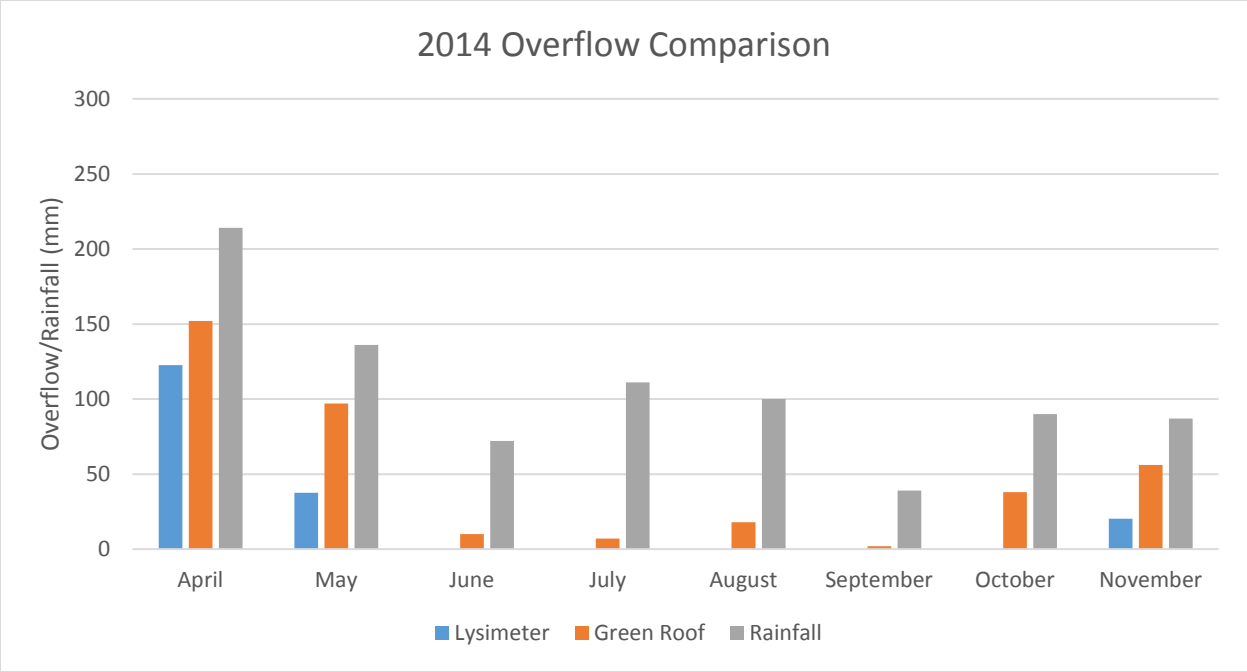

Figure 4.10: Overflow Volumes for Lysimeter and Green Roof for 2014

To help understand why there can be such a difference in performance between the systems, plots of storm size and equivalent overflow were produced for each system (Figure 4.11 and Figure 4.12). An important distinction between the two plots is the apparent "break point" for each system. We see for most of the smaller storms, there is minimal to no overflow produced which was also found by Fassman-Beck et al. (2015). For smaller events where overflow is produced, this can be attributed to antecedent moisture condition of the system where if the system is near field capacity, nearly all of the precipitation becomes overflow. As used by Davis et al. (2012) for rain garden analysis, bi-linear curve fitting was performed to come up with a line of best fit with the break point for each system. For the lysimeter, it was found that in order for a storm to produce any measurable overflow precipitation needed to be in excess of 35mm, whereas for the entire green roof, rainfall events exceeding 13.5mm typically produced measureable overflow. Note, in both systems, once an event size was large enough to generate

measurable outflow, the overflow increased linearly, but never exceeded the total rainfall, so there was still overall retention with no overflow data points above the 1:1 line.

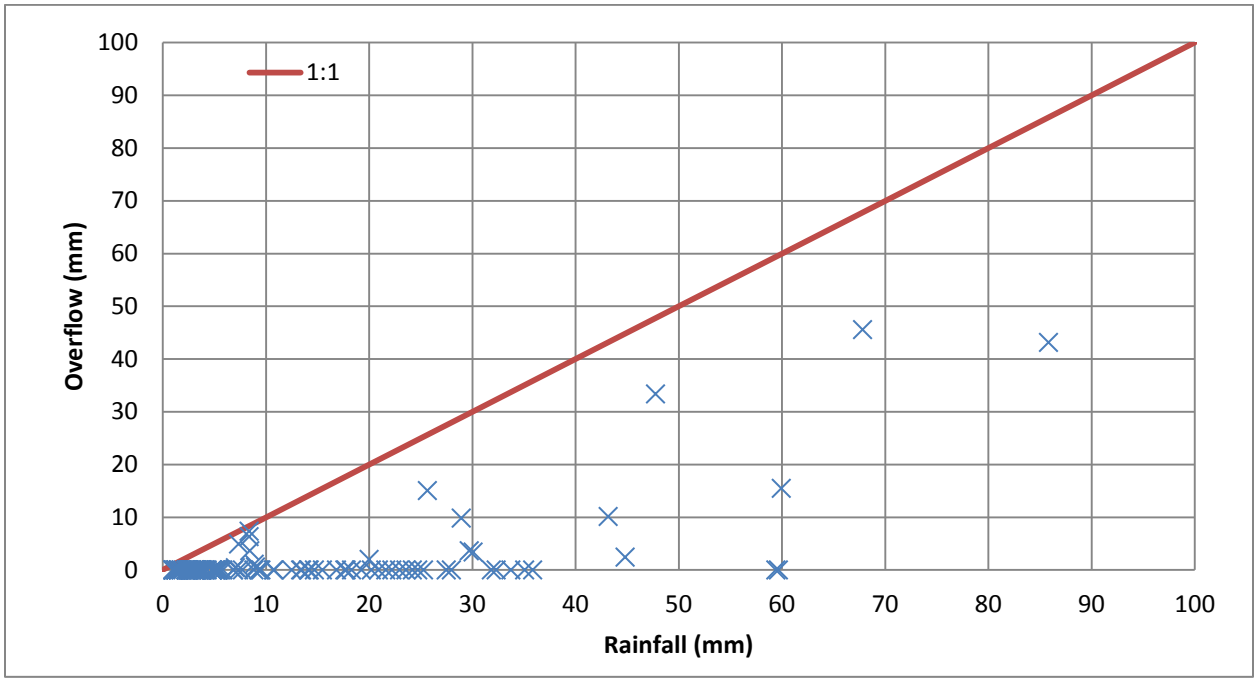

Figure 4.11: Rainfall vs. Equivalent Overflow for the lysimeter.

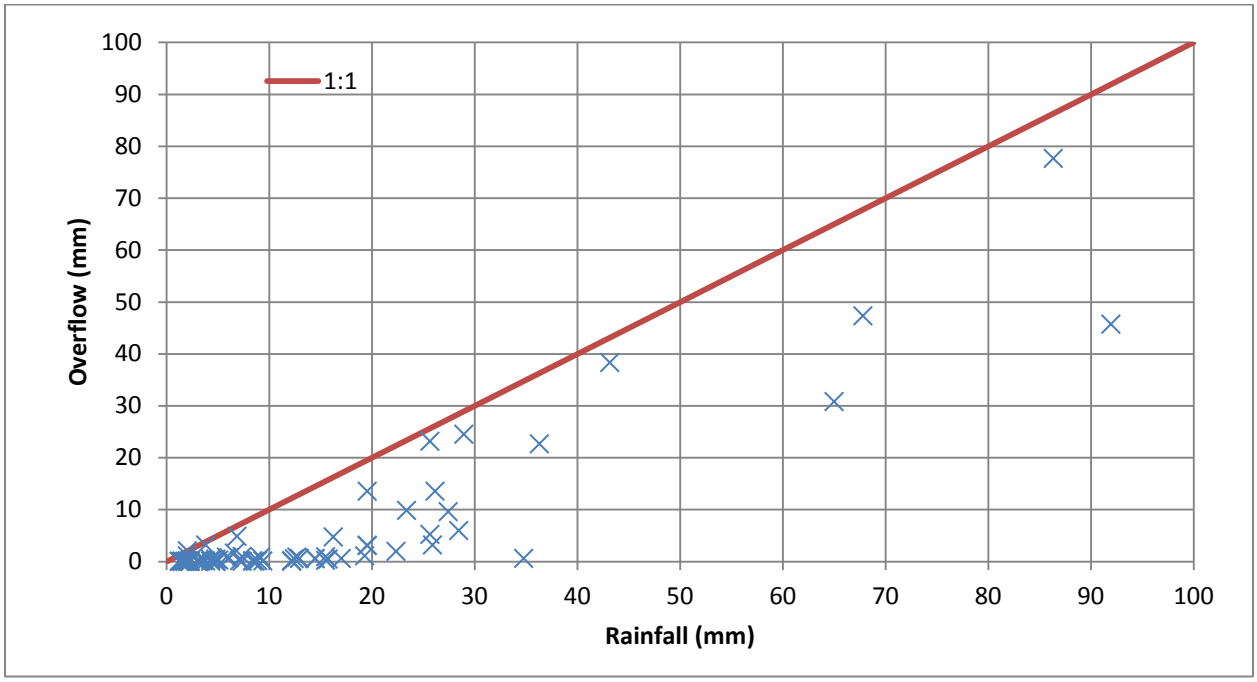

Figure 4.12: Rainfall vs. Equivalent Overflow for the entire green roof

4.1.4 Freely Drained vs. Internal Water Storage

The difference in ET and overflow for the lysimeter and entire green roof confirms that the lack of an underdrain in the lysimeter allows for a larger portion of the rainfall to be stored for ET during the following dry days. The difference in retention capacities (approximately 20mm) explains why typically more total overflow is seen from the entire green roof than from the lysimeter. The absence of an underdrain means the lysimeter could not freely drain, which allows all of the void space in the media to become fully saturated, effectively creating internal water storage. Schneider (2011) found the void space to be around 53% for the growing media used. Because of the underdrain, the entire green roof can drain freely by gravity thus limiting the maximum water holding capacity to field capacity or about 42% (Schneider 2011).

There have been concerns raised in the past about issues with oversaturating green roofs and the effect that too much water may have on plant health, in particular root rot. When roots are constantly saturated, there is also not a need for the plant to extend its roots deeper into the media to reach water. This can cause the development of very shallow root systems, which can be a problem during water stressed periods and reduces a plant's ability to provide soil stability under high winds or during periods of intense rainfall. While no quantitative analysis has been performed on comparing the health of the plants within the lysimeter or on the green roof, visual inspection of the two systems indicate that they are both healthy under normal conditions (Figure 4.13 and Figure 4.14). However, under water stressed periods, such as in 2010, the plants within the lysimeter did not appear as thin or as stressed as the plants on the green roof. As seen in Figure 4.15 and Figure 4.16, the green roof had many bare spots whereas the lysimeter still appeared relatively full and lush. Ultimately, the green roof needed to be watered and eventually replanted, whereas the lysimeter did not.

Figure 4.13 Photo of Green Roof Health. In this photo taken June 20, 2013, typical coverage of green roof under healthy, unstressed conditions. (VUSP)

Figure 4.14: Photo of Lysimeter Health. In this photo taken June 20, 2013, typical coverage of lysimeter under healthy, unstressed conditions. (VUSP)

Figure 4.15: Photo of Green Roof Health. In this photo taken October 22, 2010, during the drought, many bare spots overtook the roof requiring a replanting. (Schneider 2011)

Figure 4.16: Photo of Lysimeter Health. In this photo taken October 22, 2010, during the drought, the lysimeter still was quite healthy and did not display the same bare spots as the surrounding green roof. (Schneider 2011)

4.2 Evapotranspiration Model Performance

In this section, the results from the proposed model will be presented and compared to observed field performance. A site specific evaluation of the Hargreaves equation will be discussed as it compares to the widely accepted FAO56 methodology and the benefits of the more data intensive methodology will be assessed.

4.2.1 Lysimeter Modeled Performance

The Proposed model (Section 3.3) was run with the 6 years of lysimeter data available. Daily precipitation totals for each year (January through December), as well as maximum, minimum, and mean daily temperature, were input into the Excel spreadsheet created (Figure 4.17). In the event daily temperature or rainfall data was unavailable from the green roof site, values from nearby sites on campus were used. Daily totals of terrestrial radiation were calculated based on the Julian day of the year as discussed in Chapter 3. The model was run using the five soil moisture extraction functions described in Chapter 3 (Equations 3.11-3.15). A maximum water retention was initially set at 4.27cm (1.68in) based on the thickness of the media within the lysimeter (10cm/ 4in) and multiplied by the saturated water content (42%) (Schneider 2011). A summary of the results from the initial run can be found in Table 4.5.

																Site Latitude	47 °	0.8203	Radians
																Solar Constant	0.082 MJ m^{-2} min^{-1}		
		Maximum Storage Capacity		1.68 in.															
User Input					Hargreaves							Soil Moisture Relationship				Results			
Date	Rain in.	T_{max}	T_{min}	T_{avg}	Julian Day	PET(mmd^{-1})	Declination	Relative Distance	Sunset Hour angle	Radiation MJ/m2/Day	Radiation mm/day	Available Storage (start of day)	Available water (start of day)	RAT	SMEF	AET(mmd^{-1})	AET (in)	Overflow	
4/1/2013	0.01	18.15	2.53	9.47	91	5.54	0.07	1.00	1.65	41.54	16.95	0.78	0.90	0.54	0.57	3.18	0.13	0.00	
4/2/2013	0.00	7.54	0.16	3.83	92	2.71	0.08	1.00	1.65	41.93	17.11	0.89	0.79	0.47	0.44	1.19	0.05	0.00	
4/3/2013	0.00	9.07	-1.29	3.73	93	3.43	0.08	1.00	1.66	42.32	17.26	0.94	0.74	0.44	0.38	1.32	0.05	0.00	
4/4/2013	0.00	11.31	-1.84	4.94	94	4.23	0.09	1.00	1.67	42.70	17.42	0.99	0.69	0.41	0.33	1.38	0.05	0.00	
4/5/2013	0.00	18.15	2.66	9.86	95	5.72	0.10	1.00	1.68	43.08	17.58	1.04	0.64	0.38	0.27	1.54	0.06	0.00	
4/6/2013	0.00	12.14	1.09	6.55	96	4.06	0.10	1.00	1.68	43.45	17.73	1.11	0.57	0.34	0.21	0.86	0.03	0.00	
4/7/2013	0.00	16.13	3.03	10.01	97	5.05	0.11	1.00	1.69	43.83	17.88	1.14	0.54	0.32	0.18	0.93	0.04	0.00	
4/8/2013	0.00	25.31	10.37	17.86	98	6.91	0.12	1.00	1.70	44.19	18.03	1.18	0.50	0.30	0.16	1.07	0.04	0.00	
4/9/2013	0.00	28.81	15.50	22.32	99	7.11	0.12	1.00	1.71	44.56	18.18	1.22	0.46	0.27	0.13	0.89	0.04	0.00	
4/10/2013	0.37	31.84	16.51	23.64	100	8.19	0.13	1.00	1.71	44.91	18.33	1.25	0.43	0.25	0.10	0.85	0.03	0.00	
4/11/2013	0.00	23.21	8.95	15.79	101	6.58	0.14	0.99	1.72	45.27	18.47	0.92	0.76	0.45	0.41	2.69	0.11	0.00	
4/12/2013	1.08	9.12	5.72	7.07	102	2.12	0.14	0.99	1.73	45.62	18.61	1.02	0.66	0.39	0.29	0.62	0.02	0.06	
4/13/2013	0.00	16.48	5.19	11.00	103	4.97	0.15	0.99	1.74	45.96	18.75	0.02	1.66	0.99	1.00	4.97	0.20	0.00	
4/14/2013	0.00	16.63	6.33	12.22	104	4.80	0.16	0.99	1.74	46.30	18.89	0.22	1.46	0.87	0.98	4.70	0.18	0.00	
4/15/2013	0.00	13.84	6.96	10.27	105	3.63	0.16	0.99	1.75	46.64	19.03	0.40	1.28	0.76	0.91	3.30	0.13	0.00	
4/16/2013	0.00	21.31	8.10	15.19	106	6.27	0.17	0.99	1.76	46.97	19.16	0.53	1.15	0.68	0.82	5.14	0.20	0.00	
4/17/2013	0.00	20.42	12.01	16.16	107	4.92	0.18	0.99	1.76	47.30	19.30	0.74	0.94	0.56	0.62	3.05	0.12	0.00	
4/18/2013	0.04	16.45	11.38	13.89	108	3.45	0.18	0.99	1.77	47.62	19.43	0.86	0.82	0.49	0.48	1.65	0.07	0.00	
4/19/2013	0.66	23.96	9.76	18.16	109	7.08	0.19	0.99	1.78	47.93	19.56	0.88	0.80	0.47	0.45	3.18	0.13	0.00	
4/20/2013	0.11	15.03	5.70	10.19	110	4.54	0.20	0.99	1.79	48.24	19.68	0.34	1.34	0.80	0.94	4.26	0.17	0.00	
4/21/2013	0.00	13.05	1.53	7.25	111	4.77	0.20	0.99	1.79	48.55	19.81	0.40	1.28	0.76	0.91	4.34	0.17	0.00	
4/22/2013	0.00	13.22	2.50	7.46	112	4.66	0.21	0.99	1.80	48.85	19.93	0.57	1.11	0.66	0.79	3.67	0.14	0.00	
4/23/2013	0.01	11.38	5.06	7.96	113	3.38	0.21	0.99	1.81	49.15	20.05	0.72	0.96	0.57	0.64	2.18	0.09	0.00	
4/24/2013	0.00	20.26	4.75	14.08	114	6.95	0.22	0.99	1.81	49.44	20.17	0.79	0.89	0.53	0.56	3.87	0.15	0.00	
4/25/2013	0.00	18.26	5.98	12.03	115	5.90	0.23	0.99	1.82	49.73	20.29	0.95	0.73	0.44	0.38	2.22	0.09	0.00	
4/26/2013	0.00	19.65	7.21	12.83	116	6.20	0.23	0.99	1.83	50.01	20.40	1.03	0.65	0.39	0.28	1.75	0.07	0.00	
4/27/2013	0.00	22.62	6.63	14.59	117	7.63	0.24	0.99	1.83	50.29	20.52	1.10	0.58	0.34	0.22	1.65	0.06	0.00	
4/28/2013	0.00	21.73	8.65	15.24	118	6.78	0.24	0.99	1.84	50.56	20.63	1.17	0.51	0.31	0.16	1.10	0.04	0.00	
4/29/2013	0.70	13.67	10.79	12.09	119	2.55	0.25	0.98	1.85	50.82	20.74	1.21	0.47	0.28	0.13	0.33	0.01	0.00	
4/30/2013	0.03	21.74	8.78	14.42	120	6.82	0.25	0.98	1.85	51.08	20.84	0.53	1.15	0.69	0.83	5.64	0.22	0.00	

Figure 4.17 User Input Page of Model.

The user will input data into the first five columns (blue). All other columns are calculated using this data as well as general design parameters such as maximum storage capacity. Columns highlighted in green are a check to ensure the model does not ET more water than available and to ensure available water does not exceed maximum storage.

Table 4.5: Summary of annual model performance using the six different soil moisture extraction functions. The percentages are the percent of ET or overflow of the rainfall.

	2009				2010				2011			
	ET		Overflow		ET		Overflow		ET		Overflow	
Summary	mm	%	mm	%	mm	%	mm	%	mm	%	mm	%
Actual	784.4	68	336.3	29	723.2	88	144.1	18	929.8	74	355.5	26
Equation 3.11	694	60	442.2	38	524.8	64	296	36	673.4	48	713.5	51
Equation 3.12	670.8	58	467.4	40	509.9	62	308.5	38	642.8	46	747.6	53
Equation 3.13	785.4	68	341.2	30	574	70	248.6	30	740.1	53	641.8	46
Equation 3.14	611	53	532.6	46	473.9	58	342.5	42	588.4	42	805.9	57
Equation 3.15	706.4	61	428	37	532.2	65	286.3	35	661.5	47	728.3	52

	2012				2013				2014			
	ET		Overflow		ET		Overflow		ET		Overflow	
	mm	%	mm	%	mm	%	mm	%	mm	%	mm	%
Actual	664.5	77	203.4706	23	696.5	77	204.4	23	675.5	75	180.4	20
Equation 3.11	576.5	64	293.4224	33	639.6	71	245.1	27	580.5	66	272.8	31
Equation 3.12	558.6	62	311.1859	35	626.8	70	261	29	569.7	65	285.5	32
Equation 3.13	633.5	70	228.1532	25	686.8	76	194.5	22	615.8	73	195.9	23
Equation 3.14	516.5	57	357.5118	40	572.5	64	318.5	35	531.6	60	328.8	37
Equation 3.15	582.4	65	282.4611	31	652.1	72	235.3	26	587.6	67	264.6	30

Each soil moisture extraction function was evaluated on how close the model results came to the cumulative observed annual ET and overflow. A plot of cumulative ET for each equation as well as cumulative rainfall for 2009 can be seen in Figure 4.18. While all of the functions appeared to provide appropriate cumulative volumes early on, as it approached August, the differences grew further and further apart. It was found that equation 3.13 provided the best fit in terms of annual performance with the maximum difference between measured and modeled annual ET (measured - modeled) being 190mm in 2011 and the minimum being -1mm in 2009. The average difference across all six years was 74mm. The worst modeled years were 2010 and 2011 with differences between measured and modeled ET being 149mm and 189mm, respectively.

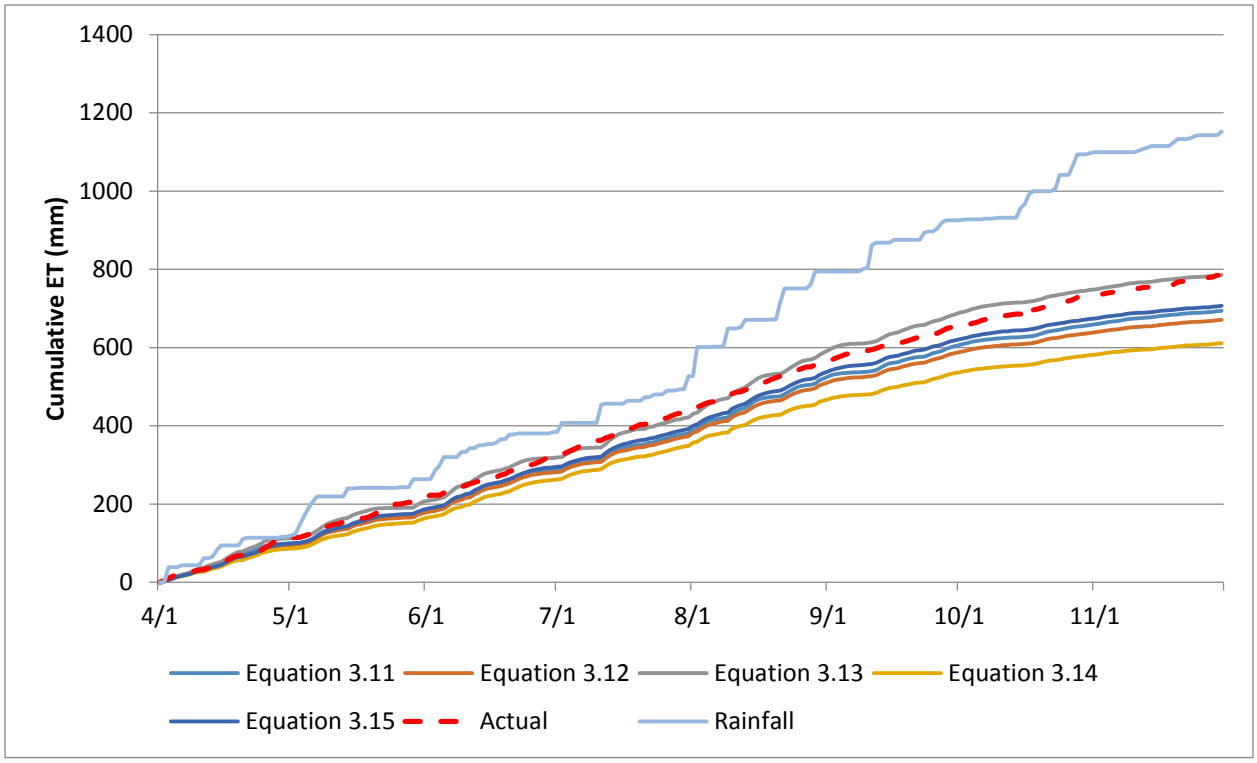

Figure 4.18: Plot of Cumulative Modeled and Measured ET and Rainfall

It is believed that larger error is due to high rainfall experienced in October 2010 and Hurricane Irene in August 2011 and the differences between measured and modeled overflow from larger

storm events such as these. During larger events, the model will only retain volume equal to the soil moisture deficit at the start of the day; however this may not be representative of what is occurring in the field. In reality, the system may be able to retain more than 4.3cm (1.68in), which explains why the annual overflow is typically less than modeled. As seen in Figure 4.19, the lysimeter may not be filled up completely to the top allowing some temporary ponding within the stalks and stems of the sedums.

Figure 4.19: Photo of Lysimeter Showing Surface of Media below the Upper Lip of Sidewalls by approximately 6.5mm (0.25in)

Equation 3.13 also performed better than the other soil moisture extraction functions on an event basis, as well as annually, because it allowed higher ET rates during higher moisture conditions and maintained a fairly constant level of ET following a storm event and tapered off as soil moisture decreased, which is more representative of the observed conditions as seen in Figure

4.20**.** This trend is expected given the nature of the growing media, the larger grain size of the media allows for more readily available water after a rain event, and as the media becomes drier, the micropores try to retain more water thus making ET more difficult.

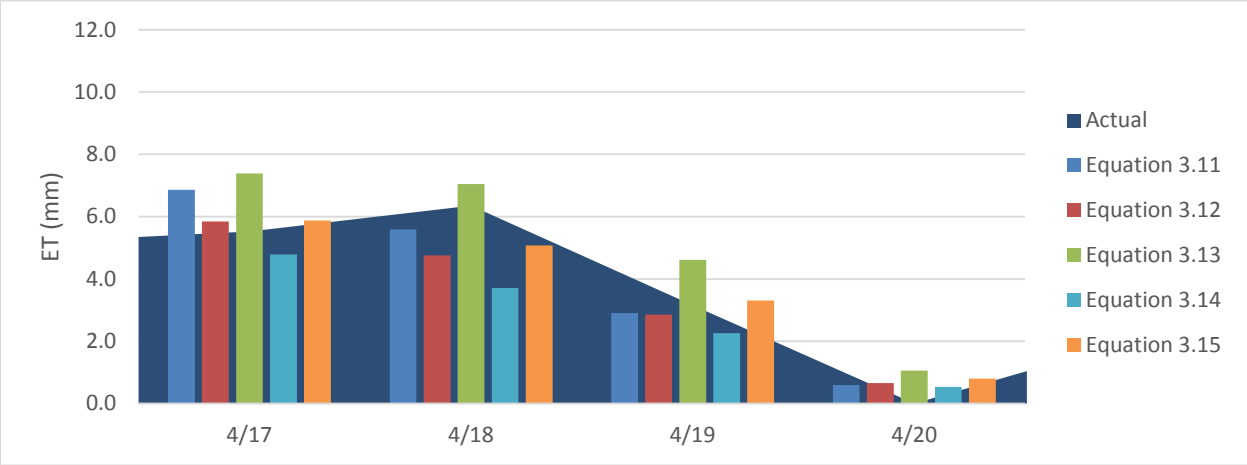

Figure 4.20: Typical Trends of Each Soil Moisture Extraction Function. Notice how equation 3.13, while fairly even with other relationships on the first day, remains higher in the following days, more indicative of reality.

On a monthly time scale, the Hargreaves equation when paired with Equation 3.13, performed quite well. A summary of monthly performance using Equation 3.13 can be seen in Table 4.6 and in Figure 4.21 through Figure 4.28. On average, the model under-predicted ET on a monthly time step by 9mm (0.35 in) with a standard deviation of 19mm (0.75 in), and over-predicted overflow by 10mm (0.4 inches) with a standard deviation of 23mm (0.9 in).

Table 4.6: Summary of Monthly Model and Actual Performance

	2009						2010						2011					
	Actual		Modeled		Delta		Actual		Modeled		Delta		Actual		Modeled		Delta	
	ET (mm)	Over (mm)	ET (mm)	Over (mm)	ET (mm)	Over (mm)	ET (mm)	Over (mm)	ET (mm)	Over (mm)	ET (mm)	Over (mm)	ET (mm)	Over (mm)	ET (mm)	Over (mm)	ET (mm)	Over (mm)
Apr	112	13	112	19	0	-6	103	0	94	0	9	0	140	31	118	32	22	-1
May	101	43	92	49	9	-6	132	8	106	17	26	-9	113	0	88	15	25	-15
Jun	110	8	113	12	-3	-4	107	0	85	20	22	-20	53	0	45	0	8	0
Jul	114	0	104	7	10	-7	131	30	109	54	22	-24	73	0	78	0	-5	0
Aug	124	144	166	113	-42	31	46	0	42	0	4	0	188	192	176	232	12	-40
Sept	91	39	98	29	-7	10	29	12	23	44	6	-32	155	88	110	195	45	-107
Oct	79	88	63	98	16	-10	120	94	81	101	39	-7	129	45	83	113	46	-68
Nov	53	1	40	15	13	-14	55	0	36	12	19	-12	79	0	44	59	35	-59

	2012						2013						2014					
	Actual		Modeled		Delta		Actual		Modeled		Delta		Actual		Modeled		Delta	
	ET (mm)	Over (mm)	ET (mm)	Over (mm)	ET (mm)	Over (mm)	ET (mm)	Over (mm)	ET (mm)	Over (mm)	ET (mm)	Over (mm)	ET (mm)	Over (mm)	ET (mm)	Over (mm)	ET (mm)	Over (mm)
Apr	58	0	52	25	3	-25	107	0	81	0	26	0	88	122	75	104	13	18
May	125	38	102	30	27	5	105	0	105	0	0	0	109	37	115	44	-6	-7
Jun	82	0	70	0	11	0	99	118	154	96	-55	22	126	0	84	0	42	0
Jul	111	0	106	10	-12	-10	117	3	108	0	9	3	91	0	105	1	-14	-1
Aug	130	38	120	45	-8	-11	108	48	107	28	1	20	94	0	87	0	7	0
Sept	95	27	91	27	7	-5	74	0	63	0	11	0	55	0	53	0	2	0
Oct	56	77	57	22	3	-4	57	6	52	30	5	-24	53	0	64	8	-11	-8
Nov	35	23	37	14	3	2	30	29	19	40	11	-11	44	20	37	66	7	-46

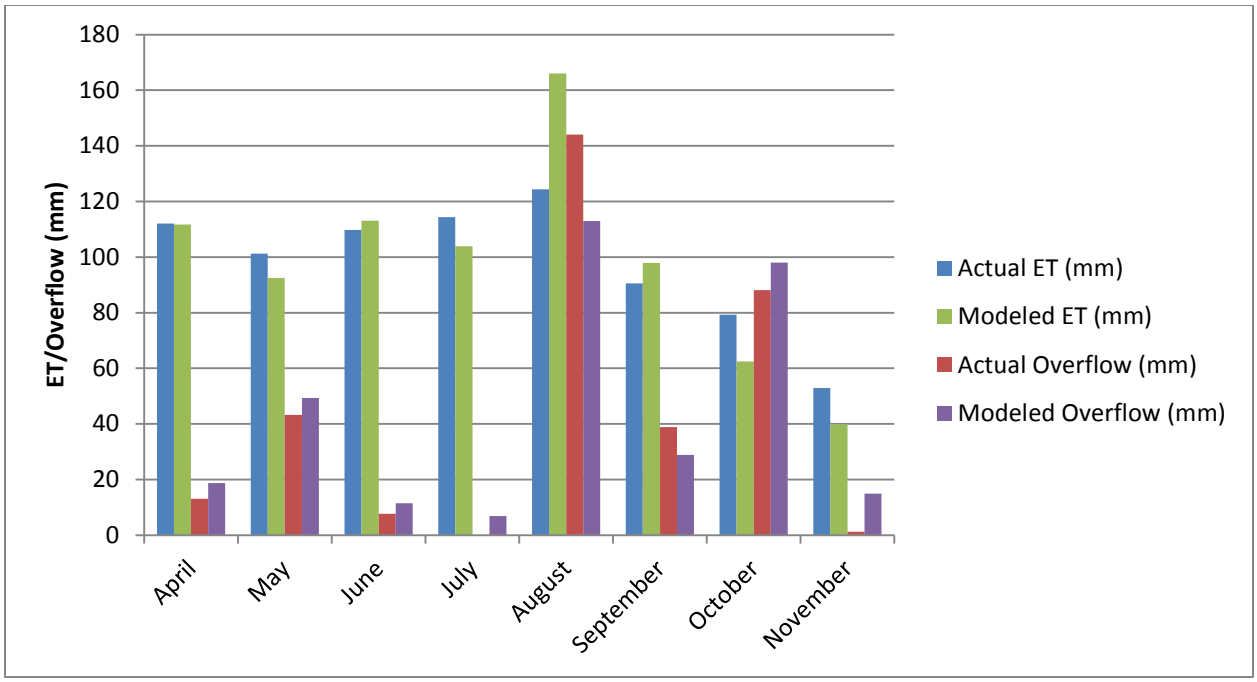

Figure 4.21: 2009 Measured vs. Modeled ET and Overflow

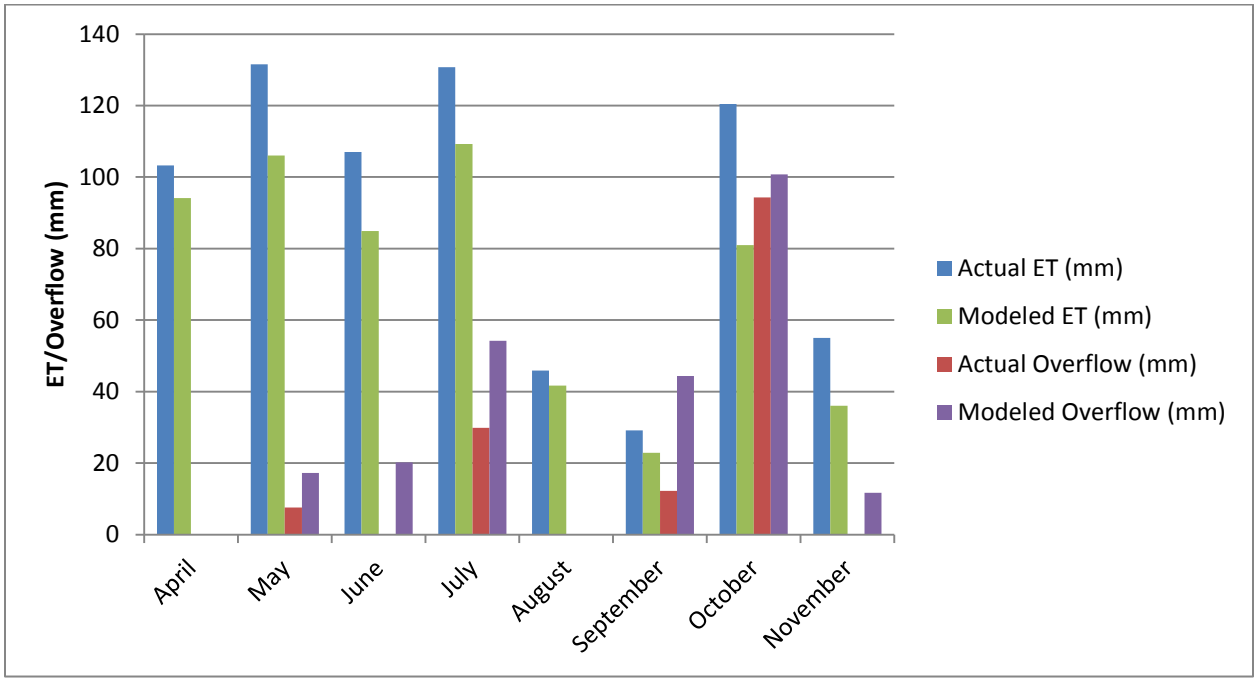

Figure 4.22: 2010 Measured vs. Modeled ET and Overflow

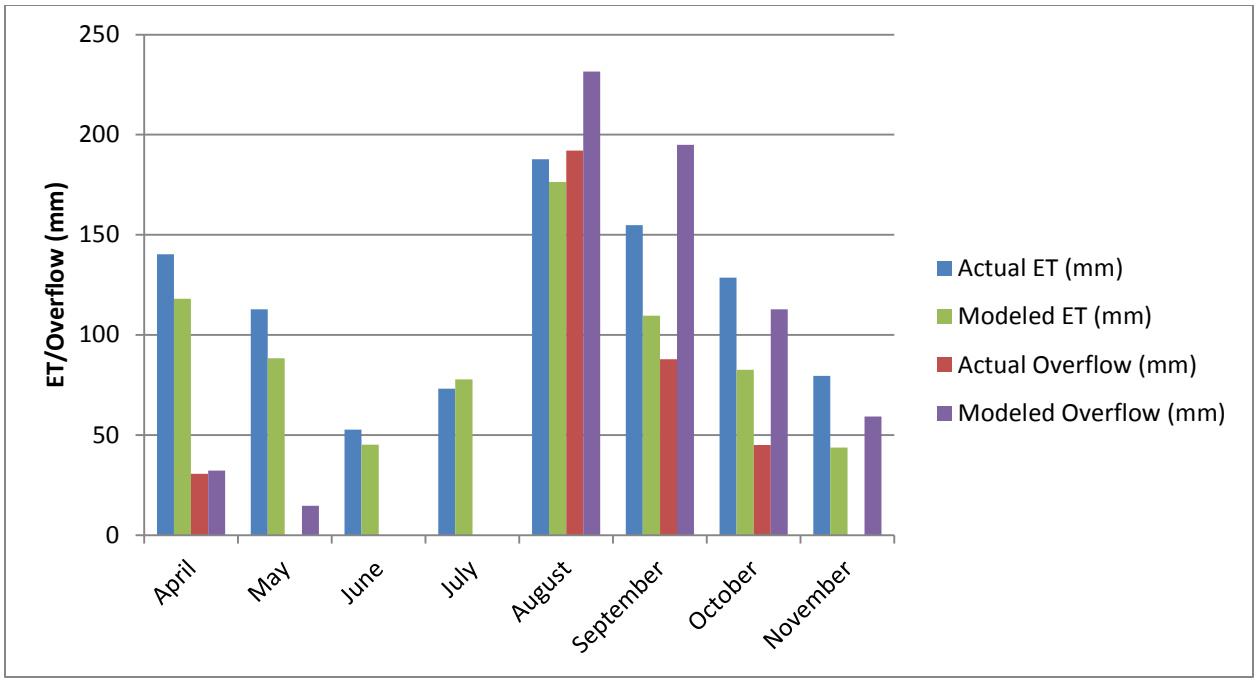

Figure 4.23: 2011 Measured vs. Modeled ET and Overflow

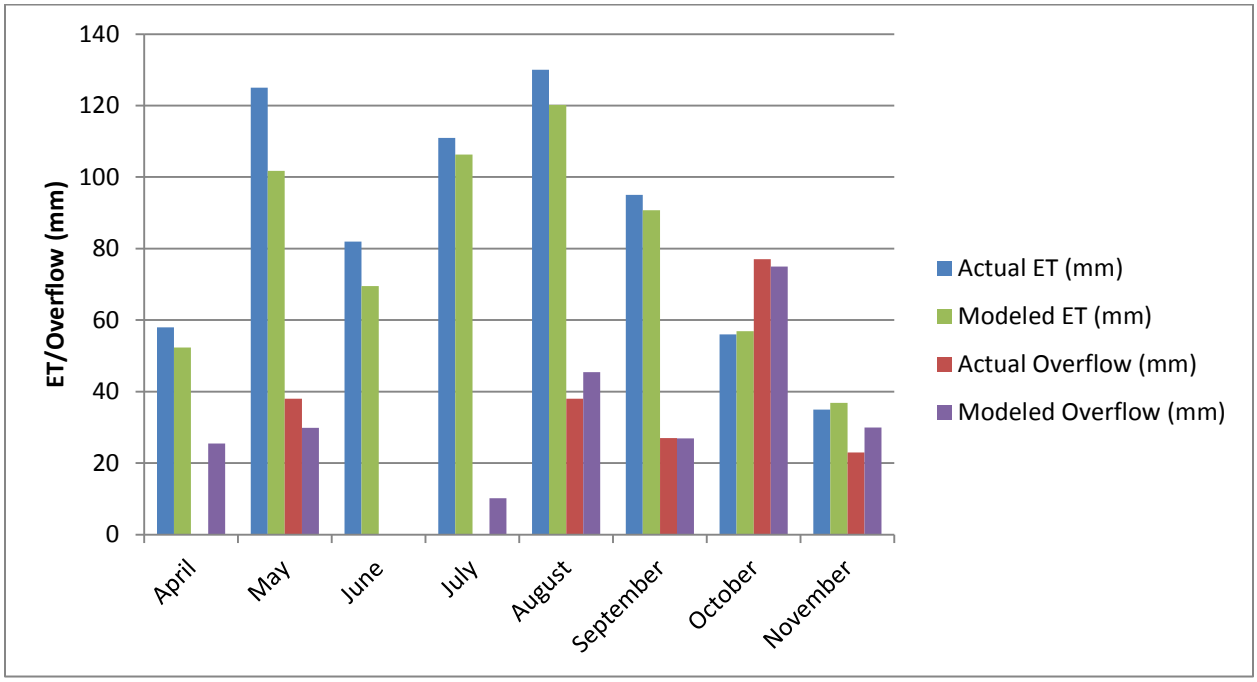

Figure 4.24: 2012 Measured vs. Modeled ET and Overflow

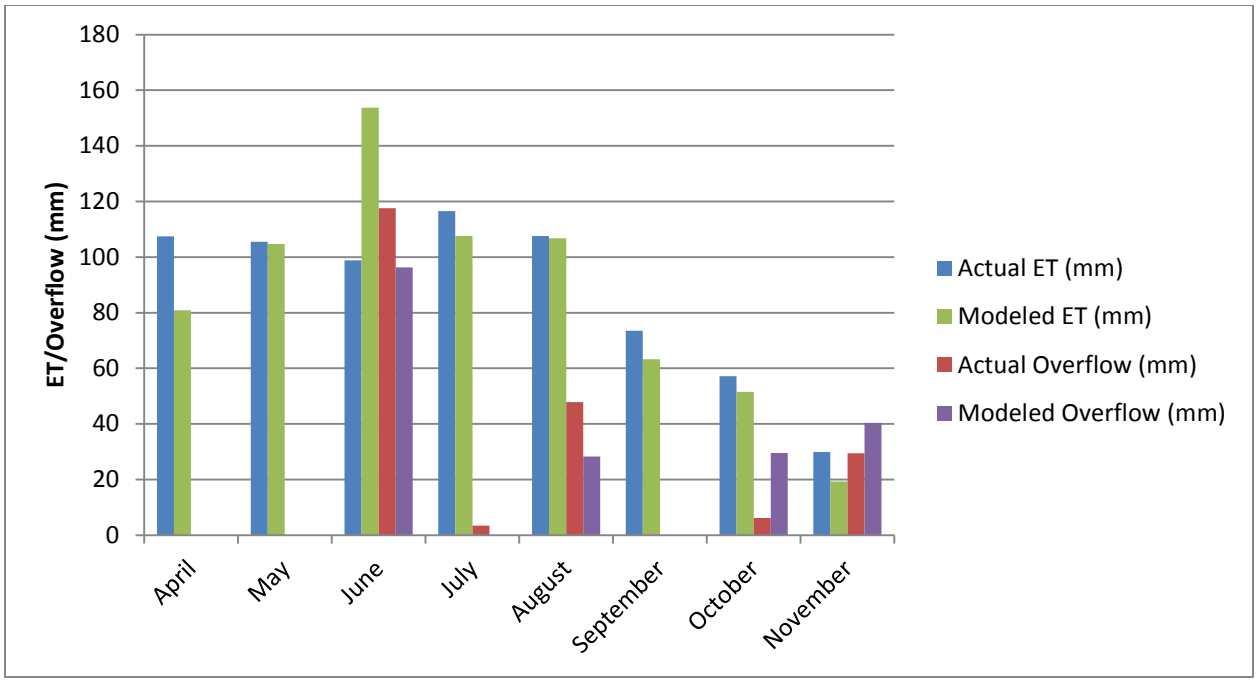

Figure 4.25: 2013 Measured vs. Modeled ET and Overflow

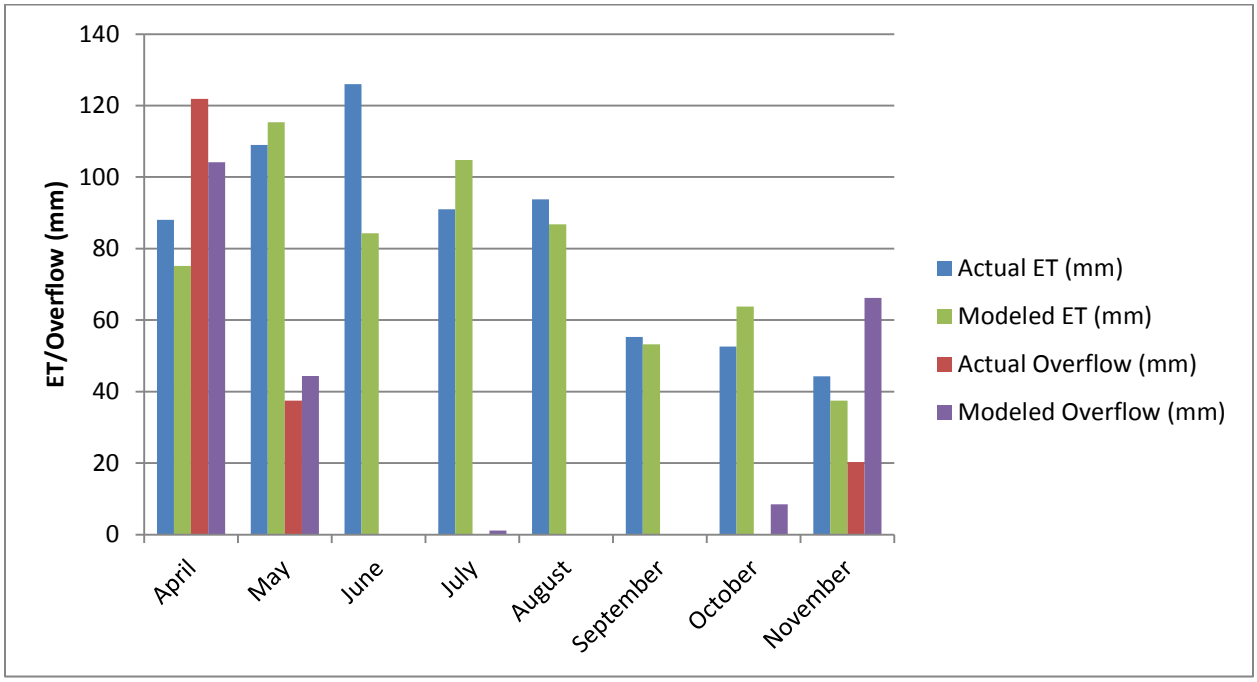

Figure 4.26: 2014 Measured vs. Modeled ET and Overflow

4.2.2 Green Roof Modeled Performance

After the model was calibrated using lysimeter data, the model was verified using data from the entire green roof to see if the predictions held true for different green roof systems. The retention capacity was set at 20mm (0.79in) based off of a visual inspection of the break point in Figure 4.11. The bi-linear curve fit parameter was not used because it did not provide enough storage for the model and therefore modeled performance was greatly below observed performance. It is believed that the bi-linear curve fit value may not have been calculated with enough storms that occurred with drier conditions therefore leading to more overflow from each event than could be expected if the system was dry. While this retention is less than the 25mm (1in) capacity that was calculated using the plant available water ($0.21 cm^3/cm^3$) (Schneider, 2011) multiplied by media thickness (100mm) and the void space of drainage board (20%) (Optigreen 2009) multiplied by its thickness (25mm), this estimated reduction should account for contributions from the rock perimeter as well as the aluminum flashing discussed previously.

A summary of annual and monthly performance for 2013 and 2014 can be seen in Table 4.7 and monthly performance for both years can be seen in Figure 4.27 and Figure 4.28.

The model overpredicted overflow from 2013 and underpredicted overflow for 2014. On average over the course of the two growing seasons, the model was within 10mm (0.4in) on a monthly basis with the model typically overpredicting overflow. The worst month was July 2014 with the model overpredicting overflow by 27mm (1 inch), or roughly 24% of the monthly total rainfall. This is quite remarkable given the high variability of the system paired with a simplistic methodology for calculating reference ET as well as a simplistic day to day water budgeting system. For future work, it will be interesting to compare predicted soil moisture with measured soil moisture using soil moisture probes.

Table 4.7: Summary of monthly and annual performance of model using green roof data.

	2013		2014	
Month	**Measured Overflow (mm)**	**Modeled Overflow (mm)**	**Measured Overflow (mm)**	**Modeled Overflow (mm)**
April	2	12	152	143
May	17	16	97	78
June	109	129	10	4
July	33	25	7	34
August	75	69	18	16
September	6	15	2	1
October	39	49	38	25
November	56	59	56	43
Yearly Total	**337**	**374**	**380**	**344**

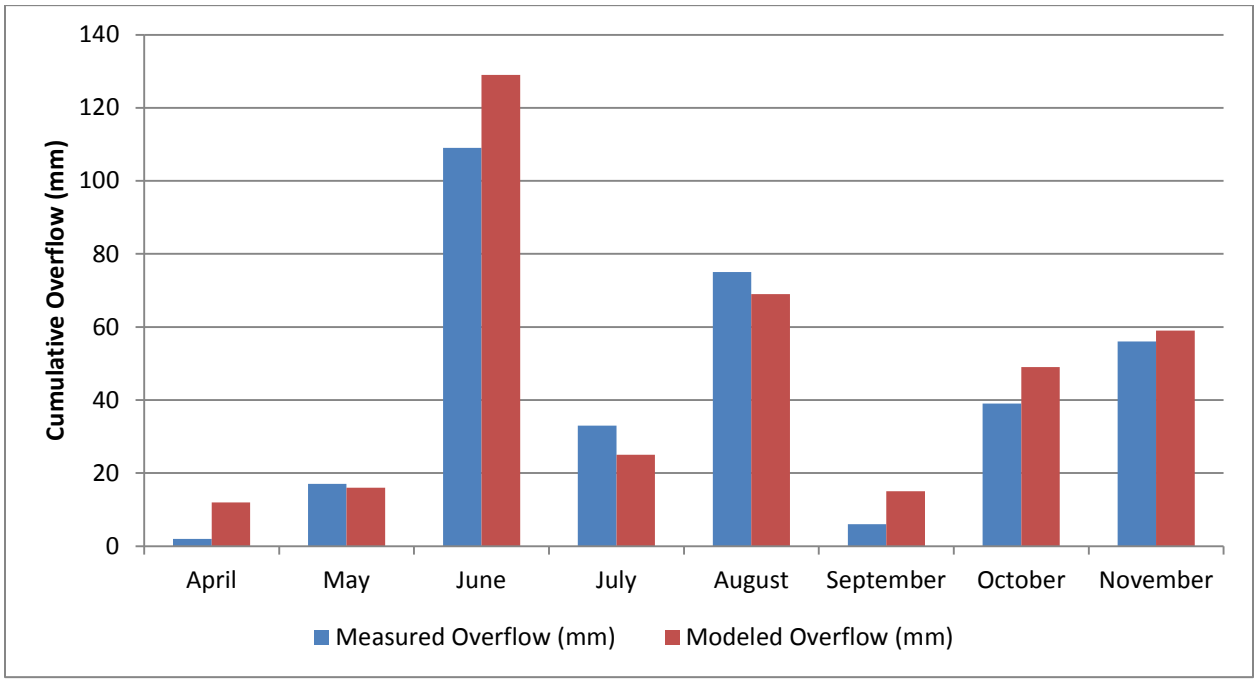

Figure 4.27: 2013 Measured vs. Modeled Overflow

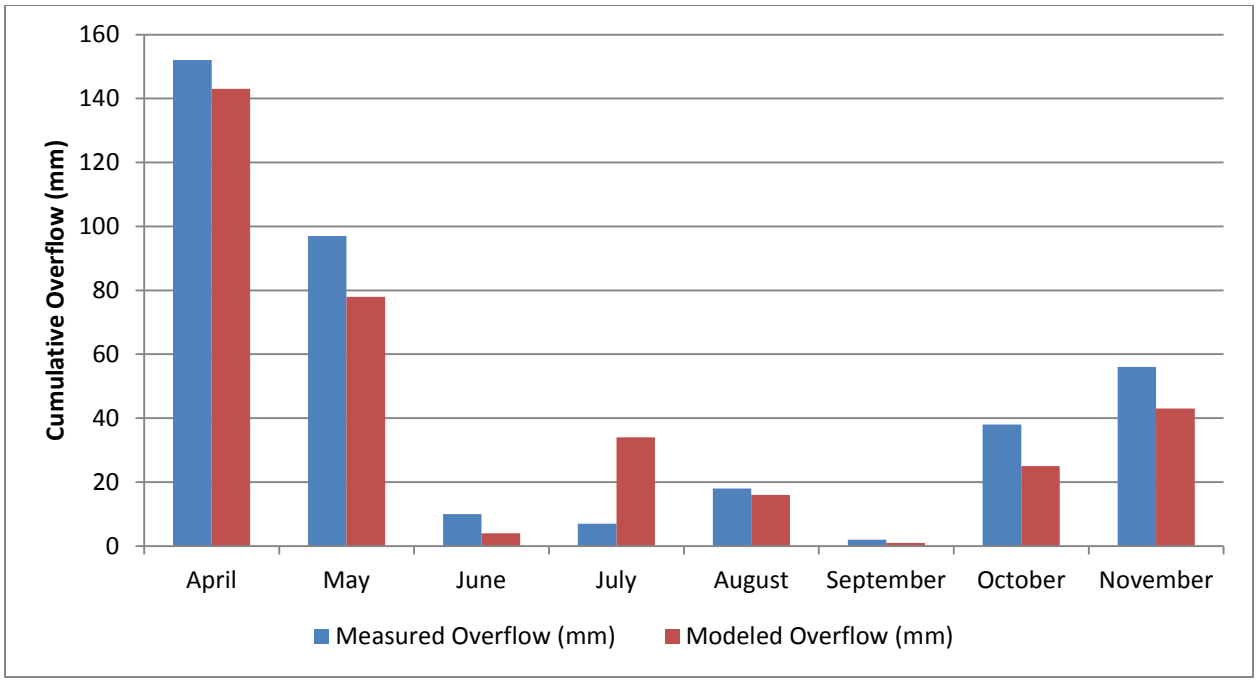

Figure 4.28: 2014 Measured vs. Modeled Overflow

The model overpredicted overflow from 2013 and underpredicted overflow for 2014. On average over the course of the two growing seasons, the model was within 10mm (0.4in) on a monthly basis with the model typically overpredicting overflow. The worst month was July 2014 with the model overpredicting overflow by 27mm (1 inch), or roughly 24% of the monthly total rainfall. This is quite remarkable given the high variability of the system paired with a simplistic methodology for calculating reference ET as well as a simplistic day to day water budgeting system. For future work, it will be interesting to compare predicted soil moisture with measured soil moisture using soil moisture probes.

4.2.3 Model Discussion

The model performed well using the original Hargreaves equation for reference ET paired with the soil moisture extraction function (Equation 3.13). On average the model was within 10% (±8%) of the measured cumulative ET and typically underpredicted it. An error of 10% is

considered to be quite good and within reasonable expectations. 2010 and 2011 had the greatest difference between measured and modeled ET with 21% and 20%, respectively. It is believed that this large difference is due to the fact that both of these years had hurricanes late in the season and the model overpredicted overflow from the system.

In the case of modeling the entire green roof, the maximum water retention was changed to reflect the differences between the freely drained green roof and the restricted drainage of the lysimeter. As expected, the total overflow increased and cumulative ET decreased because the amount of available water for ET was less than in the lysimeter. However, over the two years modeled, 2013 overpredicted overflow by ~10% and 2014 underpredicted overflow by ~10%.

Because the entire green roof is not equipped with a means to measure ET on a daily rate the model cannot be truly verified for the green roof system. However, given how well the model predicted lysimeter performance it can perhaps be used to predict daily ET values within the green roof. It follows that if the model is correctly predicting ET, then storage volume will be recharged as it is in the actual system and the model should predict similar overflow as seen in reality. Given how the model predicts actual ET as a function of soil moisture, it can be expected that when both systems are saturated, they have the same daily ET. Because of the same saturation level, the internal water storage is reduced by the same amount. Since it has been reduced similarly, the green roof will have a larger moisture deficit since its maximum storage capacity is roughly half of the lysimeter; therefore the ET for the next day will be greater in the lysimeter than it is in the green roof. Because of the lower storage capacity, the green roof system will theoretically dry out quicker than the lysimeter; this has been shown to be true by looking at total plant coverage in each system during drought periods, where the lysimeter still appears healthier than the entire green roof.

This combination of the Hargreaves equation for reference ET and the soil moisture extraction function can serve as a more appropriate model when used for predicting antecedent moisture condition when attempting to model media performance in continuous simulation models, such as that proposed by Liu and Fassman-Beck (2014). While other models, such as those proposed by She and Pang (2009), showed reasonable results using an exponential decay function, this may not be appropriate for cooler months when there is not enough energy to reach the levels of ET that were predicted using an exponential decay function. As seen in Figure 4.29 and Figure 4.30, in cooler months and in drought months, there is a more consistent rate of ET rather than the exponential decay seen in wetter periods. The Hargreaves reference ET equation, while requiring significantly fewer parameters, still provides a reasonable upper bound for ET depending on the time of year, and the soil moisture extraction function serves as a smoothing function for limiting ET based on soil moisture ensuring that ET cannot exceed available water within the system.

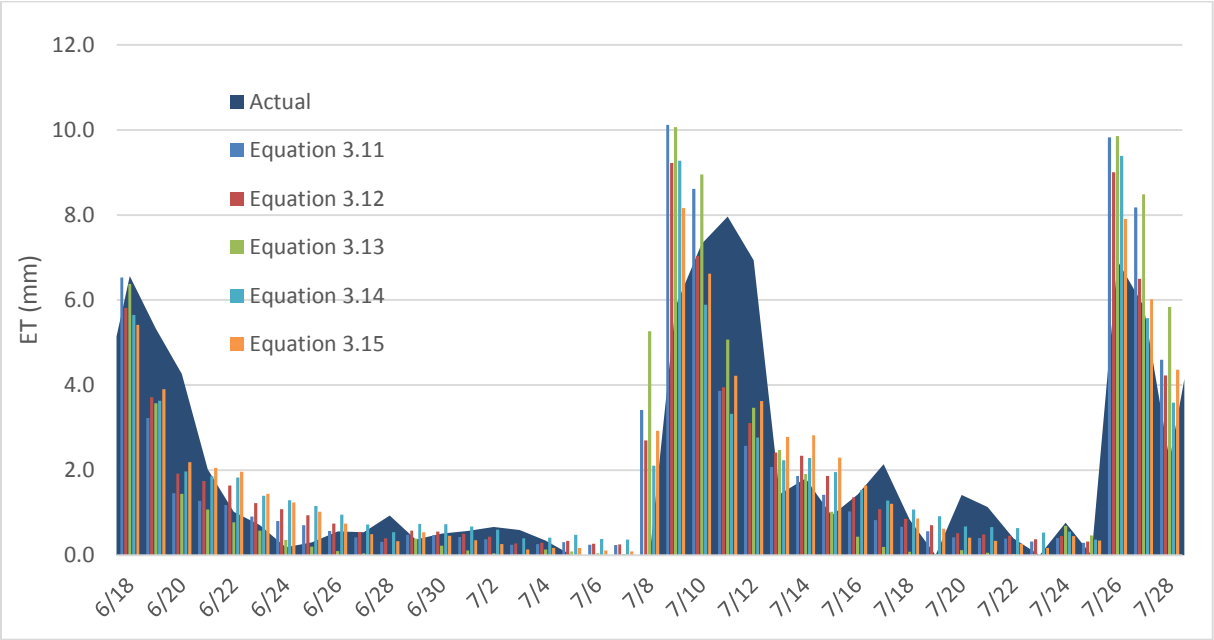

Figure 4.29: Drought Month Performance

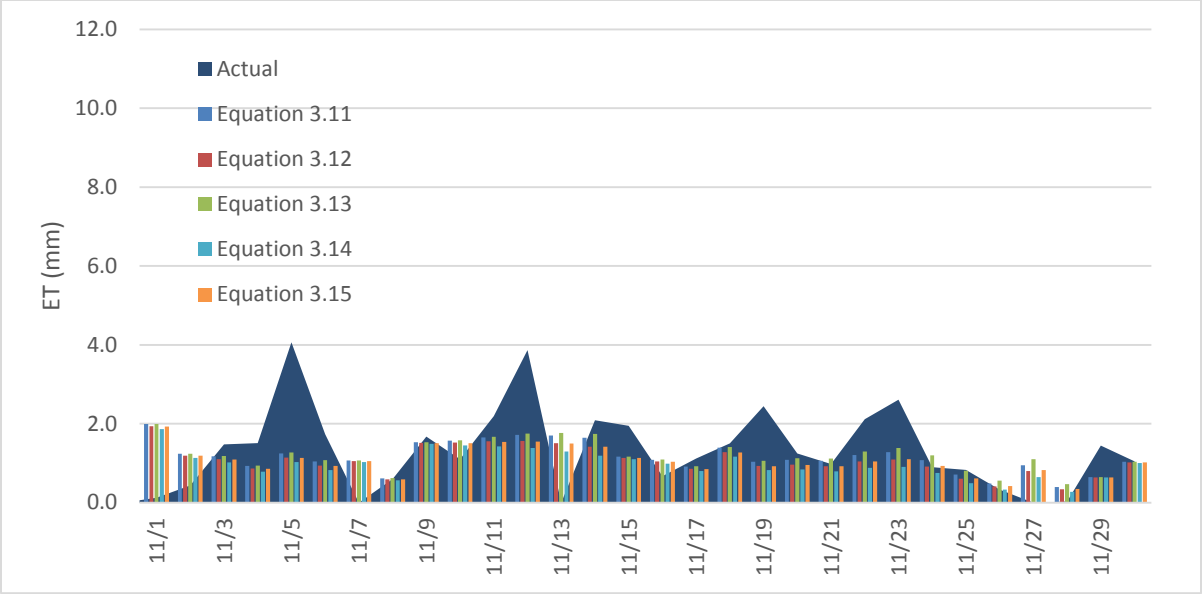

Figure 4.30: Cooler Month Performance

4.3 Hargreaves vs. FAO56

While there have been many equations proposed for calculating reference ET (ET_o) (e.g. Penman, Penman-Monteith, Thornwaite, Blaney Criddle, Hargreaves, etc.) the most widely accepted methodology is the modified Penaman-Monteith equation as described by The Food and Agricultural Organization Technical Publication 56 (FAO 1998). One of the key benefits of the FAO 56 methodology is its ability to take into account a wide range of weather parameters, such as temperature, relative humidity, and wind speed, as well as physical characteristics of the system, such as crop height and aerodynamic resistance to provide a more accurate approximation of daily ET_o. While other equations, such as the Hargreaves equation used in this model, only require daily temperature data and uses a calculated terrestrial radiation. The question remains, is a simpler model justified for evaluating green infrastructure? If you look at the historical development of reference ET equations, it was primarily driven by the need to accurately predict water usage in agricultural settings. Unlike large farm fields, green stormwater infrastructure is typically not measured in square kilometers; rather they are measured in square

meters. Also they are typically not in large expansive fields, rather tucked away in any available space on site often overshadowed by tall buildings in an urban environment. While Villanova's green roof is heavily instrumented for research purposes, most stormwater infrastructure is not, therefore trying to obtain values for wind speed, relative humidity, and solar radiation can be particularly difficult given the existence of microclimates, particularly in urban environments. As a basis for comparison, a site specific comparison of the widely accepted FAO56 methodology was compared to the simpler Hargreaves model to see if there were any significant differences between the two methodologies. Plotted in Figure 4.31 through Figure 4.36 is annual comparison of each for 2009 through 2014, the orange line on each is the 1:1 relationship. Table 4.8 summarizes statistical analysis performed for each year including total cumulative ET_o, average daily ET_o, as well as results from T-tests to determine if the two values are similar.

It is shown that for the green roof site at Villanova University, both the widely accepted FAO56 and the Hargreaves equations provide statistically similar results for reference ET. Although Hargreaves always overpredicts ET, it is not by much. 2010 was the worst year for comparison with the T-test providing a value of 0.061, which is just above the 0.05 threshold of being similar. Hargreaves also overpredicted ET by 0.5mm on an average daily basis which equated to almost 200mm on an annual basis. Interestingly the proposed model also performed the worst during 2010, severely underpredicting cumulative ET. Had the FAO56 methodology been employed, the model would have been further off given the lower ET rates estimated by FAO56. Given that green infrastructure sites are not typically the same as agricultural sites, perhaps equations for predicting reference ET for agricultural sites do not warrant the need for difficult to obtain parameters. For green infrastructure planning and crediting, simpler reference ET equations can be employed.

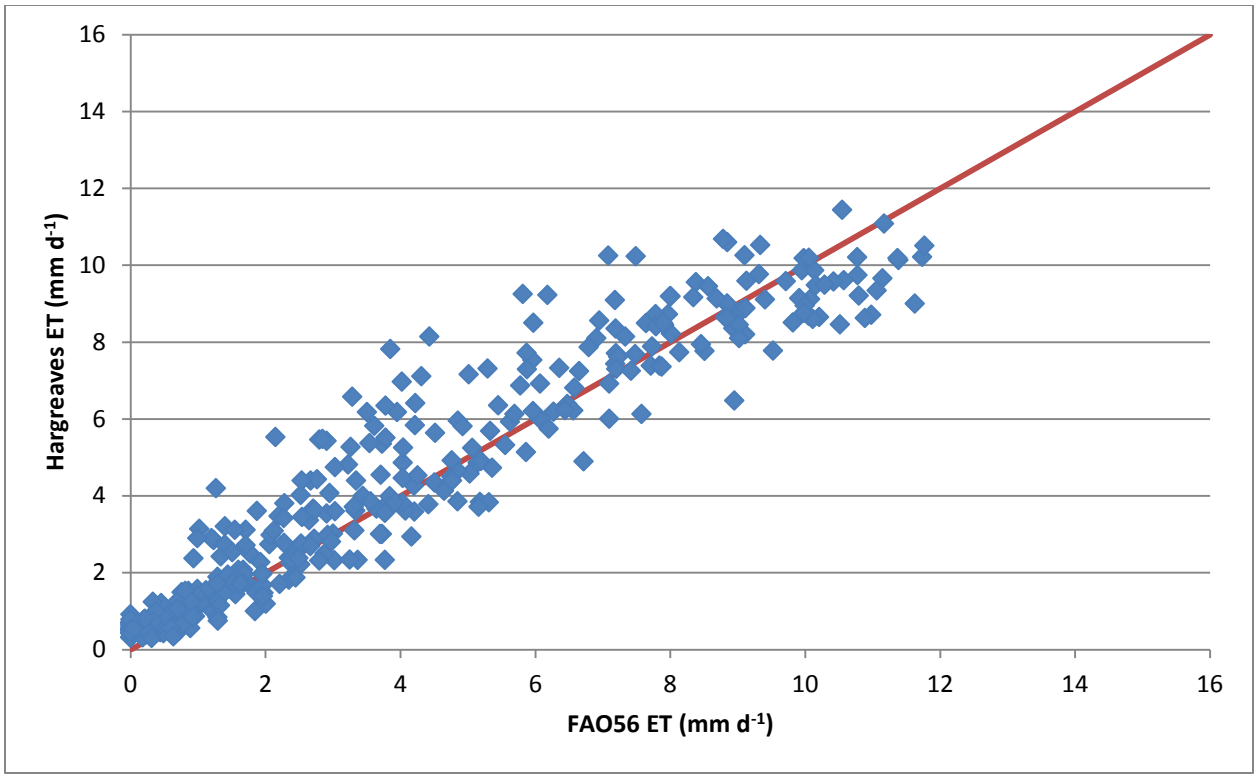

Figure 4.31: FAO56 VS. Hargreaves for 2009 Climactic Data

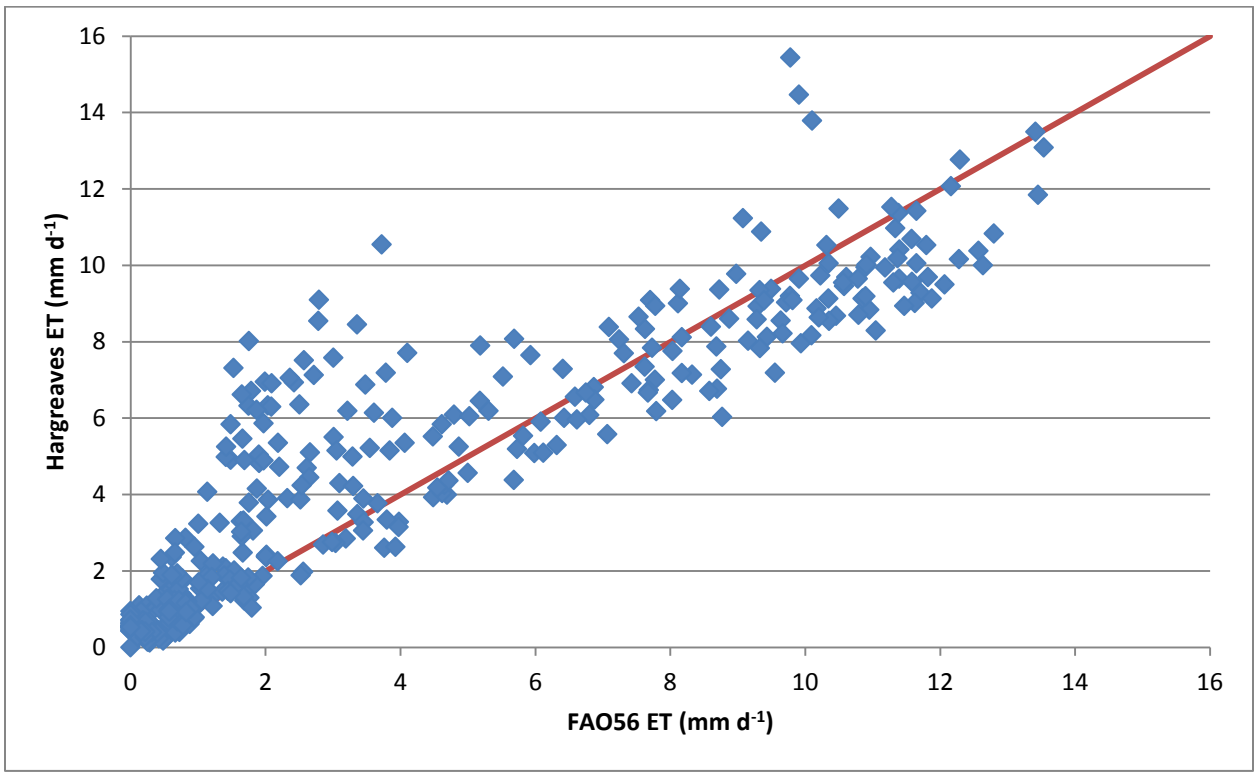

Figure 4.32: FAO56 VS. Hargreaves for 2010 Climactic Data

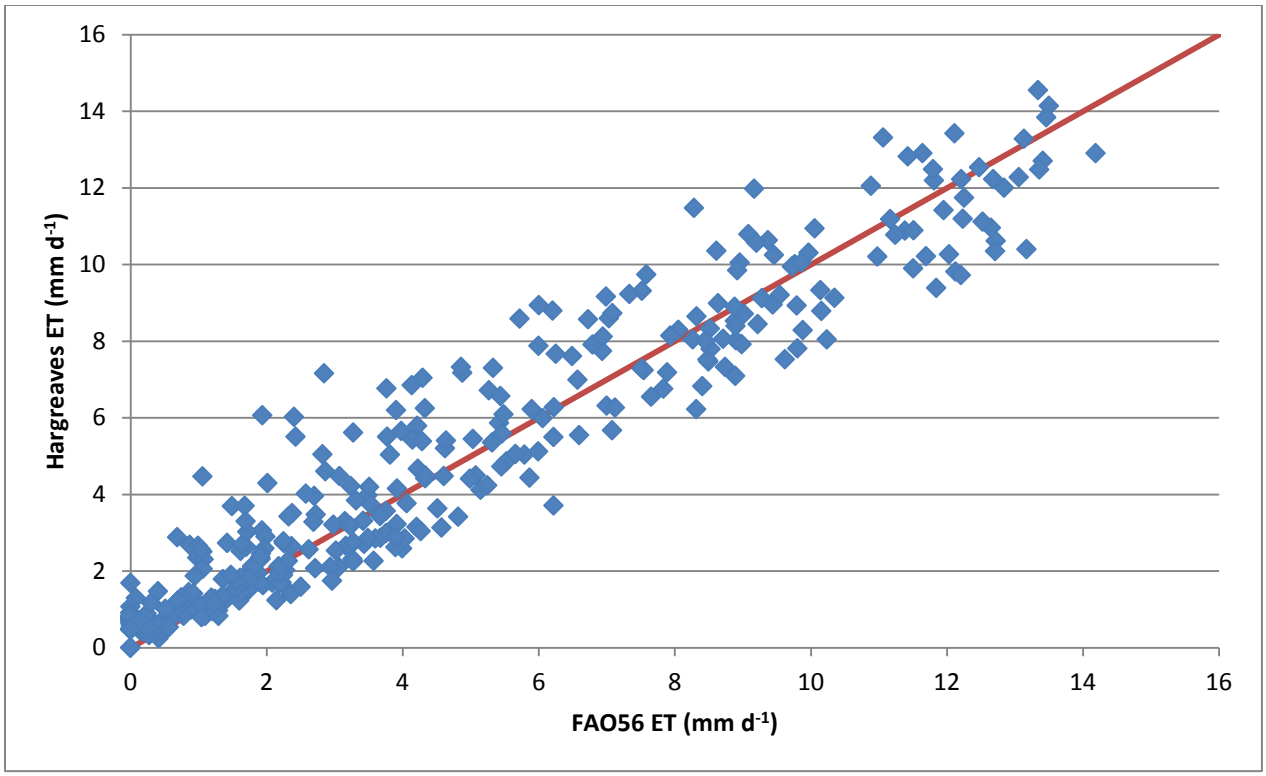

Figure 4.33: FAO56 VS. Hargreaves for 2011 Climactic Data

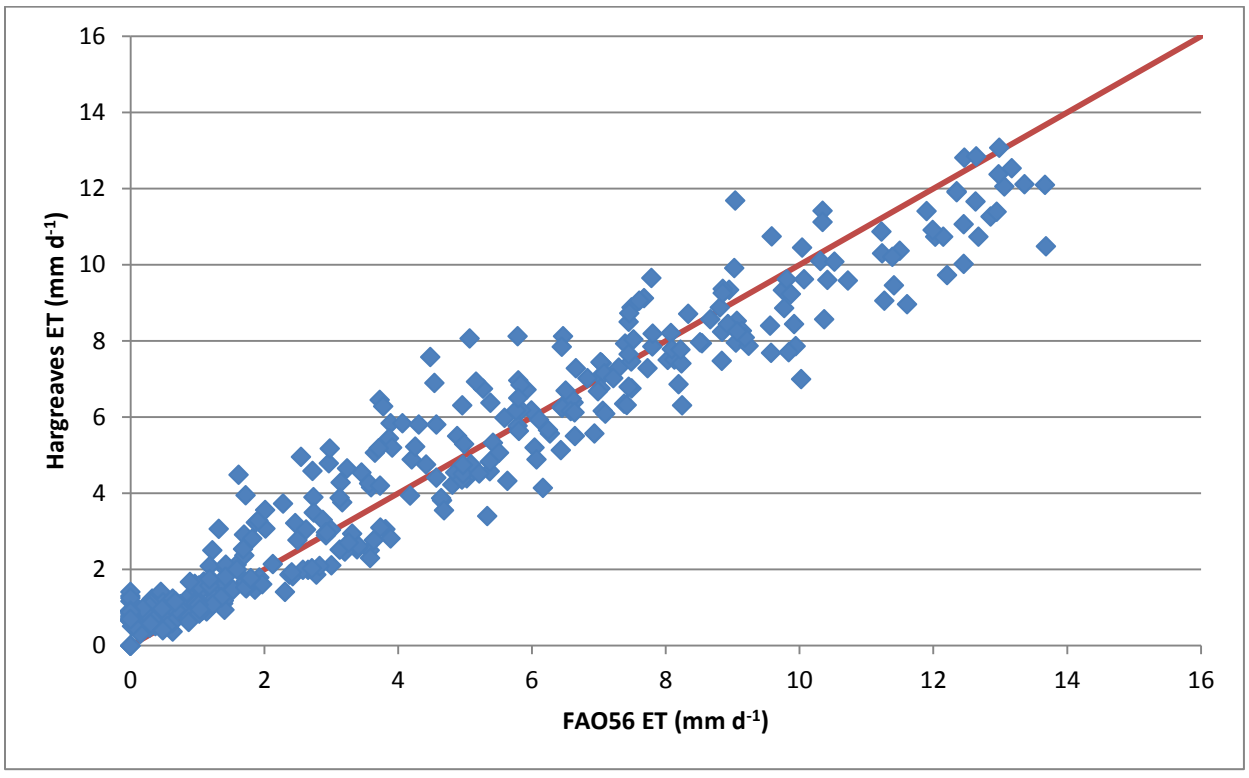

Figure 4.34: FAO56 VS. Hargreaves for 2012 Climactic Data

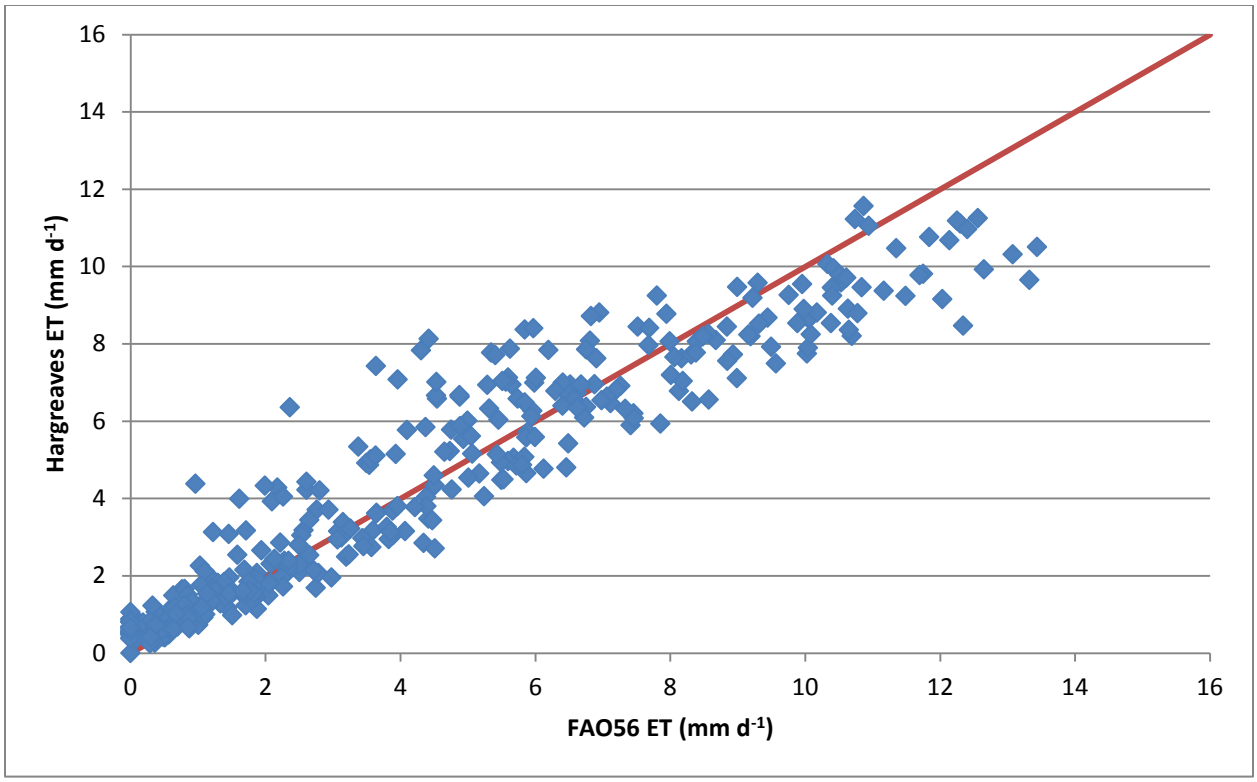

Figure 4.35: FAO56 VS. Hargreaves for 2013 Climactic Data

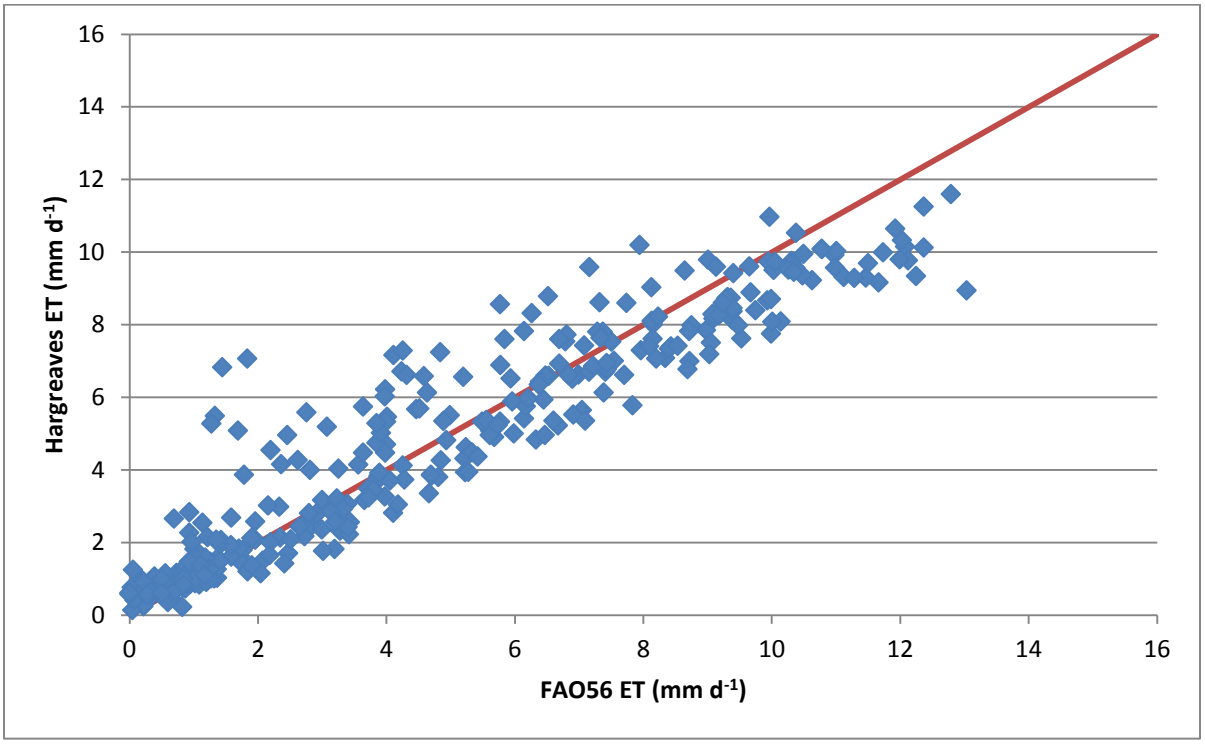

Figure 4.36: FAO56 VS. Hargreaves for 2014 Climactic Data

Table 4.8: Statistical Analysis of FAO56 vs. Hargreaves. Note, no T-test yielded a statistically significant difference between datasets.

	2009		2010		2011	
	FAO56	**Hargreaves**	**FAO56**	**Hargreaves**	**FAO56**	**Hargreaves**
Cumulative ET	1447	1563	1509	1705	1594	1682
Average Daily	4.04	4.37	4.22	4.75	4.49	4.74
Count	358	358	365	365	355	355
T-Test	0.186		0.061		0.396	
	2012		**2013**		**2014**	
	FAO56	**Hargreaves**	**FAO56**	**Hargreaves**	**FAO56**	**Hargreaves**
Cumulative ET	1638	1666	1578	1592	1580	1588
Average Daily	4.50	4.55	4.32	4.36	4.74	4.71
Count	364	364	365	365	333	333
T-Test	0.775		0.884		0.144	

CHAPTER 5. CONCLUSIONS AND FUTURE WORK

This chapter will summarize the comparisons between the weighing lysimeter and the green roof as well as the results from the proposed model. A discussion on future work and research questions is included as well as a brief overview of the future transformation of the green roof. The section concludes with closing thoughts on green roofs and how they play a role in stormwater infrastructure.

5.1 Lysimeter vs. Entire Roof Performance

One of the primary focuses of the present research was to determine how accurately the lysimeter's performance matched up with the overall performance of the entire green roof system. While the lysimeter served as an acceptable proxy to help close the mass balance for measuring ET, it consistently showed higher annual ET volumes than was estimated on the green roof from overflow data. For 2013, the green roof had 38% of its total precipitation lost to overflow resulting in 563mm of ET, for 2014, it was slightly less with 44% of total inflows becoming overflow leaving only 468mm for ET. However, for the lysimeter, 2013 and 2014 measured 680mm and 675mm of ET, respectively. It is believed that this difference in ET between the green roof and lysimeter is due to the differences in the drainage configurations of each system and how they affect available water over the course of a growing season. The lack of an underdrain in the lysimeter required the media to reach complete saturation before any overflow could occur and free drainage by gravity was nonexistent. This setup allowed the total water holding capacity for the lysimeter to be just over 43mm (1.7in) whereas with the underdrained roof system, the total water holding capacity was closer to 20mm (0.8in).

The substantially larger retention capacity meant that the lysimeter was able to completely capture more storm events, and therefore more total volume over the course of the study period, than the entire green roof. This further confirms that ET is highly available water dependent and suggests that the system would be capable of evapotranspirating more stormwater if the system was designed to retain more water within its profile.

Retaining more stormwater on the roof could be accomplished by modifying the overflow drain height to create an artificial water table within the system or even choosing a drainage board with deeper cups than discussed in Section 3.1.1 that will allow more water to be held within the profile. Restricting drainage to create a water table within the system could be done using an automatically controlled outflow drain or by a manually adjusted configuration that could be changed with the season or to meet the storage criteria for a particular event.

5.2 Predictive Evapotranspiration Model

A model was proposed to predict ET for green roof systems. The system's potential for ET, in both field conditions as well as modeled, is limited by water availability. Utilizing soil moisture extraction functions, which are a function of available water and the maximum available water of the system, reduction factors for reference ET are used to estimate actual evapotranspiration from the lysimeter or green roof. In order to track these daily changes, a simple accounting system was used for long-term modeling of the system which accounts for rainfall, overflow, and predicted ET. Results from the previously modeled day dictate the available water within the system which in turn affects system performance of the current day.

The model performed well over the course of the growing season with differences between measured and estimated ET less than 7% for the lysimeter. The predicted soil moisture also

showed a close relationship to the measured weight of the lysimeter, which could be used as a proxy for estimating actual soil moisture within the lysimeter. Total overflow volume was fairly similar between the measured and observed values for the 6 years of data with the model typically only overpredicting overflow by 10mm (0.4 in) and underpredicitng ET by 9mm (0.35 in) on a monthly timescale

While the model has only been applied to one green roof test site and needs further verification, it appears to provide a reasonable estimate for predicting antecedent moisture conditions and may prove to be more useful for continuous modeling as opposed to the exponential decay functions used in other models, such as that proposed by She and Pang (2009). While many of the soil moisture extraction functions operate as an exponential decay, pairing the soil moisture relationship discussed in this research with the Hargreaves equation for reference ET, helps to limit ET especially in the colder months in the beginning or towards the end of the growing season and better match field observations.

5.3 Future Work

Future work on the proposed model still remains. A regional calibration of the Hargreaves equation should be performed against the FAO56 methodology for reference ET as discussed by Gavilán et al. (2006). The model should also be verified at additional green roof sites both within the region, and if possible, other climate regions. Since most green roofs typically do not have the same level of instrumentation as a research site may have, a sensitivity analysis should be performed as well to study the effect of using local weather data has on modeled performance. For Villanova's green roof, the layout of the building allows for a different microclimate due to shading and wind protection that may not be represented by nearby weather station such as St.

David's Golf Course or Philadelphia International Airport, which could be used for predicting green roof performance of a non-instrumented site.

While the present research has shown the differences in performance between the freely drained green roof and the restricted drainage lysimeter to be substantial, it will be interesting to see if performance of the entire green roof is able to be enhanced by restricting the drainage. Starting in 2015, a modification will be made to the existing roof drain to elevate the overflow point too slightly above the hard surface of the roof. By doing this, any runoff from the aluminum flashing as well as the rock perimeter will be held within the system helping to eliminate any overflow from smaller storm events. This restriction will also allow the lower profile of the green roof system (drainage board and lower portion of media) to reach full saturation during larger storm events. This additional retention will help to increase total annual runoff reduction and therefore total ET.

Another area for future work is the rock perimeter as well as the aluminum flashing surrounding the green roof. While this is an essential component of all green roofs to help eliminate the possibility of damage to the structure from the plants as well as the media, this area is typically allowed to drain freely and leads to surface runoff even in the smaller events. It will be interesting to see how much this area of a green roof system actually contributes to overflow and if there is any evaporation in these areas and to quantify how much it can affect the systems total performance. One idea for reducing the amount of rapid overflow is to install baffles within the perimeter to force any small amounts of runoff into the growing media therefore increasing the total travel time and time of concentration for these areas. However, it is still important for extreme events that runoff is able to make its way to the drain to prevent flooding on the roof

therefore the top of the baffles should be below the surface of the growing media to facilitate this.

While the weight of the lysimeter served as an acceptable proxy for estimating soil moisture conditions for this study, the addition of soil moisture sensors within the growing media profile will allow for the future measurement of ET on the entire green roof for smaller time scales rather than an event to event basis. Until recently, many soil moisture sensors were either not recommended for green roofs or provided poor measurements due to the unique characteristics of the media. With the addition of several sensors across the roof, it is hoped that a fairly accurate representation of moisture condition can be used for ET measurement.

Future research on green roofs at Villanova will hopefully look into the role vegetation as well as media type and thicknesses have on overall performance. With the additions being constructed on the engineering building (CEER) it is hoped that additional green roof test sites can be constructed to further the University's green roof living laboratory. Test plots with different media thicknesses as well as varying species of plants can be independently monitored and compared. The addition of a bare media roof will also allow future research to help isolate the role plants play in these systems. While most of the research on Villanova's existing green roof has been focused on stormwater reduction as well as quantifying ET, having several test sites will allow for more interdisciplinary research on green roofs. Looking from a sustainability and heat transfer perspective, how do different plants affect internal temperatures of a building? Can green roofs be optimized for insulating structures as well as for reducing stormwater? Looking at green roofs from a social perspective can provide another interesting avenue of research. As cities continue to grow, can green roofs be used to provide an economic net benefit by serving as

either a place for growing crops for consumption or serve as an opportunity to install solar panels for power generation?

In addition to several extensive green roofs being proposed for the additions to CEER, the possibility of an intensive green roof atop one of the main portions of the remodel can serve as a valuable addition for future green roof research. Performance comparisons as well as cost benefit analysis are all interesting paths of future research.

One area of rooftop stormwater control research that has been overlooked at Villanova is the use of blue roofs. Blue roofs act as temporary detention basins reducing the time to peak as well as peak runoff from a rooftop. Blue roofs are non-vegetated roofs with restricted drainage to allow temporary ponding. These systems can be used in sites where green roofs may be too costly for the property owner or the existing structure is unable to support the additional weight of an extensive green roof.

A recently awarded grant will provide funding for research on automating the green roof for optimal stormwater performance. A tank will be located on the third floor of CEER and will collect water from a portion of traditional roof. This water will be stored and used as the green roof needs it. Soil moisture sensors will be able to indicate when the media is approaching the wilting point and trigger the irrigation of the selected region of the roof. Real time monitoring and control as well as decision making will be provided using OptiRTC. This will enable to the system to observe future weather patterns and determine how the roof should be irrigated in order to recharge the storage for any incoming weather or if it needs to drain the storage tank in order to capture more of the runoff from the traditional roof. The smart system will enable the optimization of multiple uses of the green roof. This will enable the green roof to mitigate both

rainfall landing directly on the system, as well as additional contributing area. The use of stored stormwater for irrigation purposes can facilitate the use of plants that may be less drought tolerant than the typically used sedum species. Additionally it will allow for dynamic operations of the green roof as its performance changes seasonally.

This recent grant will open up research possibilities for four key research goals. The first will be how to best design and size a self-learning and adapting green roof. Secondly, after a few years of data has been collected, comparing pre-upgrade performance and see how the system has enhanced the green roof overall. Third, comparing total volume captured and used from the traditional roof compared to the total volume of rainfall that has fallen on that portion of the roof, and seeing if this system has made a significant impact on the total stormwater generated from the site. Lastly, as systems like this become more and more common place, the need for cheap data is essential. The cost for accurate measuring and monitoring equipment could often times dwarf the cost of installing the entire green roof itself, but is this level of accuracy really necessary for these systems and can cheaper sensors be used for the same purposes and still provide relatively accurate data or data that is acceptable enough to use for non-research caliber installations of systems like these?

5.4 Closing Thoughts

Evapotranspiration is a consistent process that should be used toward reliable water volume reduction within stormwater control measures. Research at Villanova has shown that ET totals average more than 750 mm over the April through November growing season. This when extended over the course of the entire year, including a 50% reduction for winter months, still totals more than 900mm per year. On an annual basis, the ET measured from the lysimeter

accounts for over 75% of the water budget for this area and should not be neglected as a volume reduction strategy. Unfortunately many municipal and state stormwater regulatory agencies still rely on simplified methodologies and design storms for implementing SCMs. It is impossible to assign a single value on how well a green roof will perform for a design storm given the dynamic nature of the system. Each storm has different initial conditions as well as different characteristics throughout its lifespan and the green roof will elicit a different response to every storm. By changing designs of systems to retain more water, we can optimize the amount of volume reduction obtained from ET.

Designing for ET volume reduction can raise several issues. As ET is an energy dependent process, ET rates vary throughout the course of the year and therefore require a changing design strategy. Assigning a single value for daily ET volume reduction is not the most appropriate way to tackle this problem as this would likely discount the amount of actual ET occurring. Using a seasonal or monthly average would provide a better result however since ET is also highly dependent on available water, continuous simulation with a water accounting system such as the one discussed in this thesis would provide the closest to reality results.

As we move into the next generation of smart green infrastructure, the opportunities for mitigating larger volumes of stormwater in smaller spaces and in less conventional ways will revolutionize the LID community. The switch from static to dynamic SCMs will also, in my humble opinion, require the push to continuous simulation rather than the use of single event design storms. As cities stormwater regulations change such as Philadelphia's move to increase the water quality volume from 25mm (1 in) to 38mm (1.5 in) (PWD, 2015), green roofs are going to become an integral part of mitigating stormwater at the source especially given the price of real estate in the urban areas so optimizing their design for maximum performance is going to

provide a greater rate of return on investment. With these design differences, ET is going to become a more and more significant component of the hydrologic cycle and will need to be able to be measured, estimated, and most importantly credited for the affect it has on stormwater volume reduction.

References

Allen, R.G., Luis S. Pereira, Dirk Raes, and Martin Smith. (1998). “Crop evapotranspiration - Guidelines for computing crop water requirements” Food and Agriculture Organization of the United Nations (FAO). FAO Irrigation and drainage paper 56. Rome.

ASTM E2777-14 – Standard Guide for Vegetative (Green) Roof Systems

ASTM E2396-11 – Standard Test Method for Saturated Water Permeability of Granular Drainage Media for Vegetative (Green) Roof Systems

ASTM E2397-11– Standard Practice for Determination of Dead Loads and Live Loads Associated with Vegetative (Green) Roof Systems

ASTM E2398-11 – Standard Test Method for Water Capture and Media Retention of Geocomposite Drain Layers for Vegetative (Green) Roof Systems

ASTM E2399-11– Standard Test Method for Maximum Media Density for Dead Load Analysis of Vegetative (Green) Roof Systems

ASTM E2400– Standard Guide for Selection, Installation, and Maintenance of Plants for Green Roof Systems

ASTM E2788-11– Standard Specification for Use of Expanded Shale, Clay and Slate (ESCS) as Mineral Component in the Growing Media and the Drainage Layer for Vegetative (Green) Roof Systems

Beven, K. (1979). "A sensitivity analysis of the Penman-Monteith actual evapotranspiration estimates." Journal of Hydrology, 44(3), 169-190.

Boivin, M.-A., Lamy, M.-P., Gosselin, A., and Dansereau, B. (2001). "Effect of artificial substrate depth on freezing injury of six herbaceous perennials grown in a green roof system." HortTechnology, 11(3), 409-412.

Breuning, Jorg. (Personal communication, February 20, 2014).

Carpenter, D., and Kaluvakolanu, P. (2010). "Effect of Roof Surface Type on Storm-Water Runoff from Full-Scale Roofs in a Temperate Climate." *Journal of Irrigation and Drainage Engineering*, 137(3), 161-169.

Church, M. R., Bishop, G. D., and Cassell, D. L. (1995). "Maps of regional evapotranspiration and runoff/precipitation ratios in the northeast United States." Journal of Hydrology, 168(1–4), 283-298.

Cohen, D. T. (2015). "Population Trends in Incorporated Places: 2000 to 2013." U. S. C. Bureau, ed.

Czemiel Berndtsson, J. (2010). "Green roof performance towards management of runoff water quantity and quality: A review." Ecological Engineering, 36(4), 351-360.

Davis, A.P., Traver, R.G., Hunt, W.F., Brown, R.A., Lee, R. and Olszewski, J.M. (2012). “Hydrologic performance of Bioretention Stormwater Control Measures.” Journal of Hydrologic Engineering, 17(5), 604-614.

District Department of the Environment Watershed protection Division District of Columbia (DDOE). (2012). Stormwater Management Guidebook

Environmental Protection Agency (EPA). (2008). Reducing Urban Heat Islands: Compendium of Strategies (Chapter 3). Washington, DC.

Fassman-Beck, E., Voyde, E., Simcock, R., and Hong, Y. S. (2013). "4 Living roofs in 3 locations: Does configuration affect runoff mitigation?" Journal of Hydrology, 490(0), 11-20.

Fassman, E., and Simcock, R. (2011). "Moisture Measurements as Performance Criteria for Extensive Living Roof Substrates." Journal of Environmental Engineering, 138(8), 841-851.

Elizabeth Fassman-Beck, P. D., William Hunt, P. D., Berghage, R., Carpenter, D., Kurtz, T., Stovin, V., and Wadzuk, B. (2015). "Curve Number and Rational Formula Coefficients for Extensive Living Roofs." *Journal of Hydrologic Engineering*, Manuscript Draft.

Feller, Meghan. (2010). “Quantifying Evapotranspiration in Green Infrastructure: A Green Roof Study.” MS Thesis, Villanova University.

FLL (2002). "Guidelines for Planning, Implementation, and Maintenance of Green Roofs”, Forschungsgesellschaft Landschaftsentwicklung Landschaftsbau EV, Bonn, Germany.

Gavilán, P., Lorite, I. J., Tornero, S., and Berengena, J. (2006). "Regional calibration of Hargreaves equation for estimating reference ET in a semiarid environment." Agricultural Water Management, 81(3), 257-281.

Graceson, A., Hare, M., Monaghan, J., and Hall, N. (2013). "The water retention capabilities of growing media for green roofs." Ecological Engineering, 61, Part A(0), 328-334.

Green Roof Guide, (No Date). Glossary of Green Roof Terms.
< http://www.greenroofguide.co.uk/glossary/>

Green Roof Technology, (No Date). Green Roof Types.
< http://www.greenrooftechnology.com/green-roof-types>

Hanson, R.L., 1991, “Evapotranspiration and Droughts”, National Water Summary 1988-89--Hydrologic Events and Floods and Droughts: U.S. Geological Survey Water-Supply Paper 2375, p. 99-104.

Haughwout, A., Orr, J., and Bedoll, D. (2008). "The price of land in the New York metropolitan area." Current Issues in Economics and Finance, 14(3).

Hess, Amanda. (2014). “Monitoring of Evapotrasnpiration and Infiltration In Rain Garden Designs.” MS Thesis, Villanova University.

Hoban, A., and Wong, T.H.F., (2006) “WSUD resilience to Climate Change”, 1st international Hydropolis Conference, Perth WA, October 2006.

Liu, R., and Fassman-Beck, E. "Unsaturated 1D Hydrological Process and Modeling of Living Roof Media during Steady Rainfall." Proc., World Environmental and Water Resources Congress (2014) Water Without Borders, ASCE, 209-221.

Magill, John. (2007). “A History and Definition of Green Roof ETchnology With Reccomendations for Future Research” MS Thesis, *Southern Illinois University Carbondale*.

Maryland Department of the Environment (MDE). (2000). Stormwater Design Manual Volumes 1 & 2.

Mayor’s office of Long-Term Planning and Sustainability, 2008. PlaNYC Sustainable Stormwater Management Plan, New York, NY.

Met-One. (1994). Model 375c 8” Rain Gauge, Operation Manual

Miller, C. (2003) "Moisture management in green roofs." Proc., Proceedings of the 1st Greening Rooftops for Sustainable Communities Conference, 177-182.

Monteith, J. L. (1965). "Evaporation and the Environment. The State and Movement of Water in Living Organisms." Proc., Symposium of the Society of Experimental Biologists, 205-224.

Monterusso, M. A., Rowe, D. B., and Rugh, C. L. (2005). "Establishment and Persistence of Sedum spp. and Native Taxa for Green Roof Applications." HortScience,40, 391-396.

Nagase, A., and Dunnett, N. (2010). "Drought tolerance in different vegetation types for extensive green roofs: Effects of watering and diversity." Landscape and Urban Planning, 97(4), 318-327.

NRCS. (1986). Urban hydrology for small watersheds. *US Soil Conservation Service. Technical Release, 55*

New York City Department of Environmental Protection (NYC DEP). (2012). Guidelines for the Design and Construction of Stormwater Management Systems.

Penman, H. L. (1948). "Natural evaporation from open water, bare soil and grass." Proceedings of the Royal Society of London. Series A, Mathematical and Physical Sciences, 193, 120-145.

Philadelphia Water Department (PWD). (2011). Stormwater Management Guidance Manual.

Philadelphia Water Department (PWD) (2015). Stormwater Regulation Updates. < http://www.phillywatersheds.org/stormwaterregulations >

Philippi, P.M. (2006). "How to Get Cost Reduction In Green Roof Construction" *Proc., Greening Rooftops for Sustainable Communities*, Boston MA.

Philly.com. (2013). 5 Weather Records Set in Philadelphia in Summer 2013. < http://www.philly.com/philly/blogs/phillylists/5-weather-records-set-in-Philadelphia-in-summer-2013.html >

Schneider, Dominik. (2011). "Quantifying Evapotranspiration from a Green Roof Analytically." MS Thesis, Villanova University.

Schroll, E., Lambrinos, J., Righetti, T., and Sandrock, D. (2011). "The role of vegetation in regulating stormwater runoff from green roofs in a winter rainfall climate." Ecological Engineering, 37(4), 595-600.

She, N., and Pang, J. (2009). "Physically Based Green Roof Model." Journal of Hydrologic Engineering, 15(6), 458-464.

Stovin, V. (2010). "The potential of green roofs to manage Urban Stormwater." Water and Environment Journal, 24(3), 192-199.

Spatari, S., Yu, Z., and Montalto, F. A. (2011). "Life cycle implications of urban green infrastructure." *Environmental Pollution*, 159(8–9), 2174-2179.

VanWoert, N. D., Rowe, D. B., Andresen, J. A., Rugh, C. L., Fernandez, R. T., and Xiao, L. (2005). "Green Roof Stormwater Retention" J. Environ. Qual., 34(3), 1036-1044.

VanWoert, N. D., Rowe, D. B., Andresen, J. A., Rugh, C. L., and Xiao, L. (2005). "Watering Regime and Green Roof Substrate Design Affect Sedum Plant Growth." HortScience, 40(3), 659-664.

Voyde, E., Fassman, E., and Simcock, R. (2010). "Hydrology of an extensive living roof under sub-tropical climate conditions in Auckland, New Zealand." *Journal of Hydrology*, 394(3–4), 384-395.

Wadzuk, B., Schneider, D., Feller, M., and Traver, R. (2013). "Evapotranspiration from a Green-Roof Storm-Water Control Measure." Journal of Irrigation and Drainage Engineering, 139(12), 995-1003.

Wadzuk, B. (2013). “How Best to Take Credit for ET in Green Roofs – A Roundtable Discussion” PA Stormwater Symposium, Villanova University. 17 October.

Welker, A.L. (2014). CEE 8103: Geosynthetics Course. *Villanova University.*

Wolf, D., and Lundholm, J. T. (2008). "Water uptake in green roof microcosms: Effects of plant species and water availability." Ecological Engineering, 33(2), 179-186.

(WMO), W. M. O. (2008). "Guide To Hydrological Practices." *Evaporation, Evapotranspiration, And Soil Moisture*, World Meteorological Organization (WMO), Geneva Switzerland.

Zhao, L., Xia, J., Xu, C.-y., Wang, Z., Sobkowiak, L., and Long, C. (2013). "Evapotranspiration estimation methods in hydrological models." J. Geogr. Sci., 23(2), 359-369.

Appendix A

Green Roof original Specifications

rooflite®
Certified Green Roof Media

Typical Green Roof Media Analysis for rooflite® extensive mc

Results on dry weight basis unless specified otherwise

Analysis	Units	Results*	FLL** Requirements
Particle Size Distribution (See accompanying graph)			
Proportion of silting components (d < 0.063 mm)	mass %	5 - 10	< 15
Density Measurements*			
Bulk Density (dry weight basis)	g/cm^3	0.70 – 0.85	
Bulk Density (dry weight basis)	lb/ft^3	44 - 53	
Bulk Density (at max. water-holding capacity)	g/cm^3	1.15 – 1.35	
Bulk Density (at max. water-holding capacity)	lb/ft^3	72 - 85	
Water/Air Measurements			
Total Pore Volume	Vol. %	65 - 75	
Maximum water-holding Capacity	Vol. %	40 - 55	≥ 35 ≤ 65
Air-Filled Porosity (at max water-holding capacity)	Vol. %	15 - 25	≥ 10
Water permeability (saturated hydraulic conductivity)	cm/sec	0.02 – 0.08	0.001 – 0.12
Water permeability (saturated hydraulic conductivity)	in/min	0.47 – 1.89	0.024 – 2.83
pH and Salt Content			
pH ($CaCl_2$)		7.5 – 8.5	6.0 - 8.5
Soluble salts (water extract)	g /L	1.5 – 3.0	< 3.5
Organic Measurements			
Organic matter content	g/L	30 - 45	< 65
Nutrients			
Phosphorus, P_2O_5 (CAL)	mg/L	150 - 200	≤ 200
Potassium, K_2O (CAL)	mg/L	400 - 700	≤ 700
Magnesium, Mg (CaCl2)	mg/L	150 - 200	≤ 200
Nitrate + Ammonium (CaCl2)	mg/L	10 - 40	≤ 80

* *Listed range of values is typical for the Mid Atlantic region*

** *All values are based on compacted materials according to laboratory standards and testing methods defined by the Forschungsgesellschaft Landschaftsentwicklung Landschaftsbau e.V.(FLL)*
Landscape Development and Landscaping Research Society e.V.
Guidelines for the Planning Construction and Maintenance of Green Roofing, Green Roofing Guideline, 2008

www.skylandusa.us

Figure A1: Typical Green Roof Media Analysis for Rooflite Extensive MC

rooflite®
Certified Green Roof Media

Typical Particle Size Distribution for rooflite® extensive mc

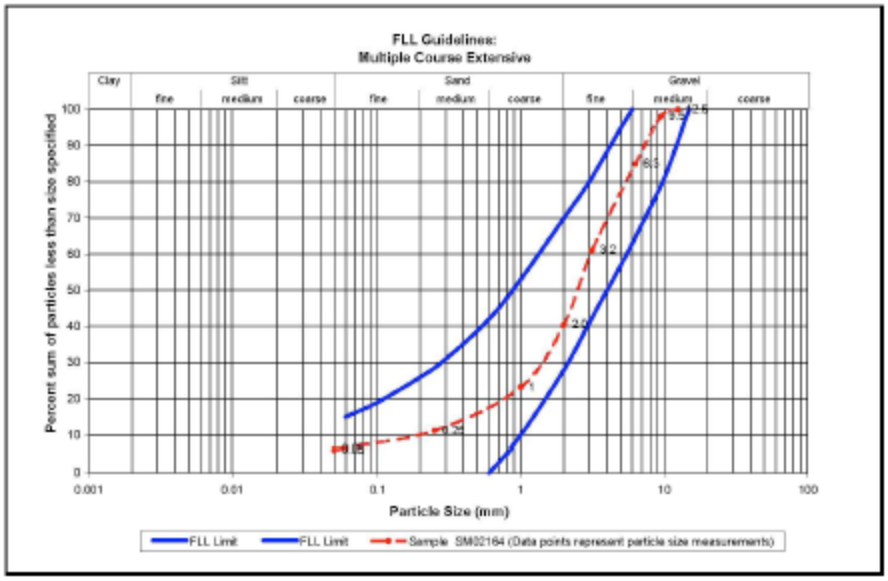

Figure A2: Typical Particle Size Distribution for Rooflite Extensive MC Media

OPTIGREEN
ROOF GREENING

Data Sheet **Optigreen-Drain-Element FKD 25 (W)**

Product Name:	Drain element FKD 25 (CE 1213-CPD-4265)	
	Made from deep-drawn, environmentally friendly, regenerated HDPE with water storage and discharge delay channels with a dewatering channel system on the underside	
	This product has received CE marking pursuant to EN 13252	
	Material:	Recycled HDPE
	Nominal thickness:	approx. 25 mm
	Area weight:	1.35 kg/sqm
	Colour:	grey-black
Technical data and Properties:	Pressure resistance pursuant to DIN EN ISO 25619-2	251 kPa
	Water discharge capacity pursuant to DIN EN ISO 12958	
	20 kPa, soft/hard, MD. With fleece layer filter mat 105 g on upper side	
		l/(s*m)
	i = 0,01 (ca. 1 %)	0,99
	i = 0,02 (ca. 2 %)	1,41
	i = 0,05 (ca. 5 %)	2,2
	i = 0,10 (ca. 10 %)	3,13
	i = 1 (senkrecht)	10,03
	Filling volume: Small knob facing upwards (inscription mirror-inverted) = approx. 14.5 l	
	Large knob facing upwards (inscription legible) = approx. 7.5 l	
	Water storage: small knob facing upwards (inscription mirror-inverted) = approx. 5 l	
	(unfilled) large knob facing upwards (inscription legible) = approx. 5 l	
Delivery form:	Boards á 2 sqm, 2 m length, 1 m width	
Area of application:	- underneath extensive greenings	
	- underneath walkable coverings for care and maintenance purposes	
Storage:	Dry, protect against UV during extended storage	
Processing:	Lay slotted on flat roof surfaces	
	On pitched roofs and with filling: 1-2 overlapping corrugations	
	Fill boards with water immediately after laying to cool in the summer and protect against wind drift. Geospacers must be covered within one day.	

The mentioned data act as guidelines discovered in the company-owned Laboratory that our supplier would want to obtain. The values underlie a Manufacturing tolerance of approximately 8-10%. Included in this product information are data corresponding to the technical information that Optigrün z.Zt has outlayed in their publication. It remains reserved with Optigrün to supplement and change new knowledge at any given time so that the properties of the products can be modified.

Optigrün international AG Am Birkenstock 19 D-72505 Krauchenwies-Göggingen
Tel.: +49 7576 7720 www.optigruen.de

Figure A3: Optigreen Drainage Board Specifications

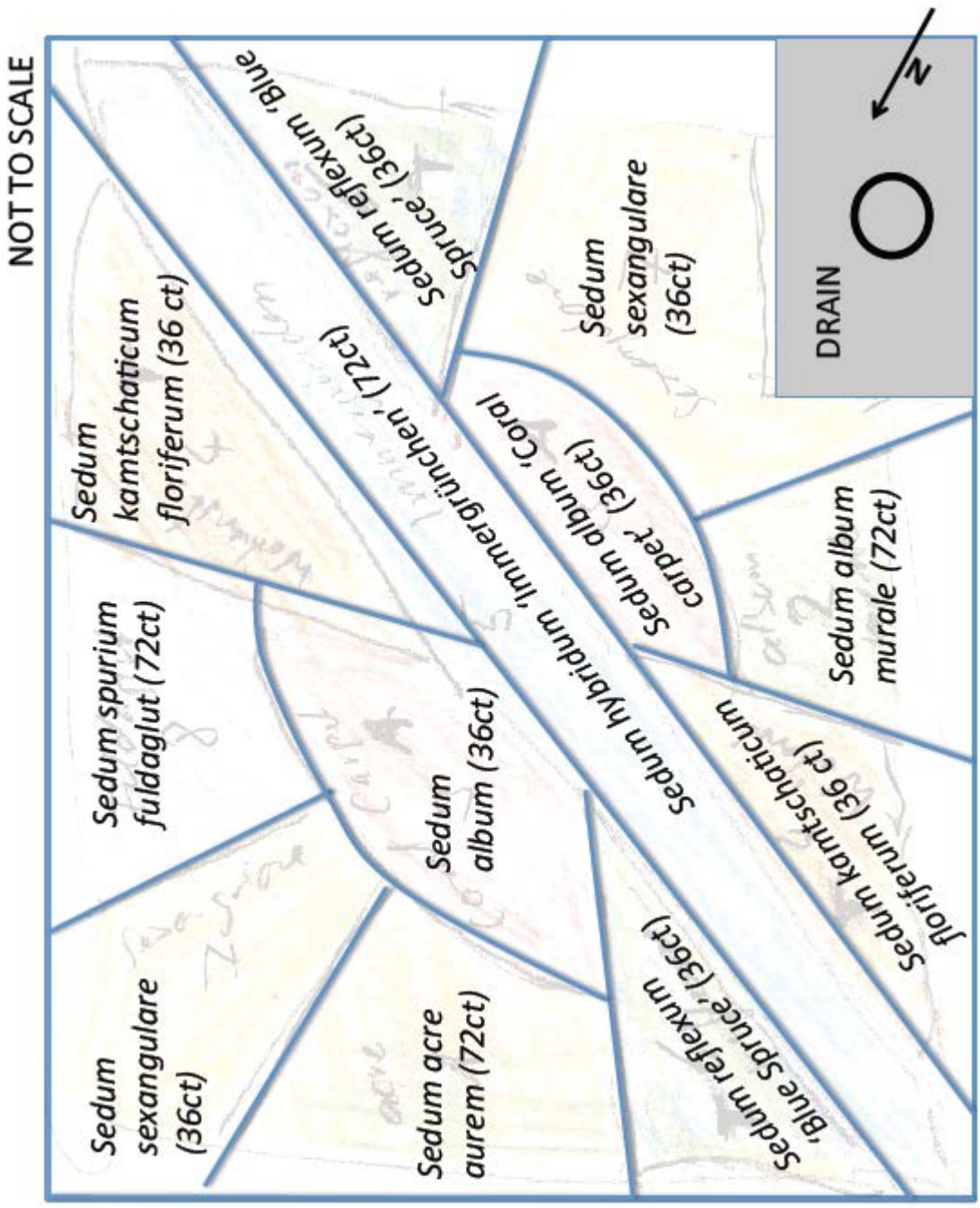

Figure A4: Original Green Roof Planting Plan (Schneider 2011)

Appendix B

Green Roof Instrumentation Specifications

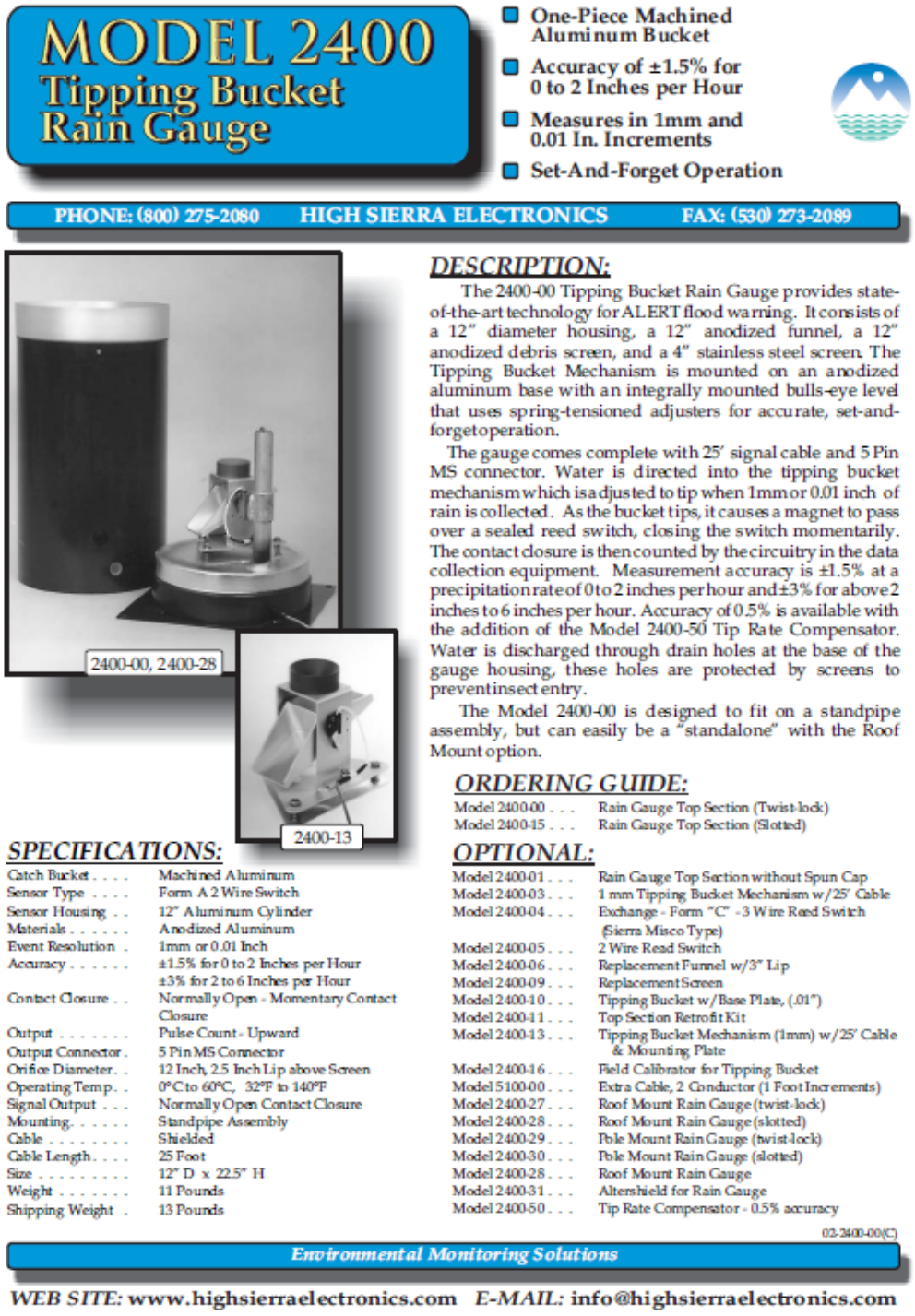

MODEL 2400
Tipping Bucket
Rain Gauge

- One-Piece Machined Aluminum Bucket
- Accuracy of ±1.5% for 0 to 2 Inches per Hour
- Measures in 1mm and 0.01 In. Increments
- Set-And-Forget Operation

PHONE: (800) 275-2080 HIGH SIERRA ELECTRONICS FAX: (530) 273-2089

2400-00, 2400-28

2400-13

DESCRIPTION:

The 2400-00 Tipping Bucket Rain Gauge provides state-of-the-art technology for ALERT flood warning. It consists of a 12" diameter housing, a 12" anodized funnel, a 12" anodized debris screen, and a 4" stainless steel screen. The Tipping Bucket Mechanism is mounted on an anodized aluminum base with an integrally mounted bulls-eye level that uses spring-tensioned adjusters for accurate, set-and-forget operation.

The gauge comes complete with 25' signal cable and 5 Pin MS connector. Water is directed into the tipping bucket mechanism which is adjusted to tip when 1mm or 0.01 inch of rain is collected. As the bucket tips, it causes a magnet to pass over a sealed reed switch, closing the switch momentarily. The contact closure is then counted by the circuitry in the data collection equipment. Measurement accuracy is ±1.5% at a precipitation rate of 0 to 2 inches per hour and ±3% for above 2 inches to 6 inches per hour. Accuracy of 0.5% is available with the addition of the Model 2400-50 Tip Rate Compensator. Water is discharged through drain holes at the base of the gauge housing, these holes are protected by screens to prevent insect entry.

The Model 2400-00 is designed to fit on a standpipe assembly, but can easily be a "standalone" with the Roof Mount option.

SPECIFICATIONS:

Catch Bucket	Machined Aluminum
Sensor Type	Form A 2 Wire Switch
Sensor Housing	12" Aluminum Cylinder
Materials	Anodized Aluminum
Event Resolution	1mm or 0.01 Inch
Accuracy	±1.5% for 0 to 2 Inches per Hour ±3% for 2 to 6 Inches per Hour
Contact Closure	Normally Open - Momentary Contact Closure
Output	Pulse Count - Upward
Output Connector	5 Pin MS Connector
Orifice Diameter	12 Inch, 2.5 Inch Lip above Screen
Operating Temp.	0°C to 60°C, 32°F to 140°F
Signal Output	Normally Open Contact Closure
Mounting	Standpipe Assembly
Cable	Shielded
Cable Length	25 Foot
Size	12" D x 22.5" H
Weight	11 Pounds
Shipping Weight	13 Pounds

ORDERING GUIDE:

Model 2400-00	Rain Gauge Top Section (Twist-lock)
Model 2400-15	Rain Gauge Top Section (Slotted)

OPTIONAL:

Model 2400-01	Rain Gauge Top Section without Spun Cap
Model 2400-03	1 mm Tipping Bucket Mechanism w/25' Cable
Model 2400-04	Exchange - Form "C" - 3 Wire Reed Switch (Sierra Misco Type)
Model 2400-05	2 Wire Read Switch
Model 2400-06	Replacement Funnel w/3" Lip
Model 2400-09	Replacement Screen
Model 2400-10	Tipping Bucket w/Base Plate, (.01")
Model 2400-11	Top Section Retrofit Kit
Model 2400-13	Tipping Bucket Mechanism (1mm) w/25' Cable & Mounting Plate
Model 2400-16	Field Calibrator for Tipping Bucket
Model 5100-00	Extra Cable, 2 Conductor (1 Foot Increments)
Model 2400-27	Roof Mount Rain Gauge (twist-lock)
Model 2400-28	Roof Mount Rain Gauge (slotted)
Model 2400-29	Pole Mount Rain Gauge (twist-lock)
Model 2400-30	Pole Mount Rain Gauge (slotted)
Model 2400-28	Roof Mount Rain Gauge
Model 2400-31	Altershield for Rain Gauge
Model 2400-50	Tip Rate Compensator - 0.5% accuracy

02-2400-00(C)

Environmental Monitoring Solutions

WEB SITE: www.highsierraelectronics.com *E-MAIL:* info@highsierraelectronics.com

Figure B1: Tipping Bucket Specifications for Low Flow Overflow measurement

15" Weir with adaptor installed in 24" pipe

Individual Volumetric Weirs are available for 6", 8", 10", 12", 14", 15" and 16" pipe. The 14" weir uses a 12" face plate, while the 16" weir uses a 15" face plate. Adaptors for 18", 21", 24", 27", 30", 36", 42" and 48" pipe are used in conjunction with the 15" weir.

Volumetric Weirs are also available in sets.
Set A consists of 6", 8", 10", 12" and 15" weirs with an 18" adaptor in a plywood storage and carrying case with handle and hasp. It measures 19½" W x 19½" D x 7½" H.

Set B is the same as set A, but has Bubbler Tubes Attached to the weirs.

Set C consists of 21" through 48" adaptors **without a storage case.**

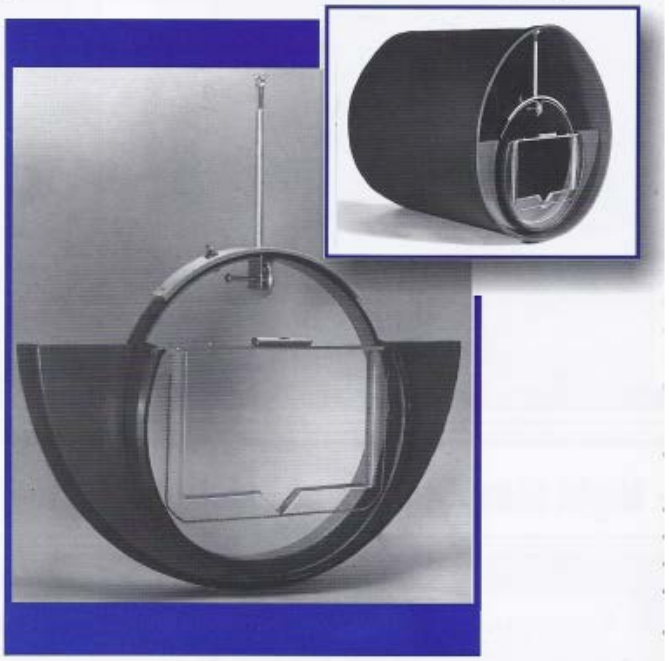

Adaptors are available individually or in sets.

WEIR CAPACITIES AND HEAD

	Capacities*		Head**
6"	57 to 3700 GPD within V-notch,	rectangular to 46,000 GPD	2.8437
8"	57 to 3700 GPD within V-notch,	rectangular to 124,000 GPD	4.0000
10"	57 to 3700 GPD within V-notch,	rectangular to 234,000 GPD	5.1250
12"	57 to 3700 GPD within V-notch,	rectangular to 361,000 GPD	5.8125
14"	57 to 3700 GPD within V-notch,	rectangular to 361,000 GPD	5.8125
15"	57 to 3700 GPD within V-notch,	rectangular to 620,000 GPD	7.3125
16"	57 to 3700 GPD within V-notch,	rectangular to 620,000 GPD	7.3125

*Calibration lines are in 2 millimeter increments
**In inches from top of rectangular opening to bottom of V-notch

Metric Flow Conversion Charts Available

Figure B2: Datasheet for Thel-Mar Weir Used For Measuring High Flows

SENTRAN

PF

PRECISION LOW PROFILE LOAD CELL

applications

- Laboratory Measurements
- Materials Testing
- Dynamic Measurements
- Process Control
- Weighing

features

- 100 to 5000 lbs. Capacities
- Compact Low Profile Design
- 500% Overload Capability
- Stainless Steel Construction
- 0.1% Accuracy Class
- High Frequency Response
- IP66/IP67 Environmental Sealing
- Low Sensitivity to Side Load and Off-Center Loading
- Two Year Warranty

SENTRAN, LLC
California Commerce Center
4355 Lowell Street
Ontario, CA 91761-2225

Toll Free: 1(888) 545-8988
Phone: 1(909) 605-1544
Fax: 1(909) 605-6305
Email: mail@sentranllc.com
URL: www.sentranllc.com

Application Tip: *The PF Series is designed for applications requiring excellent performance in an compact, rugged low profile load cell.*

The PF Series is a high performance, low profile, bonded foil strain gage load cell constructed of electro-polished stainless steel (PF3). To achieve sealing ratings of IP66 and IP67 (thoroughly sealed against airborne particles, strong jets of water and the effects of immersion up to 1 meter.) proprietary, multi-redundant environmental barriers are incorporated, including VITON® Fluorelastomer Oring seals to protect sensitive areas. The PF Series is designed to accurately measure compression forces in capacities ranging from 100 lbs. to 5,000 lbs. The integrated sensing diaphragm and precision ground base combine to produce excellent performance, superior environmental integrity and reduced sensitivity to off-center and side loading effects. Integral overload protection permits compression loads of 500% of rated capacity to be applied without adverse effects. Side loads of 50% of rated capacity can be tolerated, simultaneously. The low deflection of the PF Series yields a high dynamic response for applications in structural analysis and materials testing. The durable polyurethane jacketed cable, features a braided, tinned-copper shield for mechanical protection and to minimize the effects of common industrial electrical noise, e.g. RFI and EMI. The attributes of the PF Series make it an ideal choice for measurements in the laboratory, manufacturing and process applications, and for general force measurements and weighing situations where an extraordinarily rugged, low profile precision load cell solution is needed.

VITON® is a registered trademark of E. I. DuPont Co.

Innovative Measurement Solutions

specifications

SENTRAN

PF

performance

Rated capacities [1] (lbs.)	100, 250, 500, 1K, 2K, 3K, 4K, & 5K
Rated output (FSO)	2 mV/V ± 0.25%
Combined error	= 0.25 % FSO
Non-linearity	= 0.10 % FSO
Hysteresis	= 0.10 % FSO
Non-repeatability	= 0.05 % FSO
Creep (30 minutes)	= 0.03 % of load
Zero balance	= 10 % FSO
Zero Return (30 minutes)	Better than 0.03 % FSO

[1] ("K" = thousand)

mechanical

Material:	17-4PH Stainless steel
Finish:	Electro-polished
Safe overload	Compression: 500% FSO
	Tension: N/A
	Side load: 50% FSO
Ultimate overload	Compression: 1000% FSO
	Tension: N/A
	Side load: 100% FSO
Deflection	0.005" (.13mm) nominal
Weight	1 lbs.

electrical

Input impedance	400 ohms (nominal)
Output impedance	350 ohms (nominal)
Insulation resistance	>5000 Megohms @ 50VDC
Excitation Voltage	10 V AC/DC (15 V maximum)
Cable Color code:	+ Excitation (red)
	- Excitation (black)
	+ Output (green)
	- Output (white)
	Shield (bare)
Cable type	4-conductor, 22 AWG, tin-copper braided shield, polyurethane jacket
Cable termination	Finished conductors

environmental

Temperature, operating	-20 to +180 °F (-29 to +82°)
Temperature, compensated	+40 to +140 °F (-10 to +60°C)
Temperature effects:	Zero < 0.002% FSO/°F
	< 0.0036% FSO/°C
	Output < 0.002% of Rdg./°F
	< 0.0036% Rdg./°C
Sealing	IP66/IP67; redundant

options

Shunt calibration, Special cable lengths, High Temperature operation, MS connectors and Control Instrumentation.

dimensions

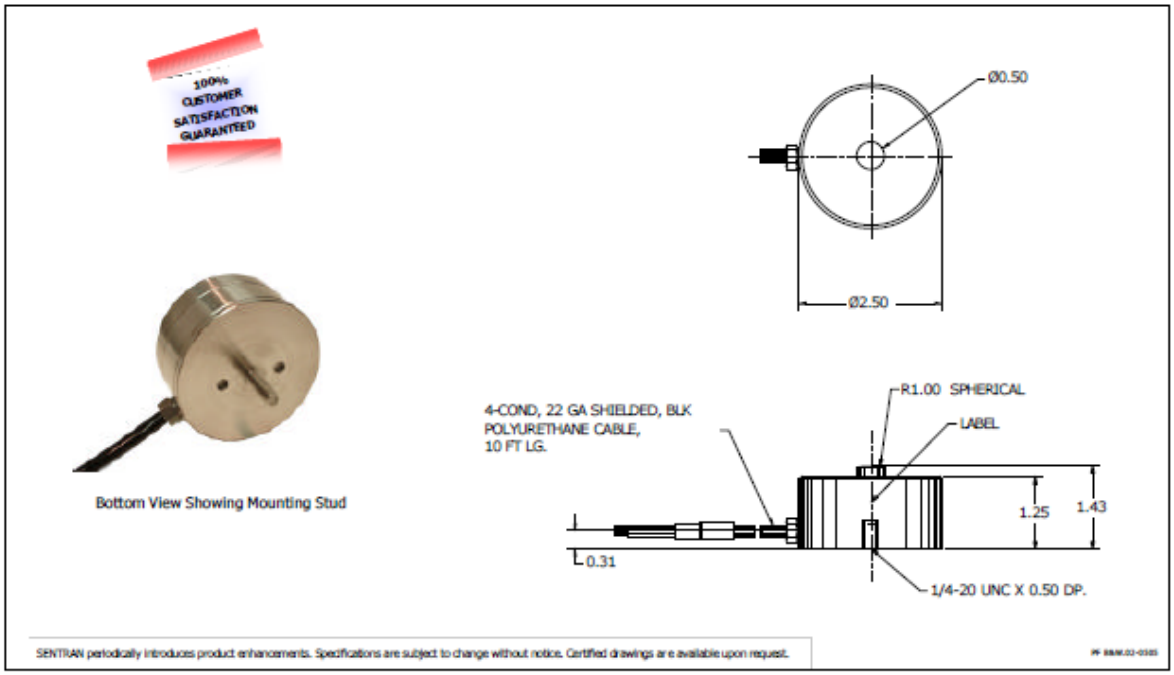

SENTRAN periodically introduces product enhancements. Specifications are subject to change without notice. Certified drawings are available upon request.

Figure B3: Load Cell Specifications for Weighing Lysimeter

APPENDIX C

2009 through 2014 Monthly Cumulative Performance Graphs of Lysimeter. Daily values of ET and overflow are represented by bar graphs in green and red, respectively, and daily rainfall totals are represented by blue dots with values on the left axis. Cumulative curves for rainfall are shaded in light blue and cumulative measured ET is represented by light green.

2009

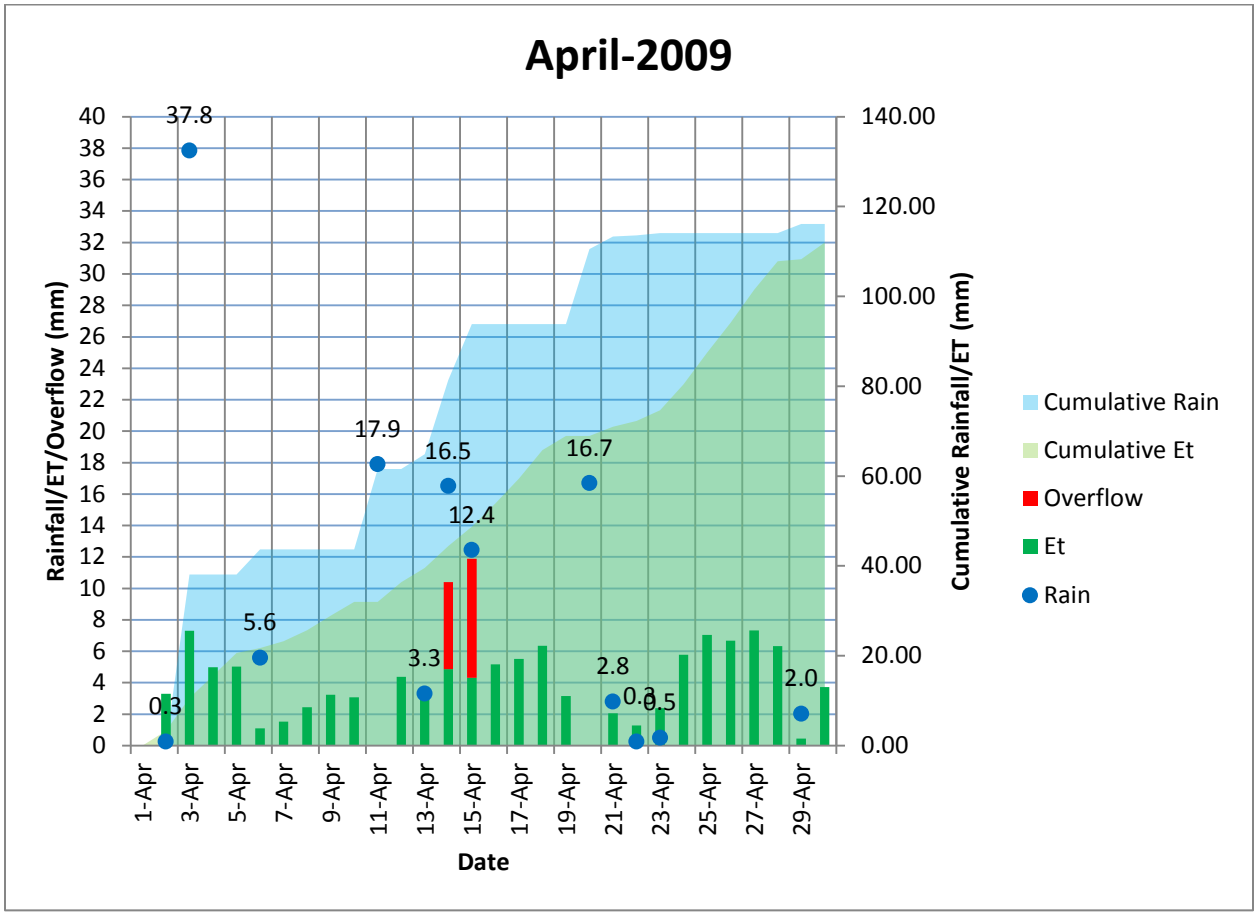
April-2009
Rainfall/ET/Overflow (mm)
Cumulative Rainfall/ET (mm)
Date
Cumulative Rain
Cumulative Et
Overflow
Et
Rain
37.8
17.9
16.5
16.7
12.4
5.6
3.3
2.8
0.3
0.5
2.0
0.3
1-Apr
3-Apr
5-Apr
7-Apr
9-Apr
11-Apr
13-Apr
15-Apr
17-Apr
19-Apr
21-Apr
23-Apr
25-Apr
27-Apr
29-Apr

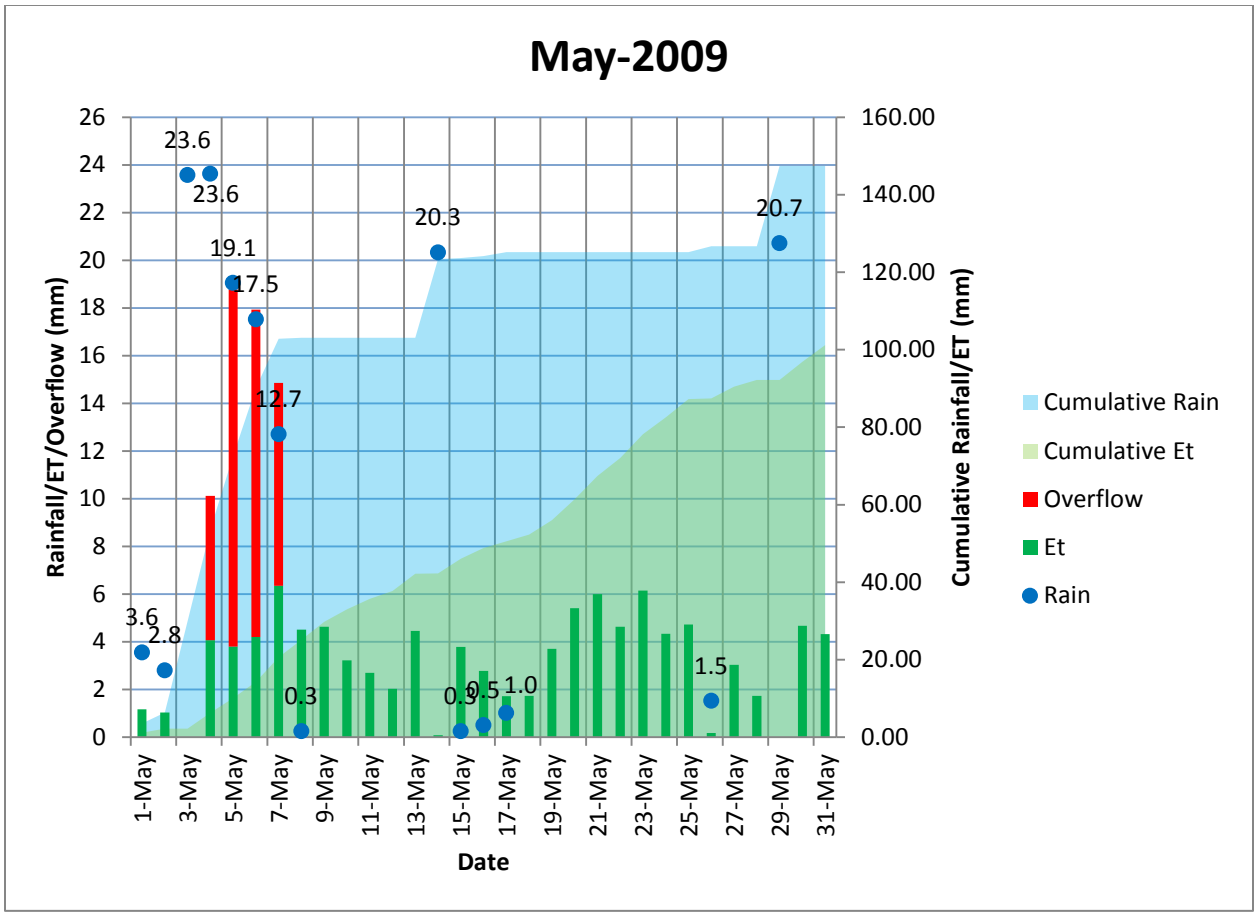
May-2009
Rainfall/ET/Overflow (mm)
Cumulative Rainfall/ET (mm)
Date
Cumulative Rain
Cumulative Et
Overflow
Et
Rain
23.6
23.6
19.1
17.5
12.7
20.3
20.7
3.6
2.8
0.3
0.9
0.5
1.0
1.5
1-May
3-May
5-May
7-May
9-May
11-May
13-May
15-May
17-May
19-May
21-May
23-May
25-May
27-May
29-May
31-May

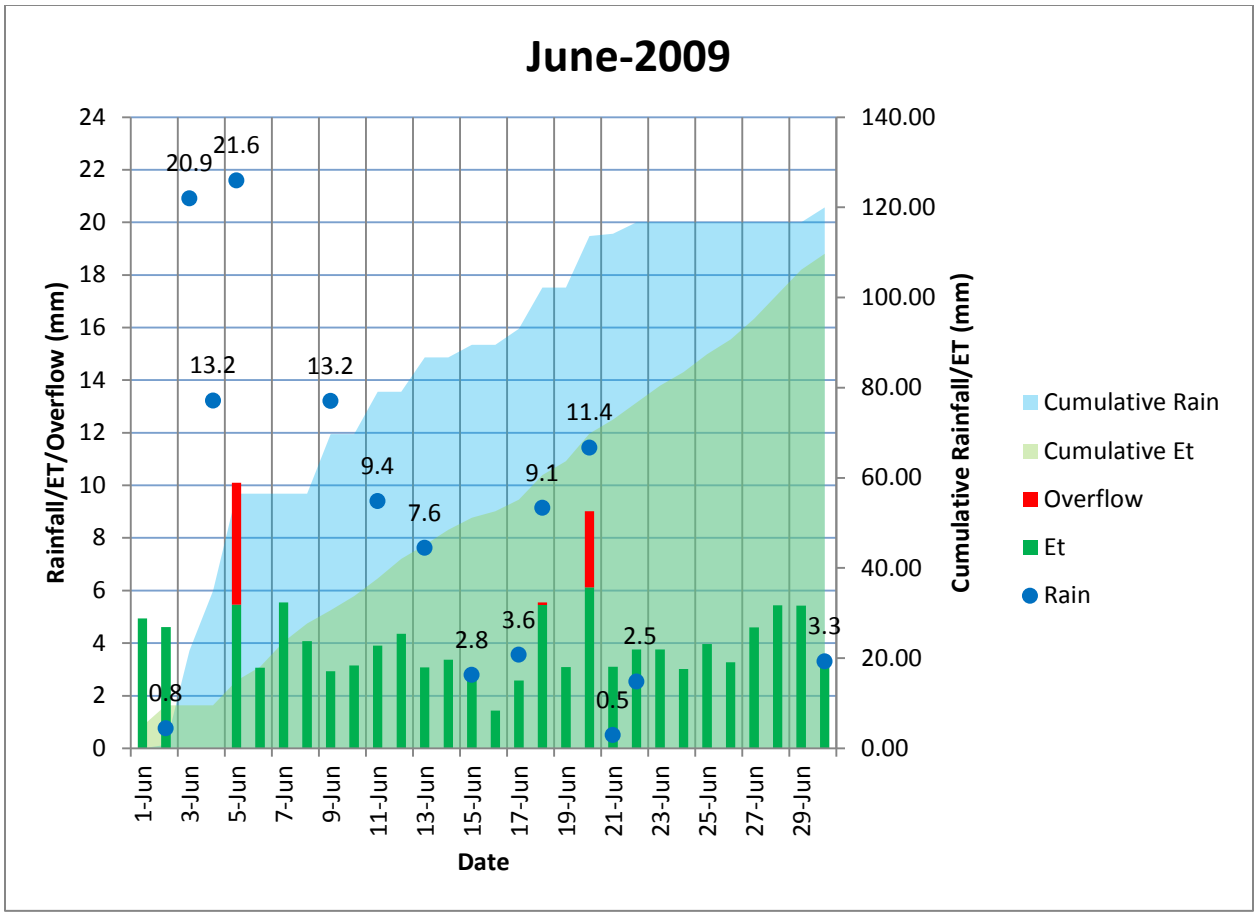
June-2009
Rainfall/ET/Overflow (mm)
Cumulative Rainfall/ET (mm)
Date
Cumulative Rain
Cumulative Et
Overflow
Et
Rain
20.9
21.6
13.2
13.2
9.4
7.6
9.1
11.4
0.8
2.8
3.6
0.5
2.5
3.3
1-Jun
3-Jun
5-Jun
7-Jun
9-Jun
11-Jun
13-Jun
15-Jun
17-Jun
19-Jun
21-Jun
23-Jun
25-Jun
27-Jun
29-Jun

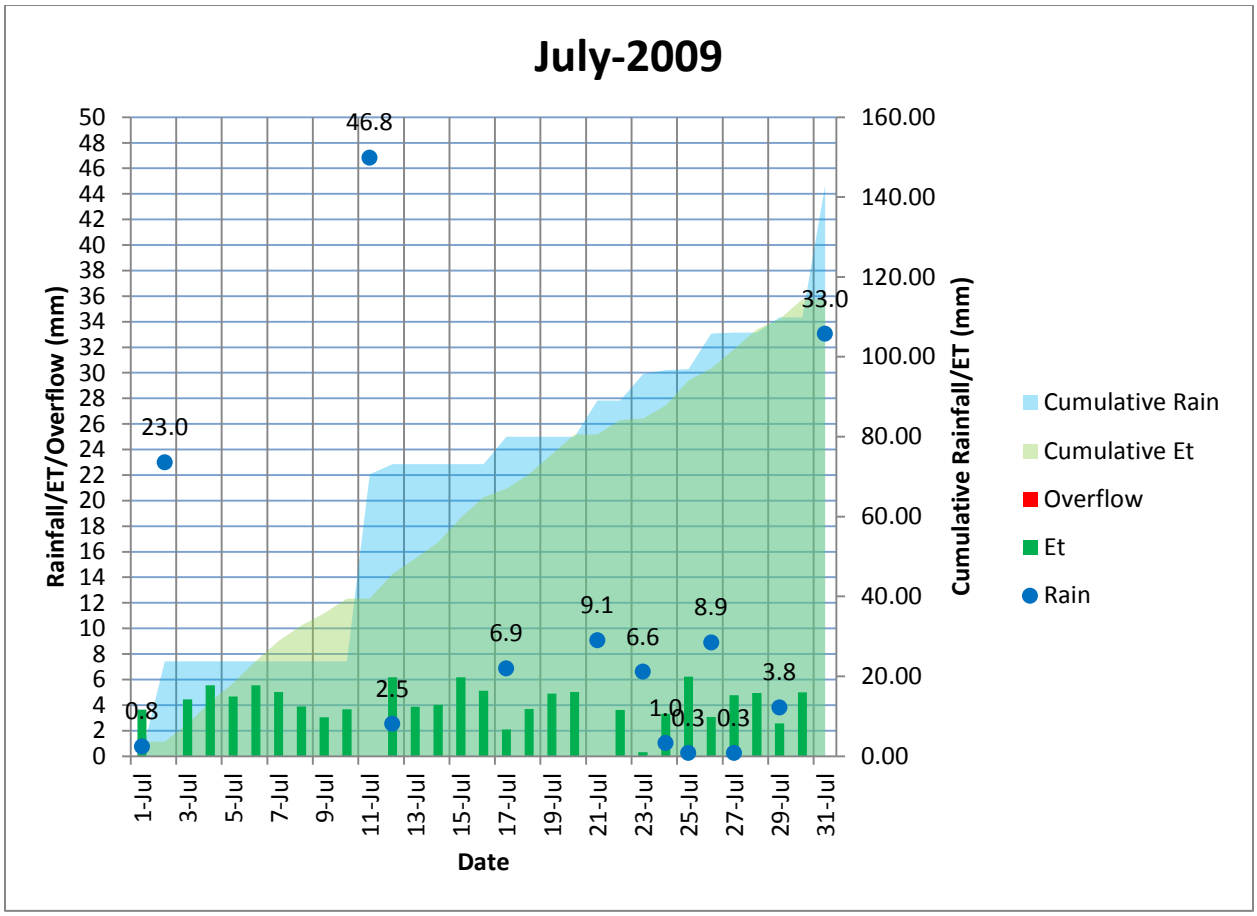
July-2009
Rainfall/ET/Overflow (mm)
Cumulative Rainfall/ET (mm)
Date
Cumulative Rain
Cumulative Et
Overflow
Et
Rain
46.8
23.0
33.0
9.1
8.9
6.9
6.6
3.8
2.5
1.0
0.8
0.3
0.3
1-Jul
3-Jul
5-Jul
7-Jul
9-Jul
11-Jul
13-Jul
15-Jul
17-Jul
19-Jul
21-Jul
23-Jul
25-Jul
27-Jul
29-Jul
31-Jul

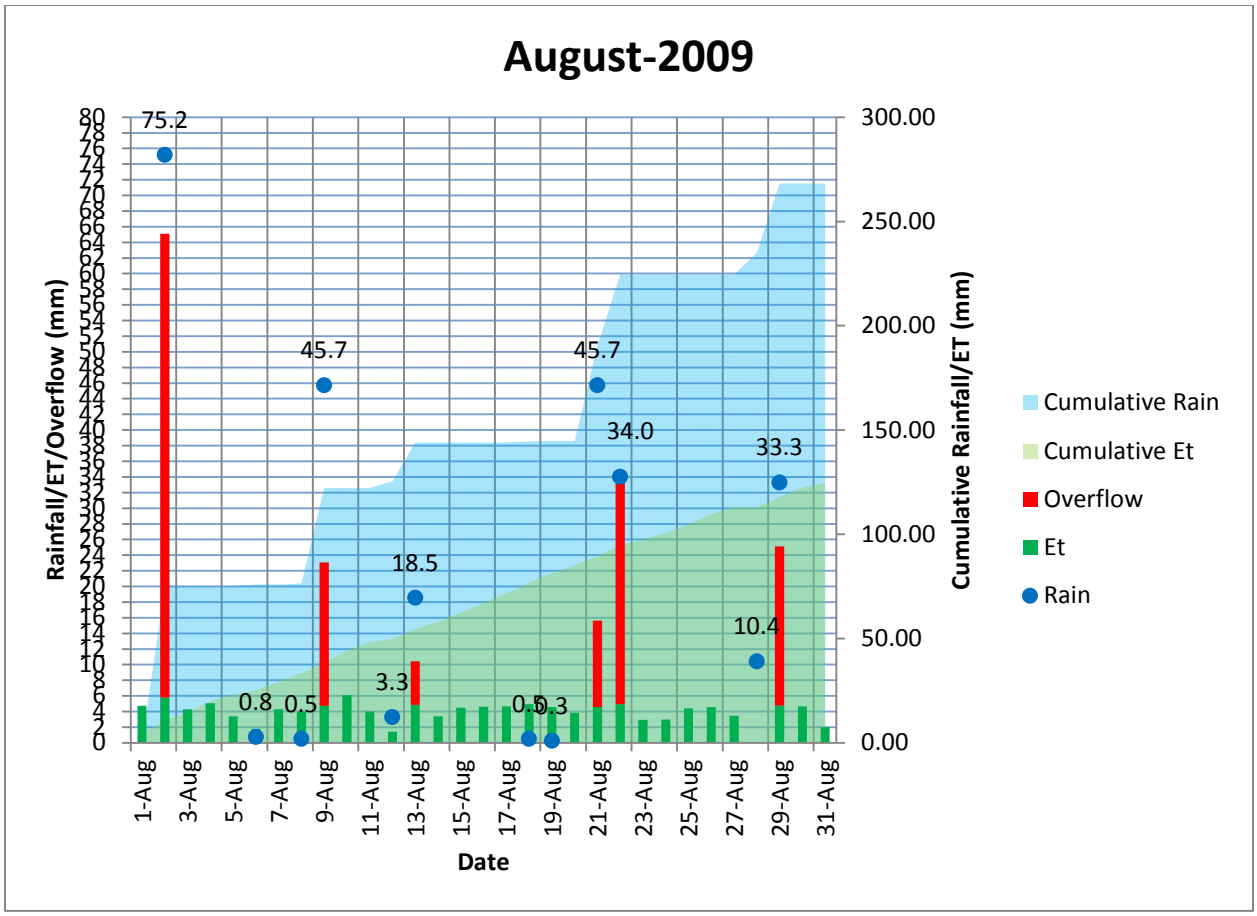
August-2009
Rainfall/ET/Overflow (mm)
Cumulative Rainfall/ET (mm)
Date
75.2
45.7
45.7
34.0
33.3
18.5
10.4
3.3
0.8
0.5
0.5
0.3
1-Aug
3-Aug
5-Aug
7-Aug
9-Aug
11-Aug
13-Aug
15-Aug
17-Aug
19-Aug
21-Aug
23-Aug
25-Aug
27-Aug
29-Aug
31-Aug
0.00
50.00
100.00
150.00
200.00
250.00
300.00
Cumulative Rain
Cumulative Et
Overflow
Et
Rain

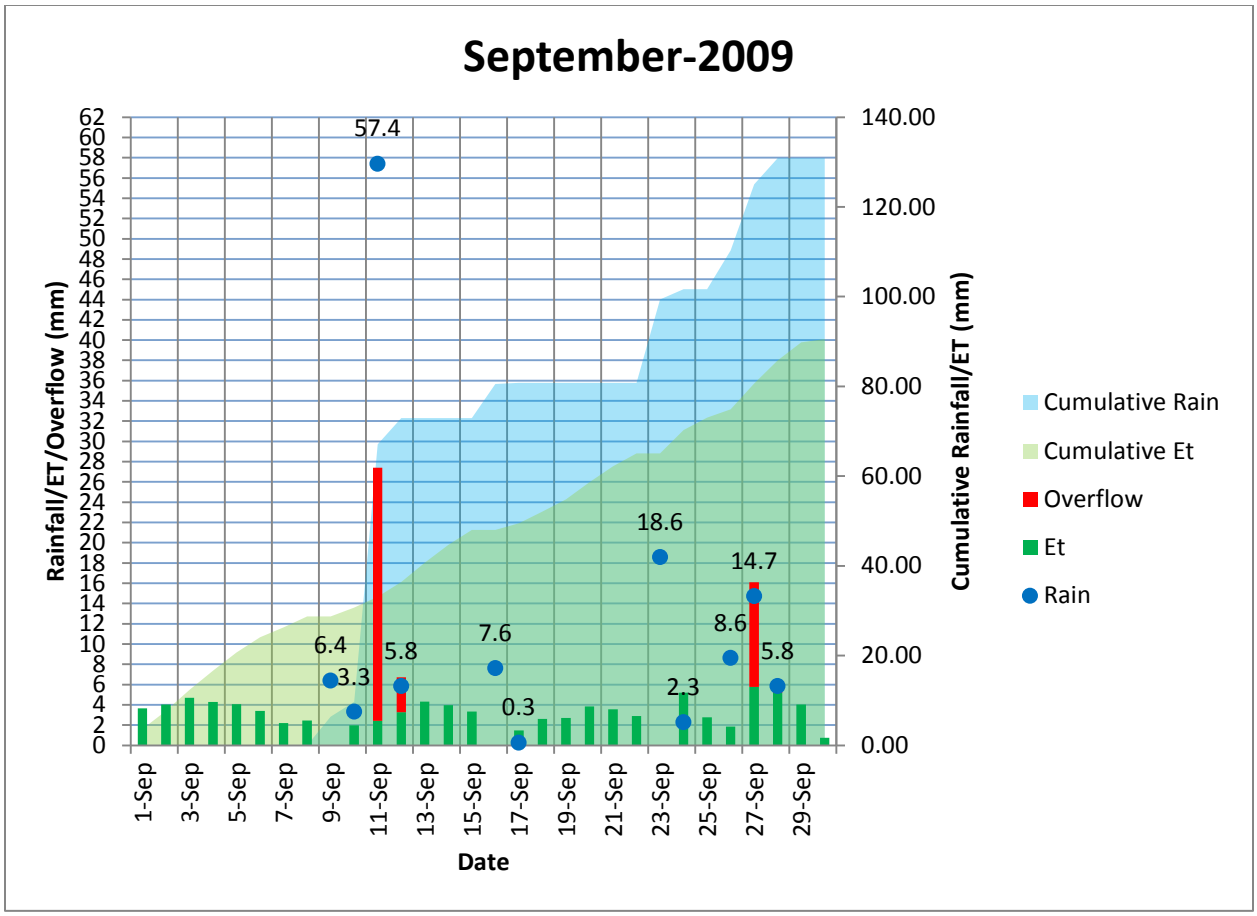
September-2009
Rainfall/ET/Overflow (mm)
Cumulative Rainfall/ET (mm)
Date
57.4
6.4
3.3
5.8
7.6
0.3
18.6
2.3
8.6
14.7
5.8
Cumulative Rain
Cumulative Et
Overflow
Et
Rain

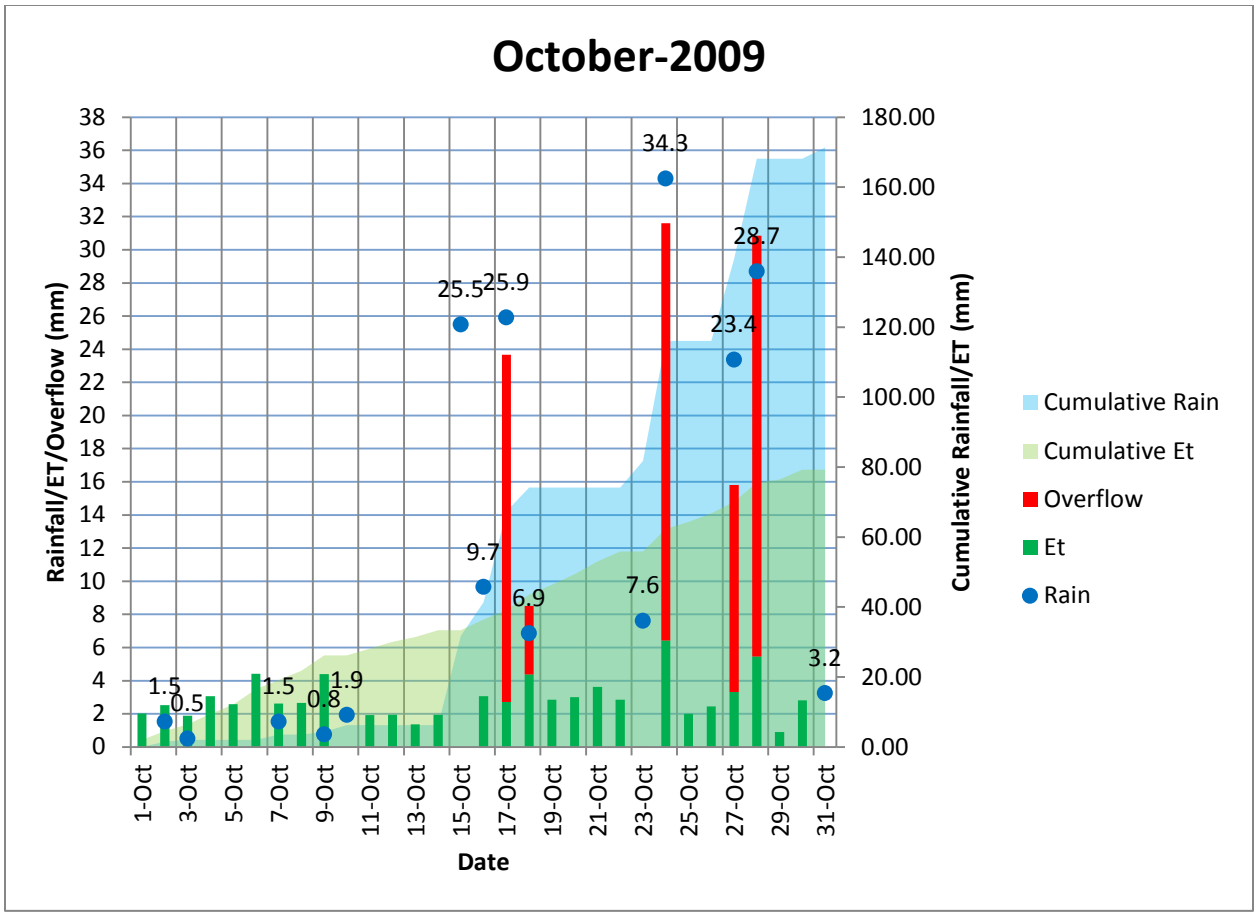
October-2009
Rainfall/ET/Overflow (mm)
Cumulative Rainfall/ET (mm)
Date
1-Oct
3-Oct
5-Oct
7-Oct
9-Oct
11-Oct
13-Oct
15-Oct
17-Oct
19-Oct
21-Oct
23-Oct
25-Oct
27-Oct
29-Oct
31-Oct
1.5
0.5
1.5
0.8
1.9
25.5
25.9
9.7
6.9
7.6
34.3
23.4
28.7
3.2
Cumulative Rain
Cumulative Et
Overflow
Et
Rain

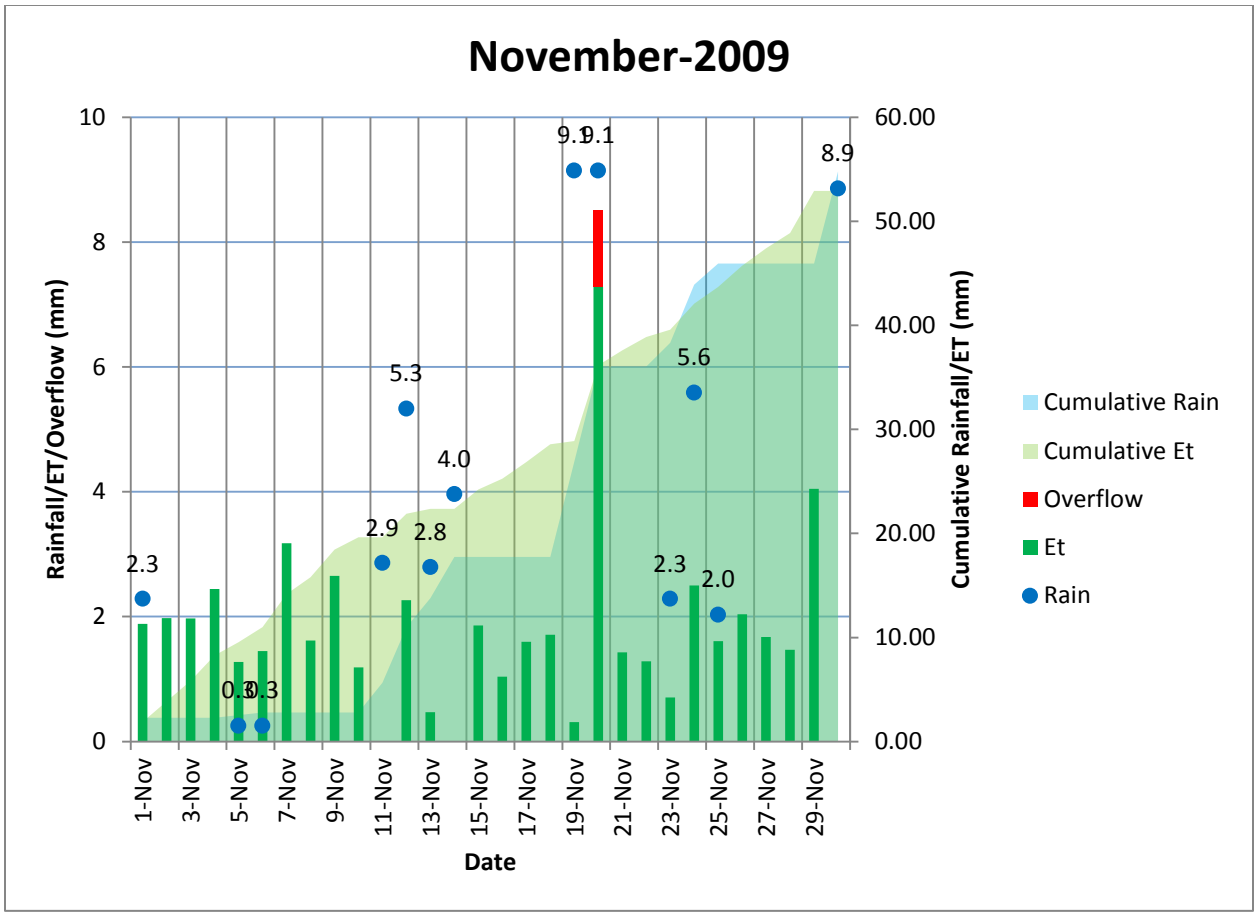
November-2009
Rainfall/ET/Overflow (mm)
Cumulative Rainfall/ET (mm)
Date
1-Nov
3-Nov
5-Nov
7-Nov
9-Nov
11-Nov
13-Nov
15-Nov
17-Nov
19-Nov
21-Nov
23-Nov
25-Nov
27-Nov
29-Nov
2.3
0.3
0.3
2.9
5.3
2.8
4.0
9.1
9.1
2.3
5.6
2.0
8.9
Cumulative Rain
Cumulative Et
Overflow
Et
Rain

2010

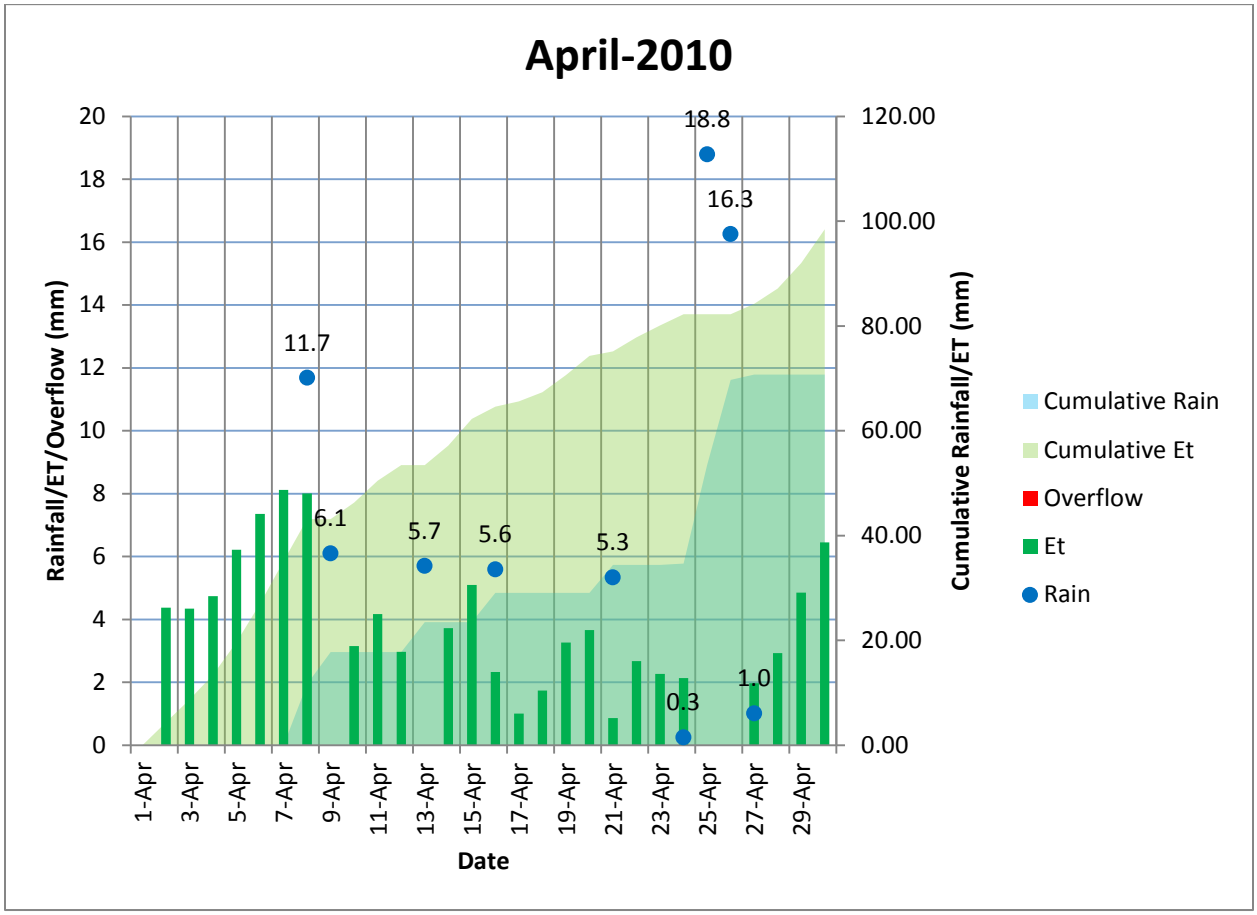
April-2010
Rainfall/ET/Overflow (mm)
Cumulative Rainfall/ET (mm)
Date
1-Apr
3-Apr
5-Apr
7-Apr
9-Apr
11-Apr
13-Apr
15-Apr
17-Apr
19-Apr
21-Apr
23-Apr
25-Apr
27-Apr
29-Apr
11.7
6.1
5.7
5.6
5.3
0.3
18.8
16.3
1.0
Cumulative Rain
Cumulative Et
Overflow
Et
Rain

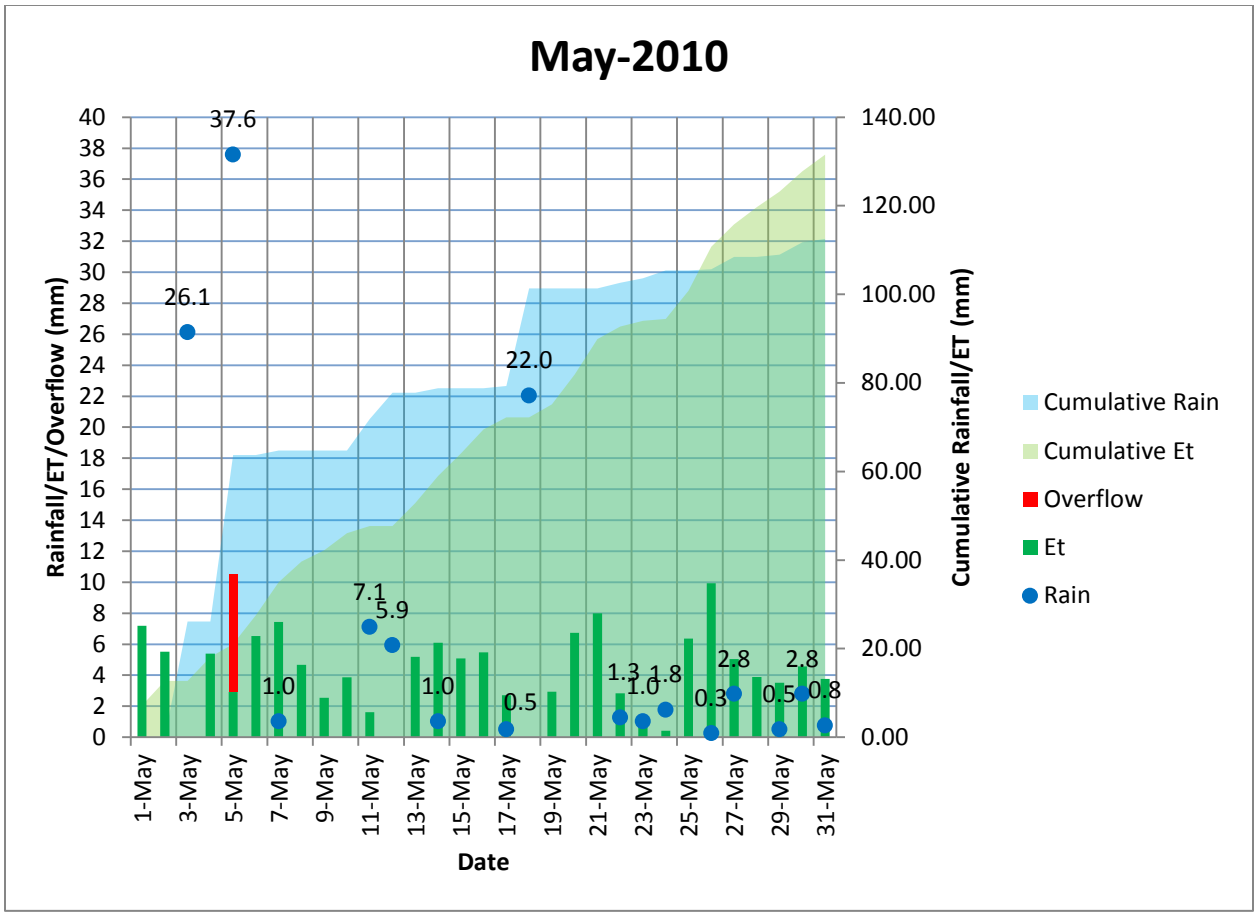
May-2010
Rainfall/ET/Overflow (mm)
Cumulative Rainfall/ET (mm)
Date
Cumulative Rain
Cumulative Et
Overflow
Et
Rain
37.6
26.1
22.0
7.1
5.9
1.0
1.0
0.5
1.3
1.0
1.8
0.3
2.8
0.5
2.8
0.8
1-May
3-May
5-May
7-May
9-May
11-May
13-May
15-May
17-May
19-May
21-May
23-May
25-May
27-May
29-May
31-May

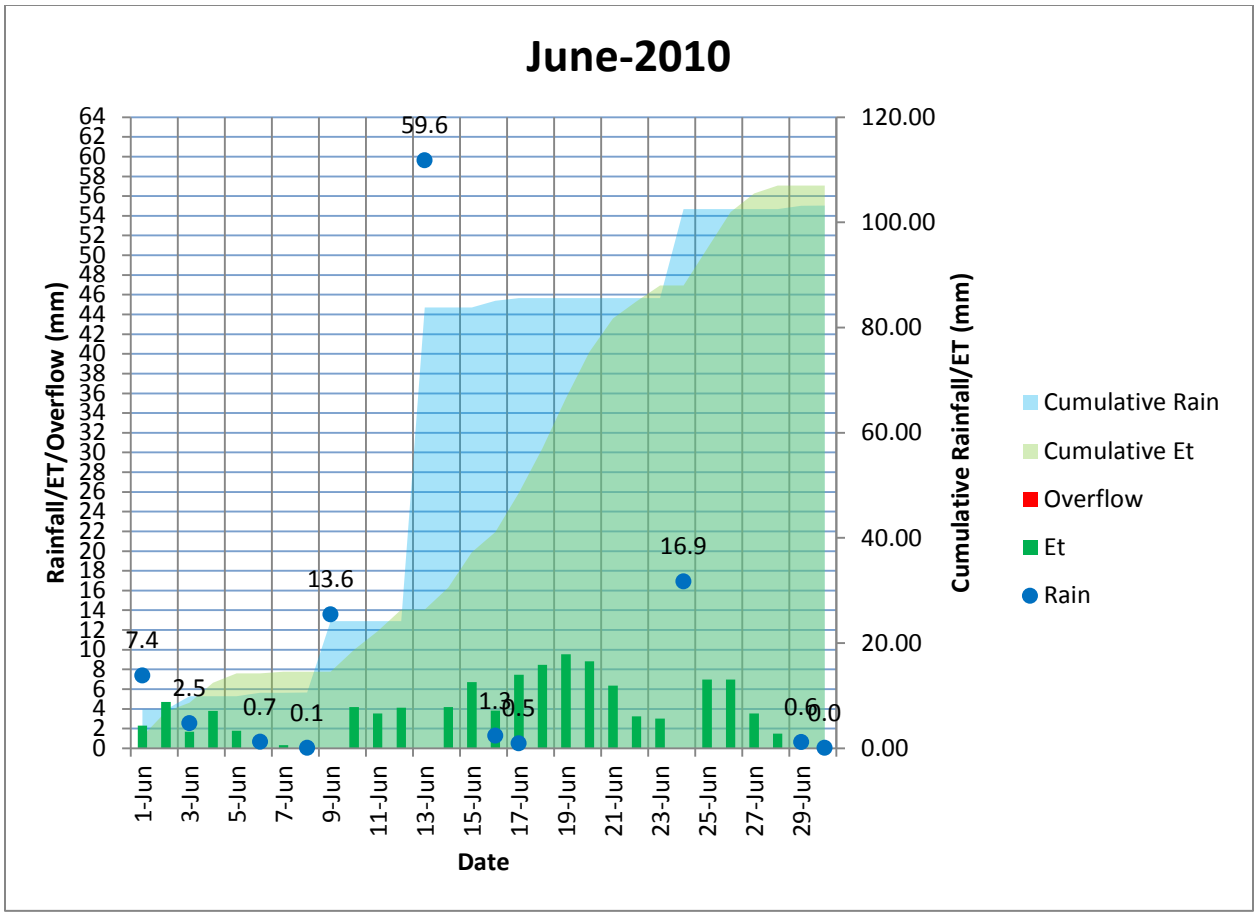
June-2010
Rainfall/ET/Overflow (mm)
Cumulative Rainfall/ET (mm)
Date
Cumulative Rain
Cumulative Et
Overflow
Et
Rain
7.4
2.5
0.7
0.1
13.6
59.6
1.3
0.5
16.9
0.6
0.0
1-Jun
3-Jun
5-Jun
7-Jun
9-Jun
11-Jun
13-Jun
15-Jun
17-Jun
19-Jun
21-Jun
23-Jun
25-Jun
27-Jun
29-Jun

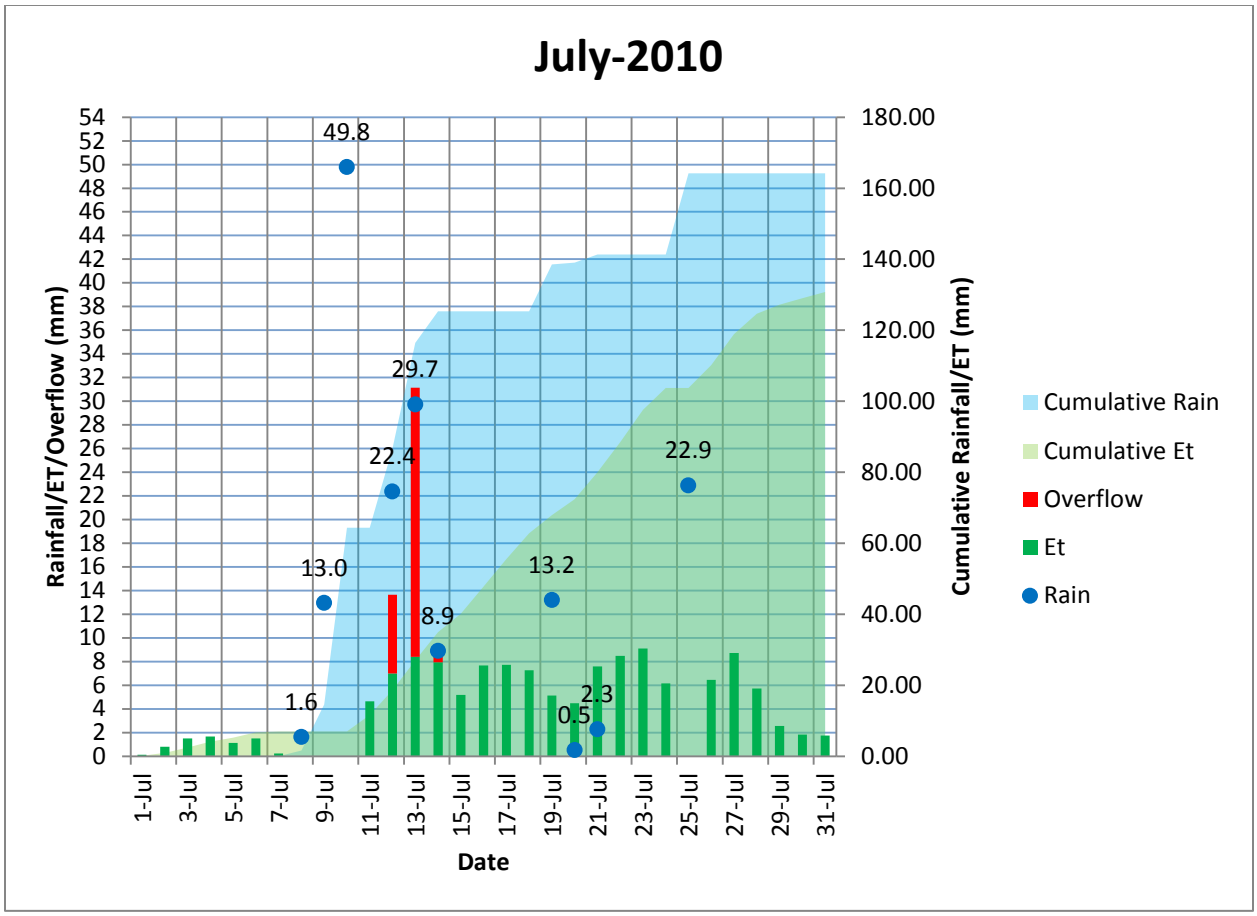
July-2010
Rainfall/ET/Overflow (mm)
Cumulative Rainfall/ET (mm)
Date
49.8
29.7
22.4
22.9
13.0
13.2
8.9
1.6
2.3
0.5
Cumulative Rain
Cumulative Et
Overflow
Et
Rain

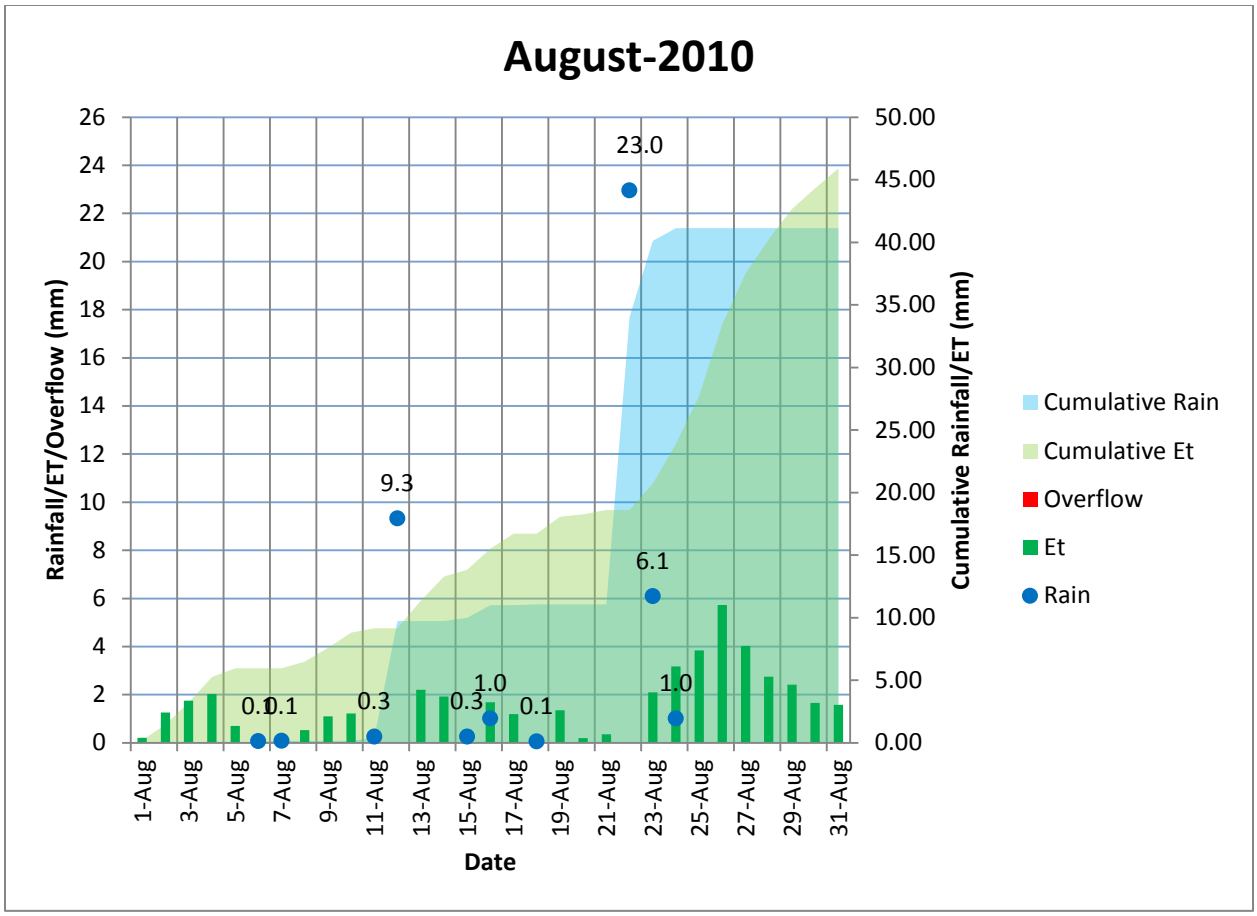
August-2010
Rainfall/ET/Overflow (mm)
Cumulative Rainfall/ET (mm)
Date
Cumulative Rain
Cumulative Et
Overflow
Et
Rain
23.0
9.3
6.1
1.0
1.0
0.3
0.3
0.1
0.1
0.1

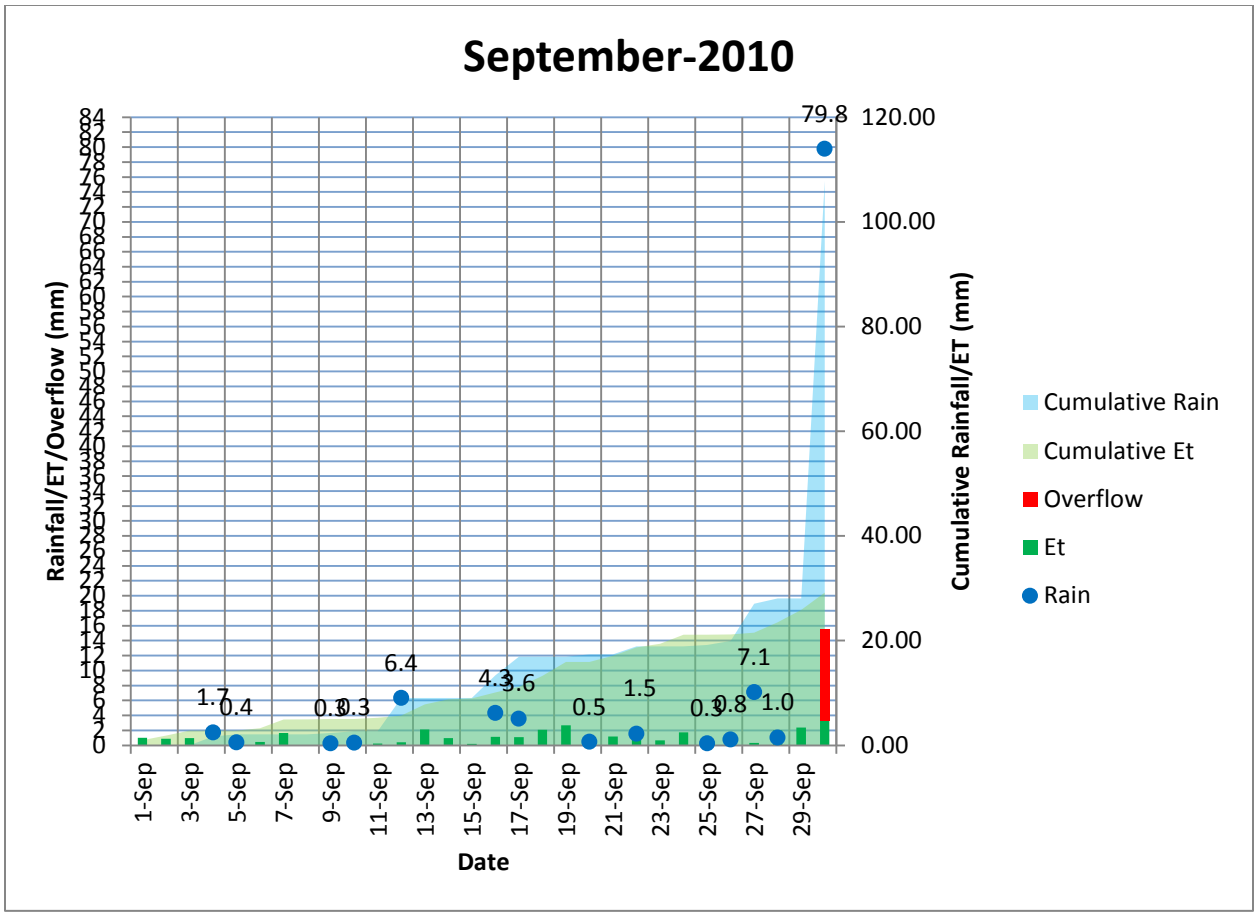
September-2010
Rainfall/ET/Overflow (mm)
Cumulative Rainfall/ET (mm)
Date
1-Sep
3-Sep
5-Sep
7-Sep
9-Sep
11-Sep
13-Sep
15-Sep
17-Sep
19-Sep
21-Sep
23-Sep
25-Sep
27-Sep
29-Sep
0.00
20.00
40.00
60.00
80.00
100.00
120.00
79.8
1.7
0.4
0.3
6.4
4.3
3.6
0.5
1.5
0.8
7.1
1.0
Cumulative Rain
Cumulative Et
Overflow
Et
Rain

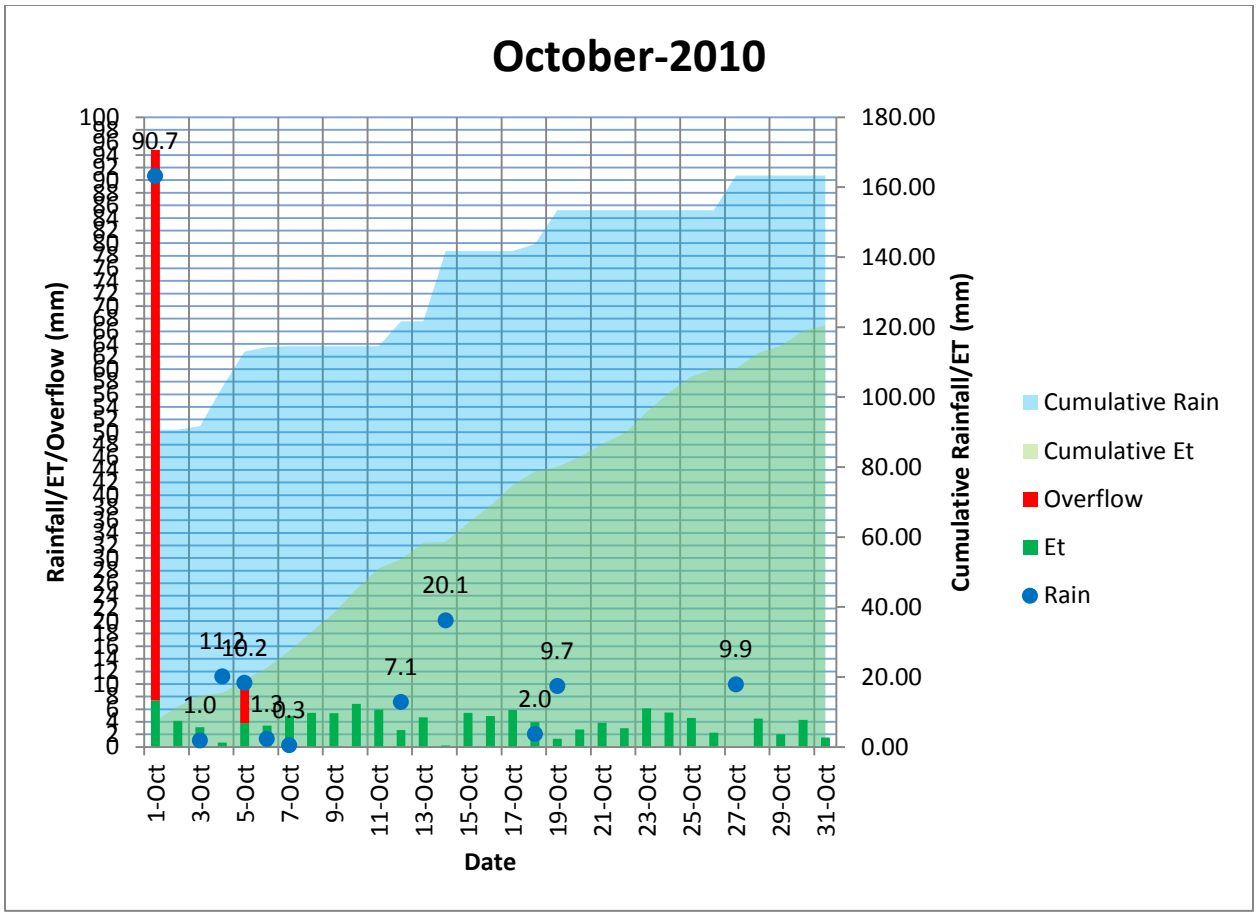
October-2010
Rainfall/ET/Overflow (mm)
Cumulative Rainfall/ET (mm)
Date
90.7
11.2
10.2
1.0
1.3
0.3
7.1
20.1
2.0
9.7
9.9
Cumulative Rain
Cumulative Et
Overflow
Et
Rain

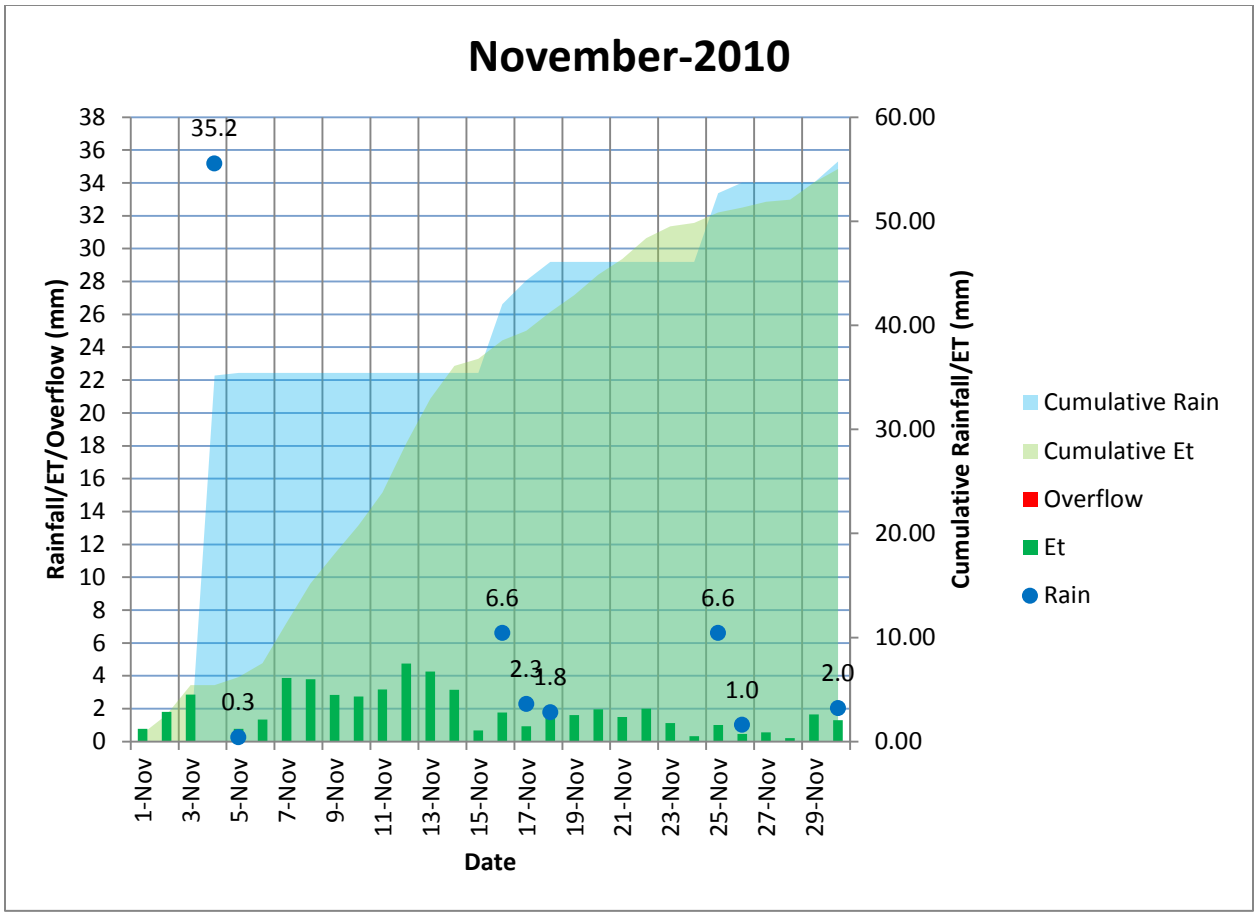
November-2010
Rainfall/ET/Overflow (mm)
Cumulative Rainfall/ET (mm)
Date
35.2
0.3
6.6
2.3
1.8
6.6
1.0
2.0
Cumulative Rain
Cumulative Et
Overflow
Et
Rain

2011

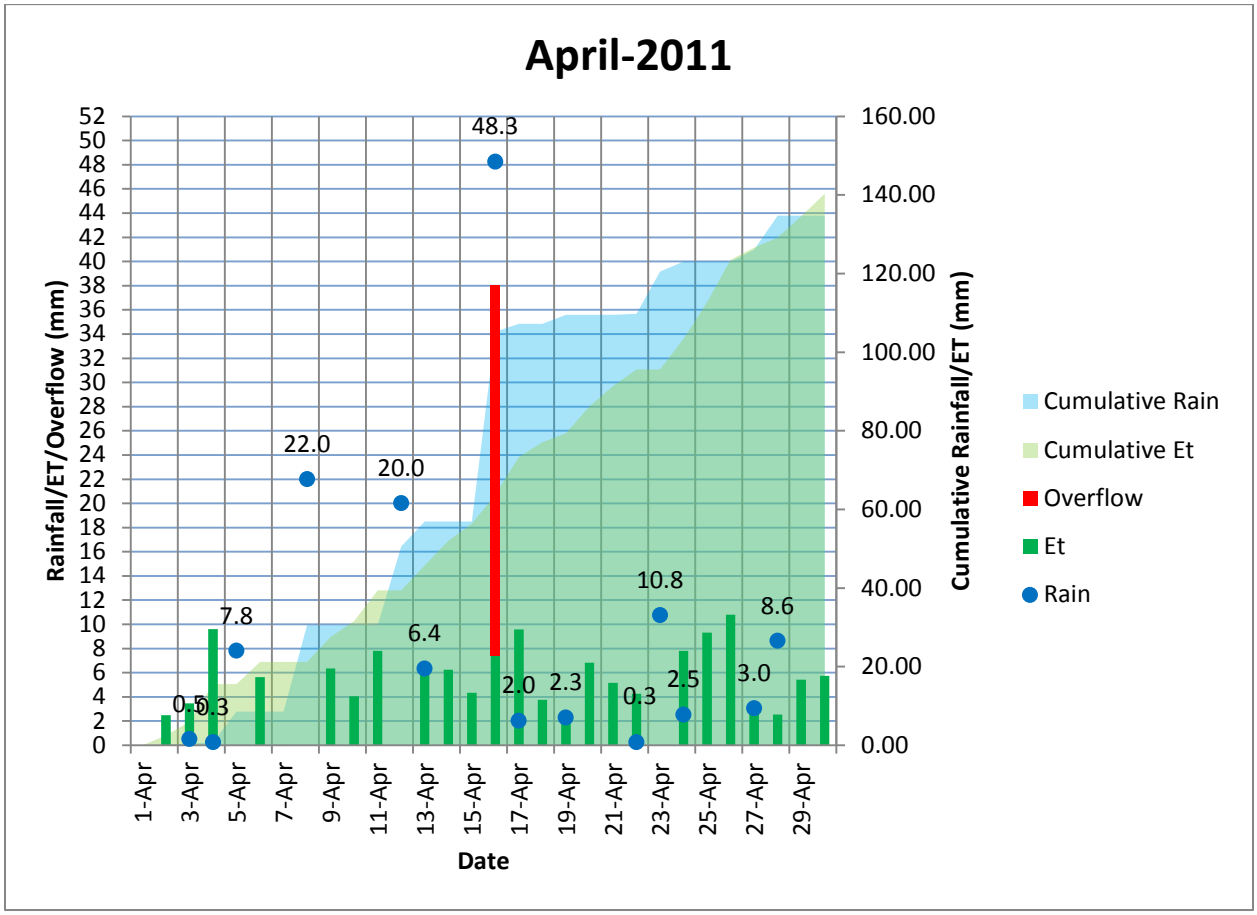
April-2011
Rainfall/ET/Overflow (mm)
Cumulative Rainfall/ET (mm)
Date
Cumulative Rain
Cumulative Et
Overflow
Et
Rain
48.3
22.0
20.0
10.8
8.6
7.8
6.4
0.5
0.3
2.0
2.3
0.3
2.5
3.0
1-Apr
3-Apr
5-Apr
7-Apr
9-Apr
11-Apr
13-Apr
15-Apr
17-Apr
19-Apr
21-Apr
23-Apr
25-Apr
27-Apr
29-Apr

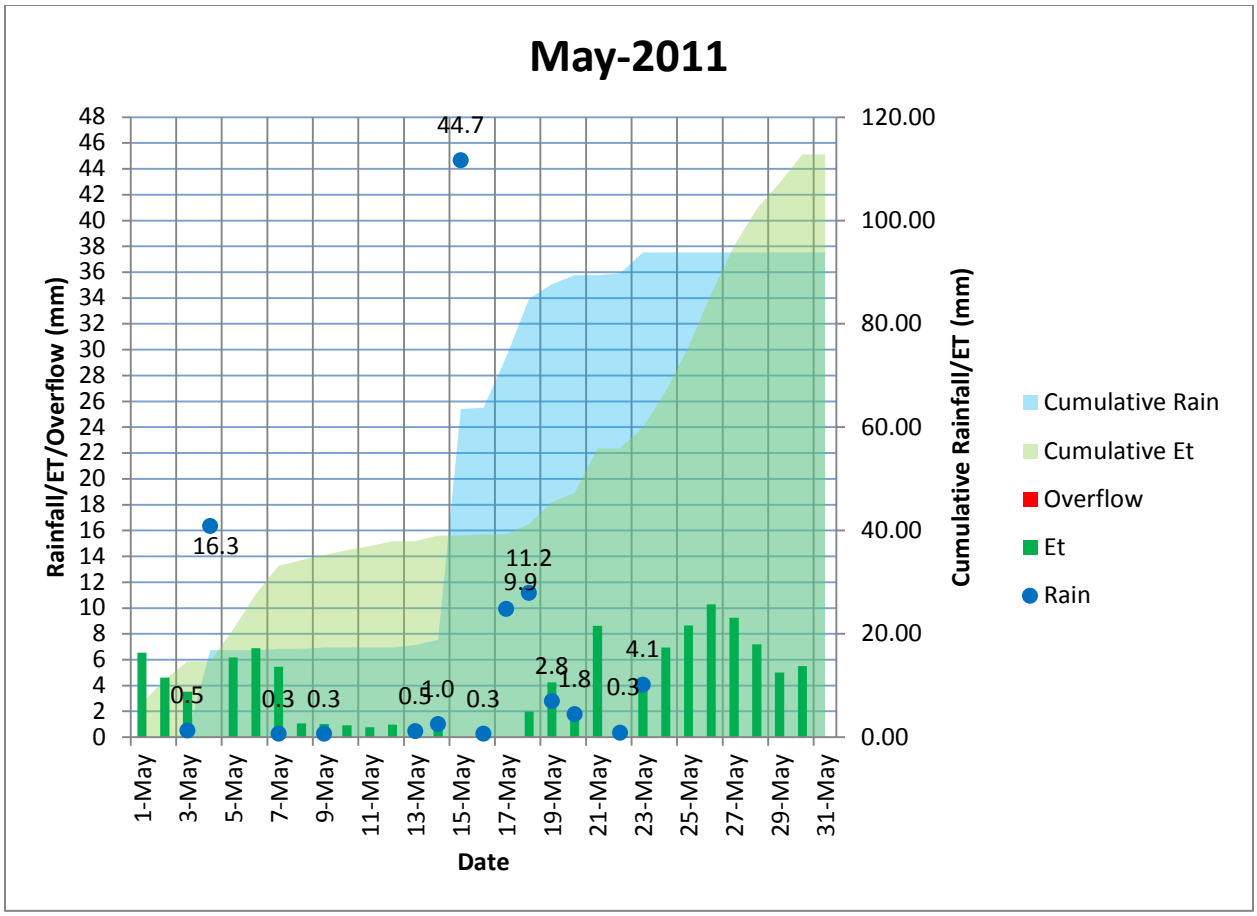
May-2011
Rainfall/ET/Overflow (mm)
Cumulative Rainfall/ET (mm)
Date
Cumulative Rain
Cumulative Et
Overflow
Et
Rain
44.7
16.3
11.2
9.9
4.1
2.8
1.8
4.0
0.5
0.3
0.3
0.5
0.3
0.3
1-May
3-May
5-May
7-May
9-May
11-May
13-May
15-May
17-May
19-May
21-May
23-May
25-May
27-May
29-May
31-May

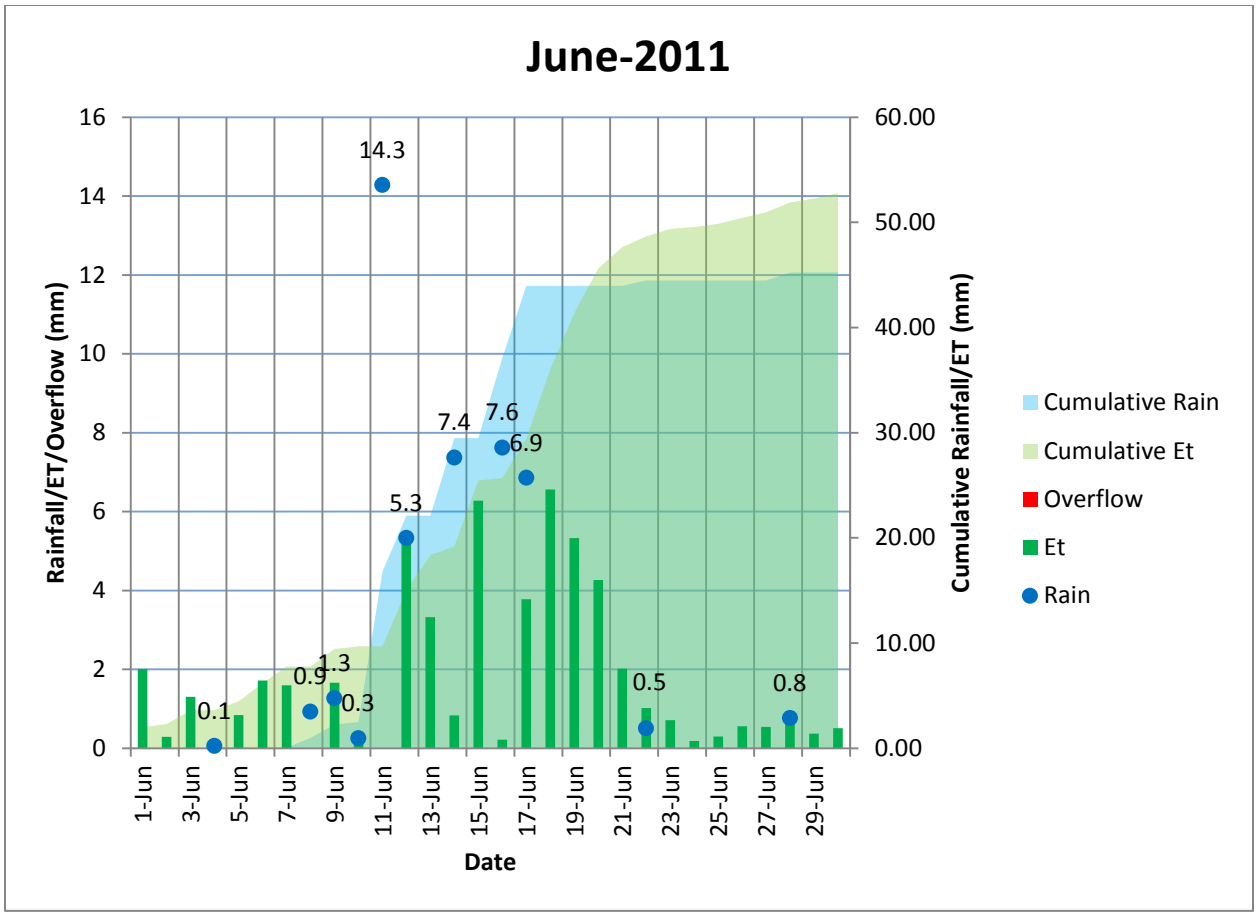
June-2011
Rainfall/ET/Overflow (mm)
Cumulative Rainfall/ET (mm)
Date
Cumulative Rain
Cumulative Et
Overflow
Et
Rain
14.3
7.4
7.6
6.9
5.3
0.9
1.3
0.3
0.1
0.5
0.8
1-Jun
3-Jun
5-Jun
7-Jun
9-Jun
11-Jun
13-Jun
15-Jun
17-Jun
19-Jun
21-Jun
23-Jun
25-Jun
27-Jun
29-Jun

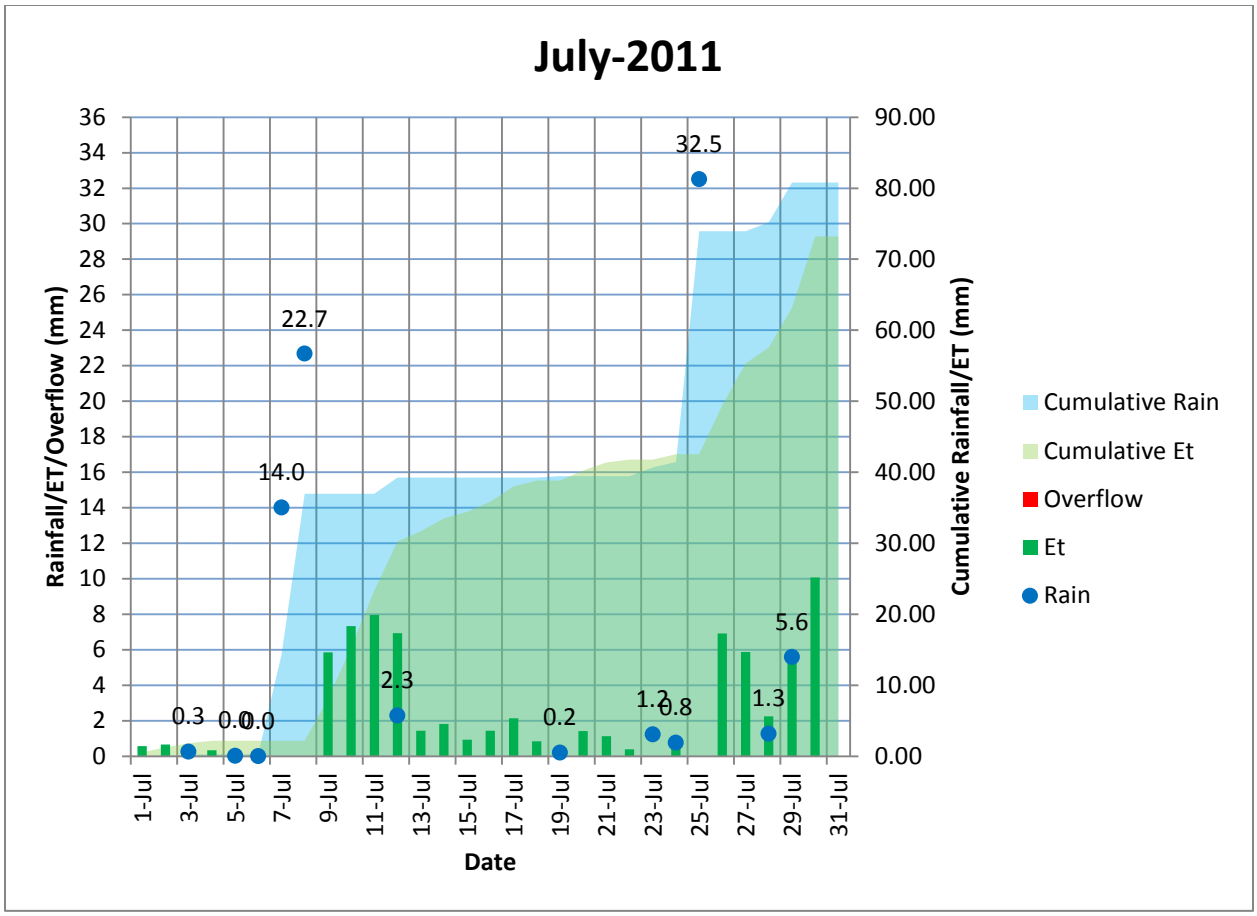
July-2011
Rainfall/ET/Overflow (mm)
Cumulative Rainfall/ET (mm)
Date
Cumulative Rain
Cumulative Et
Overflow
Et
Rain
32.5
22.7
14.0
2.3
0.3
0.0
0.0
0.2
1.2
0.8
1.3
5.6
1-Jul
3-Jul
5-Jul
7-Jul
9-Jul
11-Jul
13-Jul
15-Jul
17-Jul
19-Jul
21-Jul
23-Jul
25-Jul
27-Jul
29-Jul
31-Jul

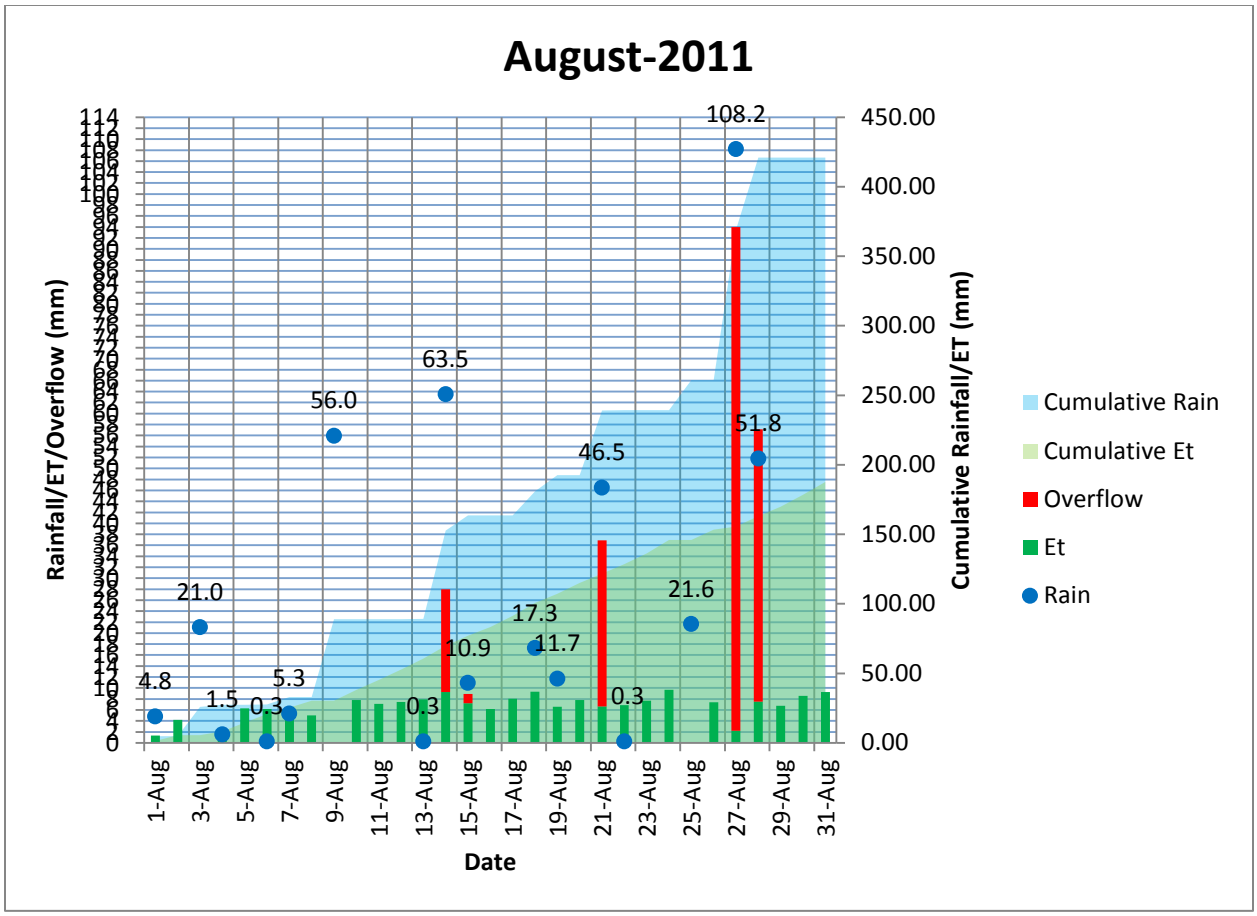
August-2011
Rainfall/ET/Overflow (mm)
Cumulative Rainfall/ET (mm)
Date
Cumulative Rain
Cumulative Et
Overflow
Et
Rain
4.8
21.0
1.5
0.3
5.3
56.0
63.5
0.3
10.9
17.3
11.7
46.5
0.3
21.6
108.2
51.8
1-Aug
3-Aug
5-Aug
7-Aug
9-Aug
11-Aug
13-Aug
15-Aug
17-Aug
19-Aug
21-Aug
23-Aug
25-Aug
27-Aug
29-Aug
31-Aug
0.00
50.00
100.00
150.00
200.00
250.00
300.00
350.00
400.00
450.00

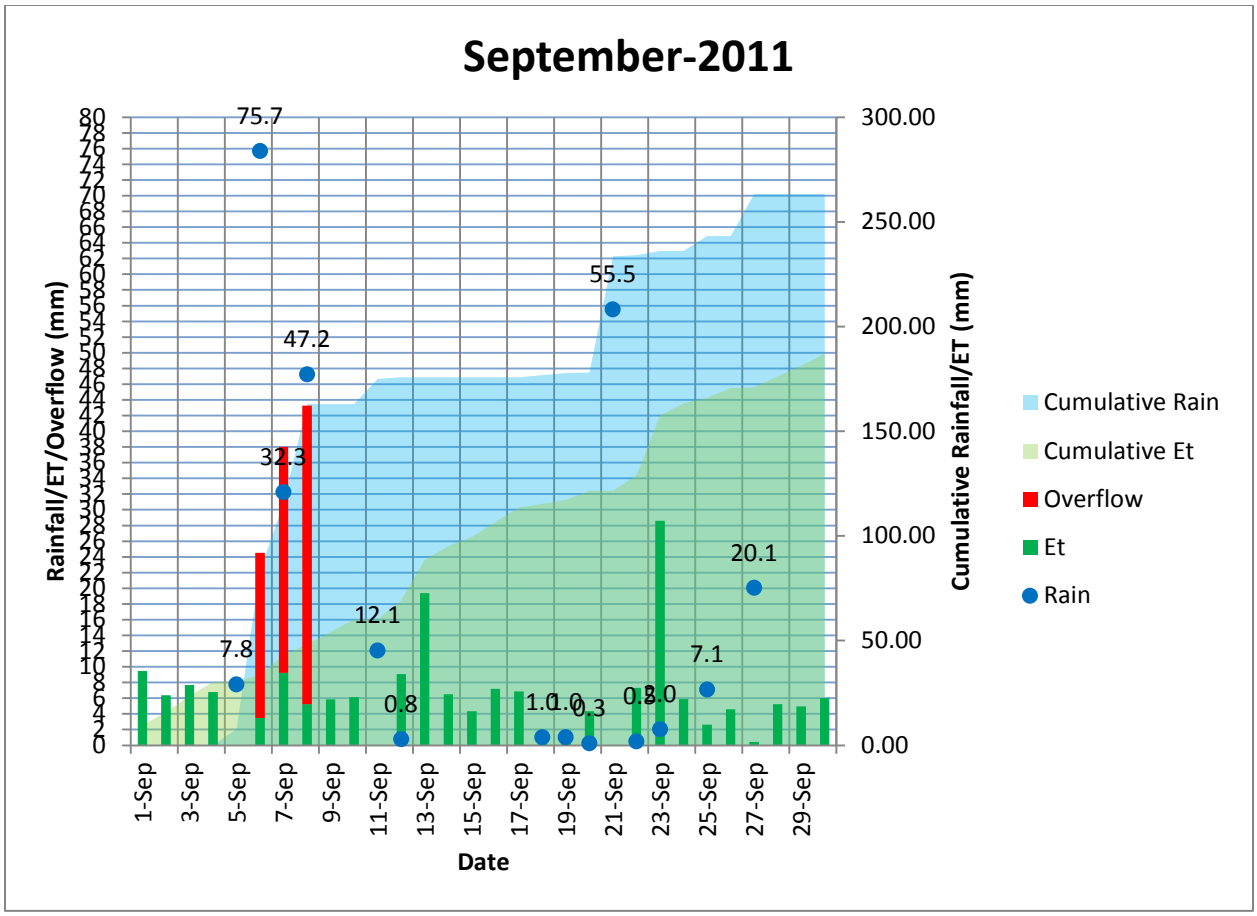
September-2011
Rainfall/ET/Overflow (mm)
Cumulative Rainfall/ET (mm)
Date
75.7
47.2
32.3
12.1
7.8
0.8
55.5
20.1
7.1
Cumulative Rain
Cumulative Et
Overflow
Et
Rain

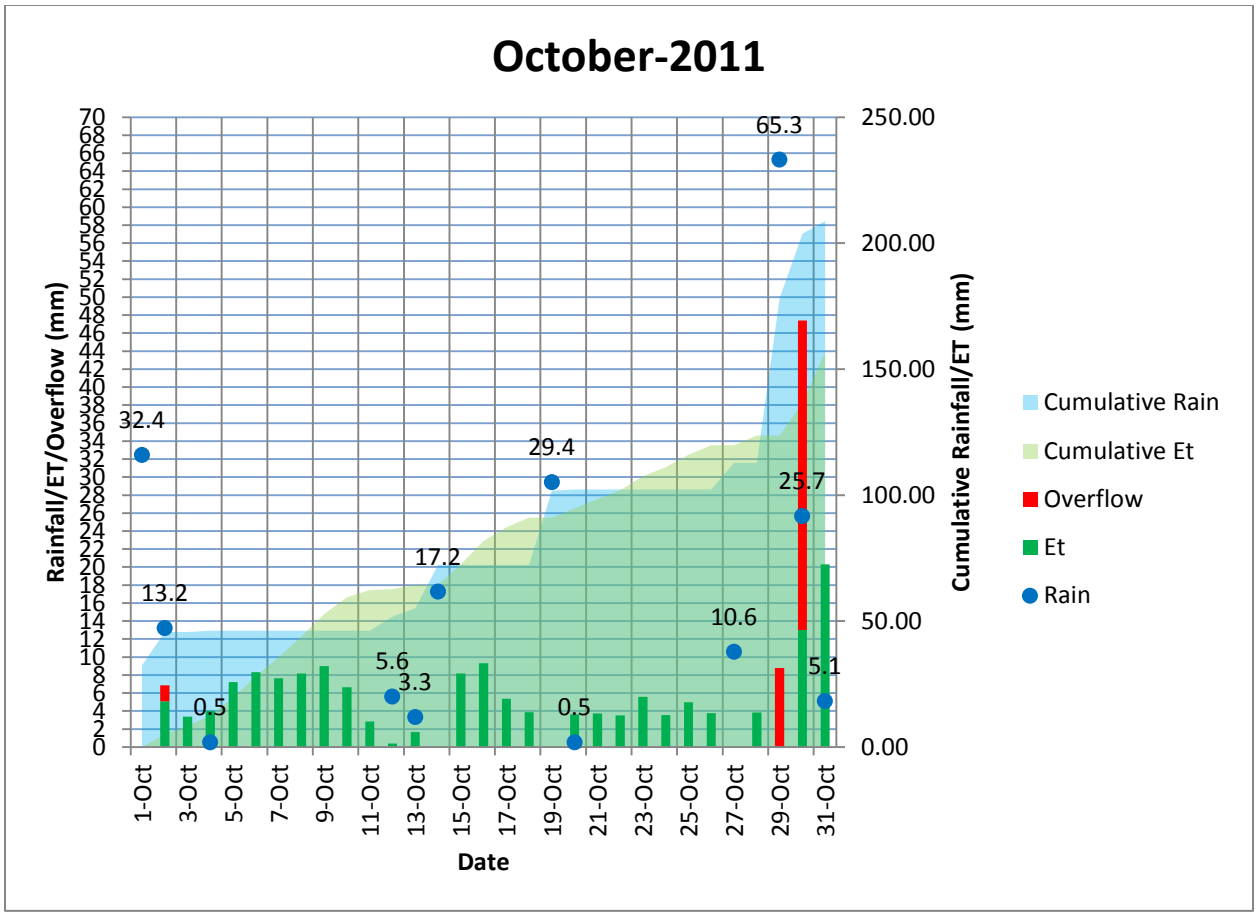
October-2011
Rainfall/ET/Overflow (mm)
Cumulative Rainfall/ET (mm)
Date
1-Oct
3-Oct
5-Oct
7-Oct
9-Oct
11-Oct
13-Oct
15-Oct
17-Oct
19-Oct
21-Oct
23-Oct
25-Oct
27-Oct
29-Oct
31-Oct
0.00
50.00
100.00
150.00
200.00
250.00
32.4
13.2
0.5
5.6
3.3
17.2
29.4
0.5
10.6
65.3
25.7
5.1
Cumulative Rain
Cumulative Et
Overflow
Et
Rain

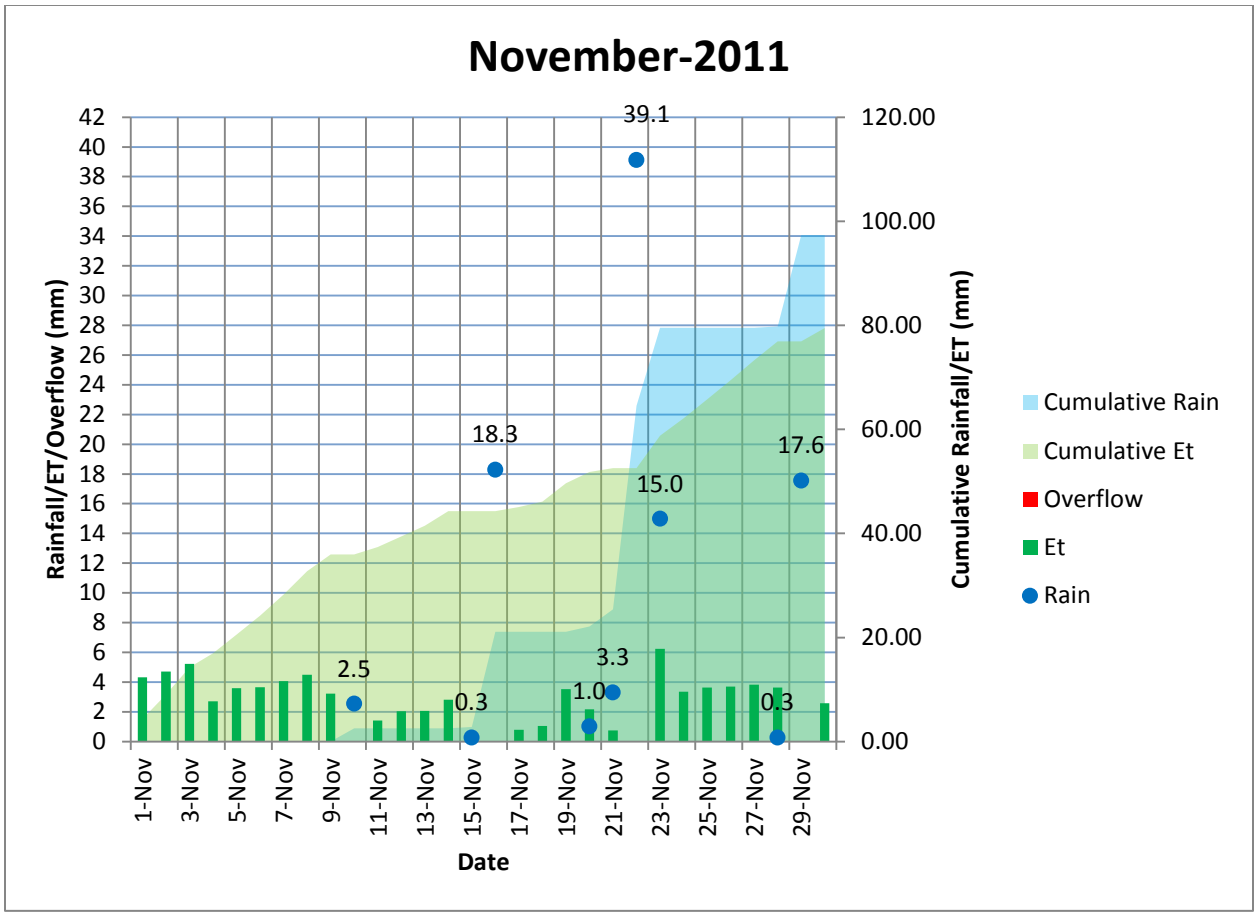
November-2011
Rainfall/ET/Overflow (mm)
Cumulative Rainfall/ET (mm)
Date
Cumulative Rain
Cumulative Et
Overflow
Et
Rain
39.1
18.3
17.6
15.0
3.3
2.5
1.0
0.3
0.3
1-Nov
3-Nov
5-Nov
7-Nov
9-Nov
11-Nov
13-Nov
15-Nov
17-Nov
19-Nov
21-Nov
23-Nov
25-Nov
27-Nov
29-Nov

2012

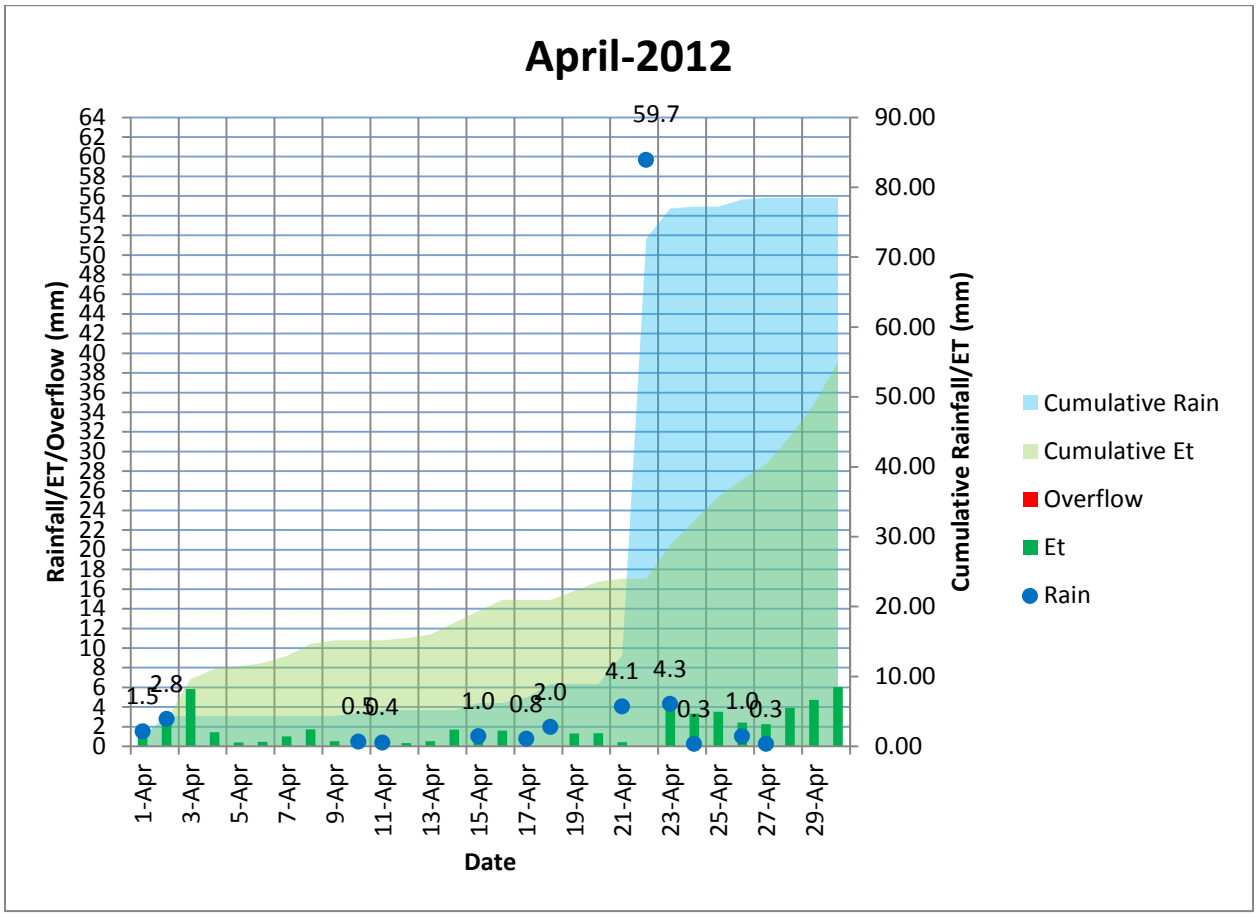
April-2012
Rainfall/ET/Overflow (mm)
Cumulative Rainfall/ET (mm)
Date
1-Apr
3-Apr
5-Apr
7-Apr
9-Apr
11-Apr
13-Apr
15-Apr
17-Apr
19-Apr
21-Apr
23-Apr
25-Apr
27-Apr
29-Apr
59.7
1.5
2.8
0.5
0.4
1.0
0.8
2.0
4.1
4.3
0.3
1.0
0.3
Cumulative Rain
Cumulative Et
Overflow
Et
Rain

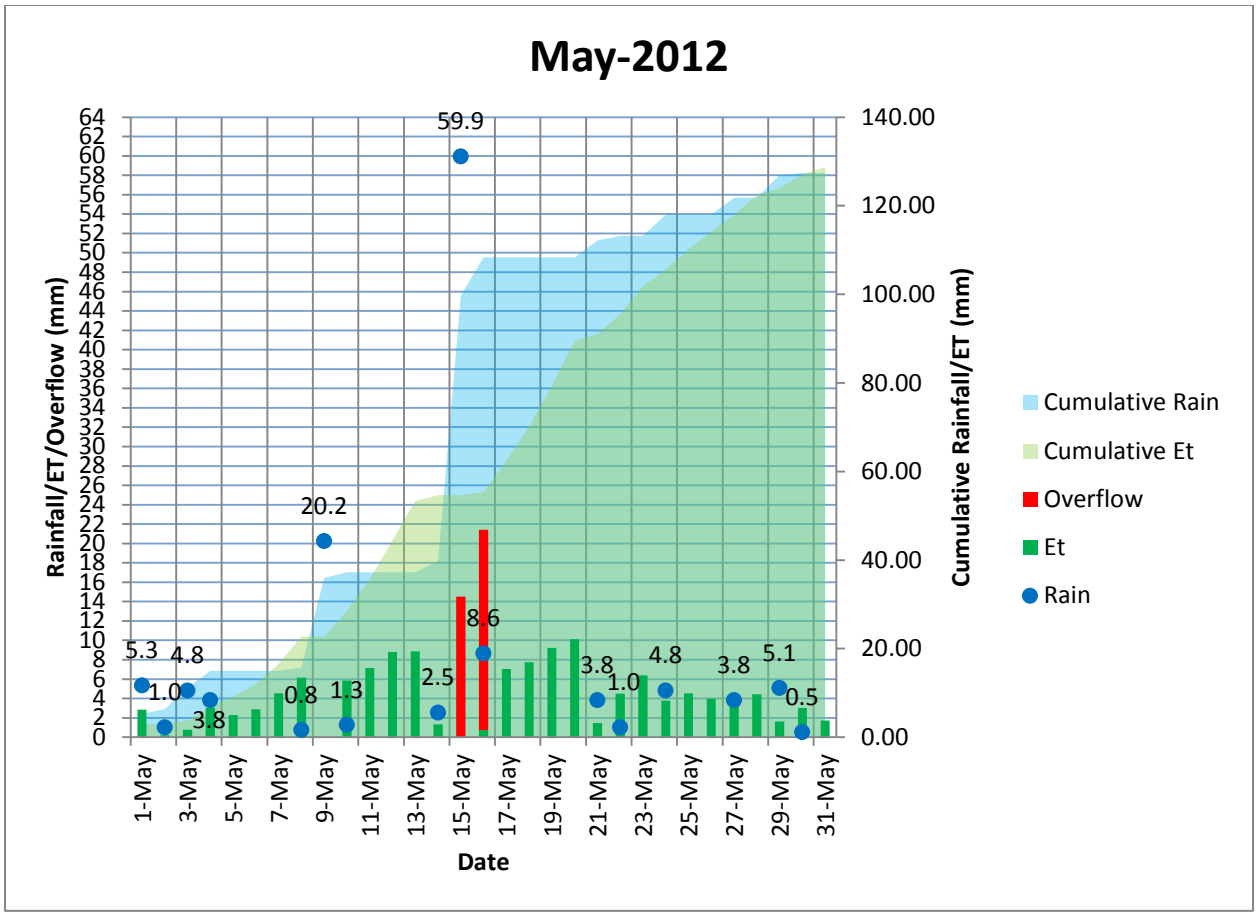
May-2012
Rainfall/ET/Overflow (mm)
Cumulative Rainfall/ET (mm)
Date
Cumulative Rain
Cumulative Et
Overflow
Et
Rain
59.9
20.2
8.6
5.3
4.8
1.0
3.8
0.8
1.3
2.5
3.8
1.0
4.8
3.8
5.1
0.5
1-May
3-May
5-May
7-May
9-May
11-May
13-May
15-May
17-May
19-May
21-May
23-May
25-May
27-May
29-May
31-May

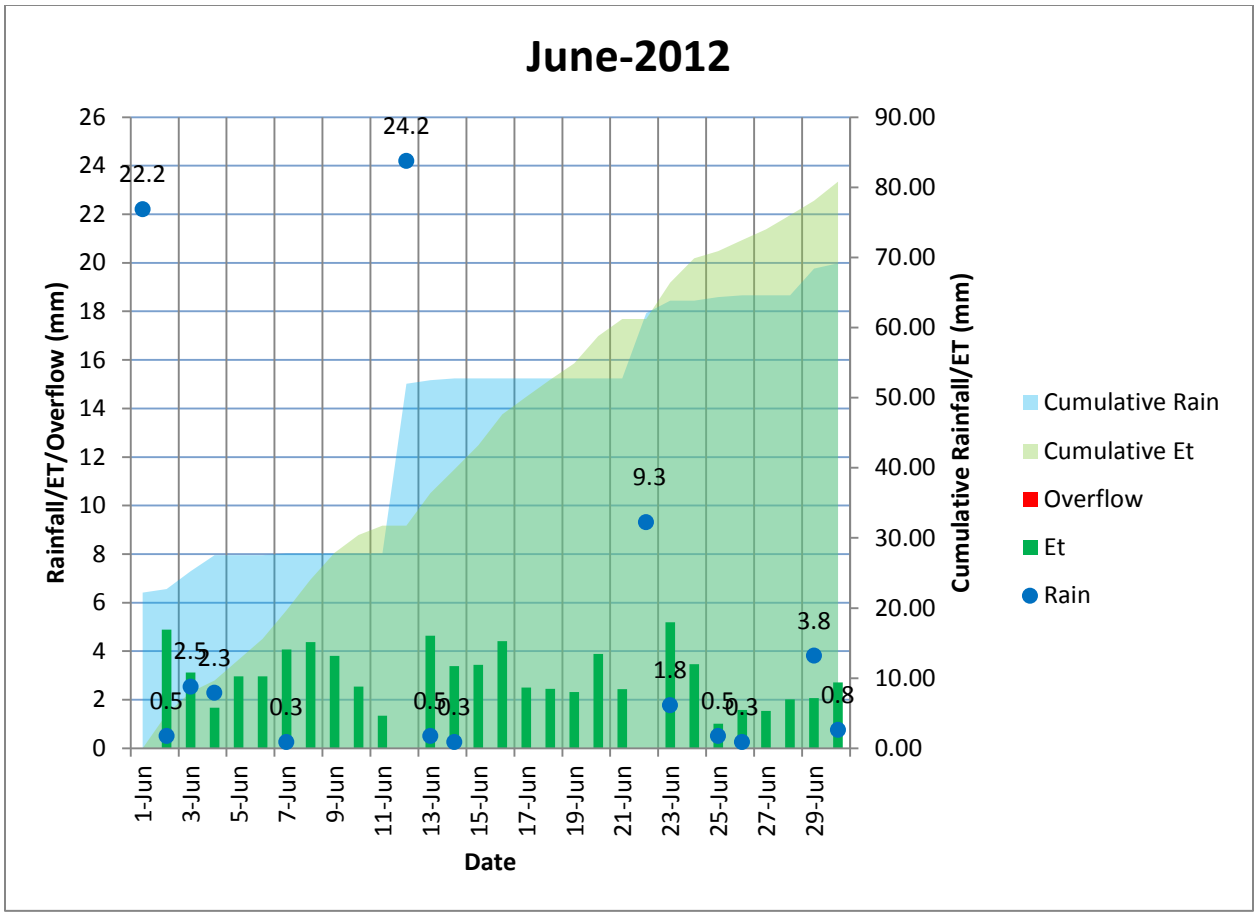
June-2012
Rainfall/ET/Overflow (mm)
Cumulative Rainfall/ET (mm)
Date
Cumulative Rain
Cumulative Et
Overflow
Et
Rain
22.2
24.2
9.3
2.5
2.3
0.5
0.3
0.5
0.3
1.8
0.5
0.3
3.8
0.8
1-Jun
3-Jun
5-Jun
7-Jun
9-Jun
11-Jun
13-Jun
15-Jun
17-Jun
19-Jun
21-Jun
23-Jun
25-Jun
27-Jun
29-Jun

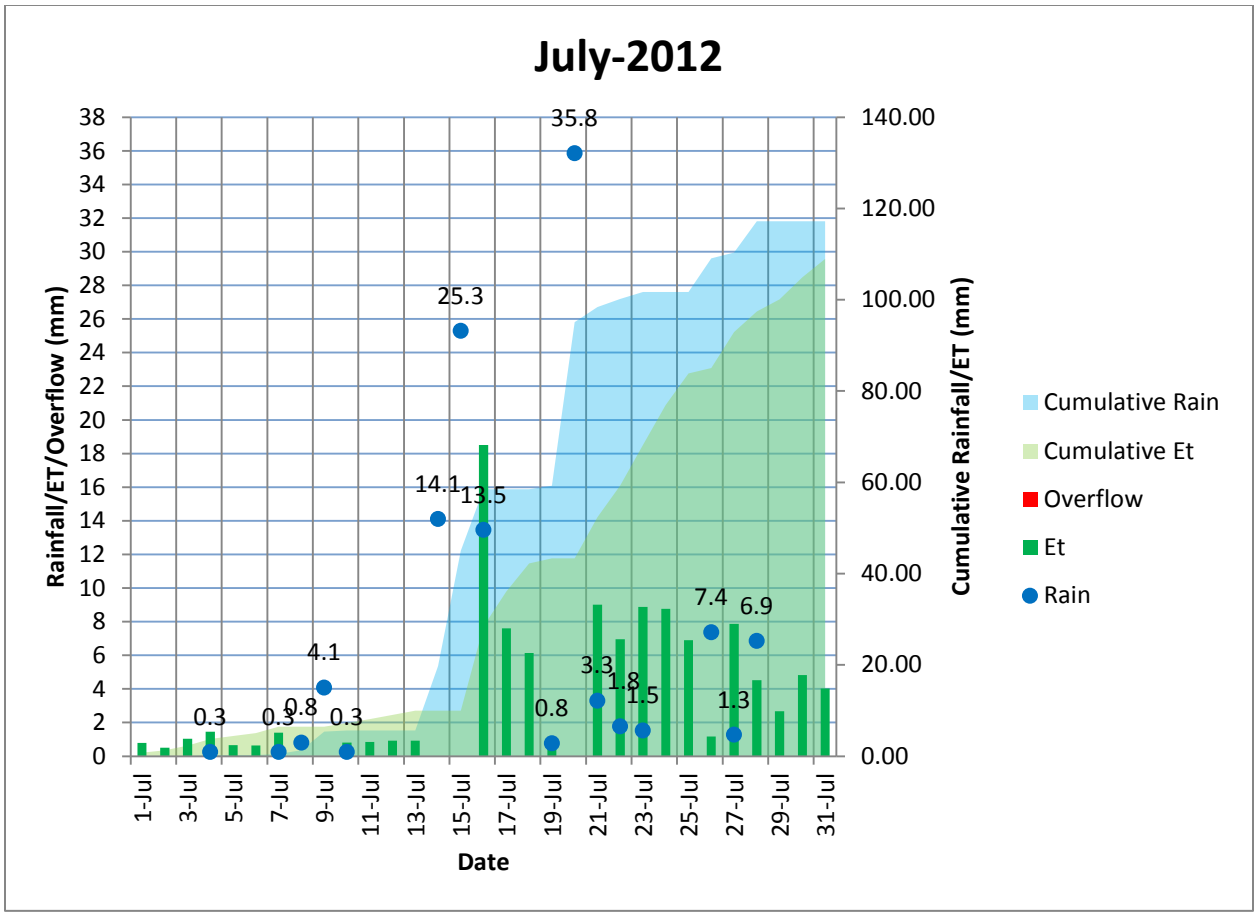
July-2012
Rainfall/ET/Overflow (mm)
Cumulative Rainfall/ET (mm)
Date
Cumulative Rain
Cumulative Et
Overflow
Et
Rain
35.8
25.3
14.1
13.5
4.1
0.3
0.3
0.8
0.3
0.8
3.3
1.8
1.5
7.4
6.9
1.3
1-Jul
3-Jul
5-Jul
7-Jul
9-Jul
11-Jul
13-Jul
15-Jul
17-Jul
19-Jul
21-Jul
23-Jul
25-Jul
27-Jul
29-Jul
31-Jul

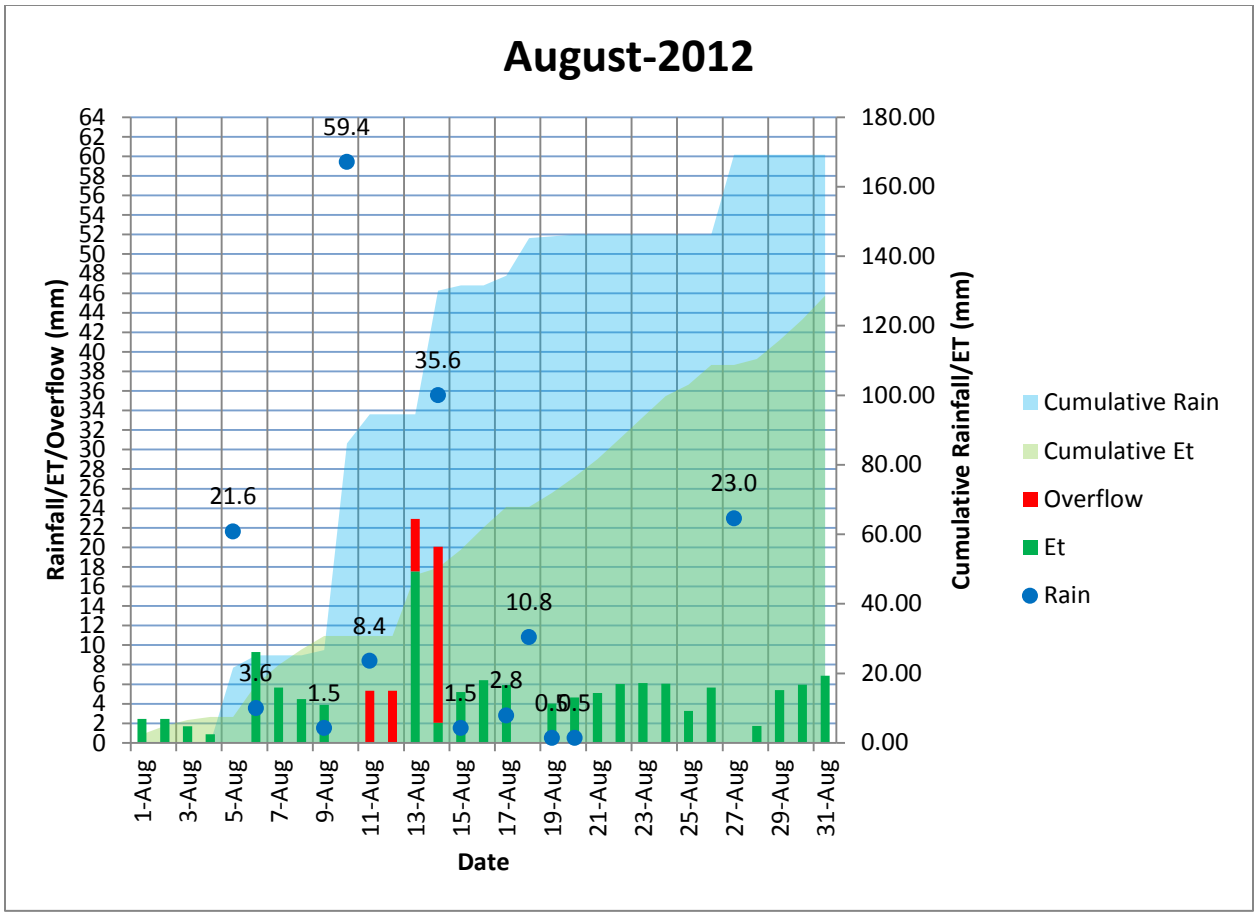
August-2012
Rainfall/ET/Overflow (mm)
Cumulative Rainfall/ET (mm)
Date
59.4
35.6
21.6
23.0
10.8
8.4
3.6
1.5
1.5
2.8
0.5
0.5
Cumulative Rain
Cumulative Et
Overflow
Et
Rain

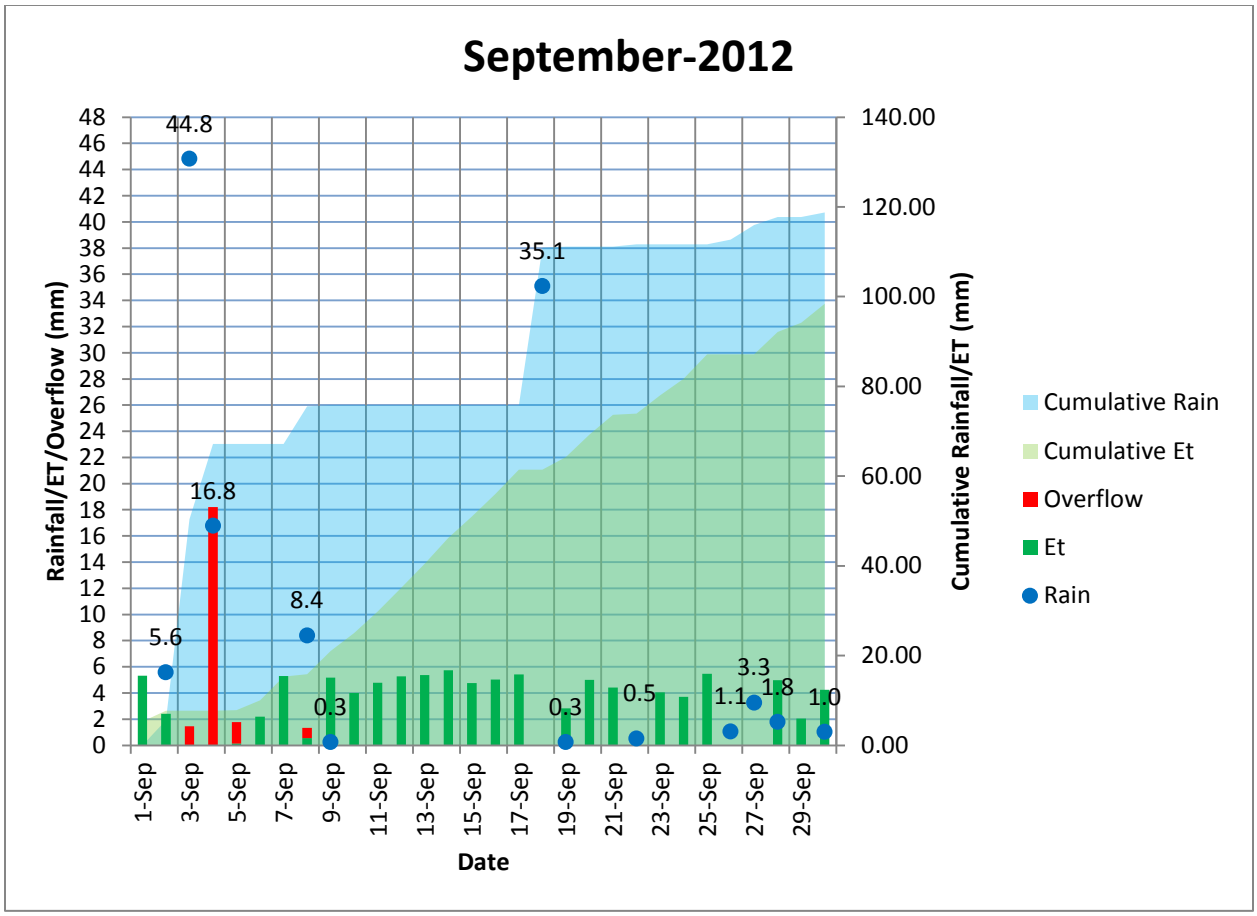
September-2012
Rainfall/ET/Overflow (mm)
Cumulative Rainfall/ET (mm)
Date
Cumulative Rain
Cumulative Et
Overflow
Et
Rain
44.8
16.8
8.4
5.6
0.3
35.1
0.3
0.5
1.1
3.3
1.8
1.0
1-Sep
3-Sep
5-Sep
7-Sep
9-Sep
11-Sep
13-Sep
15-Sep
17-Sep
19-Sep
21-Sep
23-Sep
25-Sep
27-Sep
29-Sep

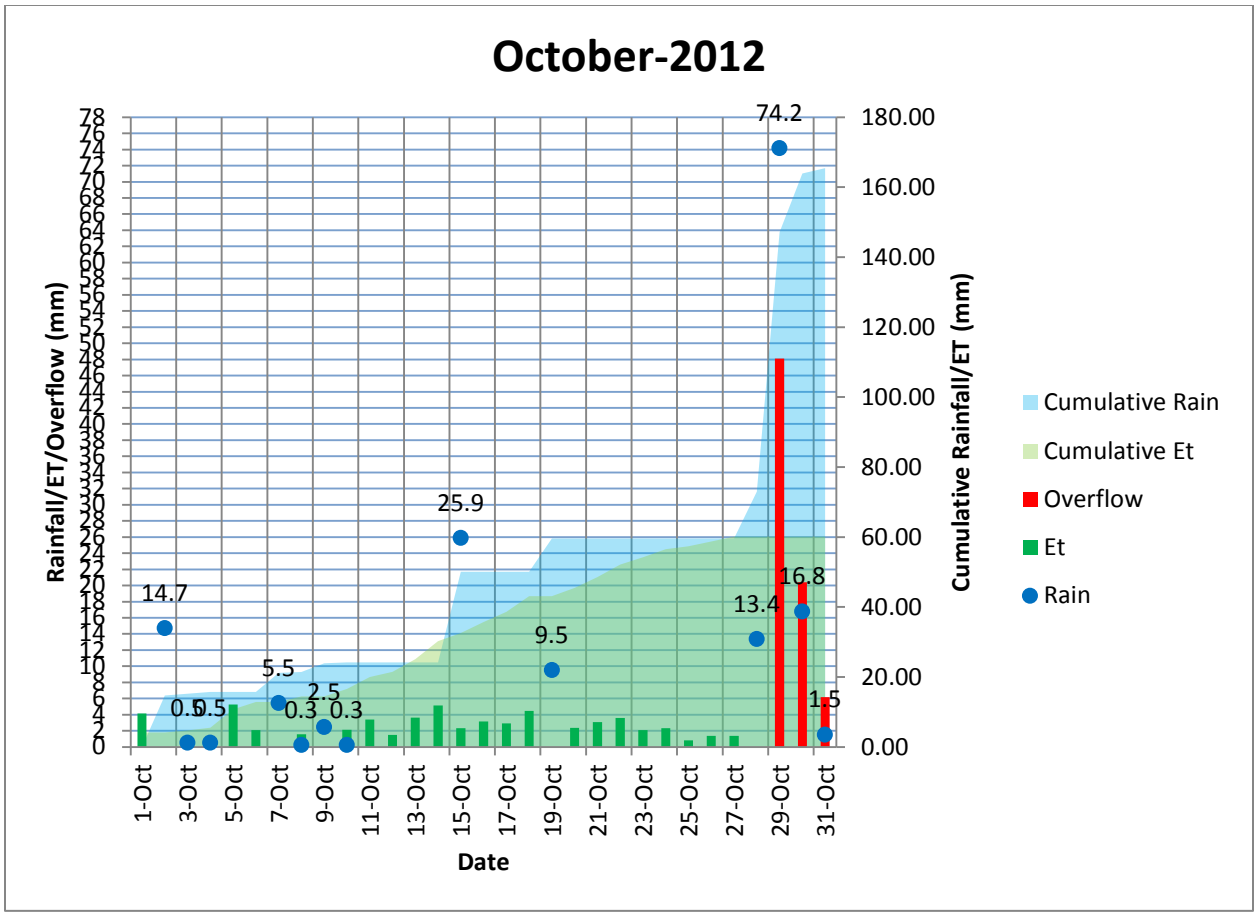
October-2012
Rainfall/ET/Overflow (mm)
Cumulative Rainfall/ET (mm)
Date
1-Oct
3-Oct
5-Oct
7-Oct
9-Oct
11-Oct
13-Oct
15-Oct
17-Oct
19-Oct
21-Oct
23-Oct
25-Oct
27-Oct
29-Oct
31-Oct
0.00
20.00
40.00
60.00
80.00
100.00
120.00
140.00
160.00
180.00
14.7
0.5
0.5
5.5
0.3
2.5
0.3
25.9
9.5
13.4
74.2
16.8
1.5
Cumulative Rain
Cumulative Et
Overflow
Et
Rain

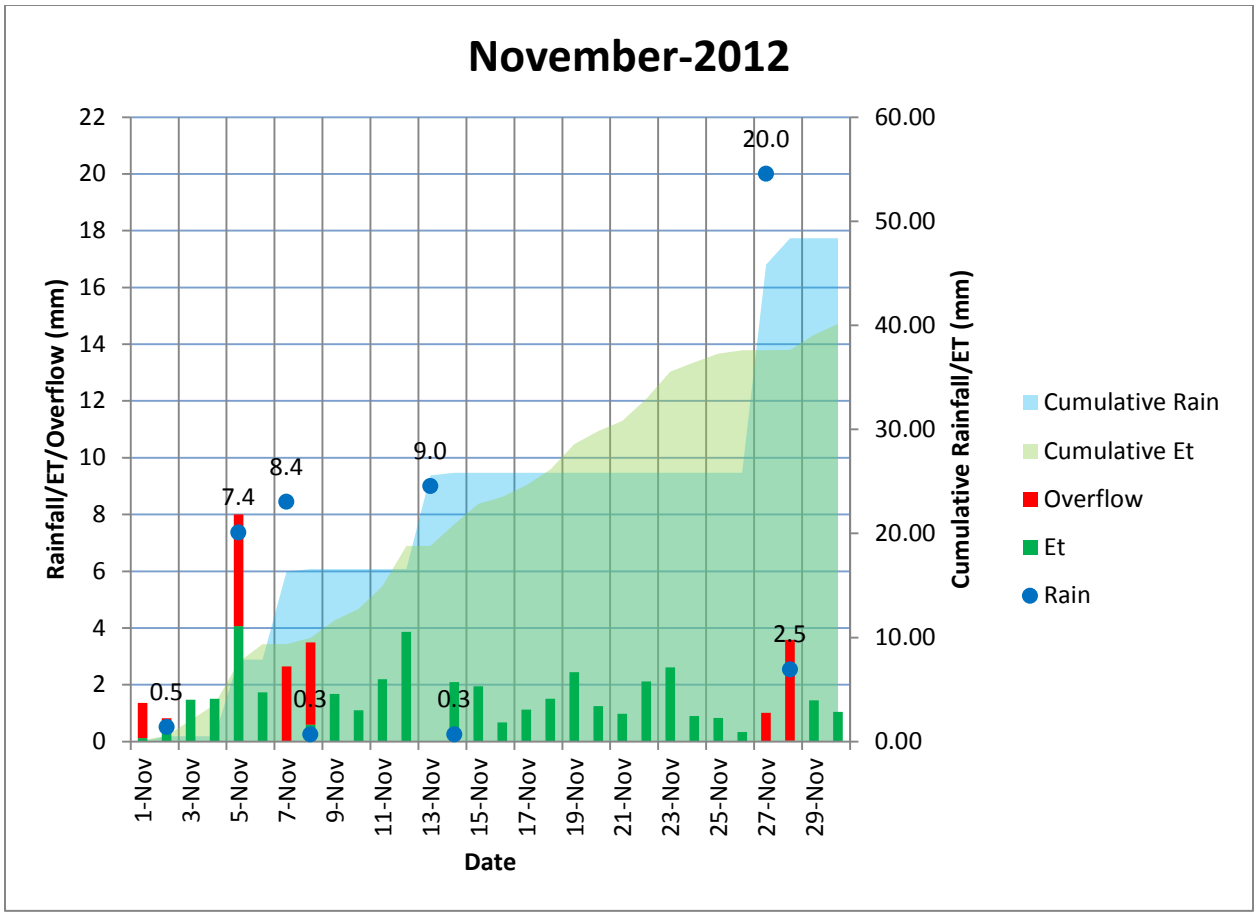
November-2012
Rainfall/ET/Overflow (mm)
Cumulative Rainfall/ET (mm)
Date
0
2
4
6
8
10
12
14
16
18
20
22
0.00
10.00
20.00
30.00
40.00
50.00
60.00
1-Nov
3-Nov
5-Nov
7-Nov
9-Nov
11-Nov
13-Nov
15-Nov
17-Nov
19-Nov
21-Nov
23-Nov
25-Nov
27-Nov
29-Nov
0.5
7.4
8.4
0.3
9.0
0.3
20.0
2.5
Cumulative Rain
Cumulative Et
Overflow
Et
Rain

2013

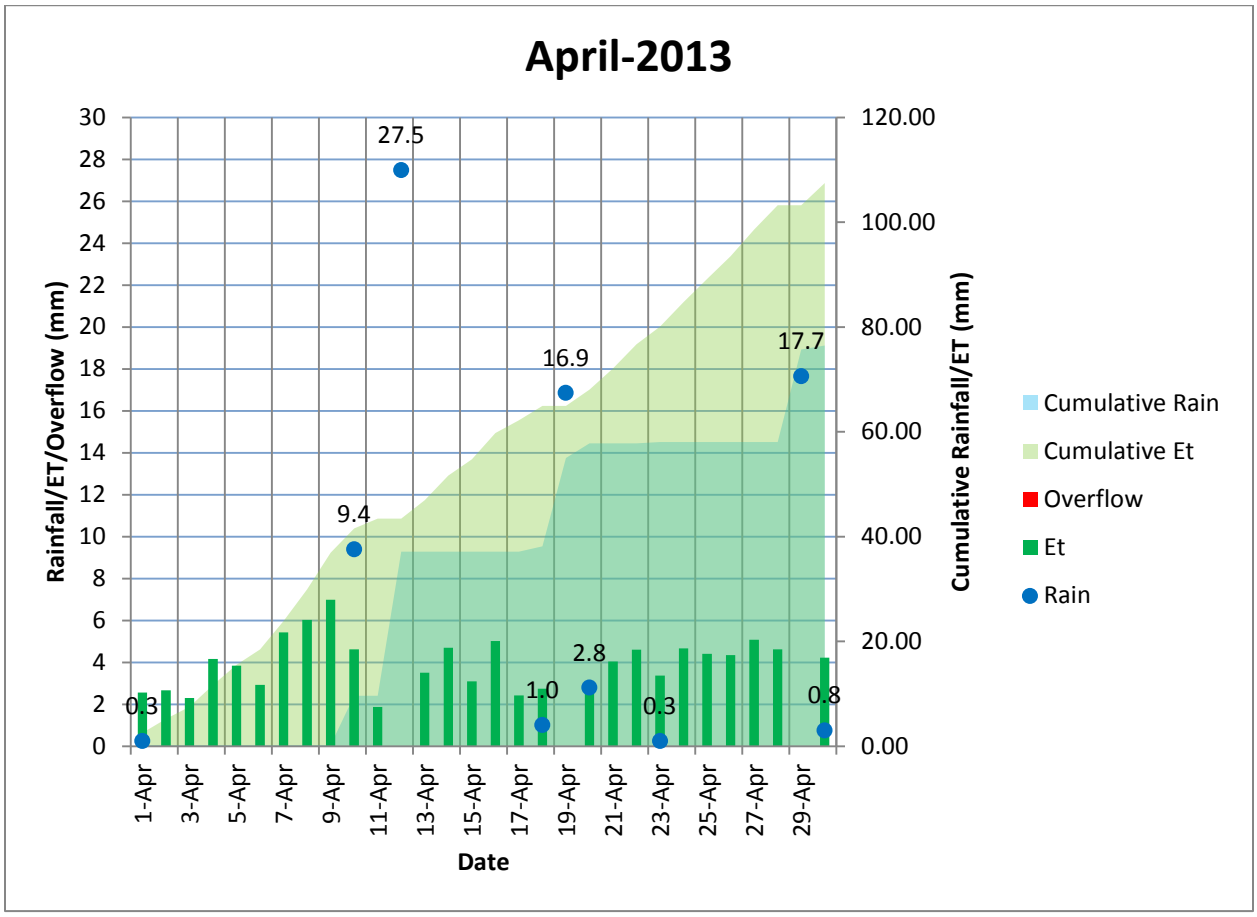
April-2013
Rainfall/ET/Overflow (mm)
Cumulative Rainfall/ET (mm)
Date
27.5
16.9
17.7
9.4
2.8
1.0
0.3
0.3
0.8
Cumulative Rain
Cumulative Et
Overflow
Et
Rain

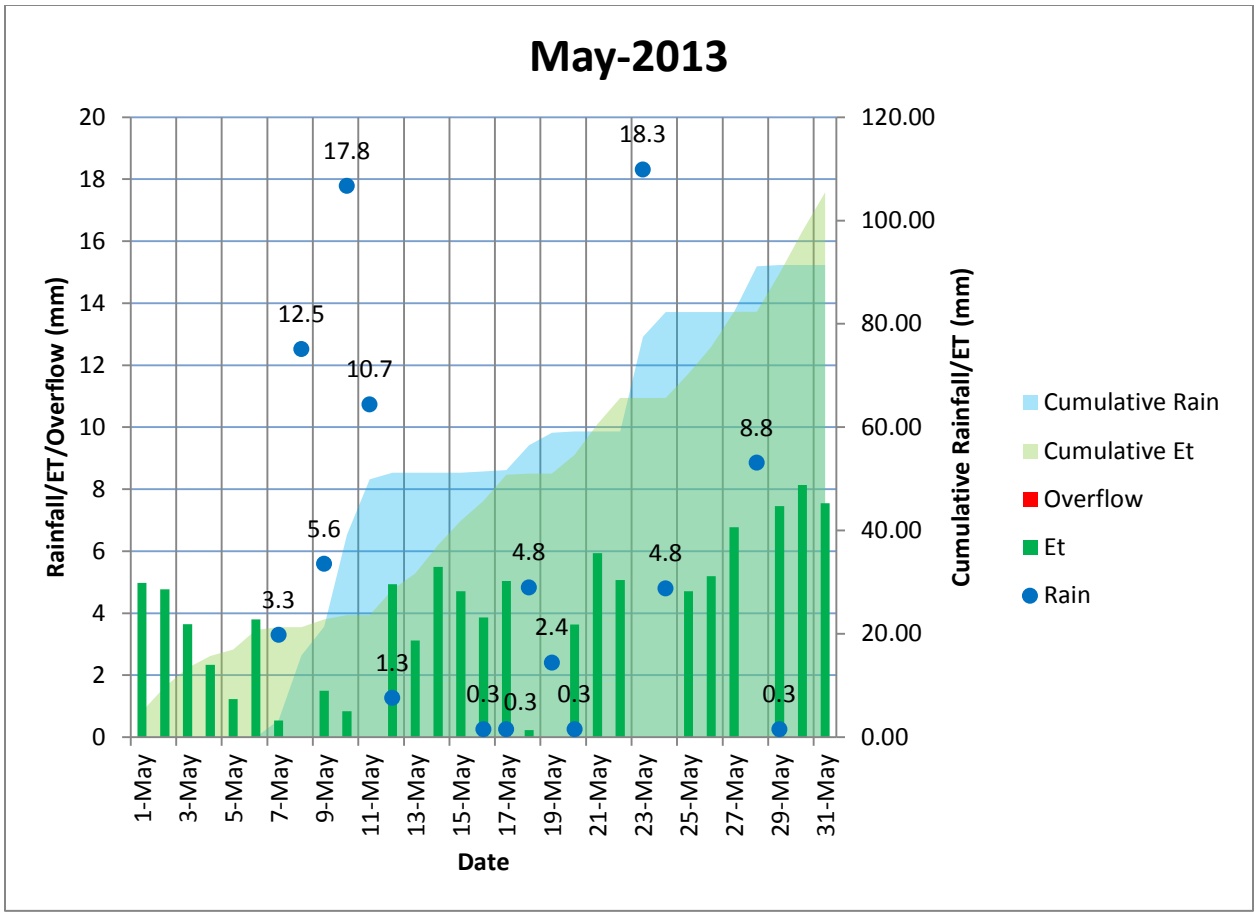
May-2013
Rainfall/ET/Overflow (mm)
Cumulative Rainfall/ET (mm)
Date
Cumulative Rain
Cumulative Et
Overflow
Et
Rain
17.8
18.3
12.5
10.7
8.8
5.6
4.8
4.8
3.3
2.4
1.3
0.3
0.3
0.3
0.3
1-May
3-May
5-May
7-May
9-May
11-May
13-May
15-May
17-May
19-May
21-May
23-May
25-May
27-May
29-May
31-May

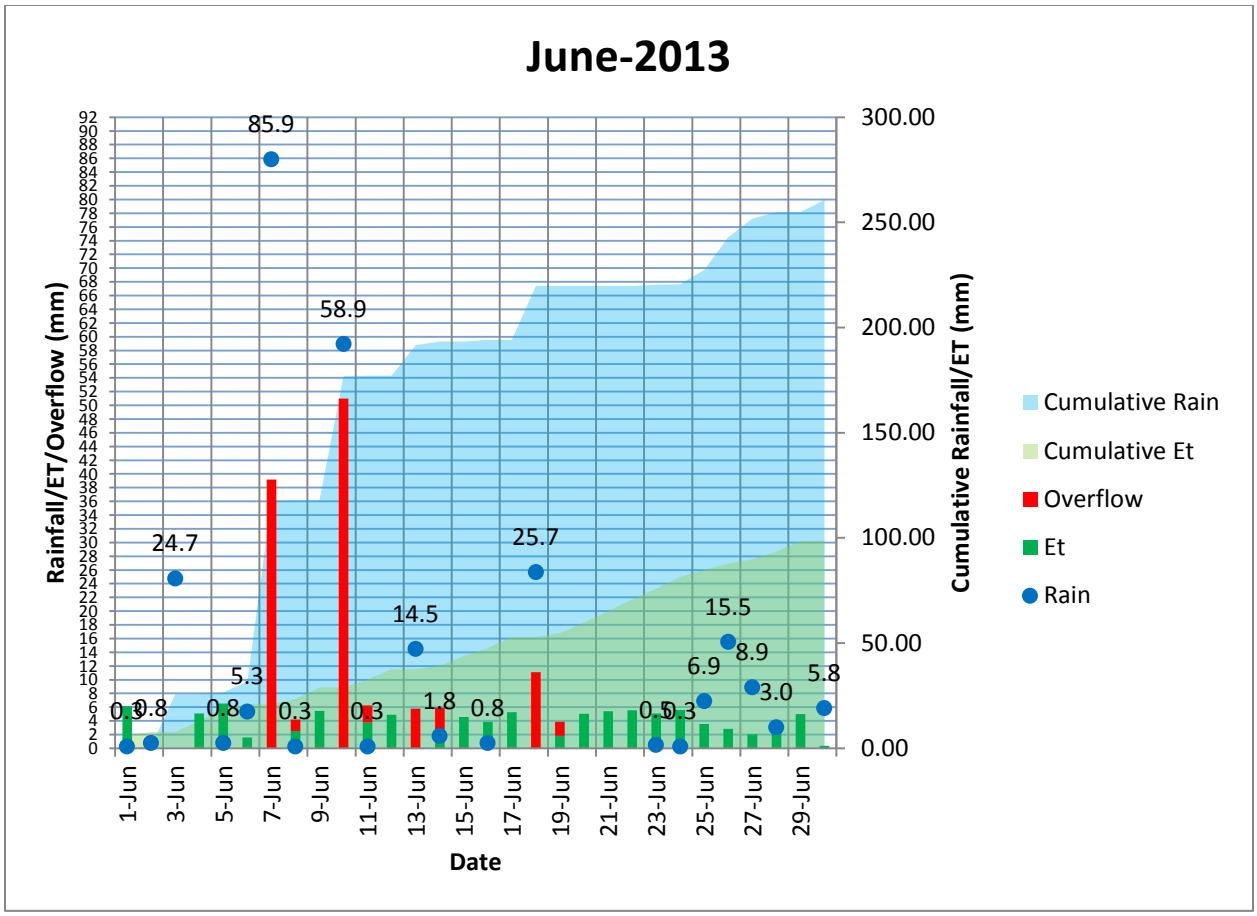
June-2013
Rainfall/ET/Overflow (mm)
Cumulative Rainfall/ET (mm)
Date
Cumulative Rain
Cumulative Et
Overflow
Et
Rain
85.9
58.9
24.7
25.7
14.5
15.5
8.9
6.9
5.8
5.3
3.0
1.8
0.8
0.3
0.00
50.00
100.00
150.00
200.00
250.00
300.00
1-Jun
3-Jun
5-Jun
7-Jun
9-Jun
11-Jun
13-Jun
15-Jun
17-Jun
19-Jun
21-Jun
23-Jun
25-Jun
27-Jun
29-Jun

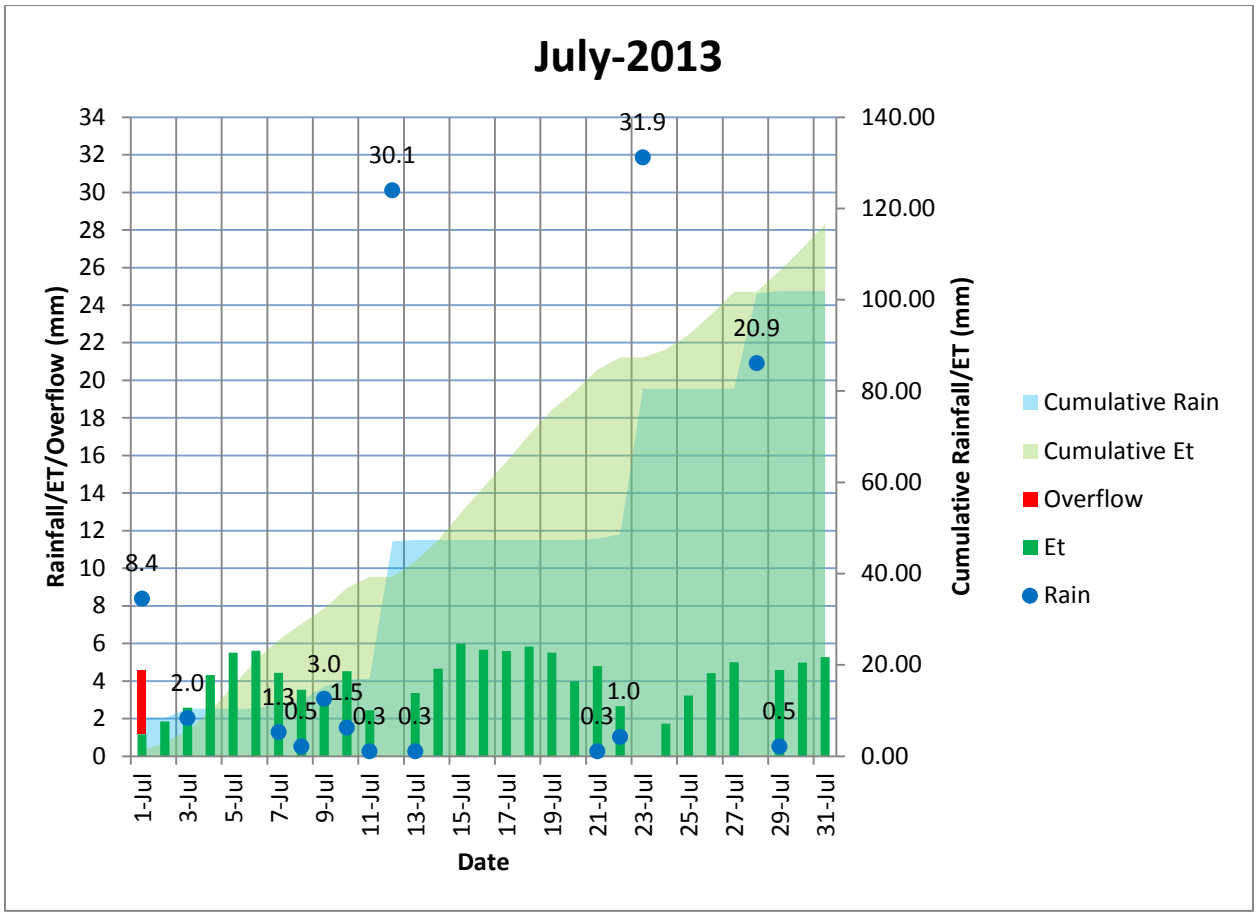
July-2013
Rainfall/ET/Overflow (mm)
Cumulative Rainfall/ET (mm)
Date
Cumulative Rain
Cumulative Et
Overflow
Et
Rain
8.4
2.0
1.3
0.5
3.0
1.5
0.3
30.1
0.3
0.3
1.0
31.9
20.9
0.5
1-Jul
3-Jul
5-Jul
7-Jul
9-Jul
11-Jul
13-Jul
15-Jul
17-Jul
19-Jul
21-Jul
23-Jul
25-Jul
27-Jul
29-Jul
31-Jul

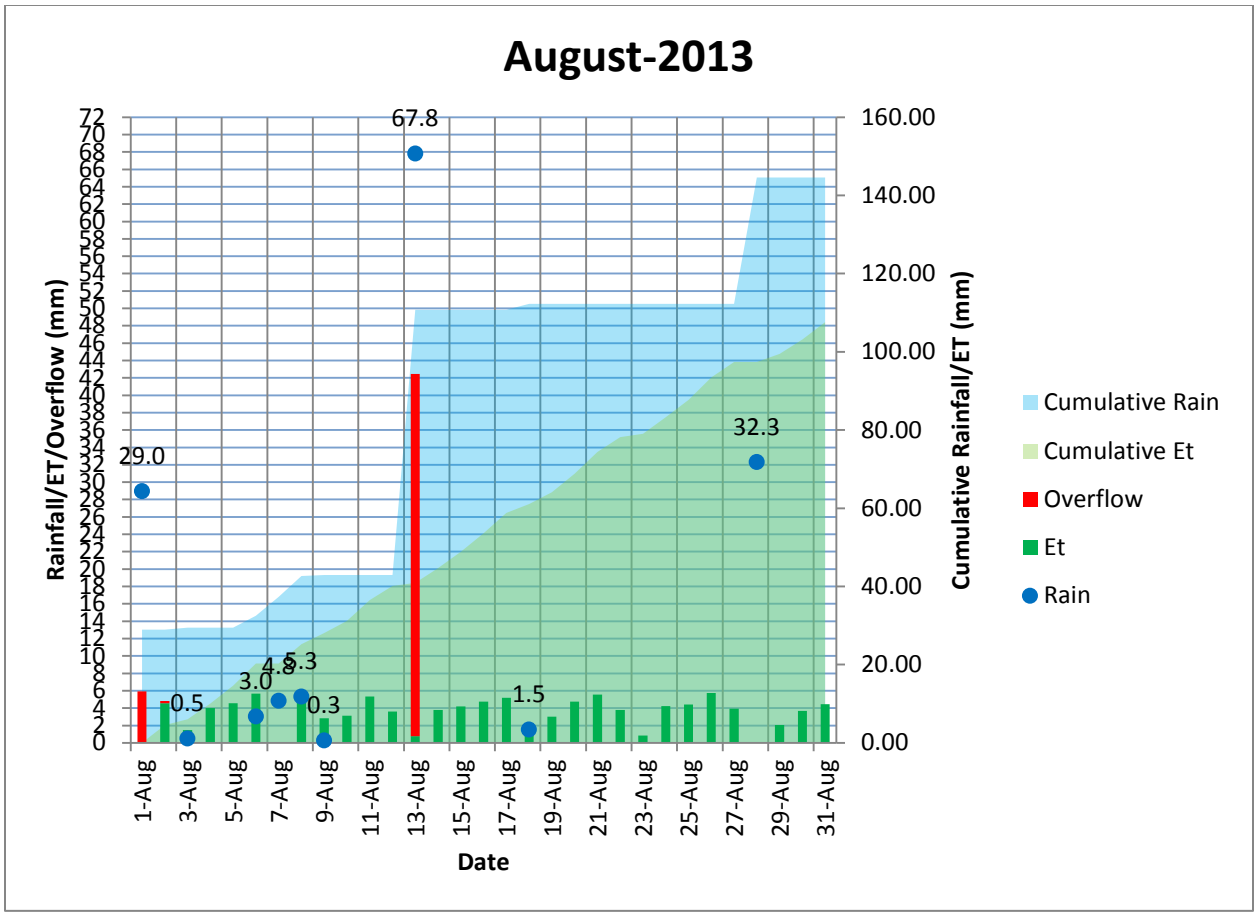
August-2013
Rainfall/ET/Overflow (mm)
Cumulative Rainfall/ET (mm)
Date
67.8
29.0
32.3
0.5
3.0
4.8
5.3
0.3
1.5
Cumulative Rain
Cumulative Et
Overflow
Et
Rain

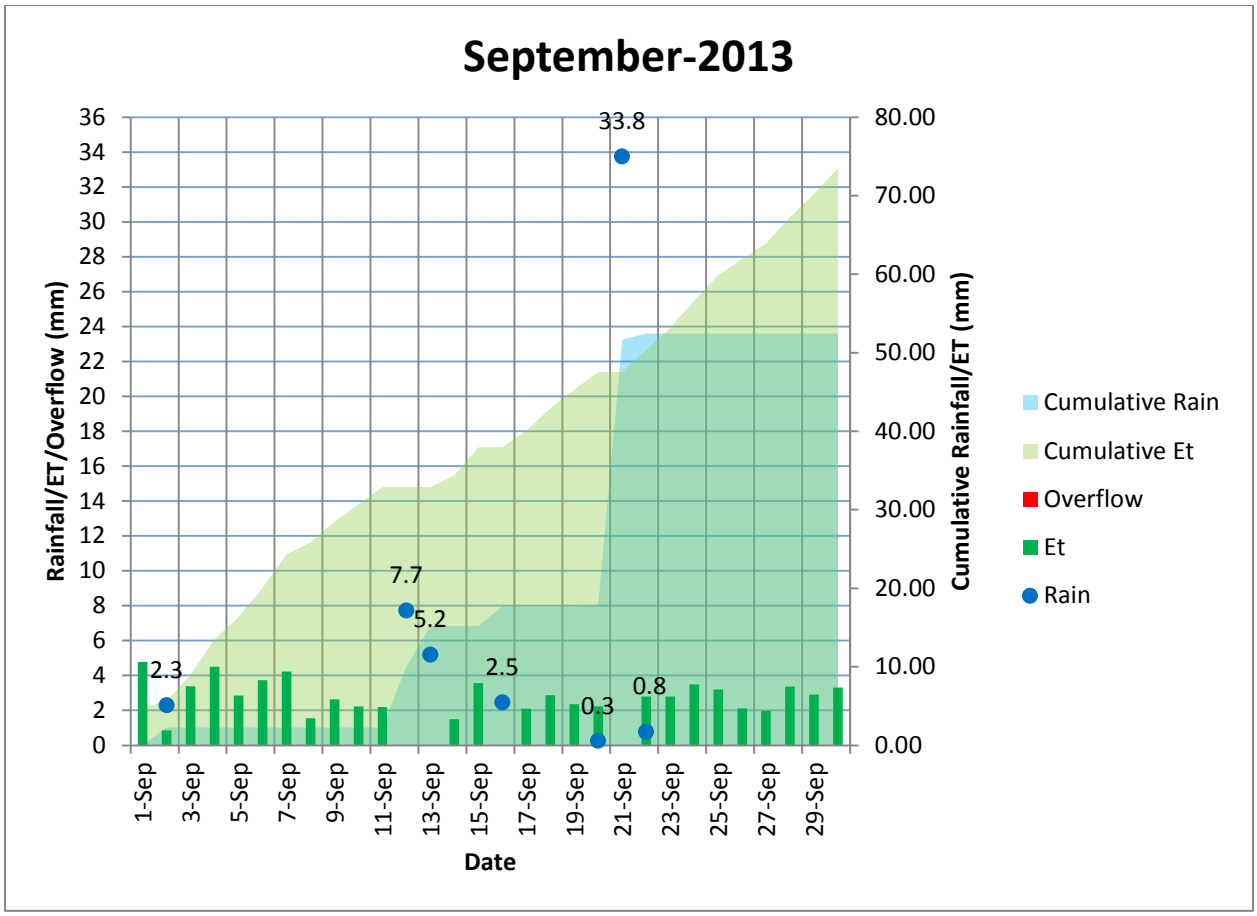
September-2013
Rainfall/ET/Overflow (mm)
Cumulative Rainfall/ET (mm)
Date
33.8
7.7
5.2
2.3
2.5
0.3
0.8
Cumulative Rain
Cumulative Et
Overflow
Et
Rain

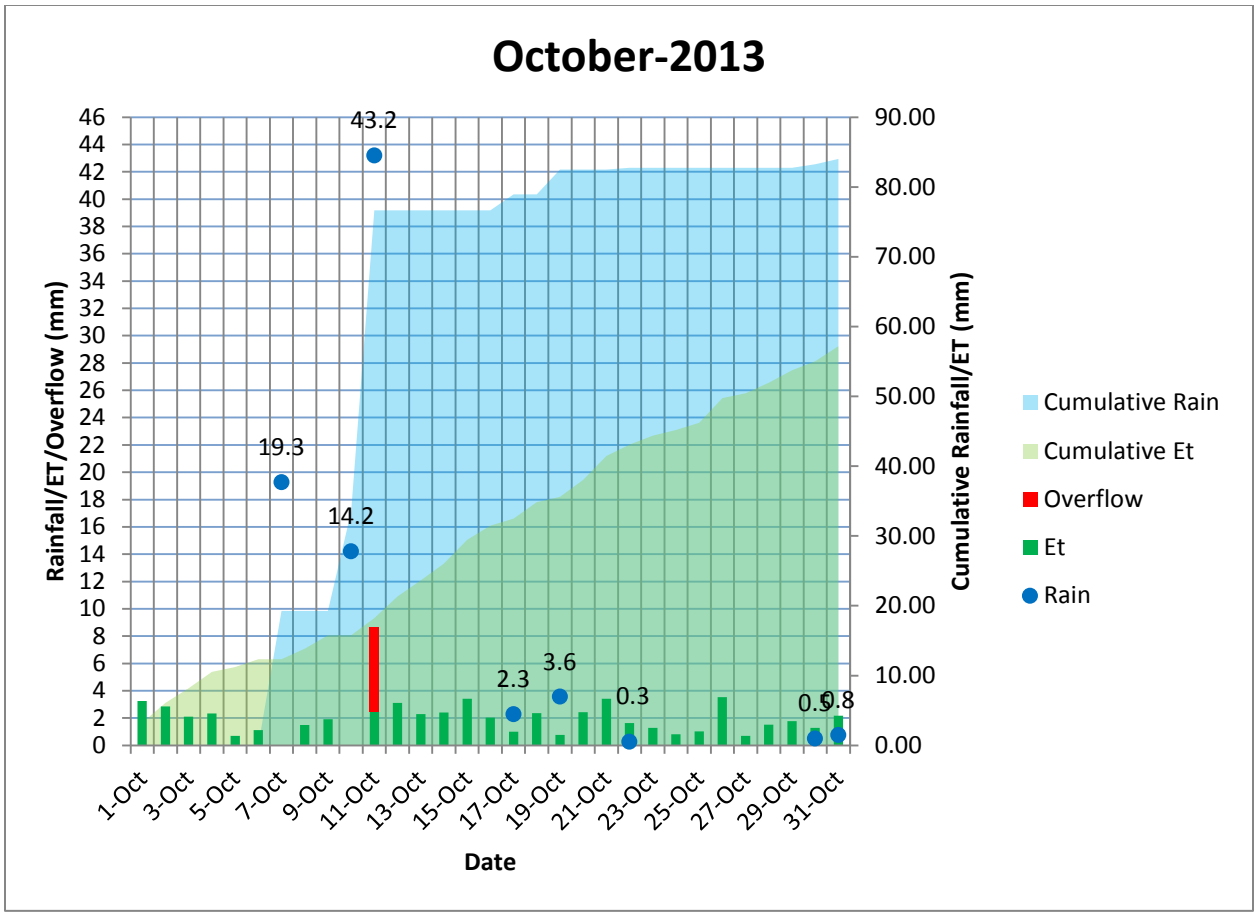
October-2013
Rainfall/ET/Overflow (mm)
Cumulative Rainfall/ET (mm)
Date
43.2
19.3
14.2
2.3
3.6
0.3
0.8
Cumulative Rain
Cumulative Et
Overflow
Et
Rain

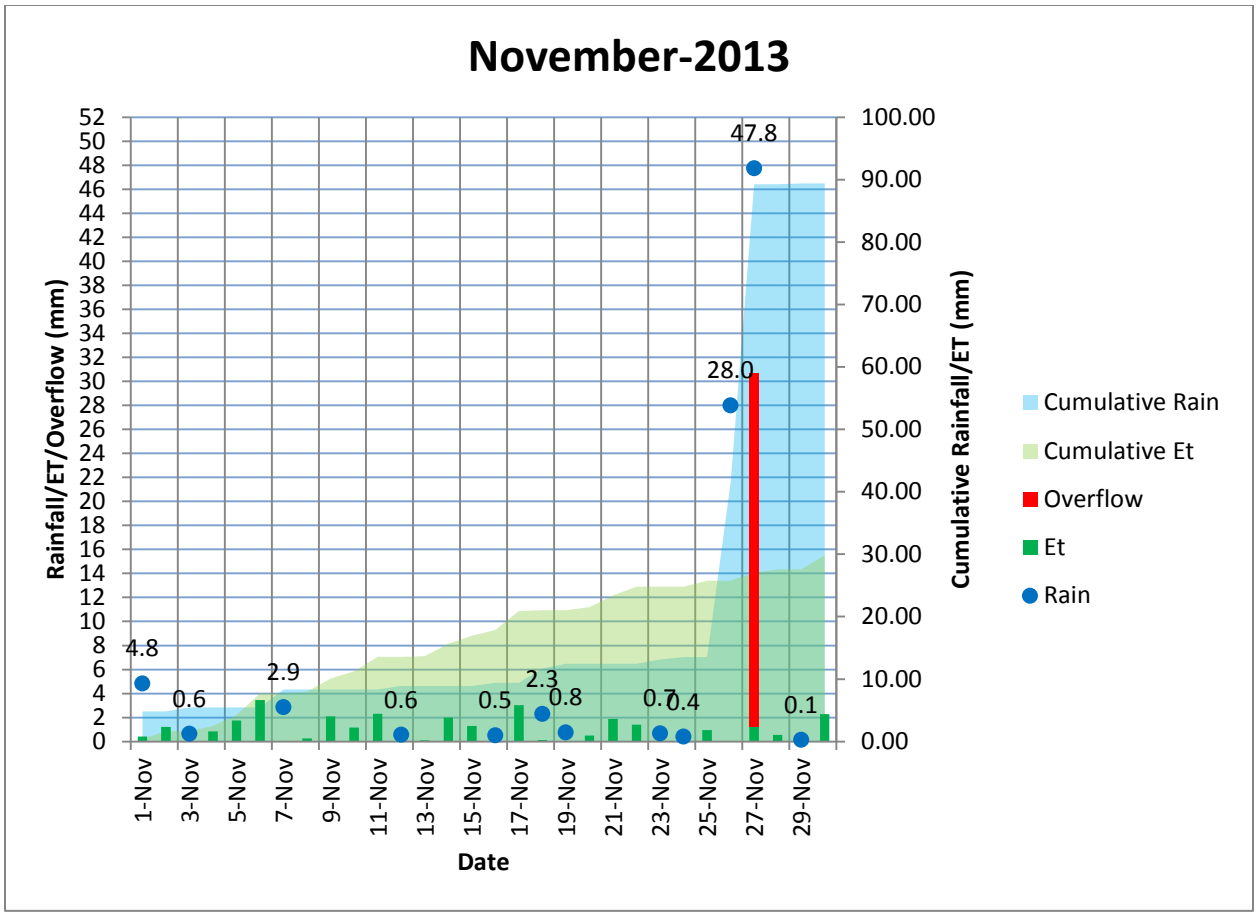
November-2013
Rainfall/ET/Overflow (mm)
Cumulative Rainfall/ET (mm)
Date
47.8
28.0
4.8
0.6
2.9
0.6
0.5
2.3
0.8
0.7
0.4
0.1
Cumulative Rain
Cumulative Et
Overflow
Et
Rain

2014

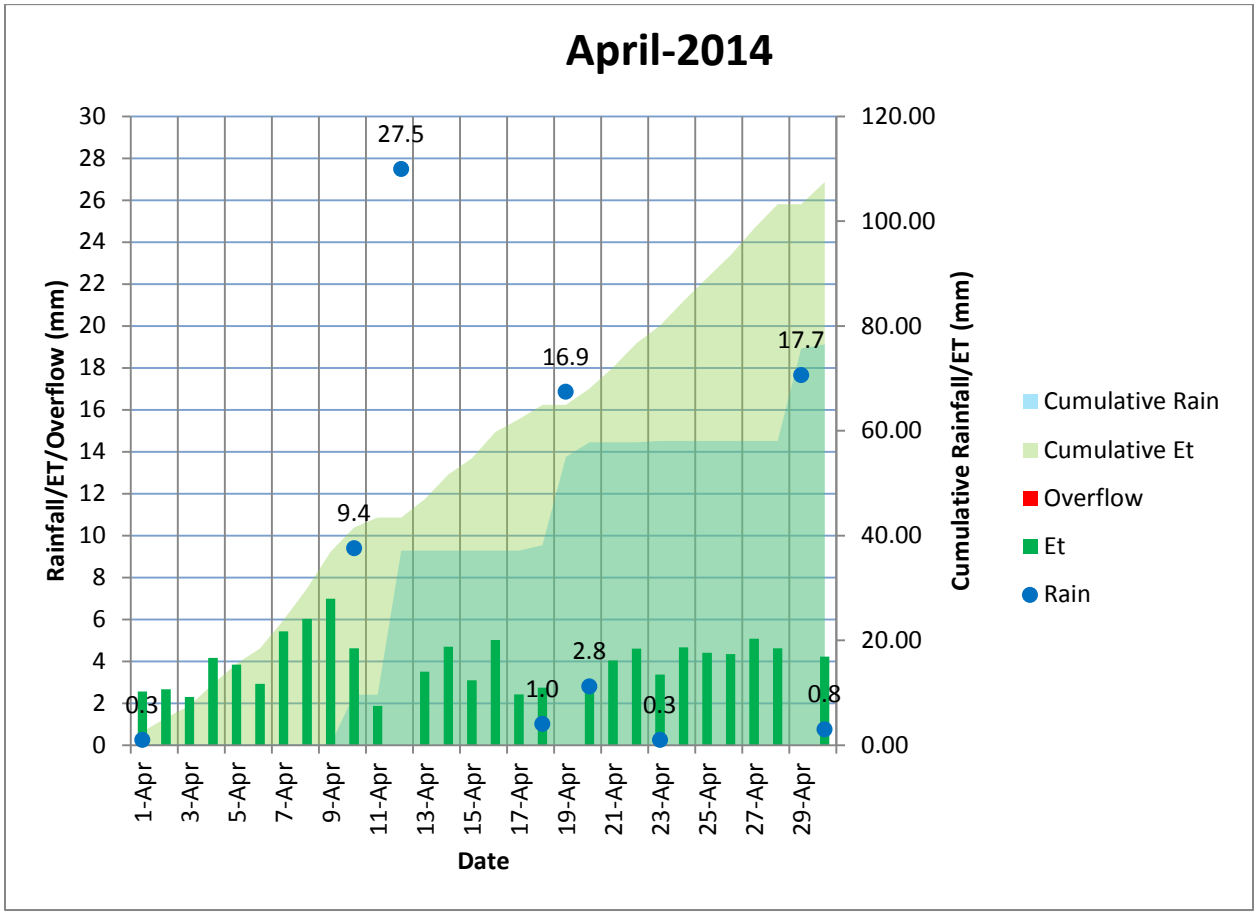
April-2014
Rainfall/ET/Overflow (mm)
Cumulative Rainfall/ET (mm)
Date
27.5
16.9
17.7
9.4
2.8
1.0
0.3
0.3
0.8
Cumulative Rain
Cumulative Et
Overflow
Et
Rain

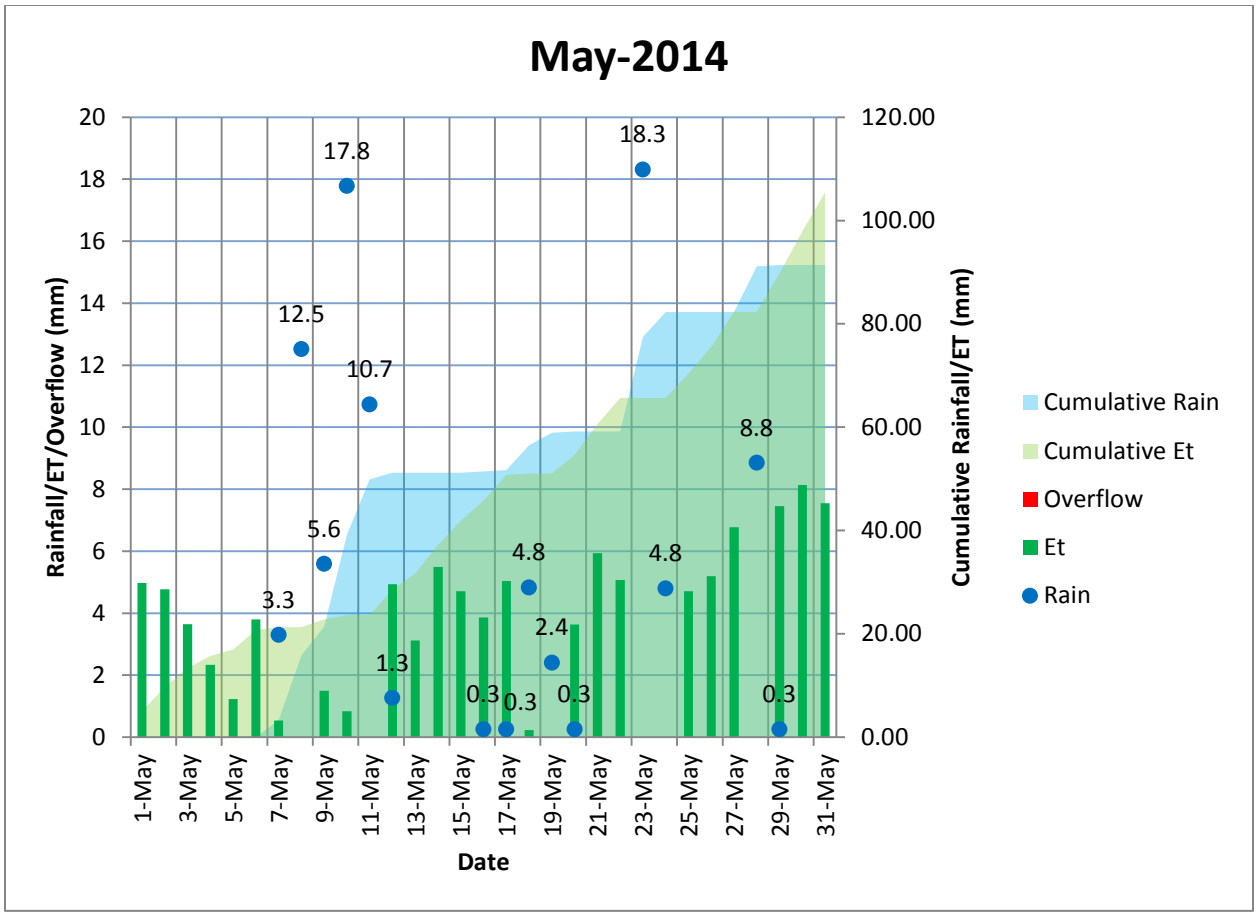
May-2014
Rainfall/ET/Overflow (mm)
Cumulative Rainfall/ET (mm)
Date
Cumulative Rain
Cumulative Et
Overflow
Et
Rain
17.8
18.3
12.5
10.7
8.8
5.6
4.8
4.8
3.3
2.4
1.3
0.3
0.3
0.3
0.3
1-May
3-May
5-May
7-May
9-May
11-May
13-May
15-May
17-May
19-May
21-May
23-May
25-May
27-May
29-May
31-May

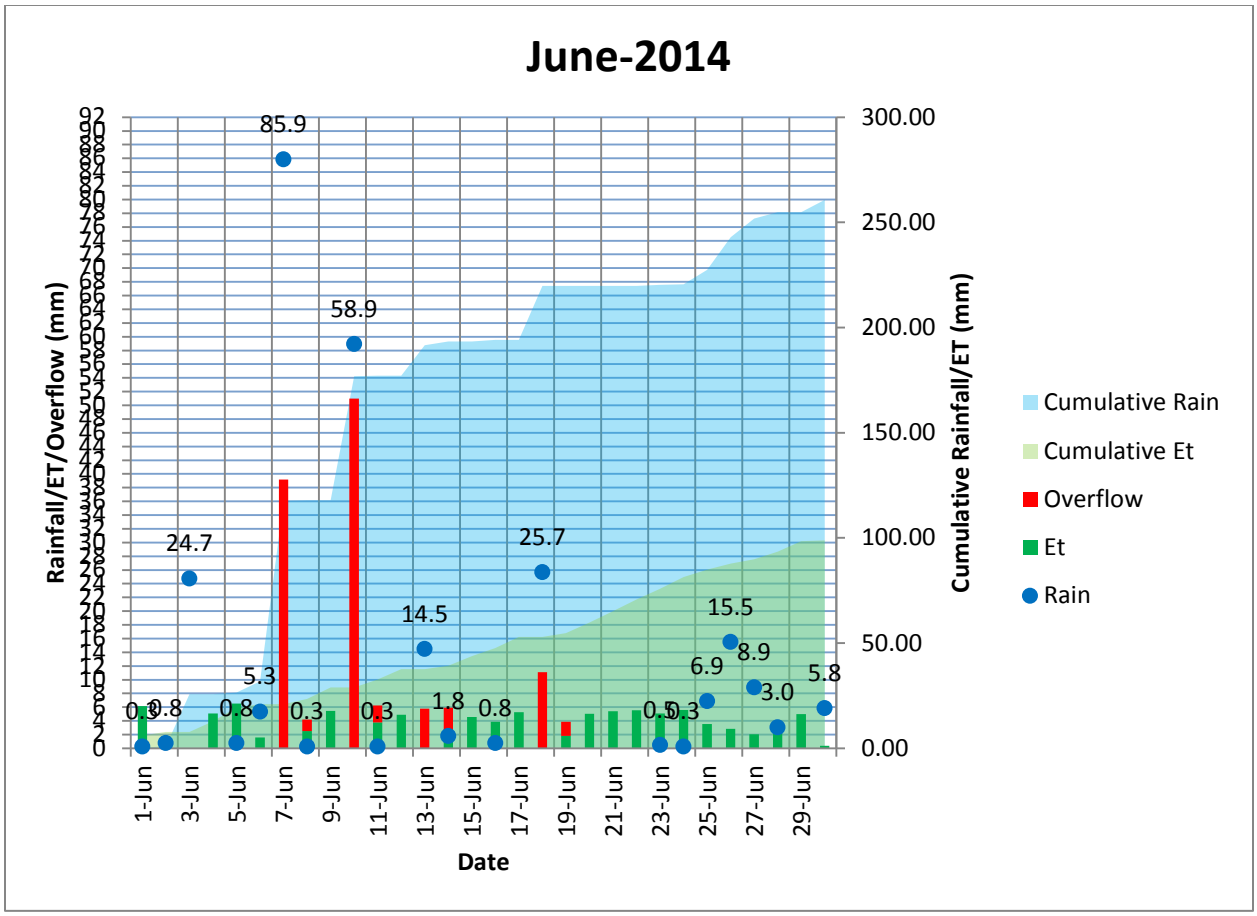
June-2014
Rainfall/ET/Overflow (mm)
Cumulative Rainfall/ET (mm)
Date
Cumulative Rain
Cumulative Et
Overflow
Et
Rain
85.9
58.9
24.7
25.7
14.5
15.5
8.9
6.9
5.8
5.3
3.0
1.8
0.8
0.3
0.00
50.00
100.00
150.00
200.00
250.00
300.00
1-Jun
3-Jun
5-Jun
7-Jun
9-Jun
11-Jun
13-Jun
15-Jun
17-Jun
19-Jun
21-Jun
23-Jun
25-Jun
27-Jun
29-Jun

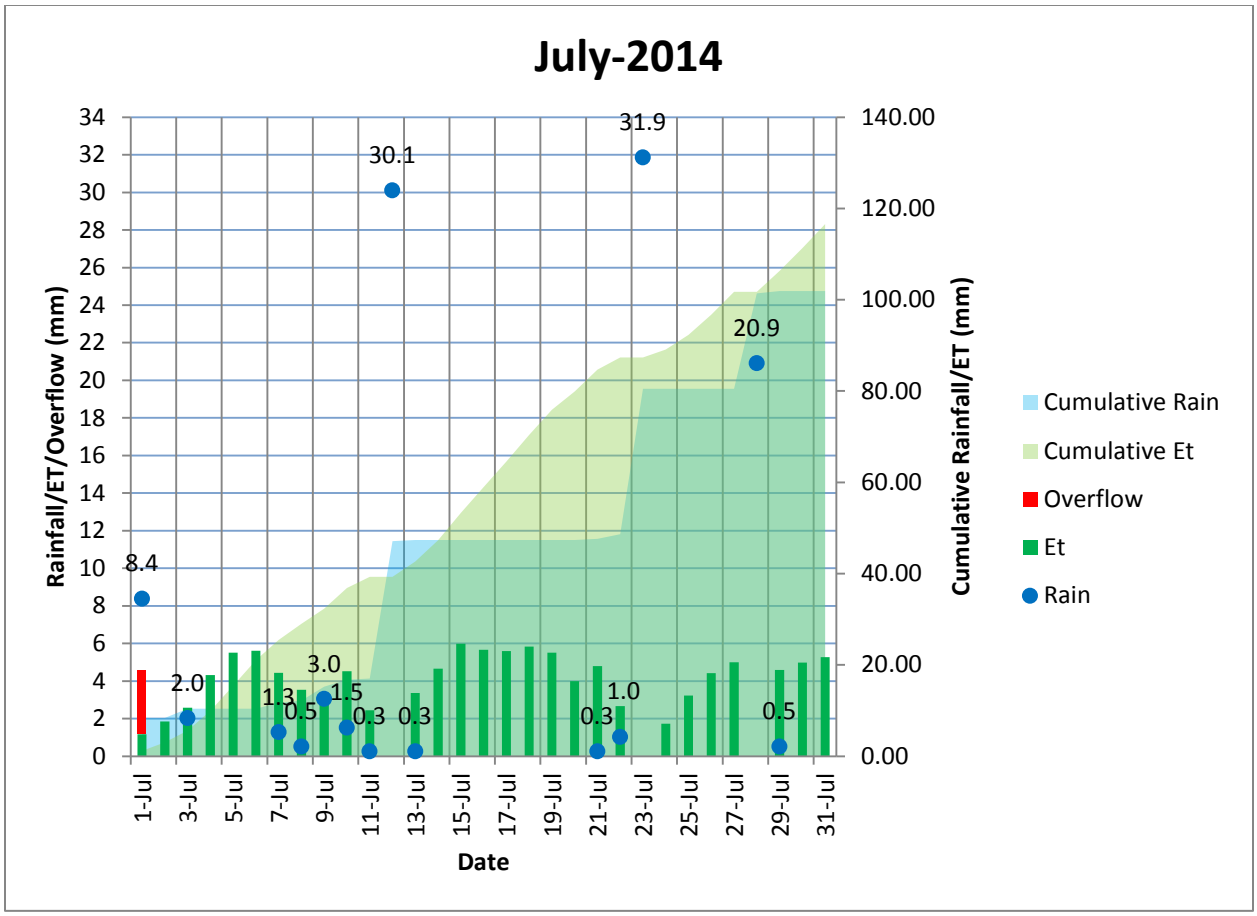
July-2014
Rainfall/ET/Overflow (mm)
Cumulative Rainfall/ET (mm)
Date
Cumulative Rain
Cumulative Et
Overflow
Et
Rain
8.4
2.0
1.3
0.5
3.0
1.5
0.3
30.1
0.3
0.3
1.0
31.9
20.9
0.5
1-Jul
3-Jul
5-Jul
7-Jul
9-Jul
11-Jul
13-Jul
15-Jul
17-Jul
19-Jul
21-Jul
23-Jul
25-Jul
27-Jul
29-Jul
31-Jul

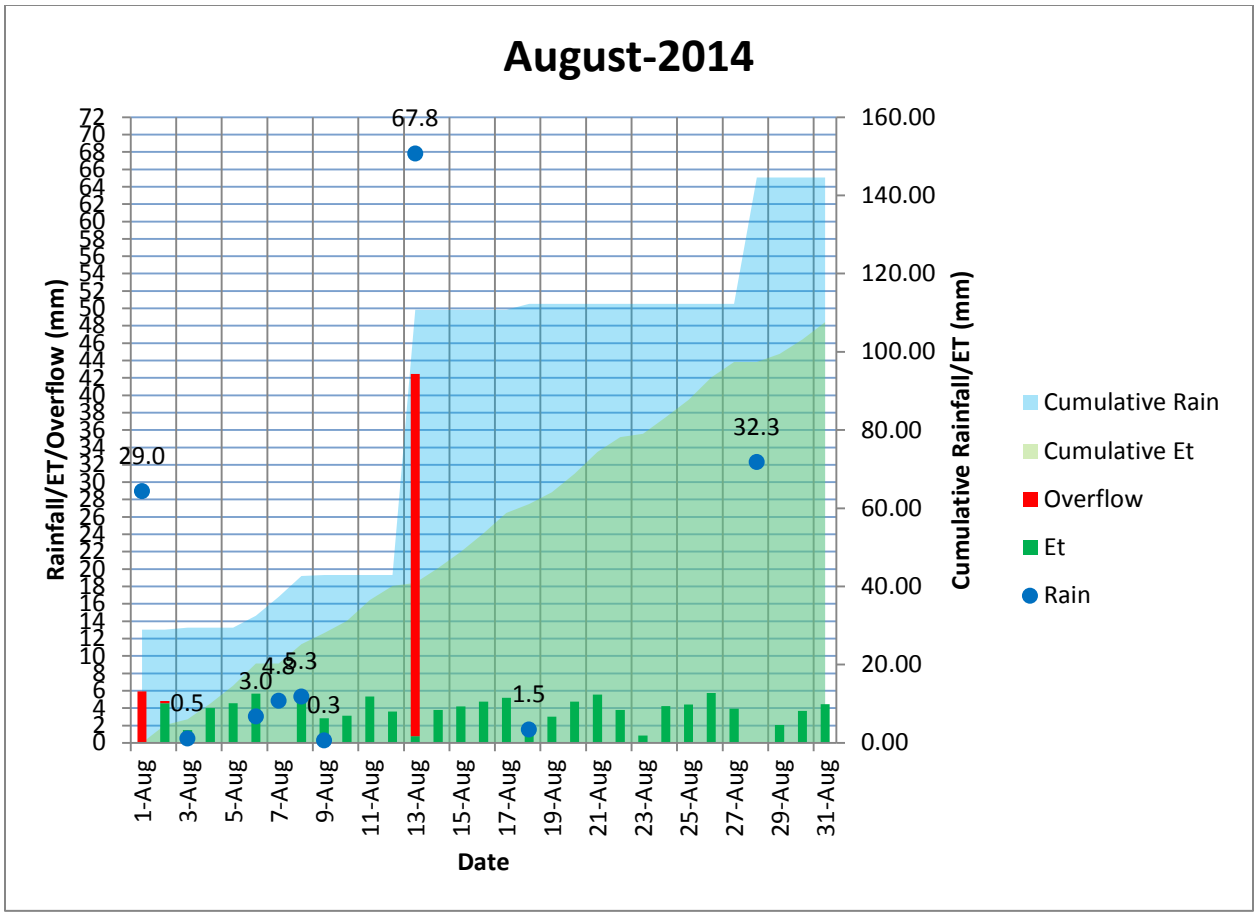
August-2014
Rainfall/ET/Overflow (mm)
Cumulative Rainfall/ET (mm)
Date
67.8
29.0
32.3
0.5
3.0
4.8
5.3
0.3
1.5
1-Aug
3-Aug
5-Aug
7-Aug
9-Aug
11-Aug
13-Aug
15-Aug
17-Aug
19-Aug
21-Aug
23-Aug
25-Aug
27-Aug
29-Aug
31-Aug
0.00
20.00
40.00
60.00
80.00
100.00
120.00
140.00
160.00
Cumulative Rain
Cumulative Et
Overflow
Et
Rain

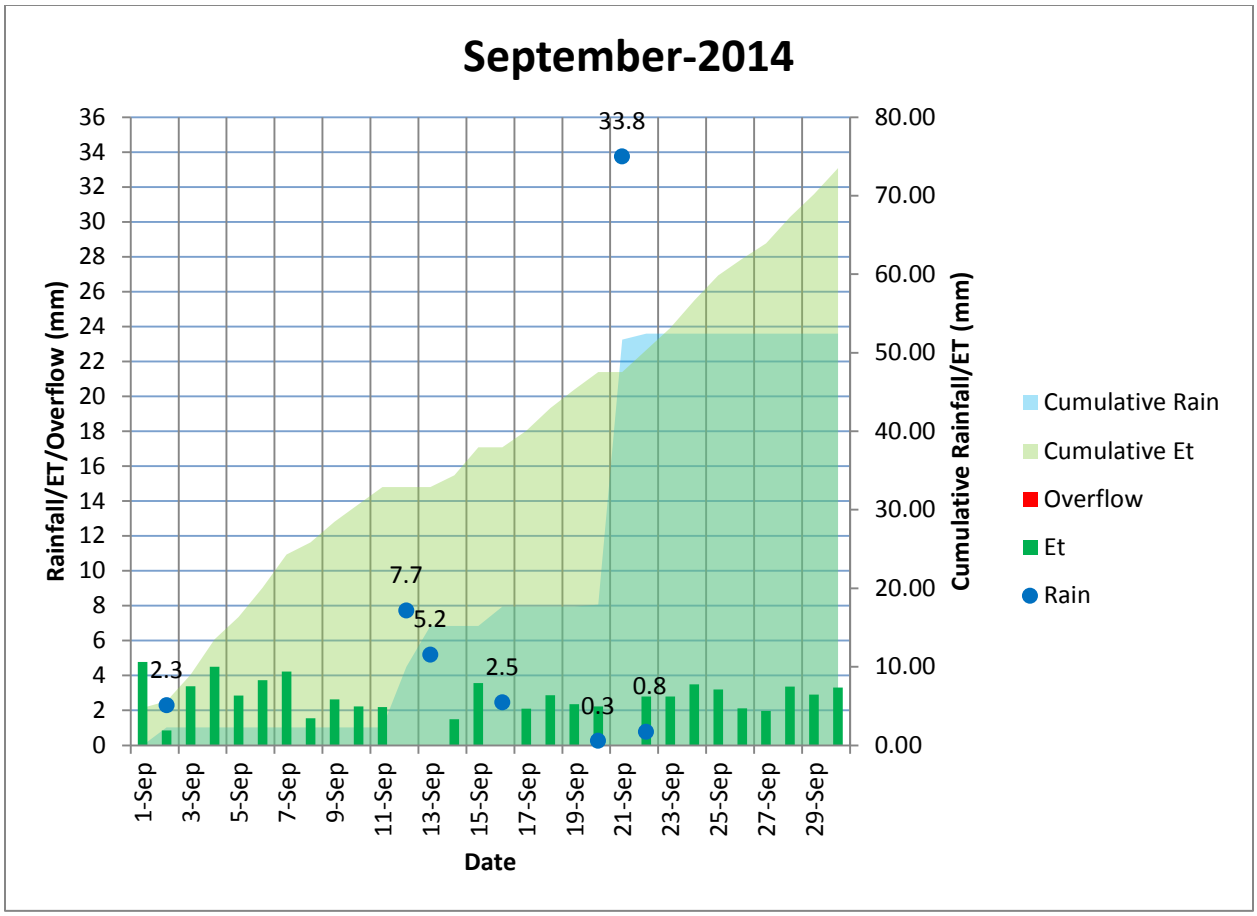
September-2014
Rainfall/ET/Overflow (mm)
Cumulative Rainfall/ET (mm)
Date
Cumulative Rain
Cumulative Et
Overflow
Et
Rain
33.8
7.7
5.2
2.3
2.5
0.3
0.8
1-Sep
3-Sep
5-Sep
7-Sep
9-Sep
11-Sep
13-Sep
15-Sep
17-Sep
19-Sep
21-Sep
23-Sep
25-Sep
27-Sep
29-Sep

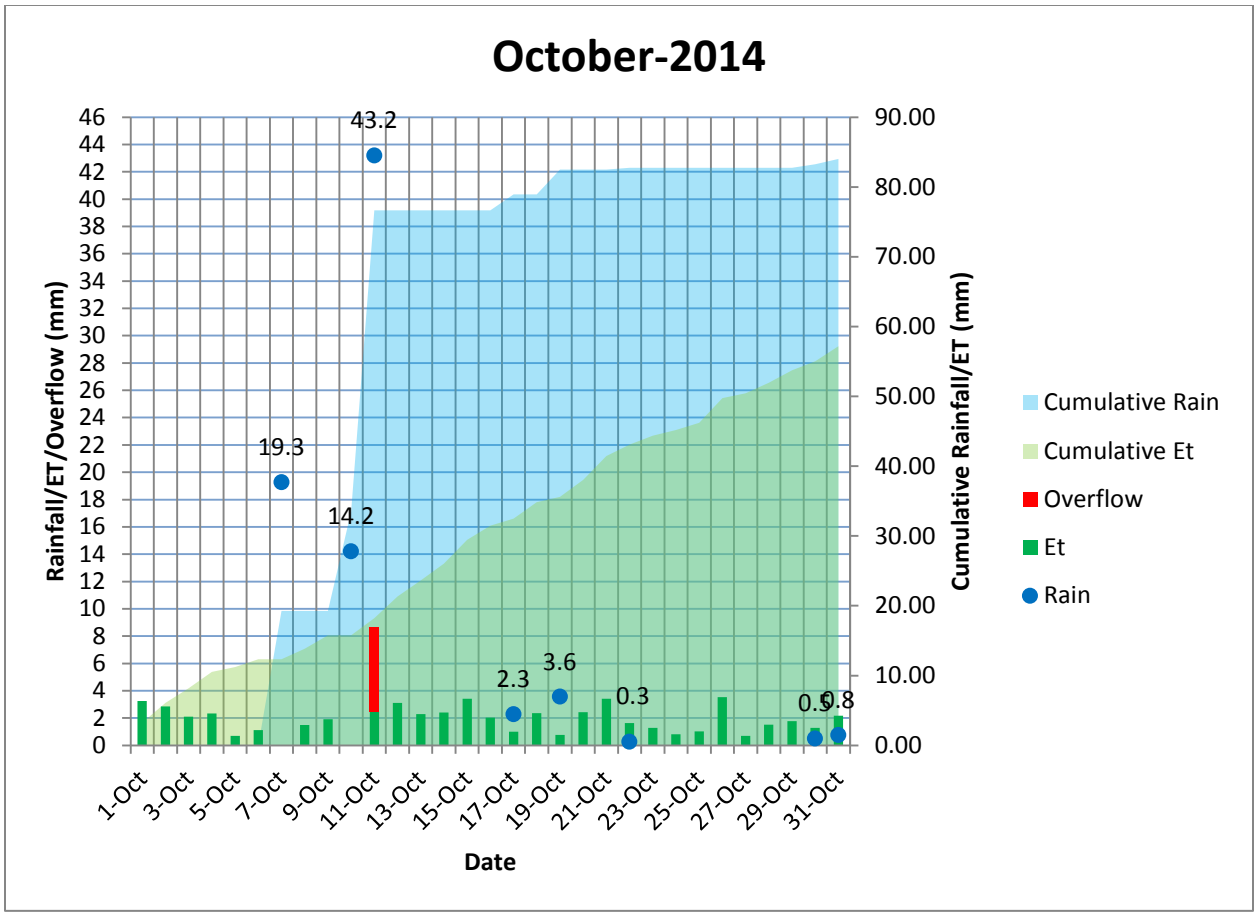
October-2014
Rainfall/ET/Overflow (mm)
Cumulative Rainfall/ET (mm)
Date
43.2
19.3
14.2
2.3
3.6
0.3
0.8
Cumulative Rain
Cumulative Et
Overflow
Et
Rain

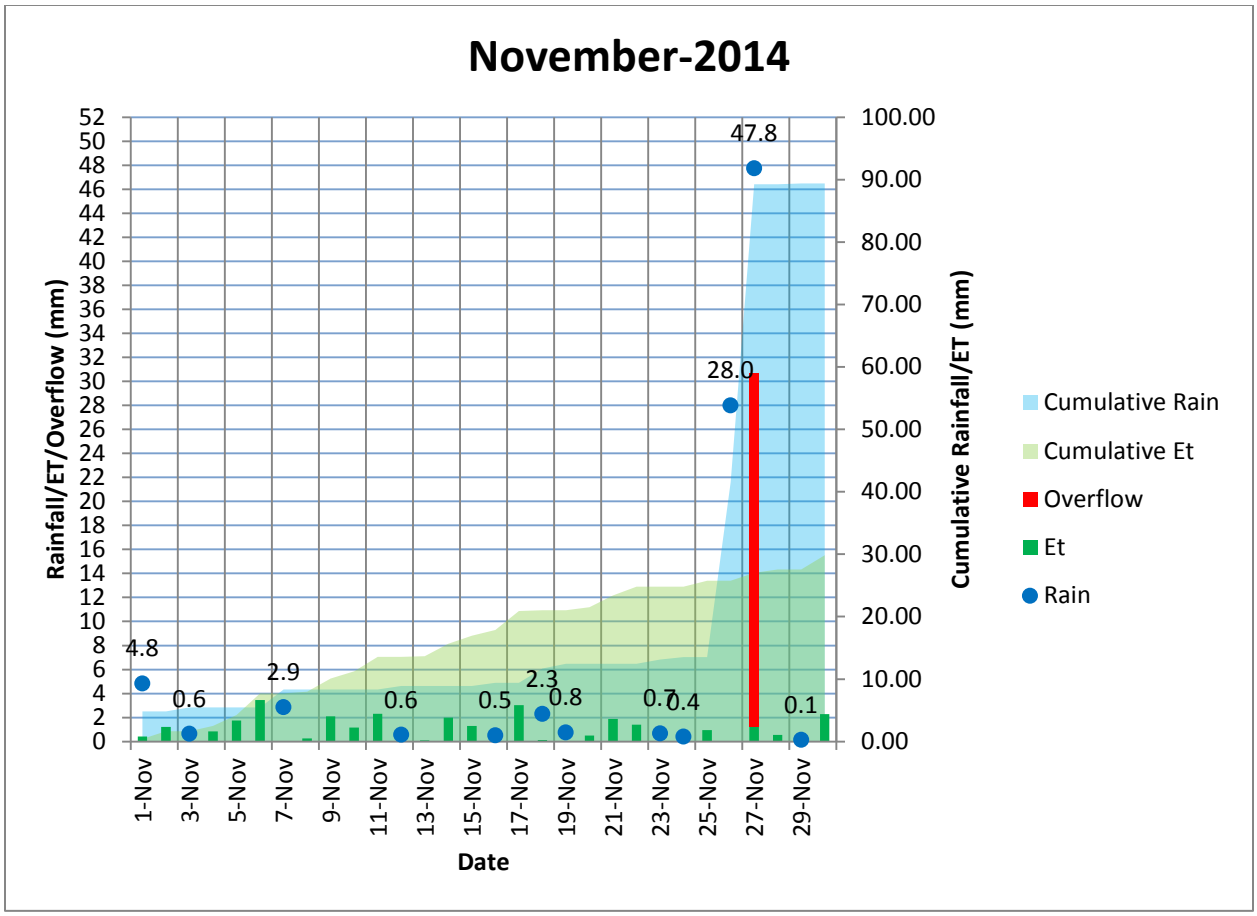
November-2014
Rainfall/ET/Overflow (mm)
Cumulative Rainfall/ET (mm)
Date
Cumulative Rain
Cumulative Et
Overflow
Et
Rain
47.8
28.0
4.8
0.6
2.9
0.6
0.5
2.3
0.8
0.7
0.4
0.1
1-Nov
3-Nov
5-Nov
7-Nov
9-Nov
11-Nov
13-Nov
15-Nov
17-Nov
19-Nov
21-Nov
23-Nov
25-Nov
27-Nov
29-Nov